A metabolism-based quorum sensing mechanism contributes to termination of inflammatory responses

Jérémy Postat

Thèse de doctorat de l'Université Sorbonne Paris Cité
préparée à l'Université Paris Diderot

Discipline : Immunologie

A metabolism-based quorum sensing mechanism contributes to termination of inflammatory responses

École doctorale Bio Sorbonne Paris Cité (ED 562 BioSPC)

UFR Sciences du Vivant
Bâtiment Lamarck Aile B
Pièce RH 71 (RdC)
35 rue Hélène Brion
75205 PARIS Cedex 13

Unité Dynamiques des Réponses Immunes

Institut Pasteur et Inserm U1223
Département d'immunologie
Bâtiment Elie Metchnikoff
25 rue du docteur Roux
75015 Paris

Thèse présentée par : **Jérémy POSTAT**

Thèse dirigée par : **Philippe BOUSSO**

Présentée et soutenue publiquement à l'Institut Pasteur le 17 octobre 2018

Composition du jury :		
	Pr. Rachel GOLUB | Univ. Paris Diderot, FRANCE	Président du jury
	Dr. Naomi TAYLOR | IGMM, FRANCE	Rapporteur
	Dr. Pierre GUERMONPREZ | KCL, UK	Rapporteur
	Pr. Andreas MÜLLER | OVGU, GERMANY	Examinateur
	Dr. Edward PEARCE | MPI-IE, GERMANY	Examinateur
	Dr. Philippe BOUSSO | Institut Pasteur, FRANCE	Directeur de thèse

Thèse de doctorat de l'Université Sorbonne Paris Cité
préparée à l'Université Paris Diderot

Discipline : Immunologie

A metabolism-based quorum sensing mechanism contributes to termination of inflammatory responses

École doctorale Bio Sorbonne Paris Cité (ED 562 BioSPC)

UFR Sciences du Vivant
Bâtiment Lamarck Aile B
Pièce RH 71 (RdC)
35 rue Hélène Brion
75205 PARIS Cedex 13

Unité Dynamiques des Réponses Immunes

Institut Pasteur et Inserm U1223
Département d'immunologie
Bâtiment Elie Metchnikoff
25 rue du docteur Roux
75015 Paris

Thèse présentée par : **Jérémy POSTAT**

Thèse dirigée par : **Philippe BOUSSO**

Présentée et soutenue publiquement à l'Institut Pasteur le 17 octobre 2018

Composition du jury :		
	Pr. Rachel GOLUB | Univ. Paris Diderot, FRANCE	Président du jury
	Dr. Naomi TAYLOR | IGMM, FRANCE	Rapporteur
	Dr. Pierre GUERMONPREZ | KCL, UK	Rapporteur
	Pr. Andreas MÜLLER | OVGU, GERMANY	Examinateur
	Dr. Edward PEARCE | MPI-IE, GERMANY	Examinateur
	Dr. Philippe BOUSSO | Institut Pasteur, FRANCE	Directeur de thèse

Abstract

Abstract

Keywords

Leishmania major | *inflammation* | *monocyte-derived cells* | *metabolism* | *collective behavior*

Abstract

Recruitment of immune cells during infection is essential to fueling the immune response but can also trigger immunopathology. A critical question is how the immune system can sense inflammation levels and self-adjust accordingly to limit tissue damage while removing the pathogen. During my Ph.D. I studied the self-resolving cutaneous infection with *Leishmania major* parasites where tissue damage arises when inflammation is allowed to become excessive. At the site of infection, the immune reaction is driven by recruited monocyte-derived cells that represents the major population of infected cells and are also actively involved in fighting the infection. They secrete pro-inflammatory cytokines but also produce nitric oxide (NO), critical to regulate the outcome of the infection: iNOS KO mice are susceptible and do not control the parasite load, subsequently developing severe tissue damage because of excessive immune cell infiltration. My work demonstrated that monocyte-derived cells at the site of infection are regulated by NO that limits their cellular respiration, lowers their energetic resources and consequently their activity *in vivo*. This regulation relies on tissue-wide NO diffusion and only exists when a sufficient cell density has been reached, revealing that monocyte-derived cells are endowed with a quorum sensing mechanism that adjusts their population size and activity in time and space to avoid immunopathology.

Résumé en français

Résumé en français

Mots-clés

Leishmania major | *inflammation* | *cellules dérivées de monocytes* | *métabolisme* | *comportement collectif*

Résumé

Lors d'une infection, le recrutement de cellules immunitaires au site inflammatoire est nécessaire pour la lutte contre le pathogène mais peut également participer au déclenchement d'une immunopathologie. Il n'est pas encore clair aujourd'hui s'il existe des mécanismes permettant au système immunitaire de percevoir l'intensité de la réponse inflammatoire pour s'autoréguler afin d'éviter une importante destruction tissulaire tout en éliminant le pathogène. Pendant mes études doctorales, j'ai étudié l'infection asymptomatique par le parasite *Leishmania major* qui peut générer d'important dommages au tissu si l'inflammation devient excessive. La réaction immunitaire contre le parasite est contrôlée par des cellules dérivées de monocytes qui sont recrutées au site inflammatoire et y forment la principale population infectée en plus de participer activement à la réaction inflammatoire. Elles secrètent des cytokines pro-inflammatoires et produisent de l'oxyde nitrique (NO) qui est essentiel pour une issue favorable de la maladie. En effet, les souris déficientes pour l'enzyme iNOS (synthétisant le NO) contrôlent moins bien l'infection et développent systématiquement de graves symptômes associés à d'importants dommages tissulaires, causés par un recrutement incontrôlé de cellules immunitaires. Mon travail a montré que les cellules dérivées de monocytes sont régulées au site d'infection par le NO qui limite leur respiration cellulaire, diminuant ainsi leur ressources énergétiques et leur activité *in vivo*. Ce mode de régulation nécessite la diffusion du NO à distance et n'existe que lorsque les cellules dérivées de monocytes sont densité suffisante. Ceci montre que ces cellules sont régulées par un mécanisme de détection du quorum, basé sur le métabolisme cellulaire, qui permet d'ajuster finement la quantité de cellules immunitaires actives dans l'espace et le temps pour éviter le développement d'une immunopathologie.

Acknowledgements

Poopy-di scoop
Scoop-diddy-whoop
Whoop-di-scoop-di-poop
Poop-di-scoopty
Scoopty-whoop
Whoopity-scoop, whoop-poop
Poop-diddy, whoop-scoop
Poop, poop
Scoop-diddy-whoop
Whoop-diddy-scoop
Whoop-diddy-scoop, poop

KANYE OMARI WEST, Lift Yourself

Acknowledgements

Ces remerciements sont l'occasion d'exprimer ma plus grande gratitude envers toutes les personnes qui m'ont aidé à la réalisation de ce projet, dont je ne suis pas peu fier !

PHILIPPE. Haha tu as une section rien que pour toi ! Tout ça pour te dire que je suis aussi chanceux que toi dans le fait d'avoir trouvé ce labo et de t'avoir eu comme directeur de thèse. Je n'ai jamais rechigné en me levant, le matin, sauf peut-être le mardi, à venir travailler ici et bien au contraire. J'ai appris beaucoup de choses scientifiques certes, mais ce que je retiendrai le plus c'est probablement ta vision de la science et ton côté si humain envers nous. Merci infiniment de m'avoir soutenu, guidé, motivé et bonifié pendant ces trois années de thèse. J'espère ne jamais avoir à dire " Philippe, mais qu'est-ce que tu as changé ! ".

AU JURY DE THÈSE. À mes rapporteurs, Naomi TAYLOR et Pierre GUERMONPREZ, ceci est probablement la première page du manuscrit que vous lirez avant suffisamment d'autres. Merci beaucoup d'avoir accepté cette lourde tâche et merci pour vos conseils et expertises respectives. J'attends vos corrections et la discussion le jour J avec impatience !
To my examiners, Andreas MÜLLER and Edward PEARCE, thank you very much for accepting my invitation to be a part of my committee. I will be delighted to discuss with

you during the defense and I'm sure your knowledge will make this thesis better. Merci également au président du jury, Rachel GOLUB, sans qui cette thèse n'aurait pas lieu.

AU LABORATOIRE. Évidemment ce travail n'aurait jamais pu être mené à bien sans le soutien quotidien de mes plus grands fans de crêpes / gâteaux, bandes de petits gloutons. Romain, je commence par toi car tu es après tout mon "maître de stage", celui qui m'a passé le flambeau sur ce super sujet et sans qui je n'aurais pas pu si bien démarrer la thèse (pas de merci pour le parasite par contre). J'espère que tu seras fier du travail accompli ! Et par ordre alphabétique pour ne pas faire de jaloux : Armelle, on commence bien la liste dis-donc, merci pour ta mémoire des scènes cultes et tes nombreux jours de congés qui ont fait passer les miens comme pas grand-chose. Béatrice B., merci pour ton enthousiasme quotidien et ta passion pour les jeux de société et le SBEA. J'ai hâte de retrouver ma cougar à SF ou NYC le plus tôt possible. Béatrice C., merci pour ta joie de vivre et ta dynamique, tu me manques le mercredi. Bérengère, merci pour ton soutien efficace dans les papiers et un bisous à Elie. Capucine, merci pour la plastifieuse, ton sens du détail, les coups de Dymo et les sessions rangement du labo (P.S. : mon bureau a besoin de toi). Merci pour les jeux et les Spritz dans ton

super "appart". David, merci de m'avoir montré que l'on peut manger sans honte au moins 2 desserts par repas. Erica, je te laisse les rênes du projet ! j'espère qu'il te plaît et je suis sûr que tu vas en faire quelque chose d'encore mieux :) et bien entendu merci merci pour tes tiramisus. Fabrice, lab manager, merci d'être l'épaule sur laquelle on peut compter en cas de soucis. Merci également pour ton aide avec Perceval, Dominique et Véronique. Idan, merci d'avoir partagé ton bureau et ta bonté avec moi au quotidien, tu es un ange aux cils de princesse. Margot, un grand merci pour ta culture jeune et ta fraîcheur, wesh tu roxes du poney meuf t'es trop chanmé. Tu as été indépendante très vite et bien débrouillarde, tu vas aller loin petite ! Maria, merci pour les séances cinéma, la charcuterie espagnole et ta ferveur politique. Marine, merci pour tes skills en danse et un grand merci du soutien que tu apportes à Ronan qui va bientôt devenir Ph.D. senior. Piv, nous ne nous sommes vu que quelques semaines mais ce fût un réel plaisir. Ronan, ah là là, merci d'avoir été mon partenaire 9GAG et Reddit pendant cette thèse et c'est non sans joie que je te proclamerai très bientôt à ton grade supérieur. Roxana, merci beaucoup pour ton rayonnement quotidien, les soirées jeux et pour Bazar Bizarre 2.0, c'est le fun ce jeu ! Tu mérites un camion entier de téquila. Susanna, merci pour tes conseils avisés sur

la réalisation de la pâte et la nourriture italienne en général. Zacarias, pour bien finir la liste, Sacha, que dire ? Je pense que tu as beaucoup de potentiel au basket. Je suis certain que l'entraînement va porter ses fruits un jour. Merci infiniment pour ta présence et ton éclat dans le labo. Vive ~~l'annexe~~ le K2, ~~Natacha~~ Mélenchon, Rihanna et j'espère que tu m'aimes autant que je t'aime même si je ne suis pas une fille.

Aux PASTEURIENS. Je remercie également les membres de l'institut qui m'ont apporté de l'aide mais aussi de très bons moments au cours de cette thèse, ils se reconnaîtrons sûrement. Mention spéciale pour Ophélie et le labo ATP pour m'avoir accepté comme membre après ~~24~~ 20 h, pour les bières et les pétanques / mölkky. Pour Jay, Dj Bianchi, pour sa maîtrise des relations sociales avec les corps de Pasteur et notre aventure en tant que Ph.D. representatives. Pour Maxime, qui fait presque partie de notre labo (ça fait longtemps que je ne t'ai pas vu d'ailleurs). Pour Freddie, Jérôme et Georges pour les pintes post boulot en compagnie de Béa. Pour Bruno et Tharshana au CIH. Pour Sophie et Sandrine à la cytométrie. Pour le staff de l'animalerie et de la cuisine parce que ça représente un gros boulot. Pour Caroline et Jim pour leur soutien lors de mes demandes de financement pour le postdoc. Merci également à Najma

pour avoir rempli avec aisance son rôle de tuteur.

A LA FAMILLE. Voilà maman, j'ai fini la thèse ! Je vais avoir plus de temps pour te téléphoner probablement, oups si. Un grand merci à toi pour ton soutien et ta patience permanente, tu es la meilleure des mamans =D Merci Alice, ma quiche, d'être toujours heureuse de me voir en vacances et merci à Morgan mon petit cordon bleu carnichon. Merci à la famille provençale de toujours être disponible quand je rentre dans le Sud en vacances. Merci également à la famille basque pour leur soutien et les moments partagés en congés - Nico, tu n'es pas là mais je pense fort à toi tous les jours et la thèse est enfin terminée ! Un grand merci à la Jaill' au complet pour m'avoir intégré si facilement dans votre famille, pour les repas du dimanche et les vacances sous le soleil du Maroc.

AUX AMIS. Le meilleur pour la fin ! Mes potes un grand grand merci pour votre présence en dehors de mes heures de boulot et pour le lolz. Merci les bios pour les sorties sur Paris, les soirées jeux, les vacances à droite à gauche, les bonnes bouffes et autres moments Loulette, Beriboubou, Chaton et Pipine, je vous aime de tout mon coeur et vous allez bien me manquer au Canada. Merci les physiciens (surtout le gang des boules): Timothée Franklin de Guillebon, Fathias Pierre, Lehébel, Briboule et Graboule sans oublier Cavillès, Maumau

et les lyonnais. Merci pour tous ces BP, soirées, quiz au BL, les vacances en Grèce, le poker des cafards... vous êtes scandaleux et j'aime ça. Big up pour Antwayne qui a réussi à me supporter pendant de longues années au quotidien, it was an intense bumpy ride. Merci aux inclassables canailles représentées par Fabienne Pelouze et sa magnifique compagne, la sacré Vernouille, Béber, Pap's, Audiot et Hélé-na. Merci à Alix et Héloïse D. pour avoir égayé mes séances de monitorat. Merci à Héloïse T. pour les japs et un grand merci à Garrone et Anaïs, je suis toujours heureux de vous voir même si c'est pas souvent.

Merci José, merci Léon et surtout merci Zizou.

Guys, it's time to get schwifty. Je vous attends tous au Canada =)

Jérem.

Table of contents

Table of contents

List of figures and tables

List of figures and tables

Table of tables

Table of figures

List of abbreviations

List of abbreviations

ACLY	ATP-citrate lyase
ADP	Adenosine diphosphate
AMP	Adenosine monophosphate
AP-1	Activating protein-1
ATP	Adenosine triphosphate
cAMP	cyclic adenosine monophosphate
BMDMs	Bone marrow-derived macrophages
CCL2, 3…	CC chemokine ligand-2, 3…
CD45, 86…	Cluster of differentiation 45, 86…
C/EBP	CCAAT-enhancer-binding proteins
cGMP	cyclic guanosine monophosphate
CL	Cutaneous leishmaniasis
CREB	cAMP-responsive element binding protein
CXCL1, 2…	CXC chemokine ligand-1, 2…
DC	Dendritic cell
ETC	Electron transport chain
$FADH_2$	Reduced flavin adenine dinucleotide (FAD)
FAO	Fatty acid oxidation
FcγRI	Fragment crystallizable-γ receptor 1
GAPDH	Glyceraldehyde 3-phosphate dehydrogenase
GLUT1	Glucose transporter 1
GM-CSF	Granulocyte-macrophage colony-stimulating factor
gMFI	geometric mean fluorescence intensity
GP63	Glycoprotein 63
HIF-1α	Hypoxia-inducible factor-1α
HSCs	Hematopoietic stem cells
IDH	Isocitrate dehydrogenase
IDO	Indoleamine 2,3-dioxygenase
IFA	Incomplete Freund's adjuvant
IFN-γ	Interferon-γ
IL-1β, 6…	Interleukin-1β, 6…
iNOS	Inducible nitric oxide synthase
IRF3, 5…	Interferon regulatory factor 3, 5…

IRG1	Immunoresponsive gene 1
JAK	Janus kinase
LC	Langerhans cells
L-NIL	N^6-(1-iminoethyl)-L-lysine
LPG	Lipophosphoglycan
LPS	Lipopolysaccharide
MAPK	Mitogen-activated protein kinase
M-CSF	Macrophage colony-stimulating factor
MCT4	Monocarboxylate transporter 4
MHC-II	Major histocompatibility complex class II
mTOR	mammalian target of rapamycin
NAD(P)H	Reduced nicotinamide adenine dinucleotide (phosphate)
NF-κB	Nuclear factor κB
NK cells	Natural killer cells
NO	Nitric oxide
OXPHOS	Oxidative phosphorylation
PAMPs	Pathogen-associated molecular patterns
PFK2	Phosphofructokinase 2
PKC	Protein kinase C
PKM2	Pyruvate kinase isozyme M2
PPP	Pentose phosphate pathway
PV	Parasitophorous vacuole
RNS	Reactive nitrogen species
ROS	Reactive oxygen species
SDH	Succinate dehydrogenase
SHP-1	Src homology region 2 domain-containing phosphatase-1
SNAP	S-Nitroso-N-acetylpenicillamine
SOCS	Suppressors of cytokine signaling
STAT	Signal transducer and activator of transduction
TCA cycle	Tricarboxylic acid cycle
TGF-β	Transforming growth factor-β
T_H1, 2 cells	T helper 1, 2 cells
TLR	Toll-like receptor
TNF-α	Tumor necrosis factor-α
WT	Wild type

Introduction

Introduction

Inflammation refers to the complex biological response consequent to harmful tissue injury by pathogens, damaged cells or irradiation, until return to tissue homeostasis. It is a protective reaction of the organism to fight and remove the injury source as well as initiate tissue healing. Upon injury, soluble mediators are released at the site of inflammation to trigger the recruitment of immune cells, as neutrophils and monocytes, circulating in the blood. This process, referred as acute inflammation, is important to eliminate the threat and avoid pathogen dissemination in the case of an infection but is also dangerous by itself. Indeed, numerous inflammatory mediators aim at killing potential pathogens and are therefore extremely toxic even for the host. When inflammation turns chronic, it can last for months or years and is often associated with the development of an immunopathology characterized by intense tissue scarring, pain and loss of function. Hence, proper control of the inflammatory reaction is critical to eliminating the threat and avoiding tissue damage.

Our perception of inflammation during physiological immune responses and pathology is constantly evolving and we are far from understanding every aspects of its control. An important question that remains to be fully answered is how an ongoing inflammatory reaction is slowed down to avoid immunopathology while having enough dominance to eliminate the source of injury?

During my Ph.D., I addressed this question in the context of the self-resolving cutaneous infection with *Leishmania major* parasites. This model has the advantage to allow a proper development of the inflammatory reaction and its fine regulation in time and space to kill the parasite without inducing immunopathology. Experimental resistant and susceptible murine models have been described and importantly, in susceptible mice, the pathology is not triggered by the parasite itself but rather by an excessive immune reaction. Therefore leishmaniasis provides a physiological model relevant to study how inflammation is regulated to eliminate stressing agents without triggering immunopathology.

In this thesis I focused on the role of nitric oxide (NO) during the inflammatory reaction against *L. major* parasites. NO has been identified several decades ago as a key effector in the control of many infection with intracellular parasites, including *L. major*. Mice deficient for the enzyme

synthetizing NO, iNOS, are susceptible to the infection and have a higher parasite load as well as extensive tissue destruction consequent to dysregulated immune cell infiltration at the site of infection. Yet, the mechanism of action of NO *in vivo* remains elusive. We know that NO is produced by monocyte-derived cells during leishmaniasis and that it is toxic for the parasite. However, decreasing the parasite load may not be sufficient to initiate the termination of the inflammatory reaction. This hypothesis was the main driving force of my Ph.D. during which I tried to elucidate whether NO participates also in a mechanism regulating the inflammatory reaction independently of the parasite.

The following introduction aims at presenting the various findings that forged the bases of my study and helped me to answer this question. In the two first chapters I will present the parasite *Leishmania major* and the immune reaction elicited by its injection into the skin. In the two last chapters I will focus more in the inflammatory reaction by presenting first a brief overview of the metabolism and activity of monocyte-derived cells and then some key mechanisms controlling the inflammation, with a special interest on cellular metabolism and NO.

Chapter I *Leishmania major* parasites: cutaneous infection and healing

I. *Leishmania* SPECIES CAUSATIVE OF CUTANEOUS LEISHMANIASIS

I.1. The genus *Leishmania*

Leishmania parasites represent the *Trypanosomatidae* members causative of leishmaniasis in vertebrates. This chronic and slow-developing disease can manifest in three different ways depending on parasite species: cutaneous, mucocutaneous, or visceral leishmaniasis (Scott and Novais, 2016; Torres-Guerrero et al., 2017). According to the World Health Organization (WHO), leishmaniasis is one of the most important tropical disease and represents a major public health problem with around 1 million new cases and 25.000 deaths occurring annually. An estimated 1 billion people are living in endemic areas at risk of infection but as only a small fraction of people that get infected develop the disease. Thus, leishmaniasis is considered as a neglected disease.

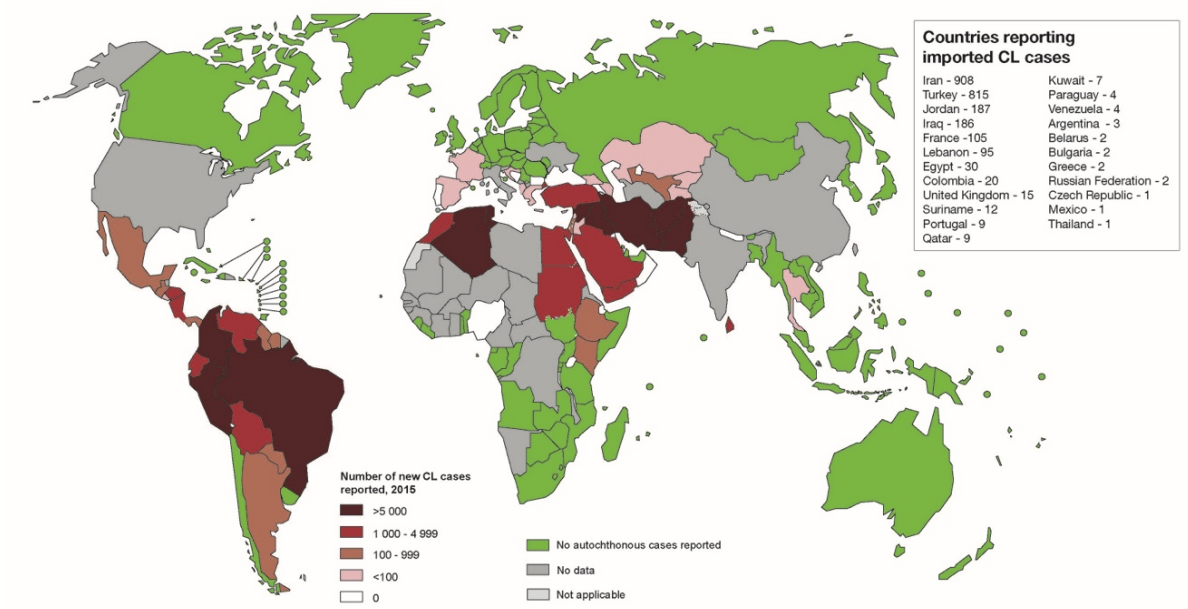

Figure 1. Status of endemicity of cutaneous leishmaniasis (CL) worldwide in 2015

This map shows the number of new cases of CL reported in 2015. The majority of CL cases (dark red color-coded countries) occurred in Afghanistan, Algeria, Brazil, Colombia, the Islamic Republic of Iran, Pakistan, Peru, Saudi Arabia and the Syrian Arab Republic. Map from WHO.

Cutaneous leishmaniasis (CL) is the most common manifestation of the illness worldwide. According to the WHO, more than 90% cases of CL are located in Northern Africa, Western Asia and Latin America countries (**Figure 1**). Different species are responsible for cutaneous lesions development according to their geographical distribution in the so-called Old World (South Europe, Africa, Western Asia) and the New World (Americas). Parasites are transmitted by sandflies belonging to the subfamily of *Phlebotominae* (**Table 1**). Old World species are spread by sandflies of the genus *Phlebotomus* mainly in semi-arid or desert conditions, whereas New World species are more specifically spread by sandflies of the genus *Lutzomyia* in forest environments.

Table 1. ***Leishmania*** **species causative of cutaneous leishmaniasis in humans**

Table adapted from (Kaye and Scott, 2011; Sacks and Kamhawi, 2001).

Leishmania **genus**	**Vector genus**	**Geographic distribution**
Subgenus ***Leishmania***		
Leishmania major	*Phlebotomus*	Western Asia | Africa
Leishmania tropica		Western Asia | Africa
Leishmania aethiopica		East Africa
Leishmania infantum		Southern Europe
Leishmania mexicana	*Lutzomyia*	Central America
Leishmania amazonensis		Latin America
Leishmania chagasi		Latin America
Subgenus ***Viannia***		
Leishmania braziliensis	*Lutzomyia*	Latin America
Leishmania guyanensis		
Leishmania panamensis		
Leishmania peruviana		

I.2. Clinical manifestations

Although most infections are symptomless or misdiagnosed, CL is characterized by a large spectrum of clinical manifestations (Reithinger et al., 2007). Disease severity, clinical appearance and curing time depend on both *Leishmania* species and host susceptibility. The first clinical manifestation is often the development of a small erythema at the site of initial infection. Localized cutaneous leishmaniasis (LCL) develops when this erythema matures into

a nodule that gradually ulcerates within 2 to 6 weeks until the final lesion is established (**Figure 2**). Diffuse cutaneous leishmaniasis (DCL) is diagnosed when multiple non-ulcerative nodules are detected in patients. Spreading of the disease by parasite dissemination to mucosal environment often implies serious complications leading to disfiguring and life-threatening situations. Whereas LCL can spontaneously heal, mucosal leishmaniasis often cannot and is challenging to heal as well as closely associated with secondary bacterial infections.

Figure 2. Clinical spectrum of localized cutaneous leishmaniasis in humans

During LCL, a small erythema develops at the site of infection (*top right image*) that gradually ulcerates (*bottom right image*) until the lesion is fully established (*left image*). LCL lesions vary in intensity and clinical appearance between patients but always remains crippling. Spreading to mucosa is often disfiguring and life-threatening. Images from (Hartley et al., 2014).

I.3. Cutaneous leishmaniasis is an immunopathology

The assumption that increased parasite load correlates with increased tissue damage is misleading during leishmaniasis. For instance, an elegant study by Naik *et al.* demonstrated that germ free mice can harbor ten-fold more parasites in the skin than SPF mice while developing reduced edema and necrosis, leading to a smaller lesion (Naik et al., 2012). Along with other studies, this support the idea that leishmaniasis is an immunopathology where tissue damage is induced by the immune reaction rather than the parasite *per se* (Nylén and Eidsmo, 2012) . Recruitment of immune cells with antimicrobial properties such as neutrophils can help to cure the infection but also leads to destruction of skin architecture and subsequent necrosis. In

response to initial tissue damage keratinocytes start to proliferate, leading to epidermis hypertrophy. Intense inflammation associated with high TNF-α levels gives rise to skin ulceration when the keratinocyte layer is shattered. This shattering appears to be a consequence of a high susceptibility of keratinocytes to apoptosis (Nylén and Eidsmo, 2012; Rethi and Eidsmo, 2012) .

Here it is clear that inflammation is needed to heal but is also responsible for tissue damage. Limiting excessive inflammation while keeping enough immune reaction at the site of infection appears to be the key for self-resolution of the disease.

I.4. Treatment and vaccines

Current treatment

Although CL is often self-resolving, medical treatment is required to accelerate the cure, reduce scarring and also prevent mucosal leishmaniasis by parasite dissemination. Chemotherapy using daily intravenous injection of pentavalent antimonial drugs during 20 to 30 days is the main current treatment (Torres-Guerrero et al., 2017). However, most of CL cases are poorly resolved mainly because of a lack of proper tools for diagnosis, expensive costs and complicated regimens. In addition, high toxicity and increased cases of co-infection by HIV (leading to immunosuppression) makes the overall treatment process poorly efficient (Gillespie et al., 2016; Reithinger et al., 2007). To circumvent these issues, current approaches aim to better control of the sandfly pool (vector) and implement an effective vaccine strategy. As CL is also an immunopathology, thinking of therapies targeting inflammation seems promising. However the immune response is so complex that it is difficult to predict the effect of a molecule blockade on both pathogen and pathology levels.

Vaccine design

Design of leishmaniasis vaccines is still a matter of intensive research (Gannavaram et al., 2016; Gillespie et al., 2016; Osman et al., 2017). Infection with live parasites in an unexposed site on the body (ancient practice called “leishmanization”) is a major vaccination process in the Middle East and Central Asia (Gillespie et al., 2016). Providing a strong immune protection towards *Leishmania* parasites to life, this practice remains to date the only vaccination process

showing efficacy in humans. However, safety concerns, lack of process standardization (dose, strain…) and potential risk of dissemination in immunocompromised patients make this procedure abandoned in most countries. Several attempts to generate leishmaniasis vaccines have been done (Gillespie et al., 2016; Kumar and Engwerda, 2014) including whole-killed (autoclaved) parasites adjuvanted with BCG, radio- and biochemically-attenuated parasites, lipid formulations of *Leishmania* antigens, recombinants proteins alone or combined with bacteria or recombinant virus and even DNA-based vaccines, but without providing enough protection levels and long-lasting immunity. Understand the determining factors allowing the immune response to cure CL may help us to better design efficient vaccines and treatments.

***

II. LIFE CYCLE OF *Leishmania* PARASITES

Leishmania parasites exist in two structural variants depending on their lifecycle stage, each one adapted to their host environment (**Figure 3**) (Kaye and Scott, 2011).

II.1. Promastigote stage

Promastigote refers to the structural stage typically found inside the sandfly midgut. At early stages, promastigotes are termed procyclic and are phenotypically short, ovoid, flagellated as well as slowly motile. Attached to the sandfly midgut epithelium, they are able to proliferate and differentiate into a highly infectious and non-diving form called metacyclic promastigotes (Sacks and Kamhawi, 2001). This differentiation process is associated with structural modifications including slimming of the cell body, elongation of the flagellum up to twice the body size and gain of high motility. Promastigotes are also highly enriched in glycoconjugates such as lipophosphoglycan (LPG) critical for promastigote adherence on midgut endothelium, limited degradation (Sacks and Kamhawi, 2001) and survival of the parasite within the host (Späth et al., 2003). Metacyclic promastigotes migrate during their differentiation towards the foregut and salivary glands were they can be transmitted to their host. Parasite transmission to host depends mostly on the ability of the parasite to become infectious in the sandfly, the quantity of parasites delivered by the sandfly bite and the host susceptibility. During blood feeding, infected sandflies can inoculate around a thousand parasites in the host skin.

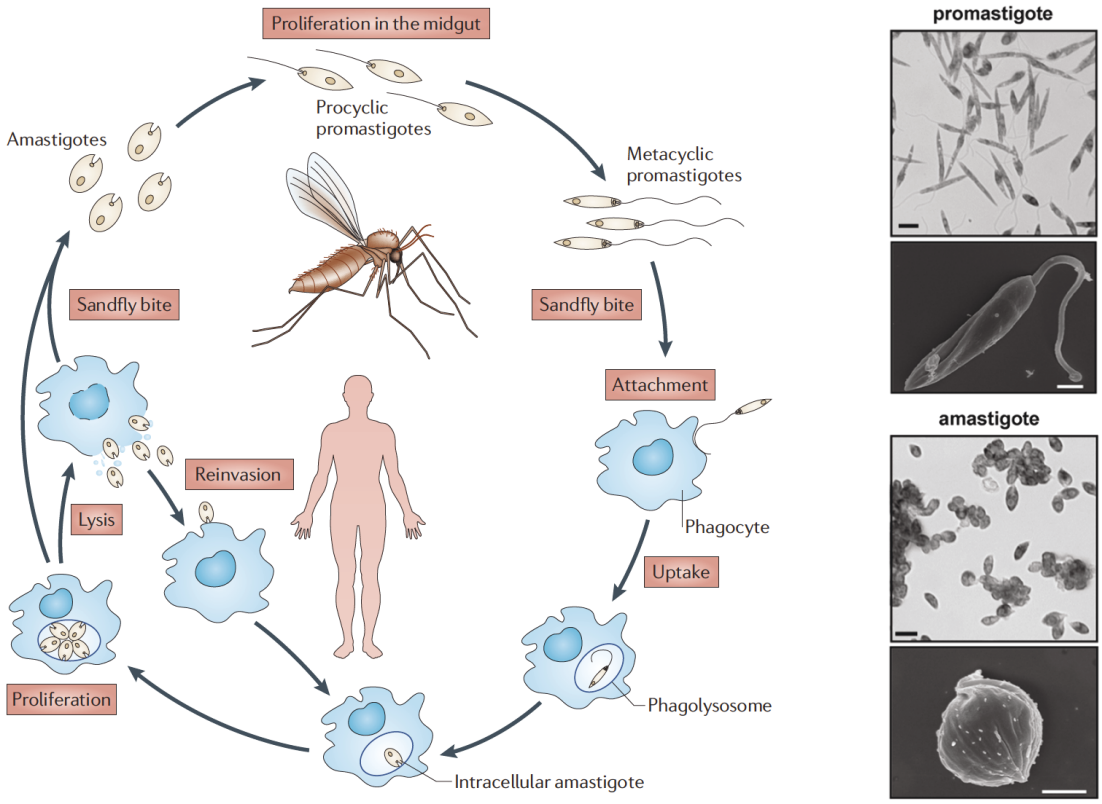

Figure 3. The life cycle of *Leishmania* parasites

Left. Procyclic promastigotes proliferate and differentiate in the sandfly midgut to give rise to infectious metacyclic promastigotes. During blood feeding, infectious promastigotes are injected into host skin and engulfed by phagocytes located at the site of injection. Into the phagolysosome, intracellular parasites resist to degradation while differentiating into their amastigote form. Amastigotes proliferate within host cells and reinfection of local phagocytes occurs when parasites are release in the environment. Transmission cycle is looped when infected phagocytes are taken up by sandflies upon blood meal and converted into their procyclic promastigote form. *Right.* Representative images of promastigotes (top) and amastigotes (bottom) stages acquired by optical or scanning electron microscopy (scale bar: 1 and 5 µm). Images from (Kaye and Scott, 2011; Yau et al., 2010).

II.2. Transition to amastigote stage

Inoculation of *Leishmania* parasites into the host skin is immediately followed by phagocytosis of promastigotes by resident mononuclear phagocytes (macrophages | dermal dendritic cells (dDCs)) but also neutrophils recruited at the site of infection (**Figure 4**) (Liu and Uzonna, 2012; Moradin and Descoteaux, 2012; Peters et al., 2008). In macrophages, the parasite triggers phagocytosis while inserting large quantities of LPG into phagosomal membranes. LPG is critical to delay phagolysosome acidification and inhibit activation of lysosomal proteases needed for antigen processing and immune response initiation (Moradin and Descoteaux, 2012;

von Stebut and Tenzer, 2018). This provides time for the parasite to switch from promastigote to amastigote. Phagosome maturation arrest and remodeling by parasite virulence factors leads to the generation of the parasitophorous vacuole (PV) that is filled with amastigotes. Transition to the amastigote stage is triggered in PVs by rising temperature and acidity (Barak et al., 2005), leading to the expression of specific genes sets (Inbar et al., 2017). Although promastigotes are phagocytosed by both neutrophils and mononuclear phagocytes, differentiation to amastigote appears to happen only in the mononuclear phagocyte population.

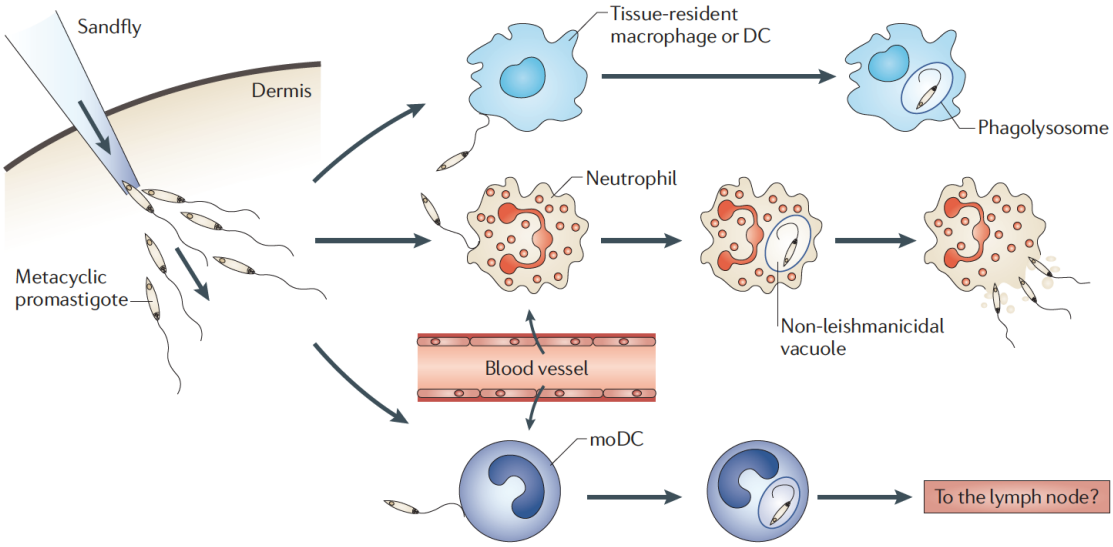

Figure 4. Uptake of *Leishmania* parasites by multiple cell types

Infectious promastigotes introduced into host skin are engulfed by tissue-resident mononuclear phagocytes (macrophages | dermal DCs) where they differentiate in amastigotes inside the PV. Neutrophils can also phagocyte many parasites but without leading to promastigote killing. Instead promastigotes are released after neutrophil death, probably introducing a population of parasites pre-conditioned for survival. Inflammatory monocyte-derived DCs recruited at later timepoints introduce a new niche for the parasite and may also be responsible for parasite dissemination to the draining lymph node. Image from (Kaye and Scott, 2011)

II.3. Amastigote stage

Amastigotes are characterized by a small rounded morphology and the near absence of flagellum (**Figure 3**). In addition to specific gene sets expression and regulation (Inbar et al., 2017), amastigotes also display changes in their core metabolism (McConville and Naderer, 2011; McConville et al., 2007). They enter a slow growth state along with a reduced metabolic

need to increase their fitness in the harsh PV environment. Amastigotes parasites differentiation and survival rely on several metabolic pathways including hexose and glucosamine catabolism but also fatty acid β-oxidation and amino acid degradation. All of this carbon processing is strictly dependent on a functional tricarboxylic acid (TCA) cycle as mitochondrial function was shown to be essential for amastigote viability (McConville and Naderer, 2011). Nutrients are often imported from the cytosol by many host and parasites transporters anchored in the PV membrane.

Summary

Cutaneous leishmaniasis is a disfiguring and life-threatening disease that represents a major world-wide public health problem. *Leishmania major* parasites represents one of the main infectious agents of leishmaniasis and live as promastigotes inside sandflies. They are transmitted to their hosts by injection into the skin where they are taken up by professional phagocytes and further differentiate into highly dividing amastigotes. The infection engages a self-resolving immune response that we will describe in the next chapter.

Chapter II The inflammatory reaction against *Leishmania major* parasites

Our knowledge about the inflammatory reaction against *Leishmania* parasites is a mosaic made from studies using different parasite species in various host models. We decided to took advantage of the self-resolving cutaneous infection with *Leishmania major* (*L. major*) in C57BL/6 mice that is the best reproducing disease outcome seen in humans (Loeuillet et al., 2016; Sacks and Noben-Trauth, 2002). In this model, the immune response can be subdivided in three main phases which are the silent, the effector and the latency phase.

I. SILENT PHASE

The silent phase corresponds to the first asymptomatic weeks of the infection with *Leishmania* parasites (Belkaid et al., 2000). Numerous cells and innate mechanisms are elicited to actively fight the infection. The development of intravital imaging technics was helpful understanding cell behavior at the site of infection during the earliest moments of the infection (**Figure 5**) (Chong et al., 2013; Ritter et al., 2009).

I.1. Initial recruitment of neutrophils

As a consequence of tissue damage induced by the sand fly bite, neutrophils are rapidly recruited to the site of infection and swarm towards the site of infection (**Figure 5**) (Peters et al., 2008). Their precise function during *L. major* infection still remains to be fully established as they can play both beneficial and detrimental roles. Following parasite injection into the skin, neutrophils appears to be beneficial as they release antimicrobial factors, participate to parasite engulfment and may produce neutrophils extracellular traps (NETs) (Ritter et al., 2009). They represent the main infected population during the first 24 hours post sand fly bite (Ribeiro-Gomes et al., 2012, 2014). Phagocytosed parasites are also exposed to deleterious enzymes, antimicrobial molecules and oxygen-derived products such as reactive oxygen species (ROS) or nitric oxide (NO). The detrimental role of neutrophils originates from the ability of *Leishmania* parasites to escape killing mechanisms and consequently survive inside neutrophils. In addition to provide a potential proliferative niche, dying neutrophils can modulate the activation and apoptotic cell clearance by mononuclear phagocytes while acting

as “Trojan horses” (Laskay et al., 2003, 2008; Scott and Novais, 2016). Yet this model needs to be further discussed as more recent intravital imaging data revealed a more complex mechanism, reported as “Trojan rabbit” (Peters et al., 2008; Ritter et al., 2009). Further studies with better tools to investigate neutrophil functions during leishmaniasis are needed to better understand the development of this disease but also better clarify the role of neutrophils during immune responses. Mouse genetic background, dose and delivery of the parasite but also appropriate antibodies for neutrophils depletions also need to be standardized in future studies.

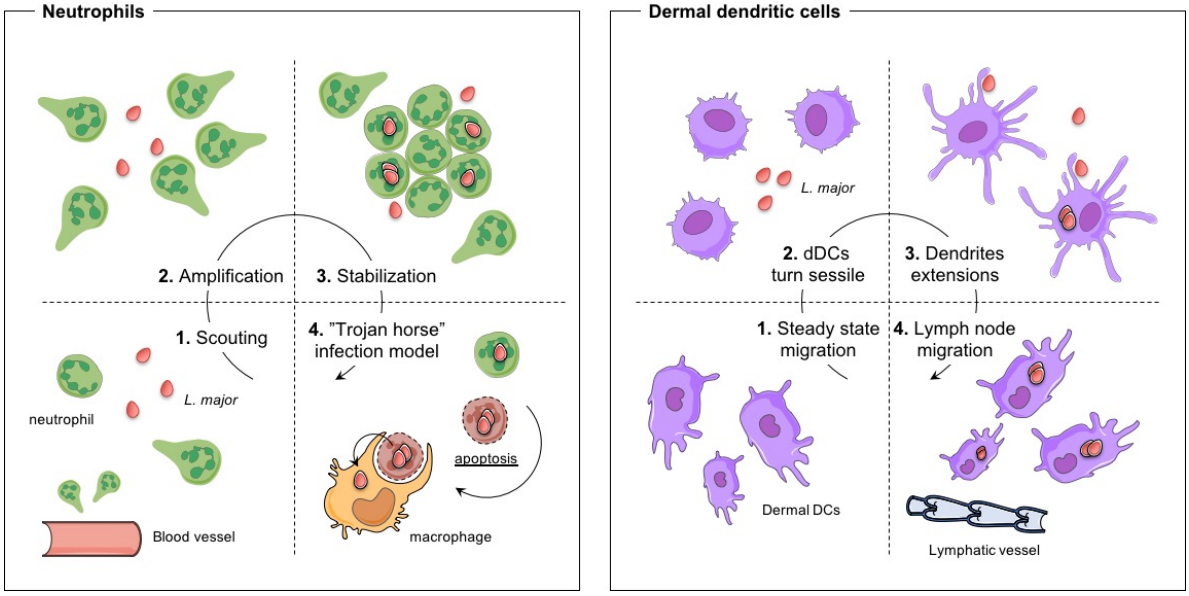

Figure 5. Neutrophils and dermal DCs behaviors during *L. major* infection

Left. Neutrophils are recruited from blood vessels upon tissue damage induced by the sand fly bite (scouting phase) and swarm towards the parasite pool (amplification phase). They cluster around the site of parasite injection (stabilization phase) while engulfing live parasites that resist to neutrophil defense mechanisms. After a few days at the site of infection, dying neutrophils carrying live parasites are phagocytosed by macrophages leading to their infection (“Trojan horse model”). *Right.* Dermal DCs patrolling the dermis layer at steady state turn sessile upon tissue damage induced by the parasite injection. They extend their dendrites and capture free living pathogens or apoptotic bodies potentially filled with parasites. Ultimately they recover motility to migrate in the draining lymph node by extravasating into lymphatic vessels and further elicit the T cell response. Picture adapted from (Chong et al., 2013).

I.2. Parasite uptake by mononuclear phagocytes at the site of infection

During leishmaniasis both resident and monocyte-derived phagocytes are involved in parasite uptake and immune control of the infection.

Resident DCs

Upon parasite deposition into the skin dermis, not principally Langerhans cells (LC) but rather resident dermal DCs were found to internalize *L. major* parasites at the site of infection (Malissen et al., 2014; Ng et al., 2008). Initially actively crawling, they turn sessile upon tissue damage induced by the sand fly bite and start elongate their dendrites to scan and engulf live parasites (**Figure 5**). After recovering motility and processing parasites antigens, they migrate to the draining lymph node by lymphatic vessels where they can initiate the T cell response (Chong et al., 2013). It is at this step important to highlight that only infected DCs and not infected macrophages are capable of a sufficient antigen processing and presentation eliciting an efficient T cell response against *L. major* parasites (**Figure 6**) (von Stebut and Tenzer, 2018). LC participation to parasite uptake needs to be better investigated as experimental injection with a needle often introduce parasites in the dermis and not in epidermis where LC reside.

Monocyte-derived DCs

Inflammatory monocytes are also recruited to the site of infection. They are attracted by neutrophil-derived CCL3 and platelet-induced CCL2 production to further differentiate into monocyte-derived DCs (Charmoy et al., 2010; Goncalves et al., 2011). A peak of recruitment occurs at 24 hours post infection. By engulfing live parasites either directly or indirectly in a "Trojan rabbit" manner, they rapidly become infected. In contrast to neutrophils, inflammatory monocytes are competent at killing *L. major* promastigotes by various intrinsic mechanisms (Scott and Novais, 2016). However, because these cells are permissive to parasite differentiation into their amastigote stage, some parasites resist and proliferate. That is how, in a few days, inflammatory monocytes represent the main infected population in the skin (Scott and Novais, 2016). How *L. major* parasites escape these intrinsic defense mechanisms by modulating monocyte-derived cell functions will be detailed later. Potentially of high importance, they may not fully explain the initial development of the pathogen burden during a primary infection. Indeed, a recent study by Romano *et al.* challenged the traditional idea that the initial pathogen burden is a direct consequence of a rapid infection of inflammatory monocytes that are next inhibited in their defense mechanism by the parasite. Instead, they propose that monocytes infected with neutrophil-originated parasites are impaired in their maturation process, leading to parasite proliferation without triggering of monocyte activation (Romano et al., 2017). This mechanism only exist for the primary infection, as they demonstrate

that during secondary infection the same inflammatory monocytes are quickly activated and able to eliminate the parasite.

I.3. Initiation of the T cell response

Initiation of an efficient T cell response against *L. major* needs parasite antigen presentation in the draining lymph node. This is performed by various DC subsets present in the infected skin that migrate to the draining lymph node (**Figure 6**).

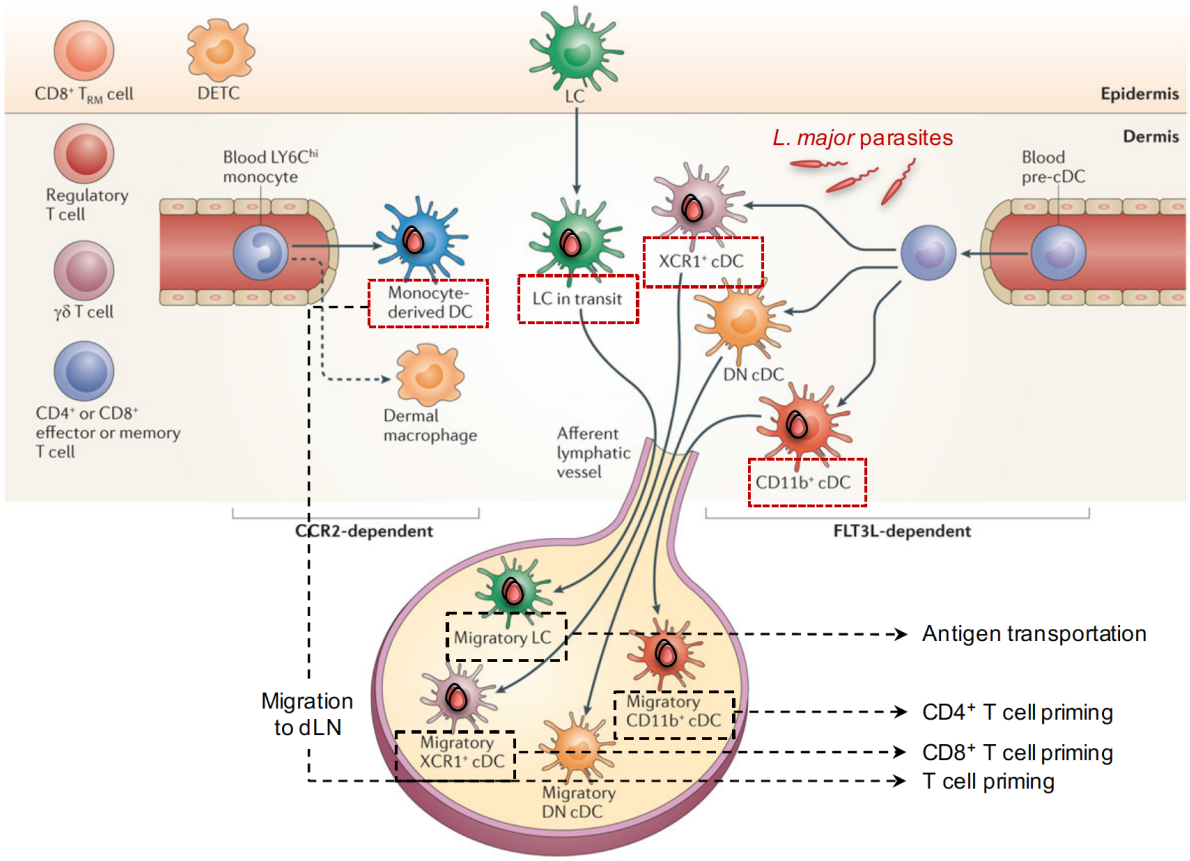

Figure 6. DC subsets involved in *L. major* antigen presentation

Parasites injected into the skin are phagocytosed by dermal DCs subsets and LC in transit. Following activation, DC but not macrophages migrate to the draining lymph node to elicit a T cell response. Each dermal DC subset have been shown to be involved in activation of specific T cell subsets while migratory LC are thought to only transport live parasites/parasite antigens into the draining LN. Picture adapted from (Malissen et al., 2014).

Antigen presentation by distinct DC subsets

LC were initially thought to be the main presenting cells in the draining lymph node during leishmaniasis but more recent studies have demonstrated that they are minimally involved in direct antigen presentation to the $CD4^+$ T cells (Ritter et al., 2004). However they still can be infected and migrate to the draining lymph node, raising the possibility that they participate indirectly to T cell priming by transporting live parasites or parasite antigens directly in the lymph node. The presentation of *L. major* antigens is primarily driven by dermal DCs where $CD4^+$ T cells are activated by migratory $CD8\alpha^-$ $Langerin^-$ DCs (Ritter et al., 2004) and $CD8^+$ T cells are activated by migratory $Langerin^+$ dermal DCs (Brewig et al., 2009) that carry parasite antigens and/or live parasites. Moreover, monocyte-derived DCs may also participate to T cell activation after parasite uptake and migration to the draining lymph node (León et al., 2007) . Additionally, more recent identification of new DC subsets in the skin (Kashem et al., 2017; Malissen et al., 2014) and new mechanisms for DC-mediated T cells activation in the lymph node (Eickhoff et al., 2015) raise the possibility that our knowledge of antigen presentation during leishmaniasis is still incomplete. Further investigations are required to increase the chance of design efficient vaccines.

$CD4^+$ T cell response initiation

Antigen presentation by DCs in the draining lymph node initiates the development of the T cell response against *L. major* parasites, essential to control the infection by mechanisms detailed later in the manuscript. The $CD4^+$ T cell response plays a critical role in determining the disease outcome: the dominance of a T_H2 response (IL-4-driven response in BALB/c background) is correlated to susceptibility and pathology development while the dominance of a T_H1 response (IFN-γ-driven response in C57BL/6 background) is correlated to resistance and self-resolution of the disease (Sacks and Noben-Trauth, 2002). However, more complex mechanisms are involved in susceptibility versus resistance than just T_H1 versus T_H2 balance (Alexander and Brombacher, 2012; Scott and Novais, 2016). In both susceptible and resistant background, activation of *L. major*-specific $CD4^+$ T cells is observed in the draining lymph node within the first days of infection (Malherbe et al., 2000). These T cells are IL-4 producers and initiate in the first days of the infection an early T_H2 response (Sacks and Noben-Trauth, 2002). This T_H2 response is maintained except if lymph node migratory DCs start to secrete IL-12. This *L. major*-driven IL-12 secretion, mainly by monocytes-derived DCs, is critical to acquire a T_H1

response and thus resistance to the parasite (León et al., 2007; Sacks and Noben-Trauth, 2002; Sypek et al., 1993) . IL-12 synthesis is triggered by IFN-γ produced in the lymph node by migratory NK cells and resident $CD8^+$ T cells (Scharton and Scott, 1993; Scott and Novais, 2016; Uzonna et al., 2004). T_H1-oriented T cells proliferate in the draining lymph node during this silent phase and reach the site of infection once they are fully activated and released in the circulation.

$CD8^+$ T cells contribution

The role of $CD8^+$ T cells during the silent phase of leishmaniasis is less clear. The most recent consensus is that $CD8^+$ T cells provide IFN-γ needed for IL-12 production by DCs, in addition to NK cells. This production appears to be relevant only when low doses of parasites are injected into the skin (Scott and Novais, 2016; Stäger and Rafati, 2012; Uzonna et al., 2004). Therefore, $CD8^+$ T cells seems to play a protective role in this context, which is not the case during the effector phase.

I.4. NK cells contribution to early parasite control

Natural killer (NK) cells are significant players during the silent phase of leishmaniasis but are not critical to ultimately control the infection. They are recruited to the site of infection and draining lymph node 24 hours after the initial neutrophil recruitment. They primarily act by secreting inflammatory cytokines such as IFN-γ and TNF-α rather than killing infected cells by their cytotoxic activity (Bogdan, 2012). Even if not required for ultimate infection resolution they nonetheless limit parasite growth and dissemination to visceral organs during the first days of infection and actively promote the development of a protective T cell response by their ability to produce IFN-γ (Scharton and Scott, 1993).

***

II. EFFECTOR PHASE

While the silent phase is asymptomatic, the effector phase starts when clinically symptoms are being detectable at the site of infection (Belkaid et al., 2000). Tissue damage is at that stage a consequence of neutrophils, eosinophils and mast cells recruitment induced by macrophage-

derived chemokines (Von Stebut, 2007). How this wave of immune cell infiltration is initiated and controlled is still unclear. One can imagine a positive-feedback loop control where the initial immune response during the silent phase triggers a very low inflammation that self-sustain and start being detectable only when a sufficient amount of cells have accumulated at the site of infection. In addition, stromal cells can participate to the initiation of monocyte infiltration as Goncalves *et al.* have shown that platelets can accumulate at the site of *L. major* inoculation and secrete platelet-derived growth factor (PDGF) that stimulate CCL2 production by local fibroblasts (Goncalves et al., 2011).

II.1. Host cells for *L. major* parasites

L. major parasites, first taken by neutrophils at the early beginning of the infection, are then phagocytosed by mononuclear phagocytes: macrophages and DCs. Which cells shelter the parasite during the effector phase is still to be clearly defined. If it is widely accepted that *L. major* reside inside mononuclear phagocytes, the true population definition is still matter of debate because of the constant remodeling of macrophage and DC subsets (Malissen et al., 2014; Mildner and Jung, 2014; Mildner et al., 2016). To date, the main infected cell population was identified as $CD11b^+$ $CD11c^+$ $Ly6C^+$ $MHC\text{-}II^+$ cells (Trez et al., 2009). Even if the authors highlight the similarity with a population named TNF-iNOS-producing DCs (Tip-DCs) (Serbina et al., 2003), the markers used for phenotyping are shared between other distinct populations such as inflammatory DCs (Segura and Amigorena, 2013) or myeloid-derived suppressor cells (MDSCs) (Veglia et al., 2018). In our hands, the main infected population is phenotypically identified as $CD11b^+$ $CD11c^+$ $Ly6G^-$ $Ly6C^+$ and $MHC\text{-}II^+$ in accordance to the aforementioned study, but most importantly they do express CD64 (FcγRI). Therefore macrophages, and not any DC population (Langlet et al., 2012; Malissen et al., 2014), form the main infected population. In addition to macrophages, neutrophils at the site of inflammation form the second sizable infected population.

II.2. T cell recruitment at the site of infection

$CD4^+$ T cell recruitment

$CD4^+$ T_H1 T cells are activated and released into circulation during the silent phase. During the effector phase, they are recruited at the site of infection by inflammation-induced chemokines

and adhesion receptors (Bromley et al., 2008; Griffith et al., 2014). Intravital imaging was useful understanding the behavior of these T cells *in vivo* at the site of infection. While $CD4^+$ T_H1 T cells infiltrate the inflamed tissue irrespectively of their antigen specificity, their distribution and trajectories depend on their ability to recognize *L. major* infected cells (Filipe-Santos et al., 2009). *L. major*-specific $CD4^+$ T cells were found to decelerate and accumulate near infected areas but without always engaging stable contacts with infected cells (Filipe-Santos et al., 2009; Müller et al., 2012) . One possible explanation can be that infected macrophages are deficient in presenting parasite-derived antigens either by a cell intrinsic or by a parasite-induced mechanism (Matheoud et al., 2013; Meier et al., 2003). As cytokines such as IFN-γ provided by T cells help macrophages to be activated and eliminate the parasite (Kima and Soong, 2013), this study raise the question of the mechanism allowing a self-resolution of the disease without engaging all the infected cells. Similar findings were shown in a model of hepatic granulomas elicited by BCG or *Mycobacterium tuberculosis* (Egen et al., 2011).

$CD8^+$ T cell recruitment

The role of $CD8^+$ T cells during the effector phase is less clear because of discrepancies between infectious models (species and doses of injected parasites). Concerning *L. major* parasites injected at low doses, it appears that the contribution of $CD8^+$ T cells during the effector phase is mainly deleterious to the host, in contrast to their requirement during the silent phase to drive an efficient T_H1 response. Indeed $CD8^+$ T cells were shown to be involved in the immunopathology development, probably by inducing tissue disruption by their cytotoxic activity (Belkaid et al., 2002a). Recently it has been shown that these cytotoxic $CD8^+$ T cells are unable to secrete IFN-γ because of a lack of sufficient local IL-12 concentration at the site of infection. This involvement in immunopathology also apply in humans where cytotoxic $CD8^+$ T cells were found in tissue lesions with a granzyme activity positively correlated to tissue damage intensity (Faria et al., 2009; Santos et al., 2013). It appears that the dual role of $CD8^+$ T cells depends on their primary function: IFN-γ $CD8^+$ T cells are protective while cytotoxic $CD8^+$ T cells are deleterious. In addition, it is important to keep in mind that studies about $CD8^+$ T cells cytotoxicity in mice can be misleading as murine $CD8^+$ T cells do not produce granulysin that is strictly required for intracellular pathogen killing (Dotiwala et al., 2016).

II.3. CD4$^+$ T_H1 T cell-derived IFN-γ activity

Several studies highlighted the importance of IFN-γ in the resolution of leishmaniasis and more generally during infection with intracellular pathogens (Kima and Soong, 2013; MacMicking, 2012; Sacks and Noben-Trauth, 2002). However its spatiotemporal activity into tissue is less trivial. Evidence that the control of the infection is correlated with only a few stably engaged infected cells were found in different contexts (Egen et al., 2011; Filipe-Santos et al., 2009). In the model of BGC infection, Egen *et al.* found that IFN-γ production and secretion were localized to the immunological synapse formed between the CD4$^+$ T cell and the infected antigen-presenting cell (Egen et al., 2011). In the model of *L. major* infection, Müller *et al.* demonstrated that the IFN-γ was able to diffuse to more than 80 µm from the immunological synapse, allowing iNOS activation and parasite control by bystander cells (**Figure 7**) (Müller et al., 2012). Hence, while IFN-γ secretion appears to be polarized inside the cell, this cannot fully predict a specific delivery to one target. IFN-γ may leak from the immunological synapse to mediate its effect on bystander cells. The relative importance of specific versus bystander activation remains to be investigated. However, bystander activation can explain how an infection can be controlled by engaging only a few infected cells. Furthermore, this mechanism allows for a fast response with a wave of IFN- γ signaling (one stable engagement is sufficient to activate numerous cells at once) that can activate infected cells with poor or deficient antigen-presenting capabilities.

II.4. Macrophage activation at the site of infection

During *L. major* infection, full macrophage activation is mainly triggered by CD4$^+$ T cells-derived cytokines such as IFN-γ and/or TNF-α (Mosser and Edwards, 2008; Mougneau et al., 2011; Olekhnovitch et al., 2014). Ultimately, macrophage activation leads to the expression of the inducible nitric oxide synthase (iNOS) that synthetize large proportion of nitric oxide (NO). The critical requirement of NO in controlling *Leishmania* parasites have been extensively demonstrated decades ago (Liew et al., 1990; Stenger et al., 1994, 1996; Wei et al., 1995) but we are still trying to understand how it acts *in vivo* at the site of infection. This will be discussed later in the next chapter. In addition to the triggering of intracellular defenses, macrophages are also professional cytokine and chemokine producers (**Table 2**) that allow them to actively participate in immune response regulation at the site of infection. The fact that they are both

the infected population and noticeable regulators raise the possibility that may constitute the principal population that sense the parasite load to accordingly adjust the immune reaction. In parallel to NO mode of action, details on macrophage activation will be discussed later.

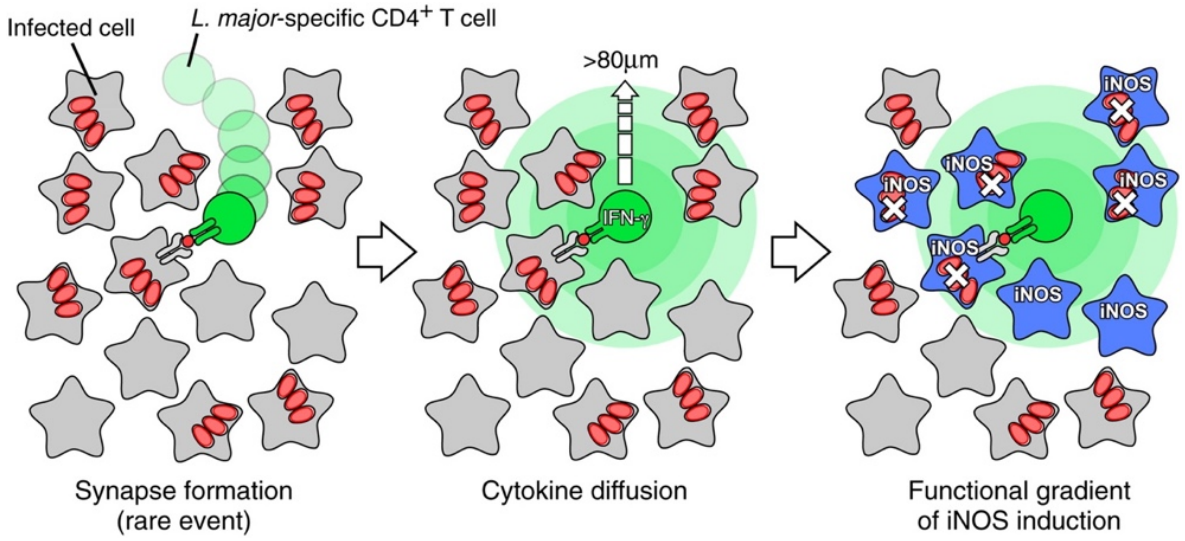

Figure 7. IFN-γ activates bystander cells by diffusion

L. major-specific $CD4^+$ T cells are recruited to the site of infection and patrol the tissue. When they stably engage an infected antigen-presenting cells, they start secreting IFN-γ that is not only targeted to the contacted cell but also diffuses at more than 80 µm away from the immunological synapse. This gradient of IFN-γ is able to activate bystander macrophages, leading to their activation and expression of iNOS. Therefore $CD4^+$ T cells can control the infection by engaging a minority of infected cells. Image from (Müller et al., 2012) .

II.5. Self-sustained recruitment of innate cells

The immune reaction against *L. major* parasites is T_H1-oriented, meaning that pro-inflammatory cytokines and chemokines are often released at the site of infection. This establish in resistant mice a transient chronic inflammation associated with immune cell infiltration from the blood, including neutrophils and inflammatory monocytes.

Neutrophils

The vast majority of studies looking at neutrophils during leishmaniasis focused on the silent phase and notably the impact of neutrophils in protection versus disease development. During

the effector phase, inflammatory chemokines produced by activated macrophages such as CXCL1 (KC) or CXCL8 (IL-8) (**Table 2**) are potent neutrophil chemoattractants and are correlated with the presence of neutrophils at the site of infection (Nylén and Eidsmo, 2012; von Stebut and Tenzer, 2018).

Table 2. Macrophage cytokines/chemokines main set

Table adapted from (Arango Duque and Descoteaux, 2014; Griffith et al., 2014).

	Name	Function
Cytokines	TNF-α	Initiation and regulation of inflammation (pro-inflammatory trio)
	IL-1α/β	
	IL-6	
	IL-12	Driving T_H1 T cell polarization | IFN-γ inducer
	IL-18	Activation of NK and T cells with IL-12 | IFN-γ inducer
	IL-23	Activation of T cells | T_H17 T cell maintenance | IFN-γ inducer
	IL-10	Suppression of macrophage, NK and T cells activation Downregulation of MHC-II expression
	TGF-β	Suppression of $T_H1/2$ polarization Suppression of macrophage | NK cells activation

	Name	also known as	Favors the recruitment of
Chemokines	CCL2	MCP-1	Inflammatory monocytes | T_M cells
	CCL3	MIP-1α	Granulocytes | Monocytes | T cells
	CCL5	RANTES	Granulocytes | Monocytes | NK | T cells
	CXCL1/2	KC/MIP-2α	Neutrophils
	CXCL8	IL-8	Neutrophils
	CXCL9	MIG	NK | T cells including T_M cells
	CXCL10	IP-10	NK | T cells including T_M cells

The interplay between macrophage activation and neutrophil recruitment during *L. major* infection have not been carefully investigated. Nonetheless, in a model of CL induced by *L. panamensis* infection in hamster, it has been shown that the effector phase harbor a second

wave of neutrophil that follows a wave of macrophage development (Peniche et al., 2017). Because neutrophils cannot kill intracellular parasites and often secrete pro-inflammatory cytokines it is likely that they are here deleterious to the host by providing a new niche for infection and inducing more tissue damage than driving inflammation resolution. However this needs to be better investigated as neutrophils can also participate to inflammation termination by various mechanisms including the expression of decoy receptors for cytokines (as CCR5 and truncated IL-1 receptors) or the induction of macrophage polarization towards a pro-resolving phenotype by anti-inflammatory molecule production (as Annexin A1 and IL-10) or by promoting efferocytosis (Jones et al., 2016; Soehnlein et al., 2017).

Monocyte-derived cells

Monocytes are also actively recruited from blood to the site of infection by macrophage-derived chemokines such as CCL2 (MCP-1) or CCL3 (MIP-1α) (**Table 2**) (Xiong and Pamer, 2015) but also with the help of stromal-derived CCL2 (Goncalves et al., 2011), neutrophil-derived cytokines and neutrophil-induced endothelial modifications (Shi and Pamer, 2011; Soehnlein et al., 2009, 2017). They originate from the bone marrow and gain access to the bloodstream after engaging the chemokine receptor CCR2 (Serbina and Pamer, 2006). Ly6C$^+$ monocytes form an heterogeneous population (Menezes et al., 2016) and can further differentiate into many types of iNOS$^+$ monocyte-derived cells (resembling Tip-DCs (Serbina et al., 2003) and inflammatory monocyte-derived DCs (moDCs) (Meredith et al., 2012; Zigmond et al., 2012)). Differentiation towards iNOS$^+$ macrophages during inflammatory processes requires a low expression of the transcription factor PU.1 (Menezes et al., 2016). The heterogeneity of monocyte-derived cells during the course of leishmaniasis have not been yet fully characterized. We know that inside the inflamed tissue, Ly6C$^+$ MHC-II$^-$ monocytes differentiate into Ly6C$^+$ MHC-II$^+$ and subsequently into Ly6C$^-$ MHC-II$^+$ cells (León et al., 2007; Olekhnovitch et al., 2014), that we identified as macrophages based on their expression of CD64 (FcγRI) (Langlet et al., 2012; Malissen et al., 2014). They express accordingly a high level of iNOS expression when activated at the site of infection (Olekhnovitch et al., 2014) and form the main infected population during *L. major* infection as aforementioned.

Contrary to neutrophils, it is likely that their presence is beneficial to the host as they represent the main source of nitric oxide, critical to parasite elimination (Liew et al., 1990; Sacks and Noben-Trauth, 2002; Scott and Novais, 2016). Of note, TNF-α at the site of infection restricts

arginase-1 activity to allow a maximal production of NO by iNOS, hence participating to pathogen control (Schleicher et al., 2016). In addition to parasite elimination, monocytes can promote inflammation resolution by numerous mechanism including the secretion of anti-inflammatory cytokines (as IL-37 and TGF-β) and decoy receptors (as truncated TNF and IL-1 receptors) (Netea et al., 2017). It is important to highlight here that the recruitment of immune cells with antimicrobial properties is essential to clear the infection but that it needs to be tightly regulated to provide efficient control while preventing immunopathology development (Murray and Wynn, 2011).

***

III. LATENCY PHASE

In self-resolving scenarios, the inflammatory reaction is controlled at the same time as the parasite load to restore homeostasis, as discussed in chapter IV. The latency phase begins when the inflammatory reaction is over, typically 3 months post infection in C57BL/6 mice (Belkaid et al., 2002b).

III.1. Development of persisting parasites

Persisting parasite genesis

Despite the self-resolution of the lesion and the strong immune response engaged against *Leishmania*, a small number of parasites (~1.000) remains in the skin to life following disease resolution. This persistence originates from the engagement of immune regulatory mechanisms that largely rely on IL-10 activity (Kaye and Scott, 2011). For instance, mice depleted of $CD4^+CD25^+$ regulatory T cells or blocked in their IL-10 signaling do not harbor persisting parasites (Belkaid et al., 2001, 2002b). However, the elimination of persisting parasites might not be the best option as the few remaining parasites confer long-lasting protection to host reinfection with several *Leishmania* species. Persisting parasites are contained by a continuous pressure coming from the immune system as inhibition of iNOS or transfer of $CD4^+CD25^+$ regulatory T cells population into clinically cured mice leads to the reactivation of the disease (Mendez et al., 2004; Stenger et al., 1996).

Host cell for persisting parasites

The main host cells in skin and lymph node for persisting parasites is still a matter of debate. In the skin, the original idea that *L. major* parasites where hiding in safe immunoprivileged environment such as fibroblasts (Bogdan, 2008) is tarnished by various studies indicating that mononuclear phagocytes must be the principal host cells for persistence (von Stebut and Tenzer, 2018). More surprisingly, a recent study by Mandell *et al.* described two populations of *L. major* persisting parasites showing different replication rates but both predominantly residing in $iNOS^+$ mononuclear phagocytes without altered morphology or genome integrity (Mandell and Beverley, 2017). This unusual finding could apply to other persisting pathogens and may be used to better understand persistence phenomenon.

III.2. Immune memory response

Resolution of a primary infection with *L. major* parasites confers a long-lasting immunity to reinfection. Persisting parasites maintain a population of effector *L. major*-specific circulating T cells that can be recruited and promote parasite killing upon secondary challenge. This population was characterized as short-lived effector cells rather than long-lived effector memory T cells (T_{EM} cells) (Peters et al., 2014; Scott and Novais, 2016). In addition to these effector cells, *L. major* infection generates a population of long-lived central memory T cells (T_{CM} cells) that can be reactivated upon secondary challenge and protects mice with delayed kinetic compared to effector T cells (Gollob et al., 2005; Zaph et al., 2004). More recently, a population of $CD4^+$ tissue-resident memory T cells (T_{RM} cells) was identified in challenged mice not only at the site of initial infection but also at distant sites. These T_{RM} cells do not need persisting parasites to survive and can be reactivated upon secondary challenge to provide an efficient control of the parasite load (Glennie et al., 2015). The protection occurs by the rapid initiation of inflammatory monocyte recruitment which limits parasite proliferation with the help of oxygen- and nitrogen-derived reactive species (ROS and NO) (Glennie et al., 2017). Interestingly, circulating memory T cells are not required to control secondary infection with a low dose of parasite. This suggests that vaccine strategies aimed at generating T_{RM} are promising in this context and should therefore be developed.

Summary

The immune response against *L. major* parasites is divided into three phases: silent, effector and latency phases. During the silent phase, parasites are taken up by professional phagocytes, survive and proliferate while DCs migrate to the lymph node to initiate a T_H1-oriented $CD4^+$ T cell response. $CD8^+$ T cells and NK cells help such activation by providing IFN-γ. During the effector phase, myeloid cells (including monocytes) and activated T_H1 $CD4^+$ T cells are recruited to the site of infection. With the help of $CD4^+$ T cells-derived IFN-γ, cells derived from the monocytes get fully activated and start express high levels of iNOS and secrete pro-inflammatory cytokines. They also represent the main infected population. iNOS activity is important to repress parasite metabolism *in vivo* and to confer resistance to the disease. Ultimately the infection is controlled, leading to the latency phase where a small number of parasites remains to life in the skin and confers long-lasting immunity to reinfection. The next introductive chapter will highlight various aspect of monocyte-derived cell activation and metabolism as they represent the main active population in the infected skin during the effector phase.

Chapter III Highlights on macrophage activity and metabolism

As mentioned earlier, it appears that macrophages are both the major infected population during the infection with *L. major* but also the main population driving disease resolution by the production of large quantities of NO. Additionally, macrophage polarization from pro-inflammatory status to a pro-resolving one is a required step for inflammation resolution (Murray, 2017). Therefore characterizing precisely their behavior during inflammation is required to understand how the inflammatory reaction at the site of *L. major* infection can be controlled and to provide strong basis for new treatments and vaccine development.

I. MACROPHAGE ACTIVATION

In response to environmental cues macrophages can adopt distinct phenotypes and functions. These changes are referred in the literature as activation or polarization, without clearer definition (Murray, 2017). The last decade was marked by a strong will to classify macrophages into distinct subsets to explain inflammation versus resolution/pathology development versus wound healing. This led to the M1 (classically activated) versus M2 (alternatively activated) macrophages classification, that mimic T_H cells nomenclature (Martinez and Gordon, 2014; Murray, 2017; Murray et al., 2014). M1 macrophages confers protection against pathogens during infections with bacterial and numerous intracellular pathogens while M2 participate in defense against parasitic infections and help to tissue repair. Nowadays this artificial dichotomy certainly needs revision as many studies *in vivo* revealed a more complex spectrum of activation, M1 and M2 representing to extreme phenotypes. Classify macrophages based on their function as inflammatory, wound-healing and regulatory macrophages may be a transitory solution while knowledge is gathered (Mosser and Edwards, 2008; Murray and Wynn, 2011).

I.1. Stimuli for macrophage activation

Macrophage stimulation and subsets

Macrophage activation occurs in response to environmental cues detected by a wide range of extracellular and intracellular receptors. Three main groups can be defined based on the main

signaling pathway they engage between NF-κB & AP-1 pathways, STAT pathways or nuclear receptor pathways (**Table 3**). The classification M1 versus M2 was dictated by the nature of the stimuli received by macrophages *in vitro*. M1 macrophages were defined as classically activated, meaning stimulated by LPS + IFN-γ while M2 macrophages were defined as alternatively activated, meaning stimulated by IL-4. The situation *in vivo* is more complex: while M1 can be roughly associated to inflammatory macrophages (IFN-γ + TNF-α stimulated), M2 cannot be associated to anti-inflammatory macrophages as this population encompass both wound-healing macrophages (IL-4 + IL-13 stimulated) and regulatory macrophages (IL-10 stimulated) arising from the same precursor but stimulated with different ligands (Mosser and Edwards, 2008; Murray et al., 2014).

Table 3. Stimuli and receptors triggering macrophage activation

Table adapted from (Glass and Natoli, 2016).

Pathway	Family of receptors	Example of ligand (receptor) couple
NF-κ B & AP-1	Toll-like receptors	dsRNA (TLR3) | LPS (TLR4) | CpG (TLR9)
	TNF receptors superfamily	TNF-α (TNFR1) | CD40L (CD40)
	IL-1 receptors	IL-1α/β (IL-1RI)
STAT	IFN receptors	IFN-α/β (IFNAR1) | IFN-γ (IFNGR1)
	Cytokines receptors	IL-4 (IL-4R) | IL-10 (IL-10R)
Nuclear receptors	Glucocorticoid receptor (GR)	Glucocorticoids (GR)
	Liver X receptors	Oxysterols (LXR)
	Peroxisome proliferator-activated receptors (PPARs)	Free fatty acids and eicosanoids (PPARγ)

Macrophage activation leads to upregulation of specific markers and functional gains depending on the stimuli (Martinez and Gordon, 2014; Mosser and Edwards, 2008; Murray et al., 2014). M1 macrophages are characterized by an upregulation of CD86, MHC-II, iNOS and the ability to produce inflammatory cytokines such as IL-1β, IL-6, IL-12 or TNF-α as well as reactive oxygen and nitrogen species. M2 macrophages on contrary are characterized by an

upregulation of CD206 (mannose receptor), arginase-1 and the ability to produce anti-inflammatory cytokines such as IL-10 and TGF-β.

Macrophages stimulation during *L. major* infection

During *L. major* infection, macrophages at the site of infection are strongly inflammatory and match the M1 phenotype described *in vitro*. They are polarized by numerous signal but mainly by $CD4^+$ T_H1 T cells-derived IFN-γ and TNF-α secreted in large quantities at the inflammatory site (Kima and Soong, 2013; Sacks and Noben-Trauth, 2002). In addition to drive M1 polarization, TNF-α is also suppressing M2 polarization by inhibiting IL-13 secretion by other cell types (Murray, 2017). These inflammatory macrophages *in vivo* are consequently expressing iNOS and a range of various cytokines (**Table 2**).

I.2. iNOS induction

iNOS is a cytoplasmic enzyme which expression is only induced during inflammation in contrast to its two other isoforms (nNOS and eNOS) that are constitutively expressed but regulated by calcium levels *via* calmodulin (Aktan, 2004; Pautz et al., 2010). After induction, this enzyme catalyzes the production of NO using arginine in the presence of oxygen by the reaction is detailed below. Its activity outperforms those of the nNOS and eNOS isoforms (by a 10-folder higher v_{max}), making iNOS the principal source of NO during inflammation processes (Lowenstein and Padalko, 2004).

NO synthesis chemical reaction. Adapted from (Daff, 2010)

1. L-arginine + O_2 + $NADPH,H^+$ ⇌ N^{ω}-hydroxy-L-arginine + $NADP^+$ + H_2O
2. N^{ω}-hydroxy-L-arginine + O_2 + 1/2 $NADPH,H^+$ ⇌ L-citrulline + NO + 1/2 $NADP^+$ + H_2O

L-arginine + 2 O_2 + 3/2 $NADPH,H^+$ ⇌ **L-citrulline + NO** + 3/2 $NADP^+$ + 2 H_2O

Modulation of iNOS expression from the transcriptional to the post-translational levels is the principal regulatory mechanism for NO synthesis. Details for these regulations are reported in **Table 4**. In addition, iNOS activity can be tuned by its substrates and cofactors availability. For

instance, decreased arginine transporter activity and increased arginase activity are two ways of regulating iNOS activity (Aktan, 2004; Pautz et al., 2010). Finally, it is important to highlight that the microenvironment may strongly impact iNOS activity by mechanisms still to be clarified. As an example, hypoxia and increased Na^+ concentrations at the site of *L. major* infection have been identified as important iNOS regulators. Although HIF-1α increases iNOS transcription (see **Table 4**) and a high Na^+ concentration favors iNOS expression and disease resolution (Jantsch et al., 2015), low oxygen availability strongly impairs iNOS-derived NO synthesis resulting in the parasite persistence (Mahnke et al., 2014; Schatz et al., 2018).

Table 4. iNOS expression regulation

Table adapted from (Aktan, 2004; Bogdan, 2015; Kone et al., 2003; Olekhnovitch and Bousso, 2015; Pautz et al., 2010).

UPREGULATION	DOWNREGULATION
At the transcriptional level by	
• ↑ NF-κB pathway (LPS|TNF-α) • ↑ JAK/STAT pathway (IFN-γ) • ↑ IRF-1 pathway (IFN-γ) • ↑ C/EBP pathway (cAMP) • ↑ HIF-1α pathway (hypoxia) • Potent synergy between NK-κB & STAT	• ↑ IκB degradation • ↑ cGMP pathway (NO) • ↑ Glucocorticoid pathway (GC) • ↑ PPARγ pathway
At the post-transcriptional level by	
• PKCα (mRNA stabilization) • cAMP(mRNA stabilization)	• ↑ cGMP pathway (NO) • ↑ Glucocorticoid pathway • TGF-β (mRNA destabilization) • Intracellular Ca^{2+} (mRNA destabilization) • miR-939 & 26a (human) or 146a (mouse) • Natural non-coding antisense transcripts
At the translational level	
Indirect evidence of translational control of iNOS mRNA	
At the post-translational level by	
• Rac-GTPases & Hsp90 (favoring dimerization)	• TGF-β & caveolin-1 (*via* proteasome) • Kalirin & NA 110 (impairing dimerization)

I.3. Cytokine production

An essential feature of activated macrophages is their ability to secrete numerous cytokines and chemokines as aforementioned (**Table 2**) (Arango Duque and Descoteaux, 2014; Griffith et al., 2014; Mosser and Edwards, 2008). They are both essential to fully activate macrophages and participate in the control of the immune response. Cytokines/chemokines are often classified in two categories: pro-inflammatory cytokines and anti-inflammatory cytokines. Upon classical activation, inflammatory macrophage can secrete numerous pro-inflammatory (type 1) cytokines including TNF-α, IL-1α/β, IL-6, IL-12, IL-18 and IL-23. They favor the inflammatory reaction by triggering numerous phenomena including vasodilatation, vascular hyperpermeability, leukocyte recruitment/extravasation, phagocytosis and the secretion of pro-inflammatory molecules as eicosanoids. By contrast, wound-healing or regulatory macrophages (Mosser and Edwards, 2008) rather secrete high quantities of anti-inflammatory cytokines as IL-10 or TGF-β to repress immune cell activity. Whether such macrophages can also secrete type 2 cytokines and how this can participate to their function is possible but yet not fully characterized (La Flamme et al., 2012).

***

II. NITRIC OXIDE FATE AND ACTIVITY

II.1. Nitric oxide fate and targets in resting cells

NO fate and biological impact depend on intrinsic factors such as its concentration, half-life and diffusion rate but also extrinsic factors such as oxygen tension, presence/absence of free radicals and other bio-reactants concentrations (Bogdan, 2015; Fang, 2004; Kelm, 1999; Olekhnovitch and Bousso, 2015). As a free radical, NO (simplified writing for $NO^{\bullet}$) is highly reactive and can undergo many chemical modifications before acting on biological structures (**Figure 8**). Most of the RNS are generated under reducing conditions when NO gains electrons to transform into nitrite NO_2^- and nitrate NO_3^-. The radical intermediate nitrogen dioxide $NO_2^{\bullet}$ can also generate dinitrogen trioxide N_2O_3 and tetroxide molecules N_2O_4 by reacting with NO or himself. In the present of other radicals, and notably the superoxide anion $O2^{\bullet-}$, NO rapidly gives rise to peroxynitrite $ONOO^-$. In biological settings, peroxynitrite protonates to form peroxynitrous acid (ONOOH) that is a potent oxidative and nitrating agent. Peroxynitrous acid

can damage numerous cellular molecules such as proteins, DNA or lipids and have been involved in many biological diseases including cardiovascular, inflammatory and neurodegenerative diseases (Pacher et al., 2007; Szabó et al., 2007). In addition to target biological molecules through its byproducts, NO can directly targets proteins in the absence of free radicals either by S-nitrosylation or by forming metal nitrosyl complexes. S-nitrosylation correspond to the reversible nitration of protein on sulfur-bearing amino acids (such as cysteine) to mediate post-translation control of protein activity (Hess et al., 2005). Metal nitrosyl complexes are stable edifices formed by nitric oxide bonded to a transition metal (such as iron). This mechanism allows NO to regulate biological processes by modifying protein activity but also by triggering intracellular signaling pathways. As respective examples, NO at high concentration can bound to iron-sulfur (Fe-S) centers to inhibit mitochondrial respiratory chain complexes (Brown, 1999) but also can bound to iron centers in soluble guanylate cyclases (sGC, a major intracellular receptor to NO) to trigger cGMP formation and consequent signaling pathway (Derbyshire and Marletta, 2012).

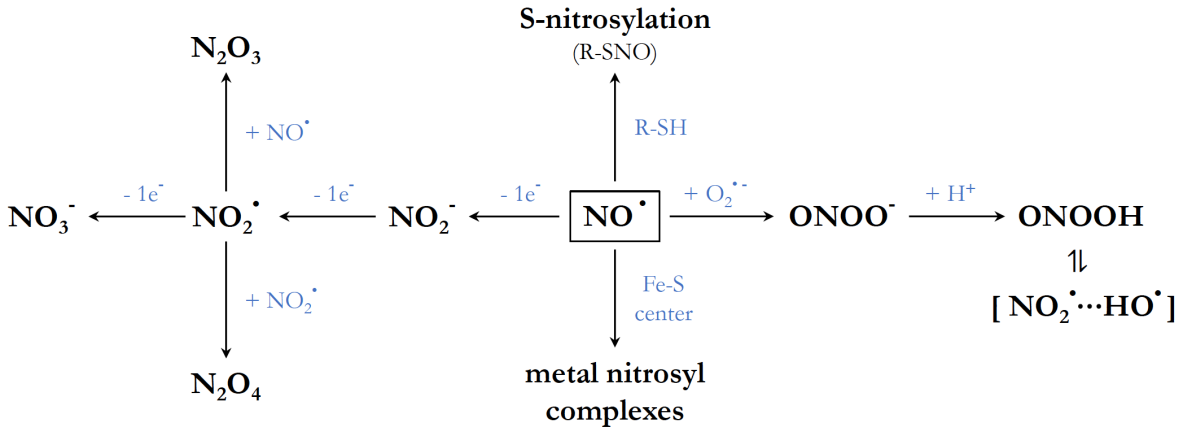

Figure 8. Major RNS and NO-derived products

Nitric oxide (NO) reacts with numerous molecules depending on its microenvironment. In an reducing environment NO mainly gives rise to nitrite (NO_2^-) and nitrate (NO_3^-). The reactive intermediate nitrogen dioxide (NO_2) can generate dinitrogen trioxide (N_2O_3) and dinitrogen tetroxide (N_2O_4) by reacting with itself or NO. In an environment rich in reactive oxygen species, peroxynitrite ($ONOO^-$) and peroxynitrous acid (ONOOH) are formed. In the absence of free radicals, NO reacts with Fe-S centers to generate metal nitrosyl complexes and with proteins by S-nitrosylation, two ways by which NO affects biological processes. Adapted from (Fang, 2004).

II.2. Nitric oxide propagation by diffusion

A key aspect of NO biology is its ability to efficiently diffuse from its production site even across biological membranes (Pacher et al., 2007). This property originates from its very low molecular size, its charge neutrality and its hydrophobicity. NO byproducts such as peroxynitrite and peroxynitrous acid have in contrary restricted diffusion capability that do not allow them to act at distance and limit their activity at their site of production. To verify whether NO is physically capable of acting on distant cells it is important to check if its half-life and diffusion rate are compatible with a long distance travel and in addition consider the concentration of oxygen as NO conversion to peroxynitrite inhibits its diffusion (Thomas, 2015). It has been shown that NO presents a very high diffusibility (~ 3300 $\mu m^2.s^{-1}$) (Lancaster, 1997) and an important half-life under hypoxia at physiological concentrations (~ 1 s) (Thomas, 2015; Thomas et al., 2001). Simple modeling of diffusion based on the Einstein-Smoluchowski equation (detailed below) show that NO is able to travel ~ 80 µm during its half-life time, which is compatible with a biological activity on distant cells.

Einstein-Smoluchowski approximation
From (Daintith, 2008)

$$\mathcal{D} \approx \frac{x^2}{2t}$$

$\mathcal{D}$	Coefficient of diffusion
x	Distance of diffusion
t	Time of diffusion

While such modeling is useful, we still critically lack proper tools to measure NO concentration and activity *in vivo*. The development of specific and sensitive sensors compatible with intravital imaging will be of a great help to better understand NO propagation in tissues and therefore to map its spatiotemporal activity during inflammatory reactions.

II.3. NO activity at the site of infection

Parasite susceptibility to NO

The toxicity of NO on *L. major* parasites was mainly assessed *in vitro* using axenic promastigotes and amastigotes cultivated with NO releasing compounds. NO exposure leads to

a dramatic loss of parasite viability and triggers apoptosis-like phenomena including cell shrinkage and DNA fragmentation (Holzmuller et al., 2006; Mauël and Ransijn, 1997). Interestingly, peroxynitrite was found inefficient to restrict *L. major* growth *in vitro*, even at high doses (Assreuy et al., 1994). This suggests that NO may act by it signaling properties rather than just causing irreversible molecular damages. Mechanistically, NO exerts its toxicity partly by disrupting parasite metabolism *in vitro*. Characteristics of this breakdown include an inhibition of key enzymes such as the glyceraldehyde-3-phosphtae dehydrogenase (GAPDH) and aconitase, a decreased in the parasite NAD^+ pool, but also an inhibition of parasite nutrient transport affecting for instance glucose, proline and adenine entry (Holzmuller et al., 2006; Lemesre et al., 1997; Mauël and Ransijn, 1997). In addition, iNOS activity can prevent parasite growth by the formation of N^{ω}-hydroxy-L-arginine (intermediate product during NO synthesis) that inhibits both host and parasite arginase (Iniesta et al., 2001). Arginase activity in parasite, by generating L-ornithine, is essential to polyamine synthesis required for parasite growth. The situation *in vivo* is less clear as Müller *et al.* revealed that NO inhibits *L. major* metabolism and growth without necessarily exerting direct killing at the site of infection (Müller et al., 2013).

Of note, the activity of iNOS at the site of infection by intracellular pathogens is complexified by the existence of indirect effects (Bogdan, 2015). For instance, in a model of infection by *Mycobacterium tuberculosis*, NO was found to elicit host cell apoptosis, restricting in turn the growth of the intracellular bacteria (Herbst et al., 2011). In a model of infection by *Pseudomonas aeruginosa*, NO was found to favor autophagosomal destruction of bacteria *via* the synthesis of 8-nitro-cGMP (Ito et al., 2013). Many others mechanisms exist including NO-mediated deprivation of iron, stimulation of phagosomal maturation and dispersion of bacterial biofilms (Bogdan, 2015).

Activity on the inflammatory reaction

During leishmaniasis, NO is essential to the self-resolution of the disease as iNOS KO mice have a higher parasite load and develop important tissue damage. However, there is no correlation between the parasite burden and the severity of the immunopathology (Nylén and Eidsmo, 2012) and it is rather the intensity of inflammation that represent the determining factor. This raises the possibility that NO also acts directly on the immune system to regulate the inflammatory reaction at the site of *L. major* infection. Also, the molecular mode of action of NO is compatible with such hypothesis as S-nitrosylation, Fe-S center chelation and RNS

formation can occur in immune cells as well. We will point out the different mechanisms by which NO can act on the immune system later in the chapter IV.

***

III. MACROPHAGE METABOLISM DURING INFLAMMATION

Cellular metabolism can be defined as all the chemical reactions that both provide energy to the cells by breaking down organic molecules (catabolism) and convert molecules to build up blocks for macromolecule synthesis (anabolism). It is a dynamic process that adapts constantly to meet the bioenergetic demand of the cells based on cell-intrinsic and environmental signals (Ganeshan and Chawla, 2014). During inflammation, the activation of immune cells can have a profound impact on the cellular bioenergetic demand and therefore on the metabolic pathways in use. We will discuss here the changes that can occur during macrophage activation and in the next chapter how metabolism is central to macrophage activity control. We will focus on the catabolic pathways as they undergo major changes during M1 macrophage activation.

III.1. Brief overview of the major catabolic pathways

Cellular activity is supported by the energy extracted from complex organic macromolecules such as glucose or fatty acids that are coming from our diet. The breaking down of those molecules is called catabolism and operates by six major pathways: the glycolysis, the citric acid cycle, the oxidative phosphorylation, the pentose phosphate pathway, the fatty acid oxidation and the catabolism of amino acids (Berg et al., 2002; O'Neill et al., 2016; Voet and Voet, 2010). In a nutshell, all together these pathway use sugars (e.g. glucose), proteins (e.g. amino acids) and fats (e.g. fatty acids) as substrate to produce energy stored as ATP (in a chemical bound) or NADH/$FADH_2$ (as electrons). They are interconnected by key metabolic intermediates as pyruvate or acetyl coenzyme A (acetyl-CoA) and therefore not independent. A brief overview is presented in **Figure 9**.

Glycolysis

Glycolysis converts glucose into pyruvate in the cytosol and provides ATP and NADH energetic molecules. Pyruvate is then either degraded into lactate by the process of fermentation

or transformed in acetyl-CoA to fuel the TCA cycle. Glycolysis is relatively inefficient to produce ATP molecules but provides key biosynthetic intermediates for many anabolic reactions (as glucose-6-phosphate for the PPP or 3-phosphoglycerate for amino acid synthesis) as well as NADH molecules. As a hub for anabolic pathways, glycolysis is often favored in rapidly proliferating cells. Glycolysis do not requires oxygen to operate and therefore can be fully functional in hypoxic environments.

TCA cycle

The TCA cycle main role is to break down acetyl-CoA into CO_2 (waste) and provide ATP as well as many NADH/$FADH_2$ energetic molecules. It takes place in the mitochondrial matrix and represents a central hub in cellular metabolism as it serves as an entry/exit point for many secondary nutrients. TCA cycle coupled to OXPHOS is highly efficient to provide ATP and is used by a vast majority of quiescent cells to produce energy.

Oxidative phosphorylation (OXPHOS)

OXPHOS function is to convert all the energy from NADH/$FADH_2$ into ATP in two steps: first NADH/$FADH_2$ molecules give their electrons to the electron transport chain (ETC) located inside the inner mitochondrial membrane to generate a H^+ gradient (oxidative step) and then this gradient is consumed by the ATP synthase to generate ATP (phosphorylation step). The electrons circulating in the inner mitochondrial membrane are ultimately taken up by oxygen molecules to give water. Thus, TCA and OXPHOS are considered as aerobic pathways.

Fatty acid oxidation (FAO)

Fatty acid oxidation takes place principally in the mitochondrial matrix after the import of "activated" fatty acids from the cytosol. They are degraded by a series of oxidations that generates many acetyl-CoA and NADH/$FADH_2$ molecules that are further used as a substrate inside the TCA cycle and OXPHOS to generate energy. ATP synthesis by this pathway gives massive yields and therefore FAO is used by a majority of quiescent cells. FAO is an aerobic pathway: it requires the presence of oxygen to be fully functional.

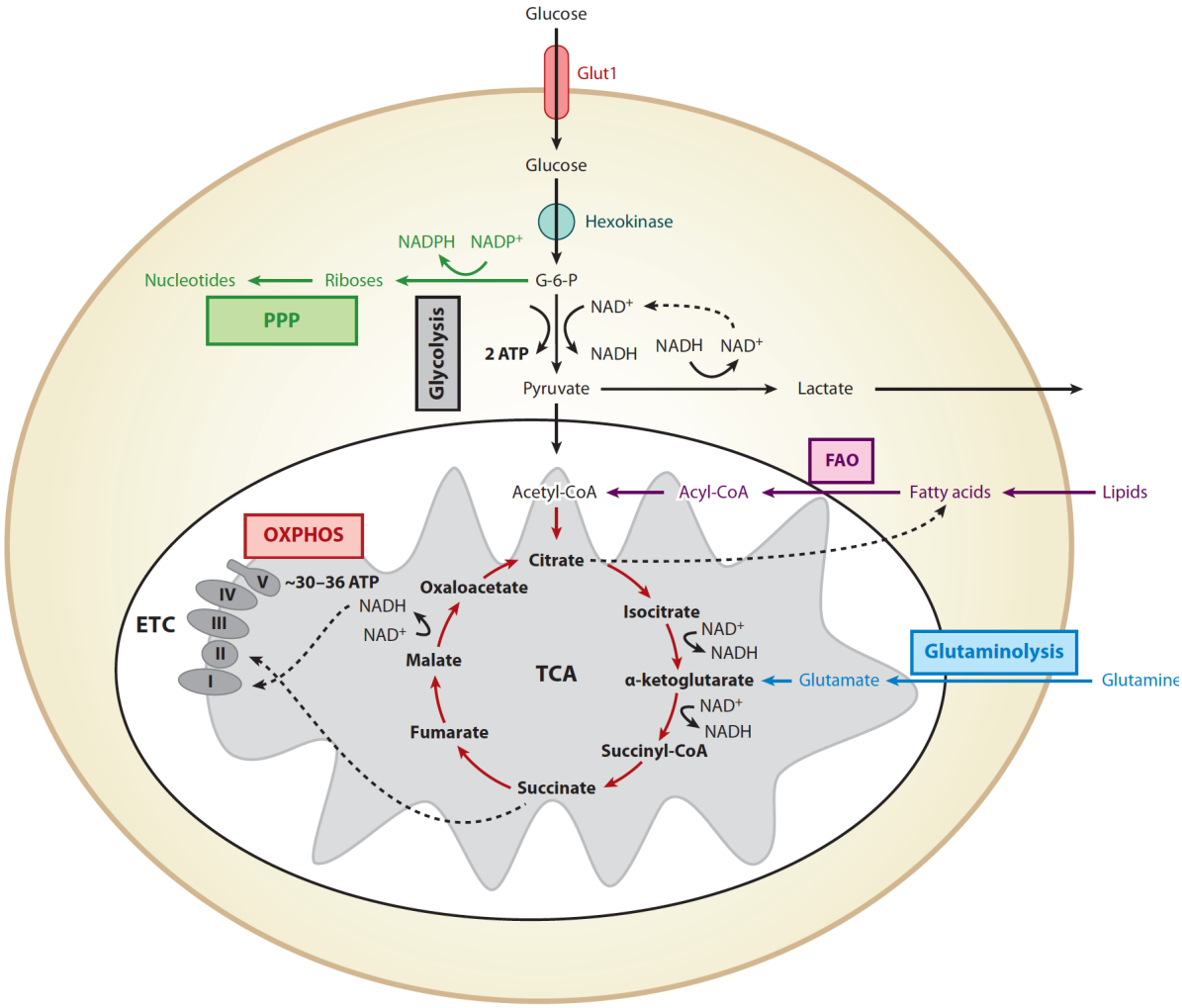

Figure 9. The major catabolic pathways are interconnected

Extracellular glucose is imported and degraded into pyruvate by the glycolysis. Pyruvate is either degraded into lactate by fermentation or directed to the TCA cycle. The TCA cycle generates many NADH and $FADH_2$ molecules that are converted into ATP by oxidative phosphorylation (OXPHOS) using the electron transport chain (ETC) as a support. TCA cycle is also fueled by fatty acid oxidation (FAO) that generates many acetyl-CoA as well as NADH and $FADH_2$ molecules in resting cells. The pentose phosphate pathway (PPP) and amino acids pathways (as glutaminolysis) are mainly anabolic pathways but participate also in catabolism by respectively generating NADPH molecules and fueling the TCA cycle (with the help of the urea cycle for toxic waste elimination). Image from (Ganeshan and Chawla, 2014).

Pentose phosphate pathway (PPP)

The cytosolic PPP branches off from glycolysis with the first intermediate glucose-6-phosphate and is one of the rare pathways generating NADPH molecules and precursors for nucleotide and amino acids generation (ribose-5-phosphate and erythrose-4-phosphate respectively). Therefore, this pathway is engaged to meet the need in cell growth and participate as a hub for various secondary anabolic reactions. It does require the use of oxygen as for glycolysis.

Amino acids catabolism

Amino acids pathways are numerous because of the diversity of amino acid substrates. They are often part of anabolic processes as amino acids are building blocks for protein synthesis and *de novo* branched chain fatty acids synthesis. During catabolism, amino acids can enter the TCA cycle *via* various entry points depending on their molecular structure. Their entry is dependent on their conversion by a transamination step and sometimes a second reaction of deamination is involved. The former reaction is an exchange of amino group between the amino acid of interest and an α-ketoacid, the latter is the removal of the amino group from the amino acid of interest as ammonium (NH_4^+, toxic waste). The transamination step concerns most of the amino acids and generates for instance pyruvate from alanine or oxaloacetate from aspartate for their entry into the TCA cycle. Almost all these transamination reactions generate glutamate that is deaminated by the glutamate dehydrogenase to give α-ketoglutarate and enter the TCA cycle. All deamination reactions generate ammonium that is eliminated by the urea cycle (also known as ornithine cycle).

III.2. Metabolism of quiescent macrophages

Our understanding of macrophage metabolism basically derives from the comparison between the extreme M1 and M2 phenotypes, which represent activated situations. Very few studies characterized and described concisely the metabolism of quiescent macrophages and one reason could be that it is supposed that such metabolism is equivalent in all quiescent cells of the body. However, it might not be the case and subtle differences between cell types can exist. For instance, it is not clear whether specific pathways are used by quiescent macrophages, what is the balance between glucose and oxygen consumption in those cells and whether specific homeostatic mechanisms exist to coordinate all the major pathways and the macrophage

functions. Most of our knowledge about quiescent macrophages comes from unstimulated macrophages *in vitro* (M0 macrophages) often used as experimental control. As for many quiescent cells, OXPHOS support energy production in M0 macrophages and is fueled by glycolysis and FAO (Nomura et al., 2016; Van den Bossche et al., 2015). Such strategy should provide the best long-term energetic yield for macrophages to perform their homeostatic maintain and proliferation *in vivo*. Recently, Liu *et al.* showed that quiescent macrophages proliferating when exposed to colony-stimulating factor 1 (CSF-1, M-CSF) can engage the c-Myc transcription factor to regulate glucose and glutamine catabolism during their cell cycle. They show that such mechanism exists only in quiescent cells as it disappears when macrophages are exposed to pro-inflammatory stimuli (Liu et al., 2016).

III.3. Metabolism switch in inflammatory macrophages

Macrophages are often part of the first line of defense against invading pathogens as bacteria and intracellular parasites. They get activated by microbe-derived molecules as well as local host signals that impose a cellular reprogramming with the emergence of new functions such as cytokine release and professional antigen presentation. In parallel, the activation triggers a metabolic reprogramming to meet the new cellular energetic demands. We will focus on the metabolism of inflammatory macrophages (M1) as they represent the main macrophage population at the site of *L. major* infection. While quiescent macrophages gain energy primarily by OXPHOS, classically activated macrophages were extensively characterized as relying on glycolysis to support their function (Ganeshan and Chawla, 2014; O'Neill and Pearce, 2016; Pearce and Pearce, 2013; Van den Bossche et al., 2017). This transition from OXPHOS to glycolysis is commonly described as the M1 metabolic switch.

Glycolysis

Upon classical activation, macrophages increase their glucose uptake via GLUT1 (Freemerman et al., 2014) and their glycolysis rate. The intermediate pyruvate is no longer directed to the TCA but is rather converted to lactate by fermentation. This pathway from glucose to lactate does not require oxygen and allows the generation of ATP and biosynthetic precursors. It occurs even in the presence of oxygen and therefore is similar the Warburg effect described for tumor cells. The function of such effect will be discussed later. The NAD^+ pool consumed during glycolysis is regenerate during the lactic acid fermentation process. The increased glycolytic

flux partly originates from a switch of the 6-phosphofructo-2-kinase (PFK2) from a poorly active isoform to the more efficient ubiquitous isoform uPFK2 (Rodríguez-Prados et al., 2010). Additionally, the activation of the NF-κB pathway and consequently the HIF-1α pathway increases the expression of several glycolytic genes as GLUT1 or MCT4 to favor glycolysis (Saha et al., 2017). The activation of macrophages by LPS also induces the expression of the glycolytic enzyme pyruvate kinase M2 (PMK2) that can dimerize and reach the nucleus to stabilize HIF-1α, therefore increasing the glycolysis rate (Palsson-McDermott et al., 2015).

TCA cycle and OXPHOS

TCA cycle. In inflammatory macrophages, the TCA cycle is disrupted in two spots: after citrate and after succinate (**Figure 10**), leading to the accumulation of both intermediates. Mechanistically, those breaks originate respectively from an downregulation of the expression of the isocitrate dehydrogenase (IDH) that catalyzes the oxidative decarboxylation of isocitrate (El Kasmi and Stenmark, 2015; Geeraerts et al., 2017) and from an inhibition by itaconate and NO of the succinate dehydrogenase (SDH) that catalyzes the oxidation of succinate to fumarate as well as participates in the electron transport chain inside the complex II (Lampropoulou et al., 2016; Van den Bossche et al., 2017). Itaconate is an organic molecule synthetized by IRG1 during inflammation from cis-aconitate (derived from citrate). Increased succinate level does not principally originate from TCA intermediates but rather by glutamine metabolism *via* anaplerosis (TCA cycle fueling by secondary reactions) (Kelly and O'Neill, 2015).

OXPHOS. In addition to a broken TCA cycle, M1 macrophages also have a deficient OXPHOS machinery (Jha et al., 2015) concomitant with increased mitochondrial fragmentation. Mechanistically, NO is able to inhibit the complexes I and IV of the electron transport chain through S-nitrosylation and/or complexation with their Fe-S centers (Brown, 1999, 2007; Cleeter et al., 1994; Clementi et al., 1998). Also, NO inhibits the complex II (SDH) as aforementioned. Therefore NO appears to be a major OXPHOS inhibitor by targeting the majority of the electron transport chain complexes.

Pentose phosphate pathway

As well, the PPP is increased in M1 macrophages and generates high amounts of NADPH and biosynthetic precursors without the need for oxygen. The increased PPP flux seems to originate

from an strong down-regulation of the PPP enzyme sedoheptulose kinase (SHPK, also known as CARKL) by LPS-induced activation (Haschemi et al., 2012). Additionally, the higher glucose uptake induced by GLUT1 upregulation may also favor a higher metabolic flux through the PPP, as well as the upregulation of the hexokinase, the first enzyme of both glycolysis and PPP (Abdel-Haleem et al., 2017).

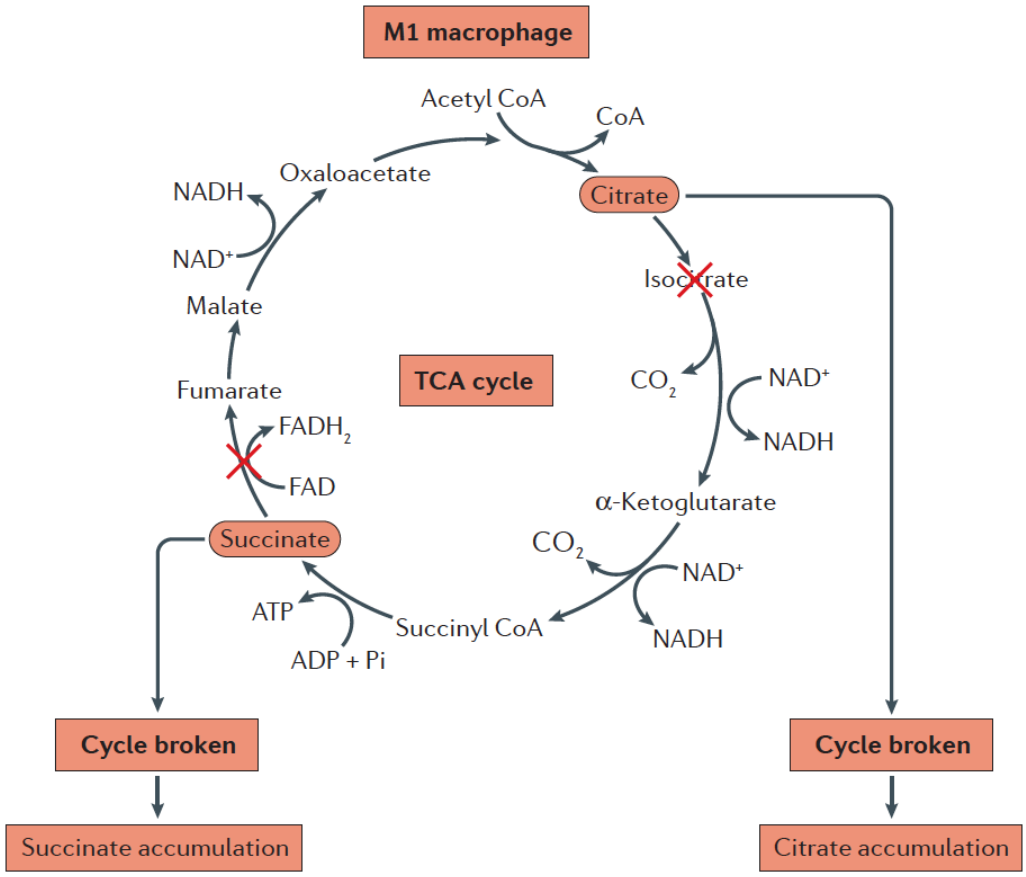

Figure 10. The broken TCA cycle of inflammatory macrophages

In inflammatory macrophages (M1), the TCA cycle is broken in two spots: after citrate and after succinate. The first break leads to the accumulation of citrate that helps in the generation of fatty acids, allows the synthesis of the antimicrobial molecule itaconate and favors NO production. The second break leads to the accumulation of succinate that stabilizes the transcription factor HIF-1α and consequently the production of IL-1β. Image from (O'Neill et al., 2016).

Lipid metabolism

Classical activation of macrophages is also followed by changes in lipid metabolism. M1 macrophages show an increased metabolism of arachidonic acid leading notably to an increased

synthesis of eicosanoids as leukotrienes, prostaglandins and thromboxanes that have pro-inflammatory properties (Greene et al., 2011; Pearce and Pearce, 2013). As well, they rely on fatty acid synthesis for their function, but the underlying mechanism supporting this switch is still unclear. It could be that in M1 macrophages there is a triggering of the sterol regulatory element-binding transcription factor 1c (SREBP1c) that enhances the transcription of several genes related to fatty acid synthesis as observed in M-CSF-stimulated macrophages (O'Neill et al., 2016).

Amino acids metabolism

Finally, the uptake of numerous amino acids is upregulated during M1 polarization. Glutamine uptake is increased in LPS-stimulated macrophages as they show higher levels of SLC3A2 (Tannahill et al., 2013). SLC3A2 interacts with SLC7A7 to form an amino acid membrane transporter that carry glutamine but also other amino acids, suggesting that M1 macrophages uptake a broad spectrum of amino acids. Tryptophan catabolism is as well increased during M1 activation (Saha et al., 2017). In that case, LPS and IFN-γ drive the switch by stimulating the indoleamine-23-dioxygenase (IDO) activity that is the rate-limiting enzyme of the tryptophan catabolism. Concerning arginine, its uptake is also increased by the specific upregulation of the CAT-2 membrane transporter during activation (Comalada et al., 2012; Yeramian et al., 2006). In macrophages, the arginine flux can be consumed by the two enzymes iNOS and arginase. While iNOS have an approximative 1000-fold better affinity for arginine than arginase, it also have an approximative 1000-fold lower enzymatic rate (v_{max}) (Maarsingh et al., 2009). Hence the two enzymes can equally compete for arginine in macrophages. However, in M1 macrophages, the level of expression of iNOS outcompete the arginase one and therefore the arginine flux is dissipated by the iNOS enzyme to produce high amounts of NO.

III.4. Functional consequences on macrophages activity

The massive metabolic switch that occurs during M1 inflammatory polarization have a profound impact on cell activity and we will explain here what are the main advantages of each metabolic modification. Such benefits are summarized per pathways in the **Figure 11**.

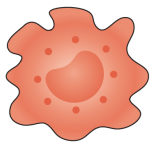

Pathways used:	
Glycolysis	Supports phagocytosis and inflammatory cytokine production
TCA cycle	Redirected to produce citrate to promote fatty acid synthesis
Pentose phosphate pathway	Supports nucleotide and ROS production
Fatty acid synthesis	Supports proliferation and inflammatory cytokine production
Amino acid metabolism	Supports proliferation and nitric oxide production

Figure 11. Functional consequences of the metabolic switch on M1 macrophage activity

M1 inflammatory macrophages undergo a massive metabolic reprogramming during their activation. They show enhanced glycolysis, PPP, fatty acid synthesis and amino acid degradation. In parallel they face a broken TCA cycle and an impaired OXPHOS machinery. All together, these changes support the proliferation and production of building blocks for fatty acids and proteins (including cytokine) synthesis as well as the production of anti-microbial products as ROS or nitric oxide. Image from (O'Neill et al., 2016).

Enhanced cellular resources

As aforementioned, inflammatory macrophages undergo a metabolic switch similar to what observed in tumor cells and named Warburg effect (Galván-Peña and O'Neill, 2014; Kelly and O'Neill, 2015; Langston et al., 2017; O'Neill and Pearce, 2016; Pearce and Pearce, 2013). It is characterized by the use of intense glycolysis followed by lactic acid fermentation even in aerobic conditions. Such effects have two majors advantages: the possibility to produce ATP rapidly and the enhanced biosynthetic precursors synthesis. The glycolysis provides a short-term and dynamic burst of energy (by ATP and NADH production) that can be rapidly triggered upon activation. Additionally, by fueling glycolysis, Warburg effect participates in the synthesis of biosynthetic precursors needed for lipid, nucleotide and protein synthesis. The increased fueling of PPP participates as well to increase the pool of biosynthetic precursors. In inflammatory macrophages, the impaired respiration also participates to resources enrichment. The broken TCA cycle makes citrate accumulate in the mitochondria. It is exported to the cytosol and can have several fates that we will describe as we go along. The first possible fate for citrate is its conversion into acetyl-CoA by the ATP citrate lyase (ACLY), which expression is enhanced in M1 macrophages by NF-κB (by LPS or TNF-α signaling) and/or STAT1 activity (by IFN-γ signaling) (O'Neill, 2011; Williams and O'Neill, 2018). This step allows citrate to enter numerous pathways of lipid synthesis including fatty acid synthesis and others described

latter. By fueling fatty acid synthesis, citrate help sustain membrane recycling by providing an important pool of available lipids.

Enhanced inflammation

Cytokine production. Glycolysis participates to fuel inflammation by increasing cytokine production in distinct ways. For instance, the first glycolytic enzyme hexokinase can regulate IL-1β and IL-18 secretion by triggering the NLRP3 inflammasome upon bacterial infection (Wolf et al., 2016). Also, commitment to glycolysis recruits the glycolytic enzyme GAPDH to the cytosol that is under basal condition bound to TNF mRNA to post-transcriptionally repress its expression (Millet et al., 2016). Moreover, the pyruvate kinase M2 (PKM2) can phosphorylate STAT3 to bolster IL-6 and IL-1β production, as well as activate the NLRP3 inflammasome (O'Neill et al., 2016). In parallel to increased glycolysis, the impaired respiration also participates in enhancing macrophage activity. Succinate oxidation by SDH and mitochondrial hyperpolarization during M1 activation lead to mitochondrial ROS generation that stabilizes HIF-1α and consequent IL-1β production (Mills et al., 2016; Tannahill et al., 2013). However, itaconate produced by citrate metabolism have anti-inflammatory effects by inhibiting SDH activity (Lampropoulou et al., 2016), activating the anti-inflammatory transcription factor Nrf2 (Mills et al., 2018) and regulating the IκBζ-ATF3 inflammatory axis by generating an important electrophilic stress (Bambouskova et al., 2018).

Lipid mediators. Citrate, by its conversion into acetyl-CoA by the enzyme ACLY, fuel not only fatty acid synthesis but also the synthesis arachidonic acid. This molecule serve as a precursor for eicosanoids production including leukotrienes, prostaglandins and thromboxanes that have pro-inflammatory properties (Greene et al., 2011; Pearce and Pearce, 2013). Therefore citrate accumulation helps inflammation by promoting eicosanoid synthesis.

Histone modification. During their activation, inflammatory macrophages undergo major epigenetic changes that imprint prolonged priming capacity for further stimulations (Saeed et al., 2014), a phenomenon called "trained immunity". In these cells the glycolysis is increased in regards to M1 macrophages, a phenomenon that increases their pro-inflammatory potential (Arts et al., 2016; Cheng et al., 2014). One mechanism responsible for "trained immunity" could be that acetyl-CoA, derived from citrate, can induce histone acetylation of genes coding for

glycolytic enzymes such as hexokinase, phosphofructokinase and lactate dehydrogenase (Arts et al., 2016). This is an example of how a metabolic switch can affect cell behavior not only transiently but in a long-term fashion to optimize its function.

Enhanced anti-microbial function

ROS | RNS. Cellular ROS and NO are produced respectively by the NADPH oxidase and iNOS, both requiring NADPH as an enzymatic cofactor. The metabolic switch operating in inflammatory macrophages provides 2 important sources of NADPH to stimulate ROS and NO synthesis (Infantino et al., 2011; O'Neill, 2011). The first source is the enhanced PPP that gives NAPDH during its oxidative part (the two first metabolic reactions) and the second one is the broken TCA cycle that makes citrate to accumulate. Citrate is exported to the cytosol where it not only sustains lipid synthesis but also fuels the NADP-malic enzyme after its conversion into oxaloacetate and then malate. Such enzyme converts malate into pyruvate while releasing CO_2 and NADPH. The pyruvate produced can return the mitochondria as part of the citrate-malate shuttle. Additionally, the use of glutamine through glutaminolysis participates in fueling NADPH synthesis (Ganeshan and Chawla, 2014). Therefore, by helping NADPH production, the PPP, TCA cycle and amino acid metabolism (**Figure 12**) help ROS and NO production. Additionally, the pool of NADPH produced bolster the activity of the glutathione reductase that maintain the reducing environment of the cell and avoid excessive ROS-induced damages (O'Neill et al., 2016). Other mechanisms unrelated to NAPDH help ROS and NO synthesis (Kelly and O'Neill, 2015; O'Neill and Pearce, 2016). For NO production, the increased arginine flux in inflammatory macrophages as well as the high iNOS expression favor the synthesis of high NO concentrations (**Figure 12**). Furthermore, the existence of an inflammatory version of the aspartate-arginosuccinate shunt that connects the TCA cycle and the NO cycle enhances the fueling of iNOS (Jha et al., 2015). For ROS production, the inhibition of the complex II of the electron transport chain drives mitochondrial ROS production in the complex I by reverse electron transport (Mills et al., 2016; Scialò et al., 2017). However, to which extend this mechanism is impaired/favored by NO-mediated inhibition of complex I remains elusive.

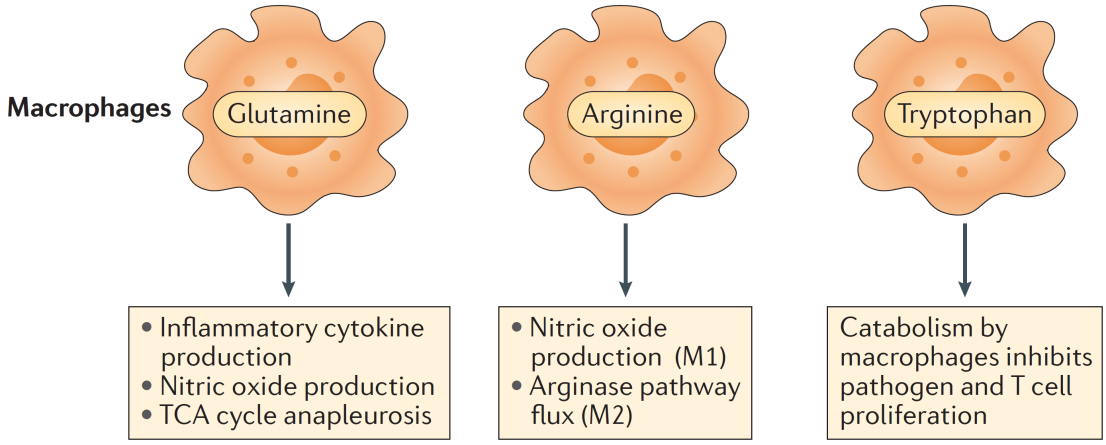

Figure 12. Amino acids catabolism helps the antimicrobial functions of macrophages

The uptake of numerous amino acids is increased inflammatory macrophages to help their functions. Glutamine uptake favors the production of inflammatory cytokines and nitric oxide production to fight pathogens. Arginine flux is redirected to iNOS in inflammatory macrophages to further enhance NO production. Finally, tryptophan is degraded by IDO and therefore limits pathogen growth as it is an essential amino acid for their survival. Image from (O'Neill et al., 2016).

Itaconate. Itaconate is a cellular antimicrobial organic molecule, synthetized by IRG1 during inflammation, that limits the growth of several bacteria including *Salmonella enterica* and *Mycobacterium tuberculosis*. Its anti-inflammatory property originates from its ability to destabilize the glyoxylate shunt by inhibiting bacterial isocitrate lyase (Michelucci et al., 2013). The glyoxylate pathway is essential for bacterial growth when glucose is near absent and simple carbon molecules remain the only carbon source (e.g. in the macrophage phagosome) (Lorenz and Fink, 2002). In inflammatory macrophages, citrate accumulation in mitochondria favors itaconate synthesis as it is converted into the intermediate cis-aconitate that accumulates and serve as a substrate for IRG1 (Lampropoulou et al., 2016; Williams and O'Neill, 2018). Itaconate could also act against *Leishmania* parasites as there are evidence that they express the two enzymes of the glyoxylate shunt (Hernández-Chinea et al., 2017; Simon et al., 1978).

Tryptophan levels. Another feature of M1 macrophages is their enhanced IDO expression (Saha et al., 2017) that lowers tryptophan availability. Tryptophan being an essential amino acid for bacterial growth, limiting its availability restricts pathogen growth (**Figure 12**). Why the macrophage do not seems impaired in its activity by the lack of this amino acid, as it is the case for T cells (Munn et al., 1999), is not clear. In addition to this effect, lowering tryptophan concentration is benefic for NO synthesis as tryptophan can selectively limits NO-synthase induction in macrophages (Chiarugi et al., 2003).

Limitations in our understanding of the Warburg effect

Several limitations still exist to our understanding of the Warburg effect (Fernandez-de-Cossio-Diaz and Vazquez, 2017; Liberti and Locasale, 2016) and they have to be taken into account here. First it is often declared that glycolysis is relatively inefficient to provide energy as ATP molecules. While it is true that glycolysis gives 2 units of ATP per unit of glucose, which is a low yield compared to OXPHOS that gives 36 to 38 units of ATP in case of complete oxidation, it has to be highlighted that the rate of glycolysis can be 10 to 100-fold higher than the rate of complete OXPHOS (Liberti and Locasale, 2016). Therefore, the final ATP synthesis can be of the same range through glycolysis and OXPHOS and macrophages could satisfy from only glycolysis as a source of ATP. Additionally, it is declared that aerobic glycolysis is the principal mean to provide biosynthetic building blocks for the cell. However, approximately 90% of the glucose is converted into lactate, without leaving any carbon behind for building blocks (Liberti and Locasale, 2016; Lunt and Vander Heiden, 2011). Therefore, only 10% of the total glucose molecules can serve a source for biosynthetic precursors. In top of that, several evidence showed that the broken TCA is still fueled by amino acid catabolism to generate building blocks for lipid and protein synthesis. Hence, TCA cycle and not only the glycolysis (via PPP or not) could act in concert in inflammatory macrophages to support the increased biosynthetic activity. Also, whether the loss of respiration is a direct consequence of the Warburg effect is still not clear (Senyilmaz and Teleman, 2015).

Summary

Macrophages are master regulators of the inflammatory reaction. They can be activated by various stimuli as PAMPs (e.g. LPS) and cytokines (e.g. IFN-γ or IL-4) that polarize their phenotype into inflammatory, would-healing and regulatory macrophages. *L. major* infection is characterized by a massive recruitment of inflammatory macrophages that are fully activated by external signals as IFN-γ and TNF-α and consequently secrete many pro-inflammatory cytokines (TNF-α, IL-1β, IL-6…) and chemokines (CXCL1, CCL2, CCL3…) but also upregulate iNOS expression to produce NO. NO mediates its action by giving rise to RNS and by directly modifying proteins by S-nitrosylation and chelation of Fe-S centers. NO is able to diffuse across membranes to act at distance on eukaryotic cells (parasites, stromal or immune cells). In parallel, the activation of inflam-

matory macrophages is concomitant with a cellular metabolic switch from mitochondrial respiration and fatty acid oxidation to glycolysis and fatty acid synthesis. Such modification supports macrophage activity as it helps increasing the cellular resources, enhancing the inflammatory reaction and boosting the production of anti-microbial factors. However, such macrophage activity can be deleterious to the host by the toxicity of the anti-microbial molecules and the important tissue damage consequent to inflammation. We will detail in the final chapter the mechanisms existing to limit inflammation that help prevent the development of immunopathology.

Chapter IV Regulation of inflammation: multiple features

Extensive work have been performed since decades regarding the regulation of inflammatory responses. We will quickly summarize the main features governing inflammation control, with a special interest in monocyte-derived cells, before addressing specific processes that appear during the infection by *L. major*. We will particularly emphasize the control of inflammation by the parasite itself but also by the immune system through NO production.

I. Basis of inflammation resolution

Inflammation is a protective reaction of the organism to fight and remove the injury source as well as initiate tissue healing. The first response is the acute inflammation, described in **Figure 13** (Netea et al., 2017). This process is elicited principally by macrophages and epithelial cells that secrete various pro-inflammatory cytokines, including the famous trio IL-1 | IL-6 | TNF-α, and chemokines such as CCL2 and CCL3. Such cytokines trigger the recruitment of immune myeloid cells at the site of tissue damage and at high concentration can reach the blood to elicit the synthesis of acute-phase proteins in the liver (such as α1-antitrypsin, C-reactive protein…) and the synthesis of lipid mediators as prostaglandins that are responsible for fever, somnolence, anorexia and pain feelings. In parallel, platelets and the complement system help to containing and eliminating the stressing agent as well as recruiting immune cells from the blood. The activation of endothelial cells by all danger signals allows them to increase vascular permeability and to express the correct set of integrins that favors immune cell extravasation. Inflammation is then prolonged until the threat is completely eliminated, fueled by a constant immune cell recruitment from the blood, and can turn chronic when the system can't return to homeostasis. Of note, the beginning of chronic inflammation is frequently considered when the activity of macrophages, and often T cells in the case of an infection, get the upper hand on neutrophil activity (Ashley et al., 2012; Medzhitov, 2008).

The resolution of inflammation does not only rely the complete elimination of the stressing agent but critically needs the establishment of active processes often including cellular reprograming through production of soluble mediators (Netea et al., 2017). We will highlight here some basic mechanisms leading to inflammation resolution as a starter before studying

more in detail the specific contribution of *L. major* and NO. Notably, we will focus on mechanisms originating from macrophages and/or regulating macrophage functions. Specifically we will not address mechanisms relative to neutrophils, even if they are of great importance in driving the resolution if inflammation (Ortega-Gómez et al., 2013; Sugimoto et al., 2016).

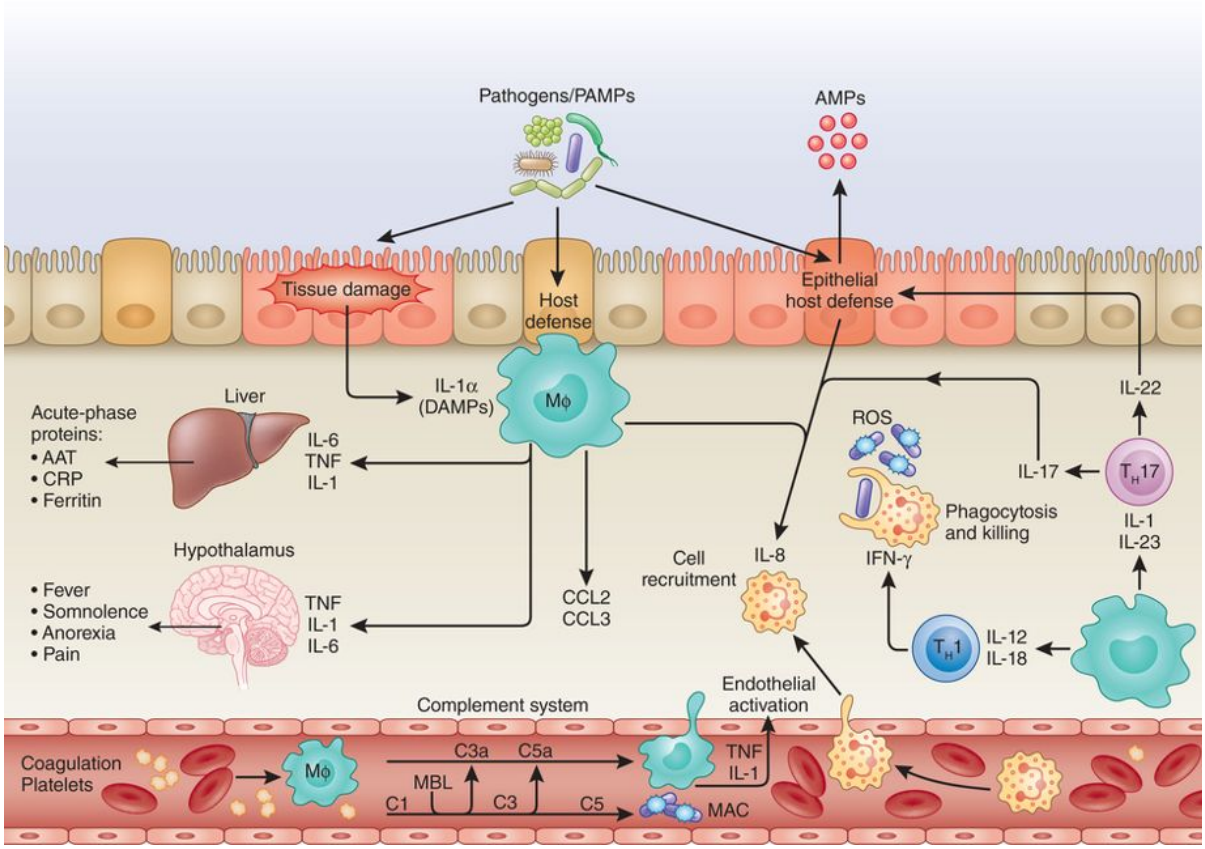

Figure 13. Cellular events occurring in a typical acute inflammatory reaction

Stressing agents introduced into the host tissue damage epithelial cells and trigger the activation of resident macrophages. They produce high quantities of pro-inflammatory cytokines such as IL-1, IL-6 and TNF-α that are responsible for the production of acute-phase proteins in the liver and that trigger fever, somnolence, anorexia and pain feelings. They also produce chemokines as CCL2 and CCL3 to recruit myeloid cells from the blood, a phenomenon bolstered by the complement system and the activation of platelets and endothelial cells. The complement system also helps containing and killing pathogens in the case of an infection. Later, the arrival of T cells helps coordinate and polarize the inflammatory response to the nature of the stressing agent. Image from (Netea et al., 2017).

I.1. Production of anti-inflammatory cytokines

IL-10

The resolution often involve the production of the anti-inflammatory cytokine IL-10. The cellular sources of IL-10 and members of its family (IL-19, 20 and 24) are extremely various as including dendritic cells, macrophages, mast cells, NK cells, neutrophils, $CD4^+$ and $CD8^+$ T cells as well as B cells (Ouyang et al., 2011). IL-10 targets principally leukocytes to dampen their pro-inflammatory functions (Filippi and Herrath, 2008; Moore et al., 2001; Ouyang et al., 2011). On monocyte-derived cells, IL-10 potently inhibits the synthesis of numerous pro-inflammatory cytokines including IL-1β, IL-6, IL-12, TNF-α… and pro-inflammatory chemokines including CCL2, CCL3, CXCLI… as well as increases the production of cytokines antagonists such as IL-1Ra and soluble p55 and p75 TNFR (**Figure 14**). Molecularly, IL-10 signals through the IL-10R coupled to JAK1/STAT3 to inhibit cytokine production by both transcriptional and post-transcriptional mechanisms (Moore et al., 2001). Notably, IL-10 is able to activate the SOCS pathway to dampen inflammation (Mosser and Zhang, 2008). Additionally, IL-10 dampens the synthesis of prostaglandin E2 through the downregulation of the expression of the cyclooxygenase 2 (COX-2) (Niiro et al., 1994, 1995). Finally, IL-10 is able to suppress antigen presentation in DCs by downregulating the expression of MHC-II molecules as well as CD80, CD86 and CD40, important for co-stimulatory signals (Gabryšová et al., 2009; Ng et al., 2013).

TGF-β

TGF-β seems to be secreted mainly by T cell subsets and is key to regulate the activity of many cell types (Letterio and Roberts, 1998; Travis and Sheppard, 2014). Macrophages can also be producers of TGF-β and in that way they contribute to tissue healing and remodeling by promoting myofibroblast proliferation, myofibroblast-derived synthesis of fibrillar collagens and metalloproteinase inhibitors expression (Ortega-Gómez et al., 2013). TGF-β is also a potent suppressor of tissue macrophage activity by limiting their cytokine production, increasing their secretion of IL-1Ra, and most importantly by downregulating iNOS expression and suppressing its activity (Letterio and Roberts, 1998). Also, TGF-β suppresses the production of ROS and the respiratory burst occurring during macrophage activation (Tsunawaki et al., 1988, 1989).

I.2. Chemokine depletion mechanisms

Chemokine truncation

Chemokines are responsible for the attraction of immune cells at the site of inflammation. Their truncation is a way to inhibit their function as they will not be recognized anymore or will be able to link their receptor but without engaging correctly their signaling pathways. Macrophages can specifically trim off chemokines by using matrix metalloproteinases to cleave neutrophil-recruiting CXC-chemokines in their ERL motif (Dean et al., 2008) as well as CC-chemokines that preferentially attract monocytes (McQuibban et al., 2002).

Decoy receptors

Decoy receptors gathered several families of proteins that can bind chemokines but do not permit their signaling. Such receptors include truncated receptors as IL-1Ra or truncated TNFR (Arend, 2002), "silent chemokines receptors" as Duffy antigen receptors (DARC), D6 and CCX-CKR (Mantovani et al., 2006) as well as atypical chemokines receptors (ACKRs) (Bonecchi and Graham, 2016; Vacchini et al., 2016). Truncated receptors are structurally similar to membrane-bound chemokine receptors but they are soluble and secreted by macrophages and others in the environment (Moore et al., 2001; Netea et al., 2017). Therefore they can catch chemokines before the membrane-bound receptor and physically suppress the signaling (**Figure 14**). Silent chemokines receptors are structurally G protein-coupled and membrane-bound receptors but they specifically lack a conserved DRY motif in their second intracellular loop (Mantovani et al., 2006). Such deficiency impairs physical coupling with the G proteins and therefore receptor signaling. They are expressed mainly by endothelial cells. ACKRs have the ability to catch chemokines to shape their gradients and sequestering them from the microenvironment (Vacchini et al., 2016). They are mainly expressed on the nonhematopoietic compartment but there are evidence that some ACKRs could be expressed on macrophages (Bazzan et al., 2013). They act either by scavenging, transporting or presenting the chemokines depending on their nature. Some ACKRs have signaling properties that can influence cellular behavior (Vacchini et al., 2016).

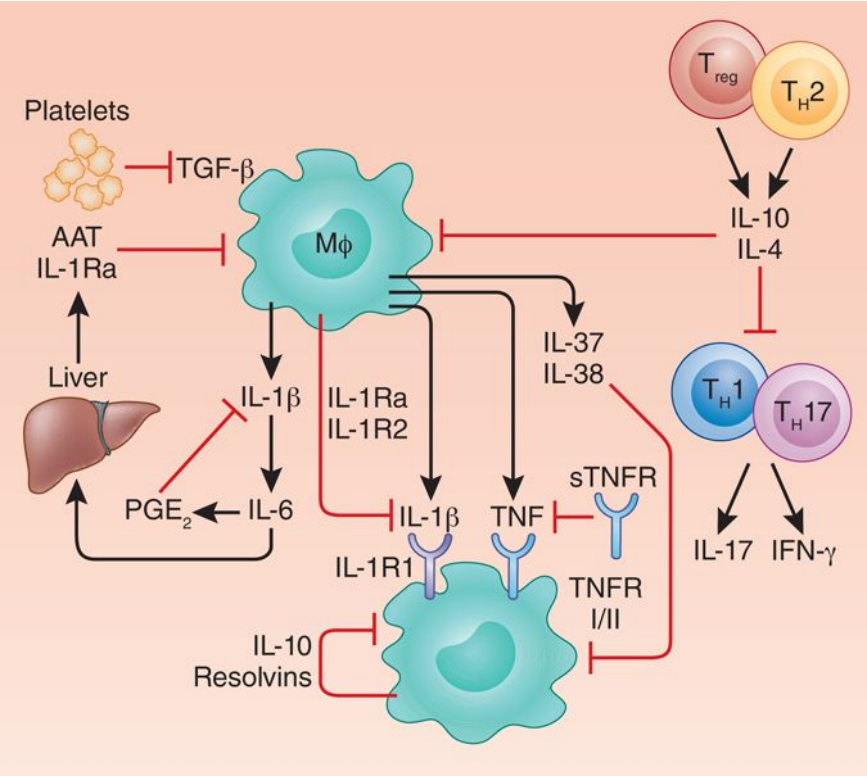

<u>Figure 14.</u> Pro-resolving soluble factors favoring the resolution of inflammation

Macrophages secrete many pro-inflammatory cytokines as IL-1β and TNF-α which actions are counteracted by various anti-inflammatory mediators. For instance truncated receptors as IL-1Ra or soluble TNFR (sTNFR) can catch chemokines before their binding to their membrane-bound receptors and prevent therefore the signaling of these molecules. The production of IL-10, TGF-β and resolvins by macrophages and other cells provides a negative feed-forward loop to regulate the intensity of macrophage activation as well as polarizing macrophage phenotype. Also, PGE_2 triggers a switch in lipid mediator production to promote the synthesis of lipoxins that favor macrophage phagocytosis and inhibit the production of IL-1β in advanced stages of inflammation. Image from (Netea et al., 2017).

I.3. A switch in lipid mediators favors inflammation resolution

Specialized pro-resolving mediators (SPMs) are derived from fatty acids and are composed of lipoxins, resolvins (of the D- and E-series), protectins and maresins (Basil and Levy, 2016; Serhan, 2014). SPMs have been described as a new class of anti-inflammatory molecules involved in the resolution of inflammatory reactions elicited by many stressful organisms as bacteria, viruses, parasites, fungi as well as non-infectious agents. In regards to macrophage biology, SPMs increase the ability of macrophage to clear pathogens and apoptotic cells by phagocytosis/efferocytosis (Godson et al., 2000; Serhan and Savill, 2005). At the site of inflammation, continuous production of pro-inflammatory prostaglandins (e.g. PGE_2) leads to

an transcriptional activation of 15-lipoygenase (15-LO) in neutrophils that in turn switch the production of lipid mediators towards the synthesis of anti-inflammatory lipoxins from arachidonic acid, such as LXA4. LXA4 triggers a rapid and concentration-dependent phagocytosis of apoptotic neutrophils by macrophages, favoring the resolution of inflammation (Godson et al., 2000). As well, SPMs enhance the production of IL-10 by macrophages and help decrease their production of pro-inflammatory cytokines (Basil and Levy, 2016).

I.4. Switch of macrophage phenotype

The switch from an M1 inflammatory phenotype to a M2 pro-resolving phenotype is often described as key to inflammation resolution (Ortega-Gómez et al., 2013; Sugimoto et al., 2016). Most of the molecular mechanisms driving this switch have been highlighted above: the secretion of IL-10 that triggers SOCS pathways, the switch from pro-inflammatory to anti-inflammatory cytokine secretion, the switch in lipid mediator synthesis that enhances wound-healing properties and the suppression of iNOS and matrix metalloproteinase-12 (MMP12) synthesis by TGF-β (Werner et al., 2000). Additional mechanisms exist to favor such transition. For instance it has been shown that resolvin E1 can bind to the leukotriene receptors BLT1 and ChemR23 on monocyte-derived cells to dampen their TNF-dependent NF-κB activation, providing a way to further dampen inflammation (Arita et al., 2007). Also, during chronic inflammation, upregulation of the cyclooxygenase-2 (COX-2) leads to the production of 15-deoxy-$\Delta^{12,14}$-prostagandin J2 that antagonizes the activity of major pro-inflammatory transcription factors as NF-κB and AP-1 while promoting the activation of the anti-inflammatory transcription factor as Nrf2 (Surh et al., 2011).

I.5. Regulation of NLRP3 inflammasome by external cues

NLRP3 inflammasome is a major signaling complex inside macrophages that triggers inflammation at early stages by enabling the secretion of IL-1 family members such as IL-1β and IL-18 (Broz and Dixit, 2016; Lamkanfi and Dixit, 2014). The activity of NRLP3 can be regulated by various external signals (Afonina et al., 2017). First, NLRP3 activation can be inhibited by effector $CD4^+$ T cells through cell-cell contacts, my a mechanism likely involving the binding of CD40 (Guarda et al., 2009). Second, type I interferons are able to dampen IL-1β production by inhibiting as well NLRP3 assembly (Guarda et al., 2011). Several mechanisms

can explain such inhibition: 1. the existence of a mechanism inhibiting NLRP3 activation by decreasing pro-IL-1β expression by the IL-10 – IL-10R – STAT3 pathway (Guarda et al., 2011) and 2. the fact that type I interferons induce the expression of 25-hydroxy-cholesterol able to suppress pro-IL-1β transcription (Reboldi et al., 2014). Finally, we will discuss later in the introduction some evidence that demonstrate a potential mechanism of NLRP3 regulation mediated by NO.

I.6. Regulation of macrophages by alteration of cellular metabolism

We illustrated earlier that classical macrophage activation is concomitant with a profound metabolic reprogramming and it is evident that both phenomenon are interconnected. This raises the possibility that external signals can control inflammation by specifically targeting cellular metabolism through unknown mechanisms. We will give some examples that support such hypothesis and will keep those relative to NO for the end of the introduction.

Example of how a cytokine can act through cellular metabolism

Ip *et al.* have recently shown that IL-10, known to regulate macrophage activity, can target cellular metabolism to mediate its anti-inflammatory function. They demonstrated that in response to inflammation, IL-10 is able to counteract the inflammatory metabolic switch in macrophages by dampening glucose uptake, promoting mitochondrial respiration (OXPHOS) and inducing the expression of DDIT4 that is an inhibitor of mTOR activity. They showed that altogether these mechanisms promote mitophagy that removes deteriorated mitochondria and consequently reduce NLRP3-driven IL-1β production to limit inflammation in both a mouse model of colitis and inflammatory bowel disease patients (Ip et al., 2017). In addition to the aforementioned properties of IL-10, this work illustrates that cytokines can target inflammation by several mechanisms including a change in the core cellular metabolism.

Example of how nutrient availability can control DC activity

Macrophages and DCs exhibit a similar metabolic switch during activation and therefore mechanisms that apply to DCs can be relevant to macrophage biology. We will illustrate here how nutrient availability can directly impact DC function by the work of Lawless *et al.* (Lawless et al., 2017). In this study, the authors showed that the maintenance of a high glucose

level is deleterious to DC activation and their ability to trigger T cell activation. They revealed that a high glucose level favors mTORC1 activation and consequent HIF-1α expression, iNOS synthesis and NO production. They show that this pathway negatively affects costimulatory molecule expression and pro-inflammatory cytokine transcription in activated DCs as well as limits DC-driven T cell proliferation. Interestingly, they showed *in vivo* that OT-I $CD8^+$ T cells can compete for glucose with SIINFEKL-pulsed LPS-activated DCs within the lymph node to deprive DCs of glucose and consequently alter their activity and to favor the T cell response. This example show that nutrient availability is not just a physiological parameter but can also locally shape immune responses, and it would be interesting to test this mechanism during the immune response elicited by a pathogen such as *L. major*.

Of note nutrient availability is also important for cell differentiation. Oburoglu *et al.* showed for instance that HSCs differentiation is governed by glutamine and glucose availability. HSCs preferentially differentiate into erythroid cells when glucose and glutamine are available while they give rise to cells of the myelomonocytic lineage in the opposite scenario (Oburoglu et al., 2014). This questions whether a similar mechanism occurs during monocyte differentiation at the site of infection by *L. major* parasites where nutrient availability can be altered.

Example of how microRNAs link cellular metabolism and activity

MicroRNAs are small non-coding and single-stranded RNAs that regulate gene expression by inhibiting translation and triggering mRNA cleavage of specific targets. It is becoming increasingly clear that microRNAs can impact cellular metabolism in immune cells to regulate their function (Yao et al., 2018) and we will take the example of the microRNA miR-33 in macrophages to illustrate this point. Ouimet *et al.* showed that miR-33 is critical for macrophage polarization by directly targeting the AMP-activated protein kinase AMPK and consequently regulating the balance between OXPHOS and aerobic glycolysis (Ouimet et al., 2015). In the context of atherosclerosis, they showed that miR-33 inhibition reduces plaque inflammation by promoting the polarization towards a M2 phenotype as well as favoring regulatory T cell induction. Also, in the context of an infection by *Mycobacterium tuberculosis*, they showed that miR-33 (in that case induced by the bacteria) diminishes autophagy and lipid catabolism (Ouimet et al., 2016). While this phenomenon could serve as an escape mechanism for the bacteria, it can also perturb lipid metabolism and therefore alter macrophage function. This idea is to consider along with the study of Rayner *et al.* showing that miR-33 represses the

surface expression of the cholesterol transporter ABCA1 that is involved in atherosclerosis pathology and further demonstrated as enhancing pro-inflammatory cytokine production in macrophages (Rayner et al., 2011; Yao et al., 2018).

***

II. REGULATION BY *Leishmania* PARASITES: SOME ESCAPE MECHANISMS

Leishmania parasites have successfully developed strategies to evade the immune system in order to survive both outside and inside its host cell. Notably they have many mechanisms to protect themselves against macrophages that are involved in their elimination, as they represent their main host cell and harbor many antimicrobial functions. By altering macrophage activity, these mechanisms can have a direct impact on the inflammatory reaction at the site of infection and therefore participate in its regulation. We will highlight here the principal escape mechanisms triggered by *Leishmania* parasites that specifically modulate macrophage functions and how they can influence inflammation levels during the infection.

Many macrophage defects originate from the effect of two major *Leishmania* virulence factors: lipophosphoglycan (LPG) and glycoprotein 63 (GP63) (Chang and McGwire, 2002; Forestier et al., 2015; Olivier et al., 2012; Späth et al., 2003). LPG is a glycoconjugate that dominates on the parasite surface by its very high level of expression. Its main roles are to circumvent parasite lysis by the complement system and interfere with host signaling pathways and notably the TLR2 pathway (Forestier et al., 2015; Späth et al., 2003). GP63 is a zinc-metalloprotease expressed in abundance on the surface of promastigote and amastigotes parasites. It have a major role in increasing parasite survival into the phagosome and influencing macrophage signaling pathways, notably on transcription factor activity (Olivier et al., 2012).

II.1. Control of host cell signaling pathways

Defective TLR pathways

The infection by *Leishmania* parasites is relatively "silent" and parasite uptake do not rely on TLR signaling. However, a few molecules have been reported as potential PAMPs, thus highly potentially pro-inflammatory, including LPG that is recognized by TLR2 (Faria et al., 2012).

Leishmania parasites can inhibit TLR2 signaling by recruiting elements of the suppressors of the cytokine signaling (SOCS) family (Veer et al., 2003) as well as by activating the host de-ubiquitinating enzyme A20 that interferes with the ubiquitination of TRAF6 (Srivastav et al., 2012). It can by the same way also inhibits TLR4 signaling, that have been reported as a critical TLR shaping the immune response against *Leishmania* parasites (Gupta et al., 2013). Therefore, by inhibiting several TLR pathways, *Leishmania* parasites can influence the level of activation of macrophages and consequently lower the intensity of inflammation in the infected tissue.

Alteration of JAK/STAT pathways

These pathways are crucial to stimulate macrophage activity as they are very often associated with cytokine receptors. *Leishmania* parasites are potent at upregulating protein tyrosine phosphatases (PTP) including the well-known Src homology region 2 domain-containing phosphatase-1 (SHP-1) regulator. SHP-1 is able to inactivate JAK2 protein, that is for instance downstream IFN-γ receptors (Blanchette et al., 2009). In addition, *Leishmania* can selectively inactivates STAT1α translocation into the nucleus by enhancing its degradation and further reducing IFN-γ signaling (Forget et al., 2005). Moreover, upregulation of SOCS members also decreases JAK-STAT pathway activity by binding to phosphorylated JAK proteins (Veer et al., 2003). Therefore, infection by the parasite decreases IFN-γ and potentially other cytokine signaling in macrophages and thus participates in decreasing the inflammation intensity and cytokine secretion.

Alteration of the MAPK pathways

In addition to inhibit JAK/STAT pathways, *Leishmania* parasites are also able to downregulate several members of the MAPK pathways. For instance, *Leishmania donovani* was shown to inhibit ERK1/2, p38MAPK and JNK activation in macrophages, leading to a decrease in pro-inflammatory cytokine production (Privé and Descoteaux, 2000). Mechanistically, *Leishmania*-induced SHP-1 participates in MAPK modules inhibition as well as *Leishmania*-induced activation of ecto-protein phosphatases that for instance inactivate ERK1/2 MAP kinase (Forget et al., 2006; Martiny et al., 1999). Also, some species of parasites, as *Leishmania mexicana*, have their own cysteine peptidase that cleaves ERK and JNK to dampen MAPK signaling (Cameron et al., 2004). Finally, increased host ceramide generation induced by *Leishmania*

parasites suppresses AP-1 and NF-κB activity by enhancing their dephosphorylation (Ghosh et al., 2002). Altogether, the inhibition of MAPK modules impairs NF-κB and AP-1 transcription factors activity that consequently affect macrophage activity (as cytokine production and iNOS expression).

Cleavage of mTOR

Finally, *Leishmania* is also able to manipulate the host energetic machinery by acting on the mammalian target of rapamycin (mTOR). Indeed, Jaramillo *et al.* demonstrated that *Leishmania* GP63 protease can cleave mTORC1 to inhibit its activity and consequently activate the translational repressor 4E-BP1. Such activation restricts macrophage translation and decreases type I interferon synthesis but increases the parasite load in macrophages *ex vivo* as well as increases the susceptibility to cutaneous leishmaniasis *in vivo* (Jaramillo et al., 2011).

II.2. Polarization of cytokine production

Increased immunosuppressive cytokine and prostaglandin production

Various species of *Leishmania* parasites can trigger TGF-β secretion both *in vitro* and *in vivo* (Bogdan and Röllinghoff, 1998). Mechanistically, TGF-β production is induced by the exposure of phosphatidylserine (PS) motifs at the surface of *Leishmania* amastigotes, probably by a mechanism similar to what happens with apoptotic cells (El-Hani et al., 2012; Wanderley et al., 2006). In addition, *L. major* can stimulate IL-10 production in *vitro* by exposure of PS motifs on its surface but also by engaging CD64 (FcγRI) (de Freitas Balanco et al., 2001; Sutterwala et al., 1998). Finally, *Leishmania* parasites can increase the production of the anti-inflammatory prostaglandin E2 by significantly increasing the expression of COX-2 in human monocytes (Matte et al., 2001).

Decreased pro-inflammatory cytokine/chemokine production

Leishmania parasites are potent at dampening the production of major pro-inflammatory cytokines such as TNF-α, IL-1β and IL-12 (Olivier et al., 2005) by mainly repressing JAK/STAT and MAPK pathways as aforementioned. Other complementary mechanisms exist

to explain the decrease in pro-inflammatory mediators. First, *Leishmania* LPG was found to act as a "gene silencer" that represses IL-1β transcription by acting through a promoter repression sequence (Hatzigeorgiou et al., 1996). TNF-α is as well reduced in infected cells but also in neighboring cells, suggesting that the repression originates from an indirect mechanism, as for instance by a parasite-induced IL-10 secretion followed by diffusion (Olivier et al., 2005). One of the most studied pro-inflammatory cytokine in the development of leishmaniasis is probably the IL-12, notably because IL-12 is crucial to the development of a protective T_H1 T cell response. IL-12 have been reported as diminished in various contexts of leishmaniasis both *in vitro* and *in vivo* (Belkaid et al., 1998; Carrera et al., 1996; Piedrafita et al., 1999). Such repression was shown to be restricted to infected cells by singe-cell analysis, mediated by *Leishmania* LPG and independent of the NF-κB pathway. The mechanism underlying IL-12 inhibition is still controversial (Olivier et al., 2005). Finally, *Leishmania* parasites can as well decrease the synthesis of pro-inflammatory chemokines as CCL2 (Lo et al., 1998; Ritter et al., 1996) and also limit the expression of cell surface adhesion molecules as E-selectin, ICAM-1 and VCAM-1 by endothelial cells (Lo et al., 1998) to decrease monocyte recruitment to the site of infection.

II.3. Protection against anti-microbial molecules

Modulation of iNOS expression and resistance to RNS

Leishmania parasites have developed mechanisms to directly or indirectly affect NO production by iNOS. First, *Leishmania* parasites are highly efficient at disrupting signals leading to full macrophage activation. For instance, the aforementioned inhibition of JAK2 and ERK1/2 by SHP-1 results in a downregulation of iNOS production, leading to decreased NO synthesis (Blanchette et al., 2009; Forget et al., 2006). In addition, pathogenic strains of *Leishmania* parasites are able to trigger arginase expression in macrophages as well as pumping host arginine by their own arginase, leading to decreased substrate availability for iNOS (Badirzadeh et al., 2017; Muleme et al., 2009). Also, it was recently described by Calegari-Silva *et al.* that *L. amazonensis*, but not *L. major*, parasites are able to dampen NO synthesis by the activity of the histone deacetylase 1 (HDAC1) that negatively controls iNOS gene expression (Calegari-Silva et al., 2009). Finally, *Leishmania* parasites may also be able to directly overcome RNS toxicity as several parasites extracted from infected patients were found to resist to NO in culture (Olekhnovitch and Bousso, 2015). While the molecular bases for such resistance is not

clear for *Leishmania* parasites, some mechanisms described for other pathogens may apply such as the production of NO scavengers (e.g. thiols), the upregulation of detoxifying enzymes and the development of mechanisms of repair (Bogdan, 2015).

Modulation of ROS synthesis

Leishmania parasites possess also strategies to escape ROS. They are able to interfere with the protein kinase C (PKC) signaling cascade that is crucial to NADPH oxidase activity to generate ROS. Such inhibition originates from *Leishmania* LPG that blocks PKC activity by interfering with the binding of Ca^{2+} and diacylglycerol (DAG) on this enzyme and *Leishmania* GP63 that cleaves several PKC substrates and making them unusable by the enzyme (Gupta et al., 2013; Olivier et al., 2005). They also impact the assembly of the NADPH oxidase complex at the surface of the parasitophorus vacuoles (Lodge et al., 2006).

II.4. Additional escape mechanisms that may indirectly affect inflammation

Alteration of phagocytosis and phagosome maturation

Inside the host tissue, many pathogens are opsonized by the complement molecule C3b, that facilitates their phagocytosis by macrophages and further elimination (Rosales and Uribe-Querol, 2017). *Leishmania* virulence factor GP63 is able to cleave C3b into its inactive form C3bi and consequently triggering a "silent entry" into macrophages by binding to the complement receptor 3 (CR3) (Gupta et al., 2013). Additionally, CR3 binding is known to inhibit IL-12 production (Marth and Kelsall, 1997). *Leishmania* parasites are also able to interfere with phagosome maturation once internalized. They for instance exclude the proton-ATPase from the phagosome and reduce the fusion with endosomes at early steps of phagocytosis by a LPG-dependent mechanisms (Dermine et al., 2000; Lodge et al., 2006). As well, GP63-depend mechanisms are responsible for phagosomal acidification impairment and lysosome fusion deficiency (Casgrain et al., 2016; Verma et al., 2017).

Modulation of DC activation

The modulation of DC activation by *Leishmania* species occurs by mechanisms targeting antigen presentation and the expression of co-stimulatory molecules. *Leishmania* parasites can

reduce antigen loading and transport to the surface membrane probably by sequestering MHC-I and MHC-II molecules in the parasitophorus vacuole (Kima et al., 1996), in addition to reducing MHC-II expression (Neves et al., 2010) and destabilizing its expression at the surface by disrupting lipid rafts (Chakraborty et al., 2005). In addition, *Leishmania* parasites can trigger the direct internalization of pMHC complexes, preventing further antigen presentation (de Souza Leao et al., 1995). Finally, *Leishmania* parasites also prevent the expression of co-stimulatory molecules on macrophages such as CD86, CD80 and CD40 (Martínez-López et al., 2018; Stebut et al., 1998) and probably also on DCs (Figueiredo et al., 2012).

***

III. IMPACT OF NO ON THE INFLAMMATORY REACTION

NO is synthetized in high amounts during pathogen-driven inflammatory responses and is key for pathogen control and killing. Several studies highlighted that NO can have a direct impact on immune cells including T cells and myeloid cells. We will summarize here the major effects of NO on immune cells during inflammatory processes.

III.1. NO impacts T cell expansion and activation

Sources of NO affecting T cells

In the lymph node, mesenchymal stem cells (MSCs) as well as fibroblastic reticular cells (FRCs) and lymphatic endothelial cells (LECs) were identified as important sources of NO that dampen T cell expansion and the DC-mediated T cell priming *in vivo* (Lukacs-Kornek et al., 2011; Ren et al., 2008; Siegert et al., 2011). The production of NO was shown to be dependent on iNOS upregulation induced by IL-1 cytokines as well as by IFN-γ and TNF-α released by the activated T cells. In tissues, mononuclear phagocytes of different phenotypes including macrophages (Bingisser et al., 1998) and myeloid-derived suppressor cells (MDSCs) (Mazzoni et al., 2002) were shown to have a severe impact on T cell expansion by mechanisms detailed in the next paragraph. Finally, T cells by themselves can produce NO by iNOS, induced by inflammatory signals such as IFN-γ, but also eNOS and nNOS (Ibiza and Serrador, 2008).

NO limits T cell activation

The role of NO on T cell activation is still unclear and that may be due to differences in the NOS isoform studied, the source of NO and its concentration. Several studies suggest that at high doses, NO represses T cell activation by reducing MHC-II transcription and subsequent expression on the surface of APCs (Harari and Liao, 2004) and as well impairing T cell binding to APCs by nitrating tyrosines within TCR complexes (Nagaraj et al., 2007). However, at low doses, NO may be beneficial to T cell responses as it seems to be critical to mitochondrial hyperpolarization needed for T cell activation (Nagy et al., 2003) and as well there is evidence that eNOS, targeted to the immunological synapse, locally increases TCR signaling and IFN-γ production (Ibiza et al., 2006). Also, NO was shown to modulate the susceptibility of T cells to death by neglect to set the levels of $CD4^+$ and $CD8^+$ T cell memory formation (Vig et al., 2004).

NO alters T cell expansion

IL-2 signaling is well known for its role in T cell expansion and studies have investigated the potential role of NO on IL-2 activity. NO was shown to block both IL-2 production (Taylor-Robinson, 1997) and signaling in T cells (Bingisser et al., 1998; Mazzoni et al., 2002), resulting in defective T cell expansion after stimulation. The blockade of IL-2 signaling occurs by the inhibition of the phosphorylation of key signaling molecules downstream the IL-2R such as JAK1, JAK3, STAT5, ERK and Akt. Such mechanism allows a control of the T cell pool size during immune responses. Another potential mechanism by which NO could impact T cell expansion is by the depletion of arginine. Indeed, NO production during T_H1 responses involves a high consumption of arginine that induces a loss of surface CD3ζ and results in a blockade of the cell cycle in G_0-G_1 phase (Rodriguez et al., 2002, 2003, 2007).

III.2. NO skews T cell polarization

T_H1 vs. T_H2

Several studies demonstrated that NO is able to alter T cell polarization following T cell activation, which effects are dependent on its concentration. At low doses, as during the silent phase of leishmaniasis, NO can skew naïve $CD4^+$ T cells differentiation to T_H1 phenotype by upregulating the surface expression of the IL-12R by cGMP signaling (Niedbala et al., 1999,

2002). However, at high doses, NO restricts T_H1 development by suppressing IL-12 synthesis by macrophages in the model of cutaneous infection with *L. major* parasites (Huang et al., 1998; Wei et al., 1995). In addition, NO enhances IL-4 production by T_H2 clones at high doses, further reinforcing the T_H1 polarization blockade (Chang et al., 1997). Interestingly, these findings also apply to human T cells (Niedbala et al., 2006).

Regulatory T cells

$CD4^+$ regulatory T cells (T_{REGS}) are a subpopulation of $CD4^+$ T cells characterized by a high expression of CD25 and that in most circumstances express the transcription factor Foxp3, but it does not seems always the case (Roncarolo and Gregori, 2008). Lee *et al.* reported that NO suppresses $Foxp3^+$ T_{REG} differentiation induced by TGF-β and retinoic acid in addition to drive T_H1 differentiation (Lee et al., 2011). Intriguingly, NO is also able to induce the proliferation of T_{REGS} that are $CD4^+CD25^+$ but $Foxp3^-$ and called NO-T_{REGS} (Niedbala et al., 2006, 2007). These cells are able to suppress the proliferation of naïve T cells *in vitro* and *in vivo* in models of colitis and collagen-induced arthritis by a mechanism depend on IL-10 production. It remains difficult to predict whether these cells are involved in the case of leishmaniasis as many different polarizing cues are present.

III.3. NO dampens leukocyte recruitment

The role of NO on leukocyte recruitment was addressed in the first place by Kubes *et al.* whose work revealed that endothelium-derived NO decreases leukocyte adherence and extravasation (Kubes et al., 1991). Mechanistically, it was shown that this effect originates from NOS-derived NO that decreases the expression of many adhesion molecules as ICAM-1 and P-selectin on endothelial cells by cGMP signaling (Biffl et al., 1996; Dal Secco et al., 2006; Hickey, 2001; Lefer et al., 1999). Of note, such effects should rely on a high NO concentration as it has been shown that low NO levels favor the expression of adhesion molecules as VCAM-1, ICAM-1 or E-selectin also on endothelial cells (Sektioglu et al., 2016). During leishmaniasis, eNOS-derived NO may limit the recruitment of granulocytes and therefore the immunopathology (Fritzsche et al., 2010). The contribution of iNOS in regulating leukocyte adhesion during the infection with *Leishmania* parasites remains to be fully characterized.

III.4. NO alters macrophage activity

Effects on cytokine production

We mentioned earlier that NO affects the transcription of several signaling pathways and gene expression, and many of these genes are necessary to regulate inflammation and cell survival (Bogdan, 2015). At low doses, NO helps inflammation by enhancing the production of pro-inflammatory cytokines such as CCL2 (MCP-1) and CCL3 (MIP-1α) while its displays opposite effects at high doses (Kobayashi, 2010). Mechanistically, the suppressive properties of NO may probably originate from its ability to limit intracellular cell signaling (Stamler et al., 2001), notably inhibiting NF-κB activity (Matthews et al., 1996) as well as dampening STAT1 activity by nitration, impairing IFN-γ signaling (Llovera et al., 2001). Also, in various models including a model of septic shock and a model of infection by *Mycobacterium tuberculosis*, NO was shown to restrict NLRP3 inflammasome activity and consequently IL-1β production (Hernandez-Cuellar et al., 2012; Mao et al., 2013; Mishra et al., 2013). Such inhibition of inflammasome activity resulted in a decreased granulocyte infiltrate that was protective against immunopathology (Mishra et al., 2017). During the infection with *L. major*, NO was equally shown to block NLRP3 inflammasome activity to mediate host protection (Charmoy et al., 2016; Gurung et al., 2015). Surprisingly, Lima-Junior *et al.* showed that inflammasome-derived IL-1β is key to induce enough NO to fight the parasite, suggesting a beneficial effect of NLRP3 during the infection (Lima-Junior et al., 2013). However, they highlight that this mechanism do not apply to all parasites species, including *L. major*. Altogether, these studies strongly support the possibility that NO limits the pathology occurring in uncontrolled infections with *L. major* by interfering with macrophage activity. Yet, the spatiotemporal activity of NO on macrophages *in vivo* is not characterized. Also, NO could act by other complementary mechanisms to repress immune cell activity.

Effects on cellular metabolism

Finally, less studies focused on the role of NO on immune cell metabolism. As aforementioned, NO targets many molecules by direct chemical modification as Fe-S complexation, that can for instance inhibit mitochondrial respiratory chain complexes (Brown, 1999). Therefore it is reasonable to hypothesize that NO could alter mitochondrial respiration that in turn modulate macrophage activity. Consistent with this idea, Everts *et al.* showed that NO produced in

inflammatory DCs dampens mitochondria respiration and that a switch to glycolysis was essential to maintain ATP levels under this circumstance (Everts et al., 2012). Therefore in DCs, the switch to glycolysis is NO-independent but the maintenance of the glycolytic program critically rely on NO. Later, Amiel *et al.* showed that NO most probably mediates this effect by a cell extrinsic mechanism (Amiel et al., 2014). To date, our knowledge about the role of NO on macrophages is less clear. For sure, many mechanisms that apply to DCs should be transposable to macrophage biology, but subtle differences may exist. Additionally, we still don't know to which extent NO can modulate macrophage activity (cytokine/chemokine secretion) by a direct effect on metabolism. Finally, most of the work have been done using bone marrow-derived cells *in vitro* or inflammatory DCs restimulated *ex vivo*. Thus, we critically lack studies using cells embedded in their complex microenvironment *in vivo*, as we can do using a model of the cutaneous infection with *L. major* using appropriate tools.

Summary

Inflammation is controlled by numerous mechanisms that prevent immunopathology development. A switch operates in the production of soluble mediators towards the synthesis of anti-inflammatory cytokines and pro-resolving lipids. Complementary, pro-inflammatory chemokines are truncated/sequestered and the NLRP3 inflammasome is disarmed. Finally, macrophages are forced to switch their phenotype and metabolism to dampen their activity. In the specific case of the infection by *L. major* parasites, additional mechanisms driven by parasite-derived factors (e.g. LPG and GP63) perturbate inflammation resolution and often favor the development of an immunopathology. Such mechanisms involve a strong perturbation of host cell signaling, a polarization of cytokine production favoring inflammation and the deployment of processes dampening ROS and RNS production. However, robust NO production by myeloid cells and stromal cells help counteract such effects. Indeed, NO limits T cell expansion and activation, restricts leukocyte recruitment and represses macrophage activity. Finally, NO targets cellular metabolism and by this way may participate in regulating macrophage activity to avoid immunopathology. Its spatiotemporal activity and mechanism of action *in vivo* in the complex environment imposed by *L. major* infection is yet to be determined.

Objectives

Objectives

In this introduction, we highlighted the complexity of the immune response against *Leishmania major* parasites as well as the multiple mechanisms operating to control inflammation. We focused on monocyte-derived cells and their ability to produce nitric oxide (NO) that have pleiotropic effects. Despite our important knowledge regarding mechanisms that control inflammation, there is still a lack of understanding of how the immune system can select the appropriate time for inflammation resolution. Specifically, whether a mechanism exists to sense when a sufficient number of immune cells have accumulated to elicit the termination of inflammation remains unknown.

The main objectives of this thesis were to investigate the potential impact of NO during inflammatory reactions as well as its spatiotemporal activity *in vivo*, using as a model the immune response at the site of *Leishmania major* infection. We investigated the influence of NO on monocyte-derived cell activity and metabolism *in vivo* and further dissected the molecular mechanism with the help of *in vitro* experiments. Specifically, we addressed these three specific questions:

1. How NO is influencing the immune reaction at the site of *L. major* infection?

2. By which mechanisms can NO control cellular metabolism and activity *in vivo*?

3. What is the spatiotemporal activity of NO within the infected tissue?

Results

I. NO DAMPENS INFLAMMATION AT THE SITE OF *L. major* INFECTION

I.1. NO dampens inflammation intensity

During infection with intracellular pathogens NO can exert pleiotropic effects altering immune responses at multiple stages (Bogdan, 2015; Olekhnovitch and Bousso, 2015). To specifically evaluate the impact of NO production on an established inflammatory reaction, we assessed the consequence of a short period of iNOS inhibition in *L. major* infected mice (**Figure 15**).

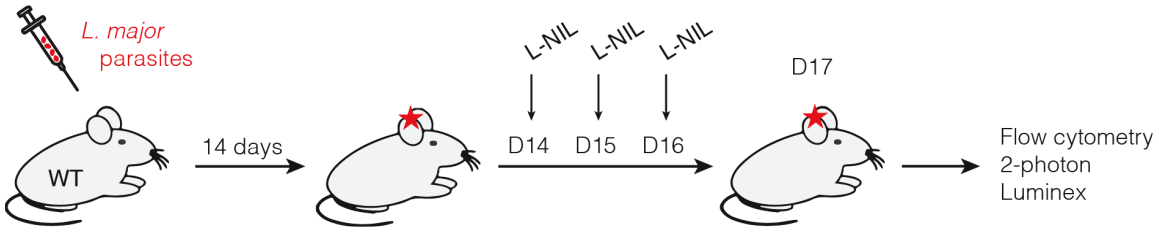

Figure 15. Experimental set-up to study the impact of NO on the inflammatory reaction at the site of *L. major* infection

Experimental set-up. WT mice were infected with DsRed-expressing *L. major* and treated 14 days later with the specific iNOS inhibitor L-NIL. Inflammatory reaction in infected ears was characterized 3 days later.

We used the specific iNOS chemical inhibitor L-N^6-(1-iminoethyl)-L-lysine (L-NIL) and treated mice 2 weeks post infection for 3 days. L-NIL is an amino acid that resemble arginine and compete with it specifically in iNOS active site (Moore et al., 1994). We found that iNOS inhibition profoundly increased myeloid cell numbers at the site of infection, with a major effect on neutrophils and monocyte-derived cells (**Figure 16**). We and others have previously shown that $Ly6C^+MHC\text{-}II^-$ monocytes (P1 population) are massively recruited at the site of infection and further differentiate into $Ly6C^+MHC\text{-}II^+$ (P2 population) and subsequently into $Ly6C^-MHC\text{-}II^+$ cells (P3 population) (León et al., 2007; Olekhnovitch et al., 2014). We found that all three populations of mononuclear phagocytes were substantially increased upon a short inhibition of iNOS (**Figure 16**).

To extend these results, we used *Lyz2*$^{+/EGFP}$ mice (Peters et al., 2008) in which both neutrophils and macrophages are labeled with GFP to visualize the effect of iNOS inhibition on myeloid cell density at the site of infection. Consistent with our flow cytometric analysis, two-photon imaging of the ear dermis revealed a significant increase in the density of myeloid cells (GFP^{+}) upon transient iNOS inhibition (**Figure 17**).

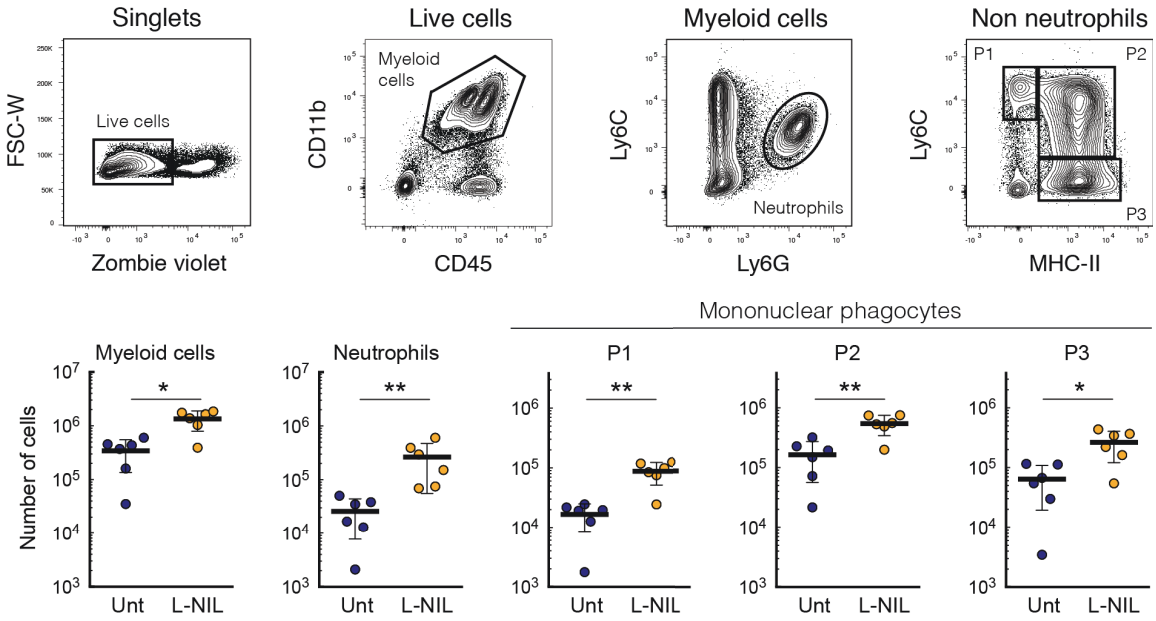

Figure 16. NO limits the accumulation of myeloid cells at the site of *L. major* infection

Top. Flow cytometry contour plots showing the gating strategy used to analyze mononuclear phagocytes (P1, P2 and P3) from extracted ear cells. *Bottom.* Absolute cell numbers of myeloid cells, neutrophils and mononuclear phagocytes in infected ears from untreated (blue circles) or L-NIL-treated (orange circles) WT mice as assessed by flow cytometry. A third of the ear cell preparation was used flow cytometric analysis and 200000 cells were acquired. Representative of 6 independent experiments.

We next investigated the effect of iNOS inhibition on the inflammatory milieu at the site of infection by analyzing cytokine and chemokine concentrations in total ear tissue. We observed an overall increase in cytokine concentrations when iNOS activity was blocked. The effect appeared very broad and concerned most of the cytokines tested, including IL-1α, IL-1β, TNF-α, IL-6, IL-12 (p40 and p70), IL-10, IL-5, IL-4 (**Figure 18**). Similarly, iNOS inhibition led to a dramatic increase in chemokine concentrations in the ear tissue, including CXCL1, CXCL10, CCL2, CCL3 (**Figure 18**).

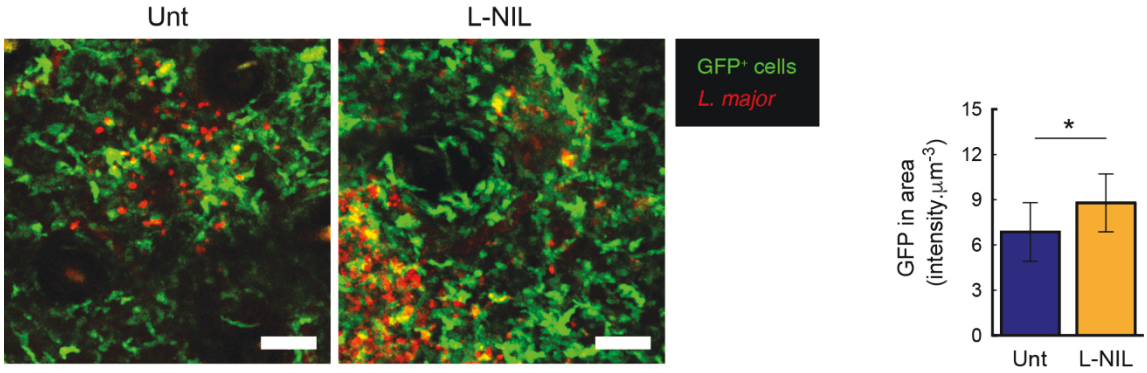

Figure 17. NO limits the accumulation of *Lyz2*$^{+/EGFP}$ cells at the site of *L. major* infection

Left. Representative images of two-photon intravital imaging performed on infected ears from untreated or L-NIL-treated *Lyz2*$^{+/EGFP}$ mice, showing DsRed-expressing *L. major* and myeloid cells (GFP+). Scale bar: 50 µm. *Right.* Quantification of GFP fluorescence in infected ears from untreated or L-NIL-treated mice. Results are representative of 2 independent experiments.

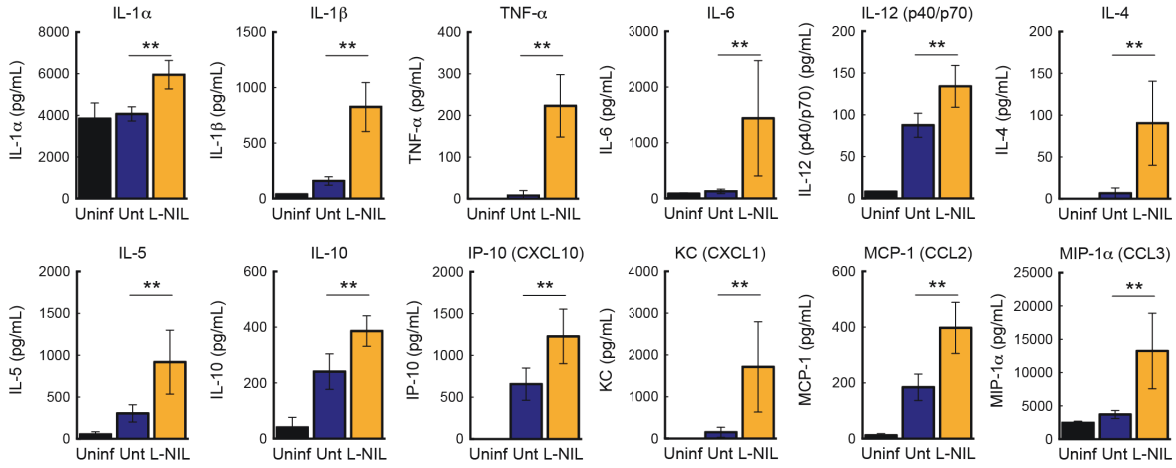

Figure 18. NO reduces cytokine/chemokine accumulation at the site of *L. major* infection

Cytokines (IL-1α, IL-1β, TNF-α, IL-6, IL-12 (p40 and p70), IL-4, IL-5 and IL-10) and chemokines (CXCL10, CXCL1, CCL2 and CCL3) quantification in ear lysates from untreated (blue bars) or L-NIL-treated (orange bars) mice as assessed by multiplex assay. Ears from age and sex-matched uninfected mice were analyzed to assess cytokine basal concentrations. Results are representative of 3 independent experiments.

Altogether, our results indicate that NO production at the site of *L. major* infection controls, either directly (acting on cells) or indirectly (acting on the pathogen), the inflammatory reaction, limiting immune cell infiltrates together with cytokine and chemokine concentrations.

I.2. NO limits myeloid cell recruitment

To specifically assess the role of NO on immune cell recruitment at the site of infection, we performed adoptive transfer of myeloid populations by injecting fluorescently-labeled bone marrow cells in infected mice. Cell recruitment in the infected ear was assessed in the presence or absence of iNOS inhibition (**Figure 19**).

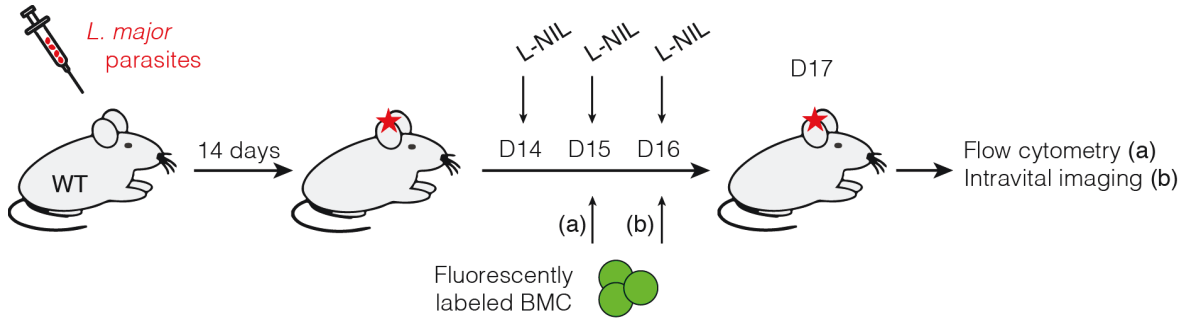

Figure 19. Experimental set-up to study the impact of NO on myeloid cell recruitment at the site of *L. major* infection

Experimental set up. WT mice were infected with DsRed-expressing *L. major* and treated 14 days later with the specific iNOS inhibitor L-NIL. Cell recruitment was assessed 3 days later by transferring i.v. fluorescently-labeled bone marrow cells.

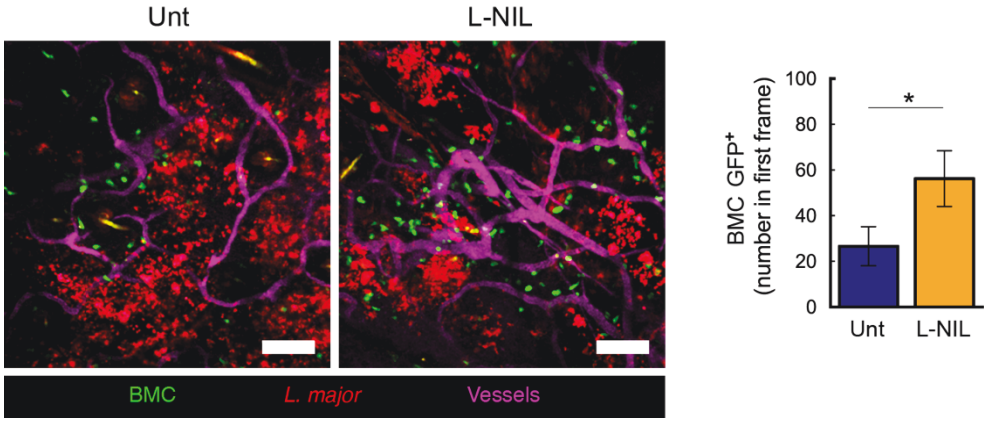

Figure 20. NO dampens the recruitment of myeloid cells at the site of *L. major* infection

Left. Representative images of two-photon intravital imaging performed on infected ears from untreated or L-NIL-treated mice, showing DsRed-expressing *L. major* (red), Evans blue-labeled vessels (magenta) and GFP^+ extravasated cells (green). Scale bar: 100 µm. *Right.* The absolute numbers of extravasated cells in the imaging field were measured for untreated (blue bar) or L-NIL-treated (orange bar) mice. Representative of 2 independent experiments.

Using intravital imaging, we detected the recruitment of transferred cells at the site of infection with a marked increase in GFP$^+$ cell numbers upon suppression of iNOS activity (**Figure 20**).

We confirmed this result using flow cytometry with a significant enhancement of myeloid cell (including neutrophils) recruitment upon iNOS inhibition (**Figure 21**).

Notably, a sizable fraction (~6%) of newly recruited cells including neutrophils and monocyte-derived cells became infected in wild-type mice during this short window of time (**Figure 22**).

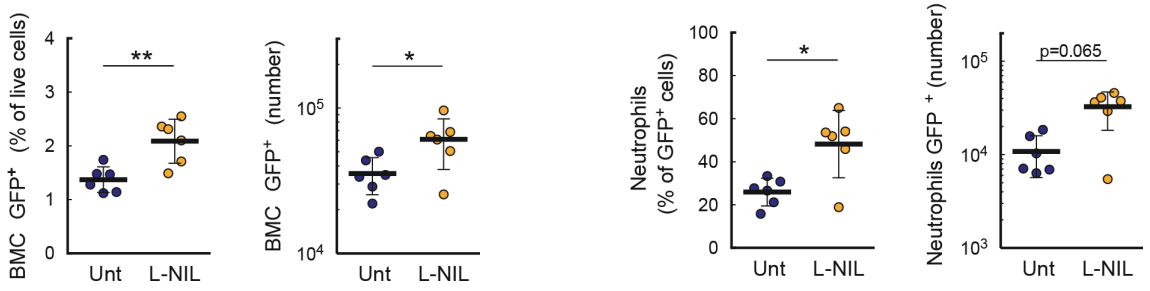

Figure 21. NO limits the accumulation of recruited cells at the site of *L. major* infection

Percentages and absolute cell numbers of total GFP$^+$ cells and GFP$^+$ neutrophils in infected ears from untreated (blue circles) and L-NIL-treated (orange circles) mice as assessed by flow cytometry.

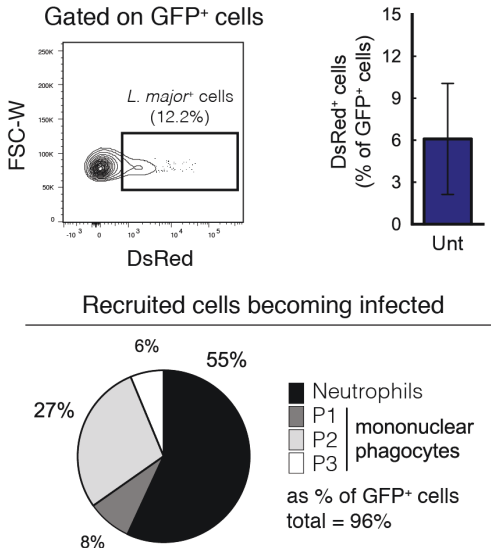

Figure 22. The infection by *L. major* is fueled by a regular recruitment of myeloid cells

Top. Contour plot and quantification of infection among recruited GFP$^+$ cells in untreated mice. *Bottom.* Pie chart showing the cellular composition of infected cells among the recruited GFP$^+$ cells. Results are representative of 6 independent experiments.

Our results suggest that the constant recruitment of myeloid cells contributes to fuel *L. major* infection and, most importantly, that iNOS activity limits such a self-sustained process.

***

II. NO RESTRICTS MACROPHAGE FUNCTION *in vivo* AND *in vitro*

II.1. NO dampens monocyte-derived cell activity at the site of *L. major* infection

Having shown that NO limits the overall cytokine production in the infected tissue, we asked whether this effect was uniquely due to a reduced accumulation of cytokine-producing immune cells or whether NO exerted an additional effect on immune cell activity. We focused on monocyte-derived cells, the major population of myeloid cells at the site of infection and analyzed cytokine production at the single cell level, in infected mice upon transient inhibition of iNOS (**Figure 23**).

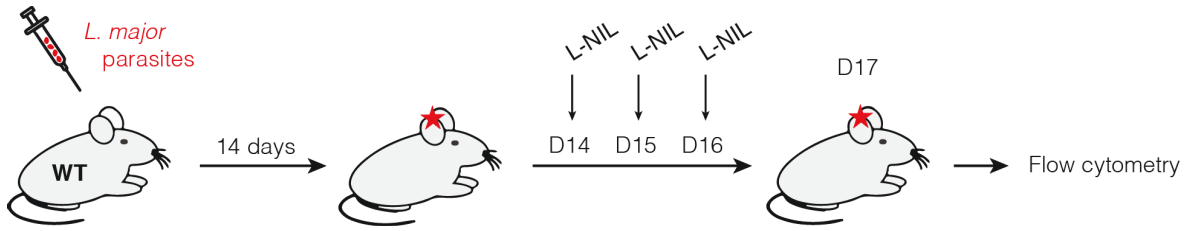

Figure 23. Experimental set-up to study the impact of NO on monocyte-derived cell activity at the site of *L. major* infection

Experimental set-up. WT mice were infected with DsRed-expressing *L. major* and treated 14 days later with the specific iNOS inhibitor L-NIL. Monocyte-derived cell activity (P2 and P3 gates) was assessed 3 days later by intracellular cytokine staining on isolated ear cells.

As shown in **Figure 24**, we observed an increased percentage of TNF-α-producing cells as well as an increased cytokine production on a per cell basis in infected mice in which iNOS activity was suppressed. This effect was not specific to TNF-α since we obtained similar results by analyzing the production of two other cytokines: pro-IL-1β and CCL3 (**Figure 24**).

Similar effects were observed when either total or infected cells were analyzed (**Figure 25**). These results indicate that NO produced by monocyte-derived cells at the site of infection dampens their ability to produce cytokines and chemokines.

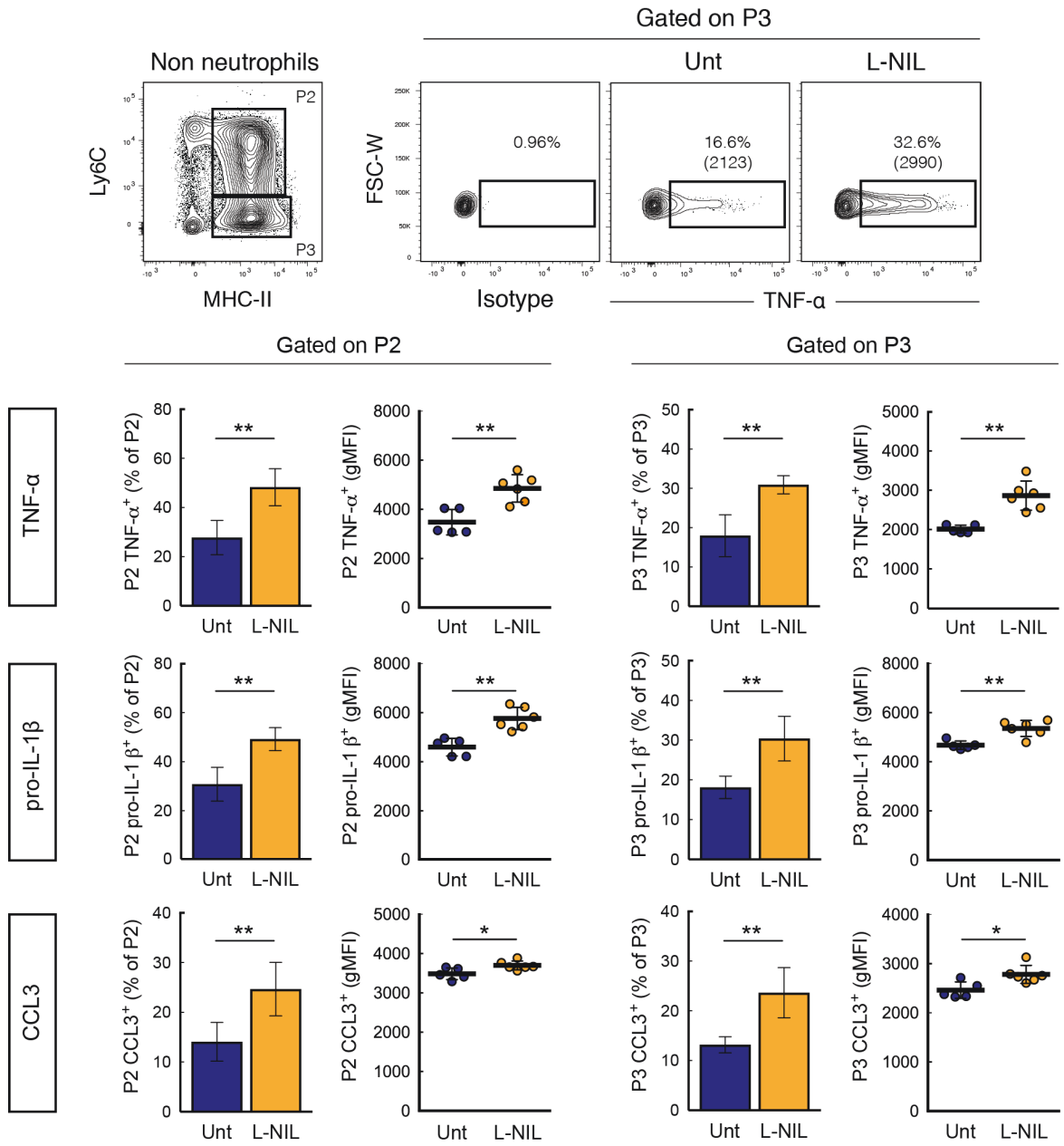

Figure 24. NO dampens monocyte-derived cell activity at the site of *L. major* infection

Top. Contours plots showing TNF-α staining in monocyte-derived cells from untreated or L-NIL-treated mice. Percentages and gMFI (in brackets) of producing cells are shown in respective plots. *Bottom.* Percentages (bars) and gMFI (scatter dot plots) of TNF-α-, pro-IL-1β- or CCL3-producing monocytes-derived cells (P2 and P3 gates) from untreated (blue) and L-NIL-treated (orange) mice as assessed by flow cytometry. Results are representative of 2 independent experiments with 6 ears analyzed per group and per experiment.

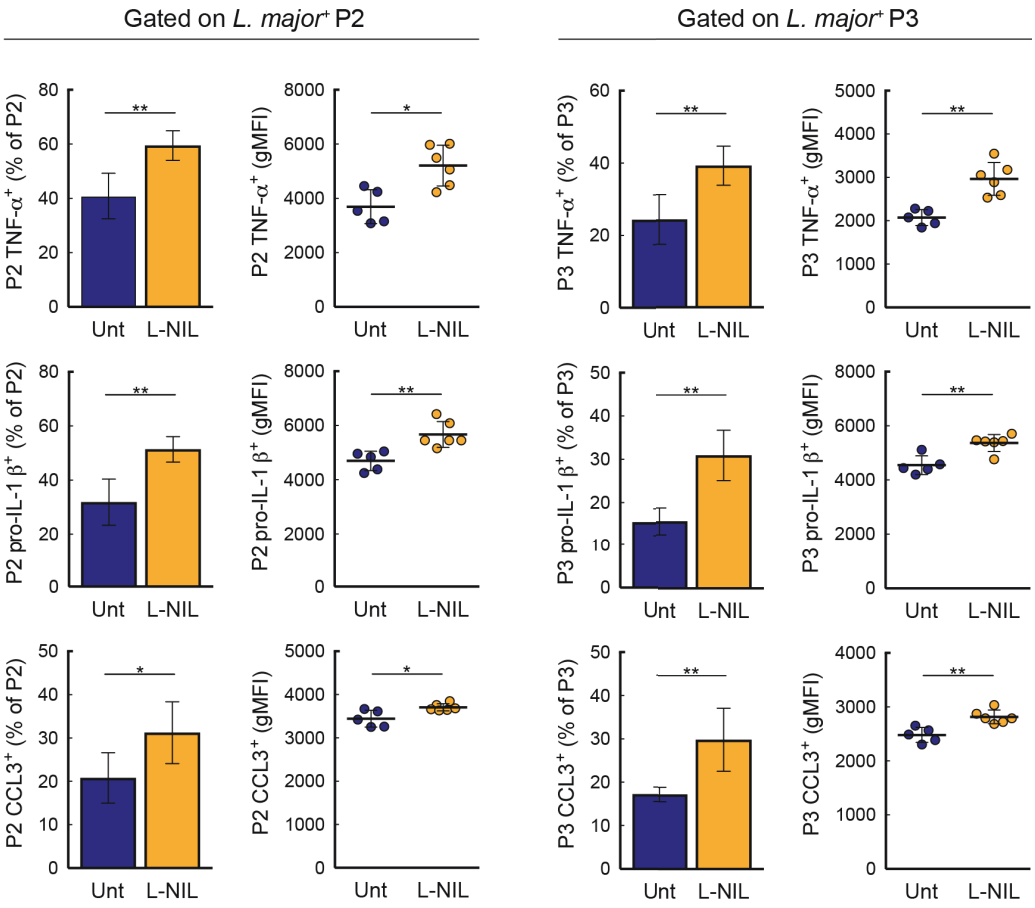

<u>Figure 25.</u> NO limits infected monocyte-derived cell activity at the site of *L. major* infection

WT mice were infected with DsRed-expressing *L. major* and treated 14 days later with the specific iNOS inhibitor L-NIL. The activity of infected (DsRed$^+$) monocyte-derived cells was assessed 3 days later by intracellular cytokine staining on isolated ear cells. Percentages (bars) and gMFI (scatter dot plots) of TNF-α-, pro-IL-1β- or CCL3-producing monocytes-derived cells in P2 (left) or P3 (right) gates.

II.2. NO limits monocyte-derived cell activity during IFA-induced inflammation

When assessing the effects of L-NIL treatment, we found that a 3-days inhibition of iNOS also increased the percentage of infected monocyte-derived cells (**Figure 26**).

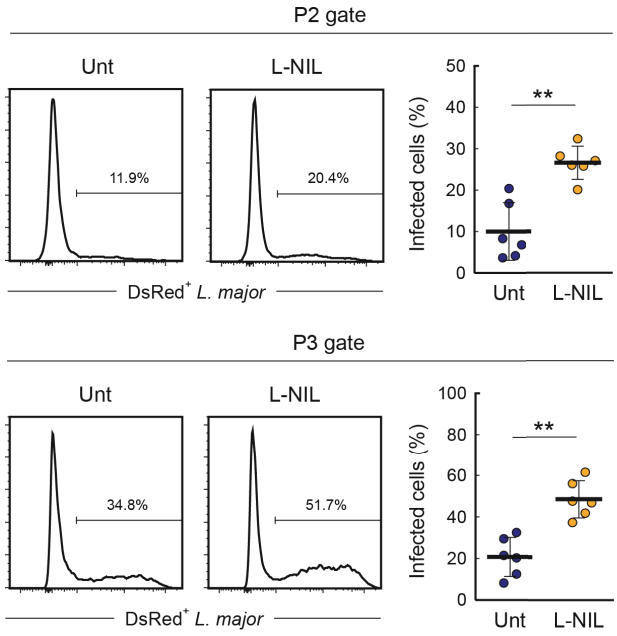

Figure 26. Effect of iNOS inhibition on monocyte-derived cell infection

WT mice were infected with DsRed-expressing *L. major* and treated 14 days later with the specific iNOS inhibitor L-NIL. Three days later, the percentage of infected monocyte-derived cells in the P2 (top) and P3 (bottom) populations was measured by flow cytometry. Numbers indicate the percentage of $DsRed^+$ cells. Plots shows the percentage of infected cells in individual ears.

While this could be the result of the increased immune cell recruitment at the site of infection, it could also reflect NO antimicrobial activity. Therefore, it was important to test whether NO mediated its effects indirectly by influencing pathogen load or by direct alteration of cellular activity. To test the latter possibility, we analyzed how NO affects monocyte-derived cell activity in a non-infectious model of inflammation using emulsified incomplete Freund's adjuvant (**Figure 27**).

In this model, we observed massive recruitment of myeloid cells including the three aforementioned mononuclear phagocytes populations (P1, P2, P3) (**Figure 28**) and a robust induction of iNOS (**Figure 29**).

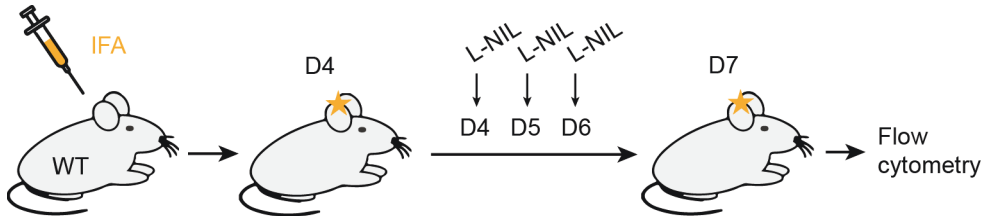

Figure 27. Experimental set-up to study the impact of NO on monocyte-derived cells during IFA-induced inflammation

Experimental set-up. WT mice were intradermally injected with emulsified incomplete Freund's adjuvant (IFA) and treated 4 days later with the specific iNOS inhibitor L-NIL. Monocyte-derived cells activity in inflamed ears were characterized 3 days later.

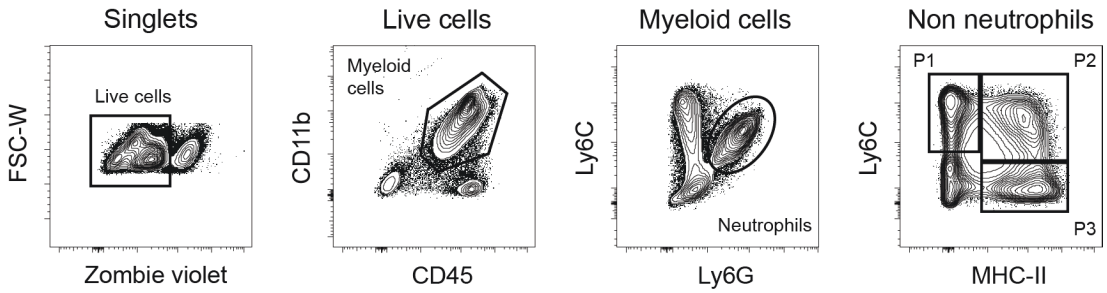

Figure 28. IFA induces inflammation that recruit monocyte-derived cells as at the site of *L. major* infection

Flow cytometry contour plots showing the accumulation of mononuclear phagocytes (P1, P2 and P3) in the inflamed ear. A third of the ear cell preparation was used flow cytometric analysis and >200000 cells were acquired.

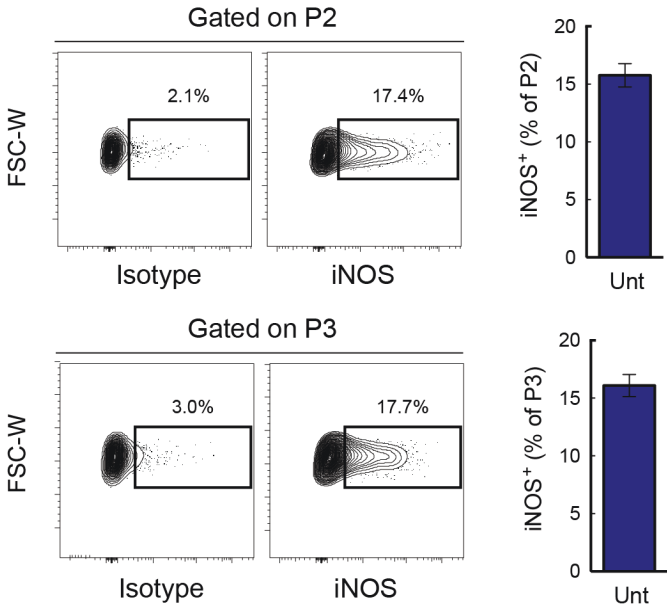

Figure 29. IFA-induced inflammation is associated with a high iNOS expression in monocyte-derived cells

Left. Contour plots showing iNOS staining in monocyte-derived cells isolated from a WT mouse. *Right*. Percentages of iNOS expressing monocyte-derived cells in inflamed ear from untreated mice. Data are represented as mean ± SEM with 16 ears analyzed for each condition.

Importantly, treatment with L-NIL increased monocyte-derived cell activity as measured by TNF-α, CCL2 and CCL3 production (**Figure 30**).

These results suggest that NO can restrict monocyte-derived cell activity independently of any potential effect on pathogen burden

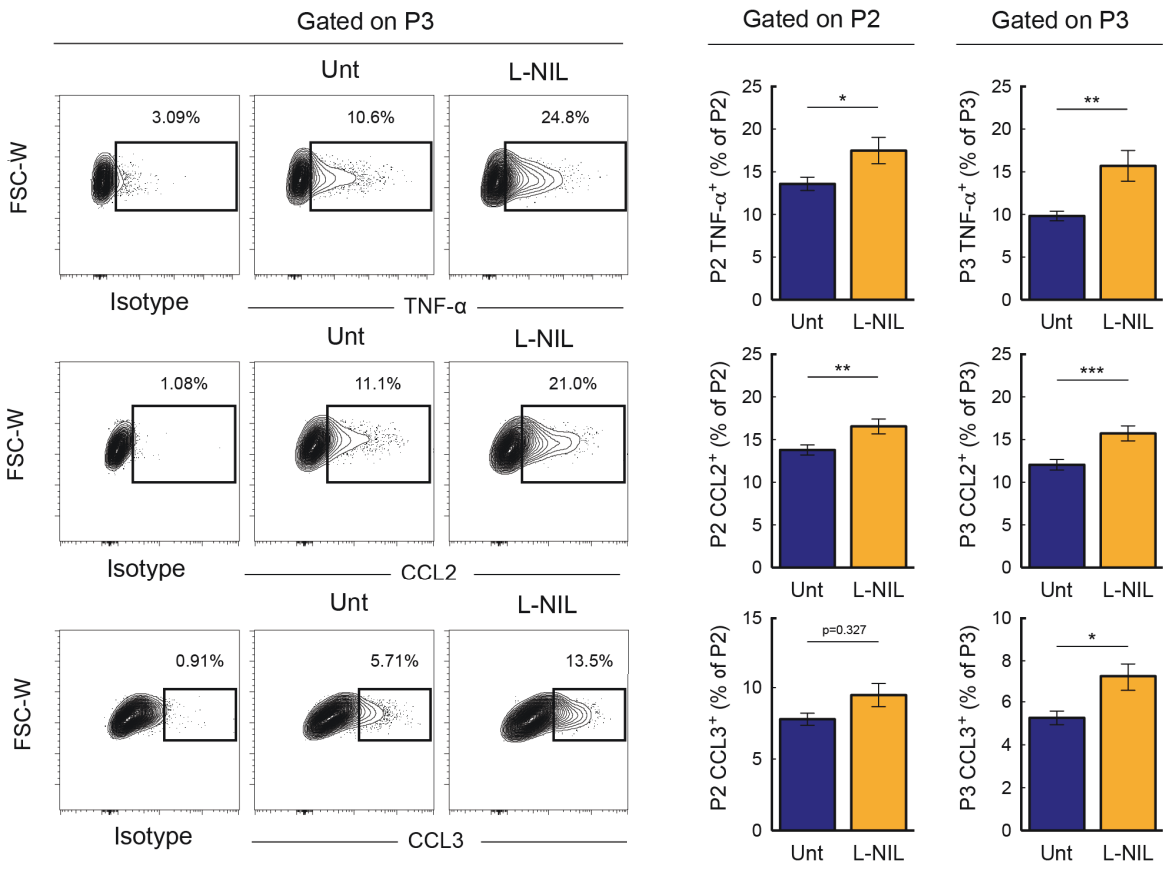

Figure 30. NO limits monocyte-derived cell activity during IFA-induced inflammation

Left. Representative contour plots showing cytokine stainings in monocyte-derived cells. *Right.* Percentages of TNF-α-, CCL2- or CCL3-producing monocytes-derived cells (P2 and P3 gates) from untreated and L-NIL-treated mice as assessed by flow cytometry. Data are represented as mean ± SEM with 16 ears analyzed for each condition.

II.3. NO broadly restricts BMDM activity *in vitro*

To further confirm and dissect the direct effect of NO on immune cells, we activated WT or *Nos2*$^{-/-}$ bone marrow-derived macrophages *in vitro* and in the absence of pathogen with

LPS+IFN-γ, a treatment that induces iNOS expression in WT cells. As shown in **Figure 31**, LPS+IFN-γ treatment induced the intracellular production of the tested cytokines (pro-IL-1β and CCL2) in both WT and *Nos2*$^{-/-}$ macrophages. However, cytokine production was significantly higher in *Nos2*$^{-/-}$ macrophages.

We repeated these experiments by treating WT macrophages with L-NIL to suppress NO production in order to exclude any potential additional defect of cells isolated from *Nos2*$^{-/-}$ mice. Consistently, we observed higher production of pro-IL-1β and CCL2 in the presence of iNOS inhibition (**Figure 32**).

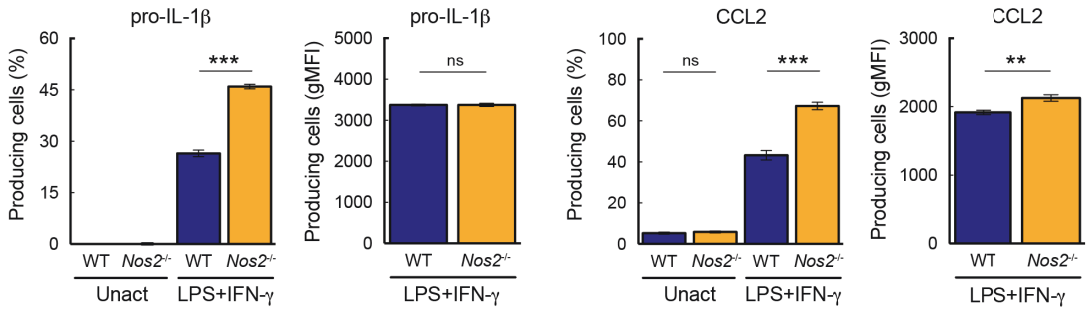

Figure 31. NO dampens uninfected BMDM activity

WT or *Nos2*$^{-/-}$ BMDMs were activated 24 h with LPS+IFN-γ or left unactivated. Percentages and gMFI of pro-IL-1β (left) and CCL2 (right) producing WT (blue bars) or *Nos2*$^{-/-}$ (orange bars) cells as assessed using intracellular cytokine staining. Representative of 4 independent experiments.

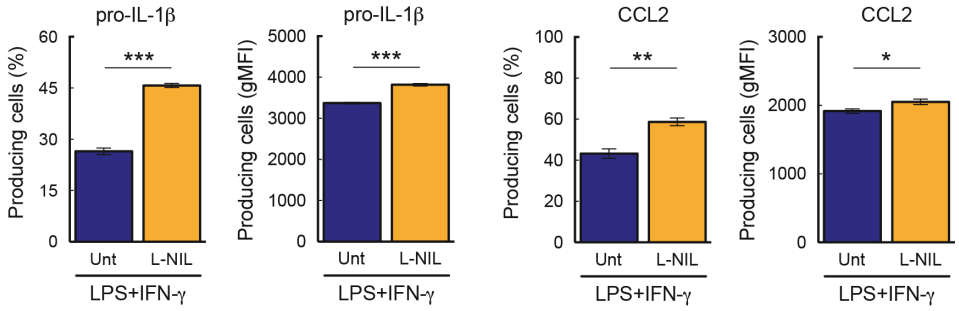

Figure 32. Treatment with L-NIL increases uninfected BMDM activity

WT BMDMs were activated 24 h with LPS+IFN-γ or left unactivated. Percentages and gMFI of pro-IL-1β- (left) and CCL2- (right) producing BMDMs cultured in the absence (blue bars) or presence (orange bars) of L-NIL.

As expected, L-NIL had no effects on *Nos2*$^{-/-}$ macrophages or on WT unactivated macrophages (**Figure 33**).

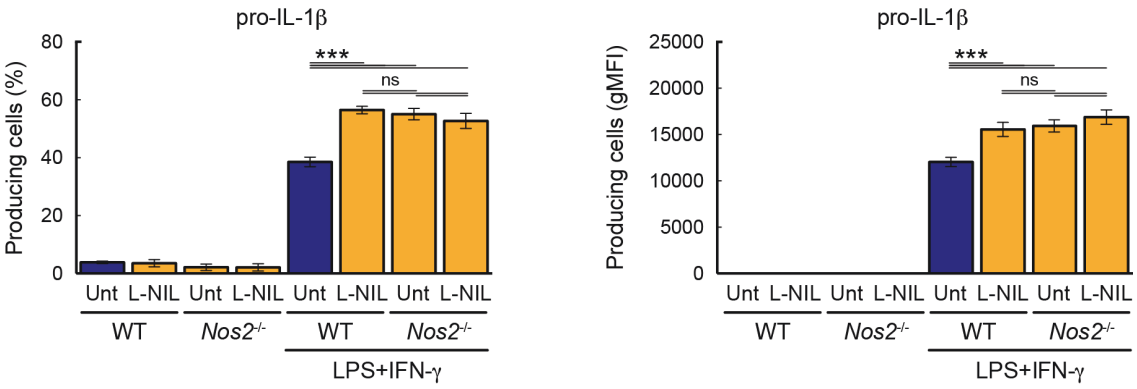

Figure 33. L-NIL-induced effect is not mediated by an off-target mechanism

WT or *Nos2*$^{-/-}$ BMDMs were activated 24h with LPS+IFN-γ or left unactivated in the presence or absence of L-NIL. Percentages (left) and gMFI (right) of pro-IL-1β producing WT or *Nos2*$^{-/-}$ cells treated with L-NIL or left untreated as assessed by intracellular cytokine staining.

We extended the aforementioned results obtained with intracellular cytokine staining by performing multi-analyte cytokine profiling on macrophage supernatants. Reflecting the effect of iNOS inhibition during *L. major* infection, *Nos2*$^{-/-}$ macrophages exhibited an overall increased production of inflammatory cytokines and chemokines, including IL-1α, IL-1β, IL-6, CXCL10, CCL2, CCL3 (**Figure 34**).

These results suggest that NO acts on macrophages to limit cytokine and chemokine production both *in vitro* and *in vivo*.

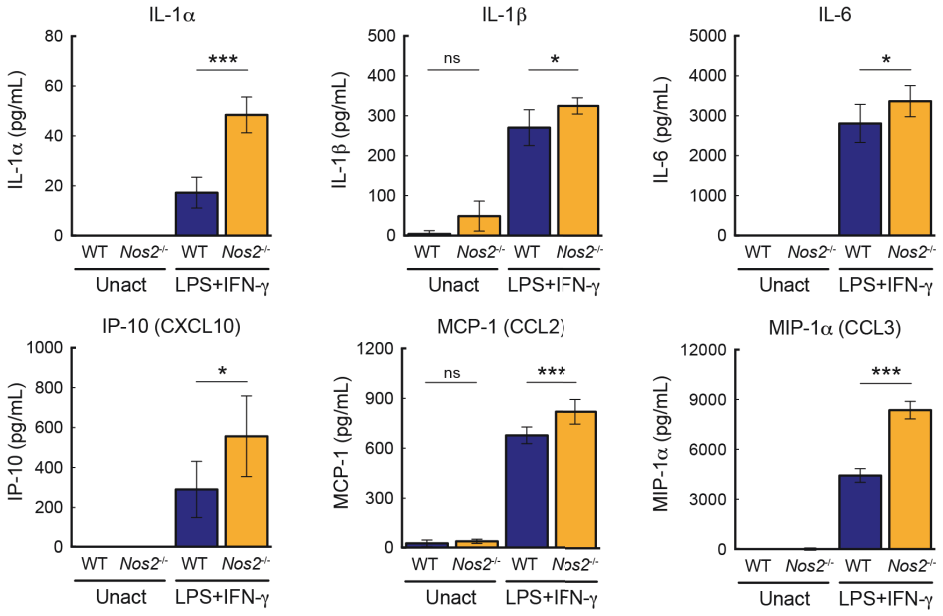

Figure 34. NO restricts cytokine/chemokine secretion by uninfected BMDMs

WT or *Nos2*$^{-/-}$ BMDMs were activated 24 h with LPS+IFN-γ or left unactivated. Cytokines (IL-1α, IL-1β, IL-6) and chemokines (CXCL10, CCL2 and CCL3) quantification in WT or *Nos2*$^{-/-}$ BMDM supernatants as assessed by multiplex assay. Results are representative of 2 independent experiments with 6 replicates per conditions and per experiment.

***

III. NO BLOCKADE OF MITOCHONDRIAL RESPIRATION RESTRICTS ATP:ADP RATIO AND MACROPHAGE ACTIVITY

III.1. NO blocks mitochondrial respiration in macrophages

Given the broad suppression of cytokine production by NO, we asked whether this effect could originate from a change in cellular metabolism (Biswas and Mantovani, 2012; Everts et al., 2012; Lu et al., 2015; Na et al., 2018; Sancho et al., 2017; Thwe and Amiel, 2018; Van den Bossche et al., 2016, 2017). Consistent with this idea, we observed that WT macrophages engage glycolysis but stop relying on oxidative phosphorylation upon activation as measured by decreased basal respiration and ATP synthesis (**Figure 35**). By contrast, *Nos2*$^{-/-}$ macrophages used both respiration and glycolysis upon activation (**Figure 35**). Overall, glycolytic activity (**Figure 36**) and glucose uptake (**Figure 37**) were not affected by iNOS activity.

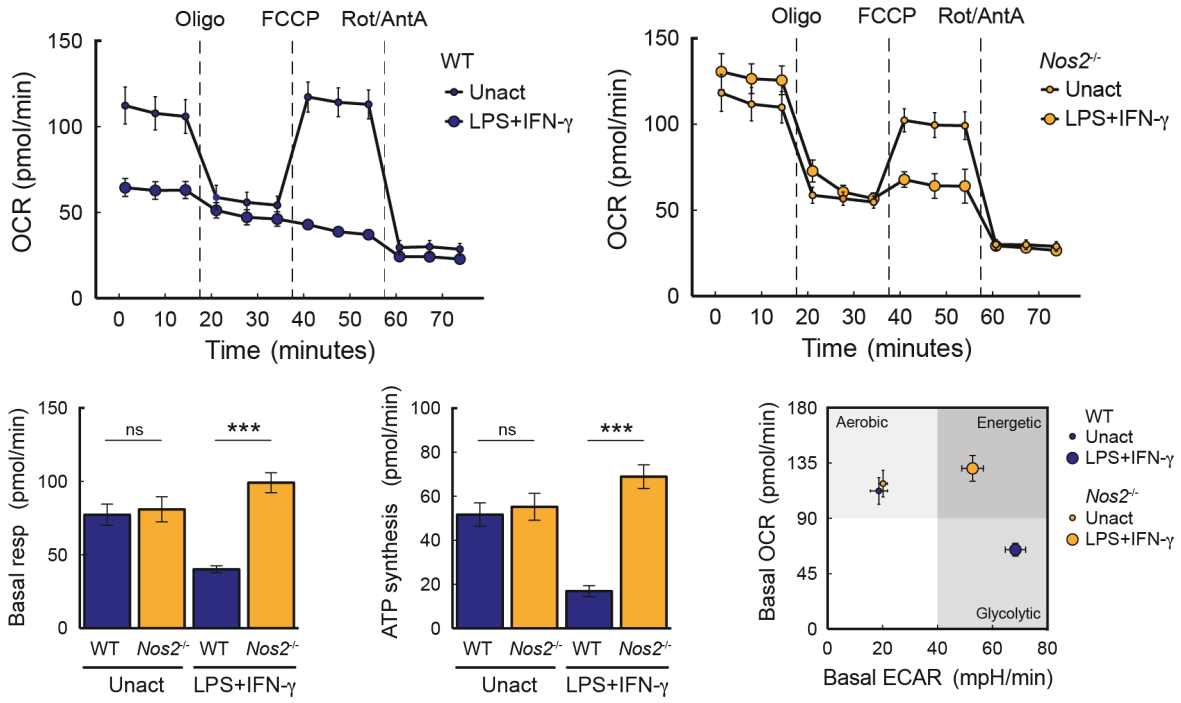

Figure 35. NO dampens respiration in uninfected BMDMs

WT or *Nos2*$^{-/-}$ BMDMs were activated 24 h with LPS+IFN-γ or left unactivated before extracellular flux analysis. *Top.* Oxygen consumption rate (OCR) measured during sequential treatments with oligomycin, FCCP and rot/antA on WT and *Nos2*$^{-/-}$ BMDMs. *Bottom.* Quantification of ATP synthesis and basal respiration based on OCR variations for WT (blue bars) and *Nos2*$^{-/-}$ (orange bars) BMDMs. Basal OCR and ECAR are graphed for the indicated populations to represent their metabolic phenotypes. Representative of 3 independent experiments.

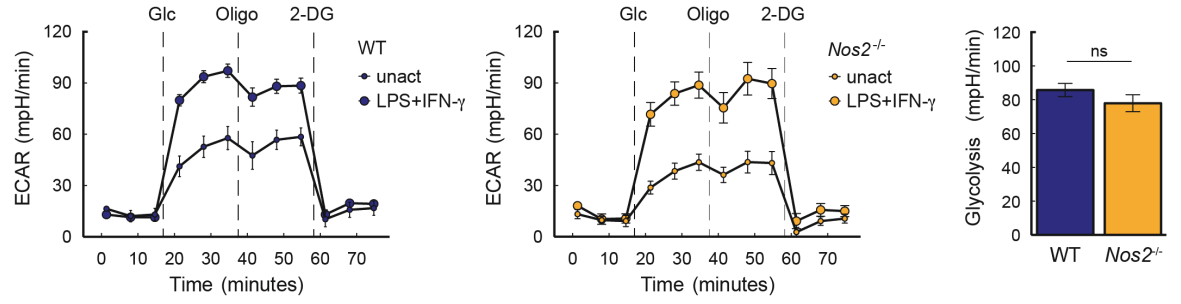

Figure 36. NO activity does not impact glycolysis in uninfected BMDMs

WT or *Nos2*$^{-/-}$ BMDMs were activated 24 h with LPS+IFN-γ or left unactivated before extracellular flux analysis. Extracellular acidification rate (ECAR) measured during sequential treatments with glucose, oligomycin and 2-DG on WT and *Nos2*$^{-/-}$ BMDMs (left and middle panels). Quantification of glycolysis based on ECAR variations is shown for on WT and *Nos2*$^{-/-}$ BMDMs (right panel).

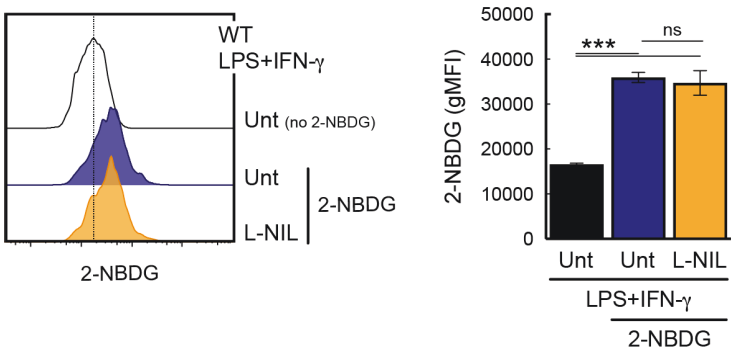

Figure 37. NO activity does not impact glucose uptake in uninfected BMDMs

WT BMDMs were activated 24 h with LPS+IFN-γ in the presence or absence of L-NIL and incubated with 2-NBDG for an additional hour. Uptake was measured by flow cytometry. Representative histograms (left) and bar plots (right) are shown for the indicated conditions.

Similarly, blocking iNOS activity with L-NIL in WT macrophages restored their respiratory capacity when activated (**Figure 38**).

To confirm these findings at the single cell level, we used a combination of dyes to measure total (MitoTracker GreenFM) and respiring (MitoTracker Red CMXRos) mitochondria by flow cytometry. A drop in cell respiration was seen upon activation of WT but not *Nos2*$^{-/-}$ macrophages (**Figure 39 left**). Again, blocking iNOS activity in WT macrophages was sufficient to restore respiration (**Figure 39 right**).

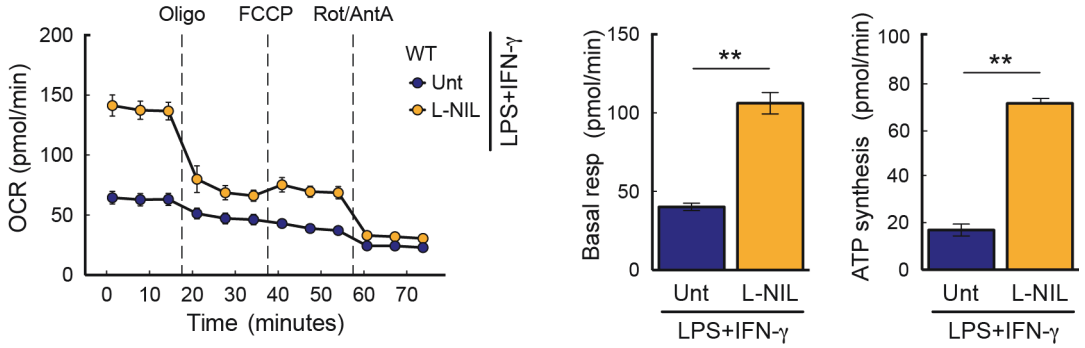

Figure 38. Treatment with L-NIL restores respiration in uninfected BMDMs

Left. OCR was measured on untreated or L-NIL-treated WT activated BMDMs. *Right.* Quantification of ATP synthesis and basal respiration based on OCR variations for untreated (blue bars) or L-NIL-treated WT (orange bars) activated BMDMs.

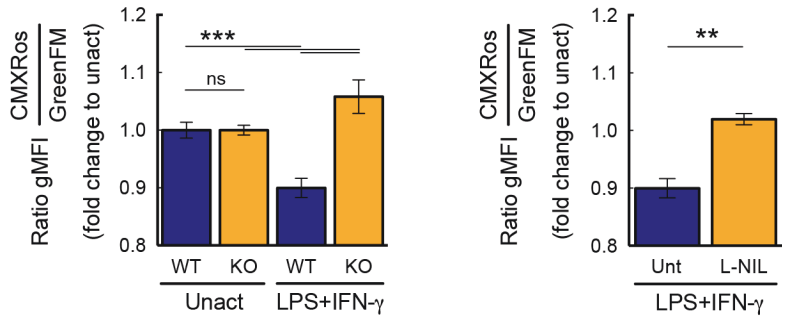

Figure 39. NO limits respiration at the single cell level in uninfected BMDMs

WT or *Nos2*$^{-/-}$ BMDMs were activated 24 h with LPS+IFN-γ or left unactivated and loaded with MitoTracker GreenFM (total mitochondria) and MitoTracker CMXRos (respiring mitochondria) to assess mitochondrial activity by flow cytometry. The ratio between MitoTracker CMXRos gMFI and MitoTracker GreenFM gMFI was calculated for each condition. Results are shown as fold change for the activated compared to the unactivated condition for (left) WT and *Nos2*$^{-/-}$ cells or (right) untreated or L-NIL-treated WT cells.

To test whether these findings pertain to monocyte-derived cells *in vivo* at the site of *L. major* infection, we sorted monocyte-derived cells from the ears of infected WT mice and subjected them to metabolic flux analysis in the presence or absence of L-NIL. As observed with *in vitro* macrophages, *ex vivo*-isolated WT monocyte-derived cells displayed a block in respiration that was relieved by a short incubation (2h) with L-NIL (**Figure 40**).

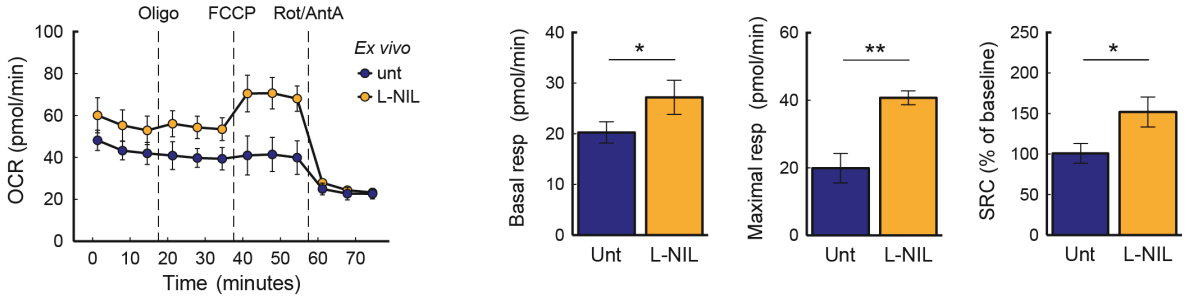

Figure 40. Transient treatment with L-NIL restores respiration in monocyte-derived cells at the site of *L. major* infection

Left. OCR was measured on monocyte-derived cells isolated from infected ears. Cells were left untreated or treated with L-NIL for 2 h *ex vivo*. *Right.* Quantification of basal respiration, maximal respiration and spare respiratory capacity (SRC) based on OCR variations for untreated (blue bars) or L-NIL-treated (orange bars) cells. Results were evaluated using a two-tailed unpaired Student's t-test with Welch's correction. Results are representative of six mice analyzed in 2 independent experiments.

These results demonstrate that NO production by macrophages drastically suppresses their respiratory capacity, in both BMDMs and monocyte-derived cells at the site of infection.

III.2. NO dampens ATP:ADP ratio in BMDMs that limits their activity

To further characterized the impact of NO on cellular metabolism, we relied on PercevalHR, a genetically-encoded fluorescent probe for monitoring ATP:ADP ratio hence providing a readout for the energetic status of individual cells in real-time (Tantama et al., 2013). Upon NO exposure, we observed a drop in ATP:ADP ratio in activated and L-NIL-treated PercevalHR-expressing macrophages within less than 10 minutes, as measured by time-resolved flow cytometry (**Figure 41 left**). These findings were confirmed by following individual PercevalHR-expressing macrophages using live-imaging (**Figure 41 right**).

Thus, one important consequence of NO targeting of mitochondrial respiration is the rapid and substantial reduction in the cellular ATP:ADP ratio. We next ask whether such energetic changes could explain the reduced cytokine production in macrophages exposed to NO. We therefore specifically inhibited the ATP synthase using oligomycin (that targets the F0 subunit of the ATP synthase). We noted that oligomycin treatment induced a drop in ATP:ADP ratio similar to that observed with NO (**Figure 42**).

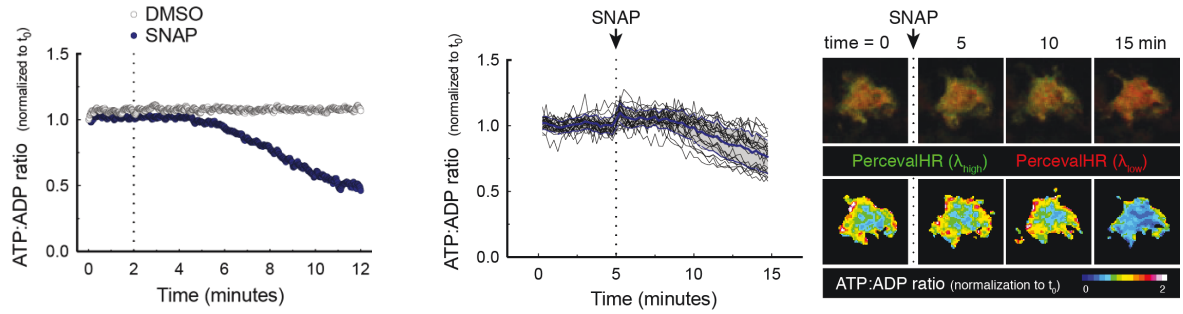

Figure 41. NO dampens ATP:ADP ratio in uninfected BMDMs

Single-cell measurement of ATP:ADP ratio in BMDMs. PercevalHR-expressing BMDMs were activated 24 h with LPS+IFN-γ in the presence of L-NIL. *Left.* ATP:ADP ratio was calculated using PercevalHR fluorescence measured at λ_{low} = 405 nm and λ_{high} = 488 nm excitation wavelengths (see Experimental procedure). The graph shows the geometric mean for the normalized ATP:ADP ratio as a function of the acquisition time. *Right.* Live-imaging of ATP:ADP ratio in BMDMs exposed to SNAP (100 μM) using two-photon excitation λ_{low} = 830 nm and λ_{high} = 1040 nm). Quantification for multiple cells (left) and representative time-lapse images (right) are shown.

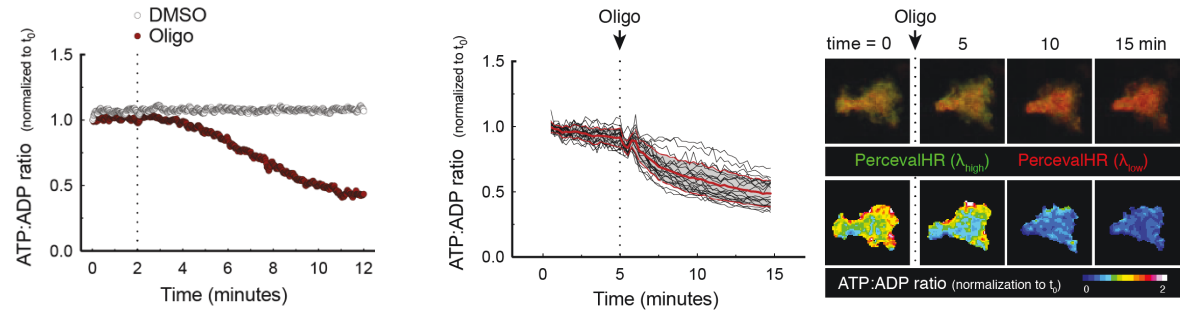

Figure 42. Oligomycin dampens ATP:ADP ratio similar to SNAP in uninfected BMDMs

Single-cell measurement of ATP:ADP ratio in BMDMs. PercevalHR-expressing BMDMs were activated 24 h with LPS+IFN-γ in the presence of L-NIL. *Left.* ATP:ADP ratio was measured in BMDMs immediately following incubation with the ATP synthase inhibitor oligomycin (1 µM) (or DMSO as a control) by time-resolved flow cytometry. *Right.* Live-imaging of ATP:ADP ratio in BMDMs exposed to oligomycin (1 µM). Results are representative of three independent experiments.

Most importantly, a short term (4 h) inhibition of ATP synthase in macrophages was sufficient to reduce cytokine and chemokine production as measured by intracellular cytokine staining (**Figure 43**) and multi-analyte cytokine profiling (**Figure 44**).

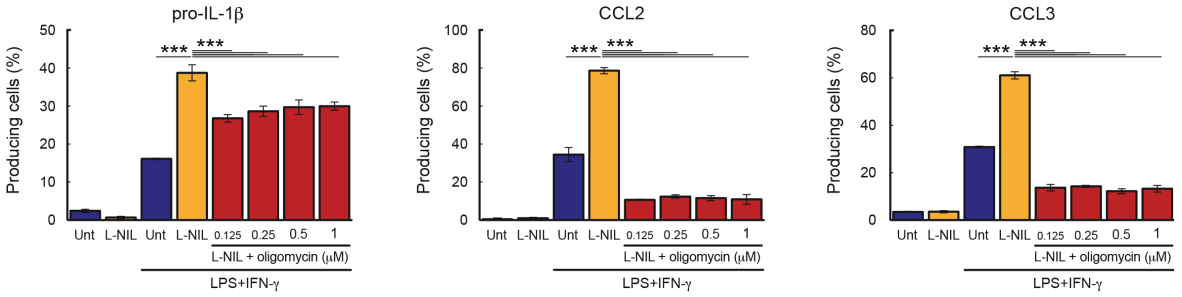

Figure 43. Oligomycin in the absence of NO limits uninfected BMDMs activity

BMDMs were activated 24 h with LPS+IFN-γ in the presence or in the absence of L-NIL or left untreated. When indicated BMDMs were incubated with various concentration of oligomycin for the last 4 h of the culture. Percentages of cytokine-producing cells were assessed by intracellular cytokine staining for pro-IL-1β, CCL2 and CCL3. Representative of 3 independent experiments.

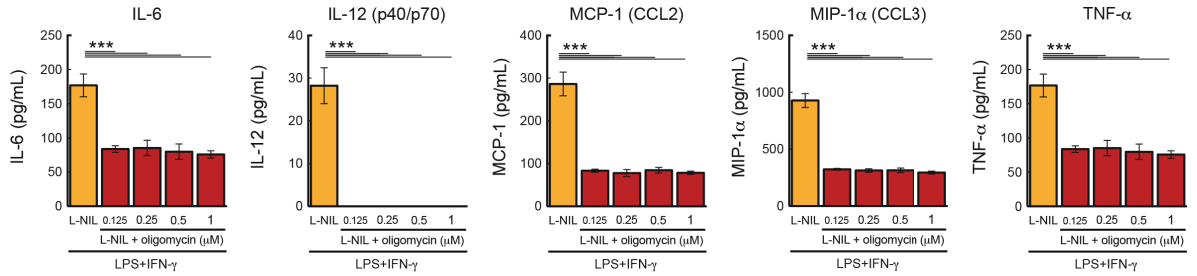

Figure 44. Oligomycin in the absence of NO limits cytokine/chemokine secretion of uninfected BMDMs

BMDMs were activated 24 h with LPS+IFN-γ in the presence or in the absence of L-NIL or left untreated. When indicated BMDMs were incubated with various concentration of oligomycin for the last 4 h of the culture. Cytokines and chemokines in BMDM supernatants cultured in the presence or absence of oligomycin were measured by multiplex assay. Medium was changed in all samples at the time of oligomycin addition.

Similar results were observed by performing the experiment by blocking respiration with azide that targets complex IV of the mitochondrial respiratory chain, which activity precedes that of the ATP synthase (**Figure 45**) or in hypoxic condition (**Figure 46**).

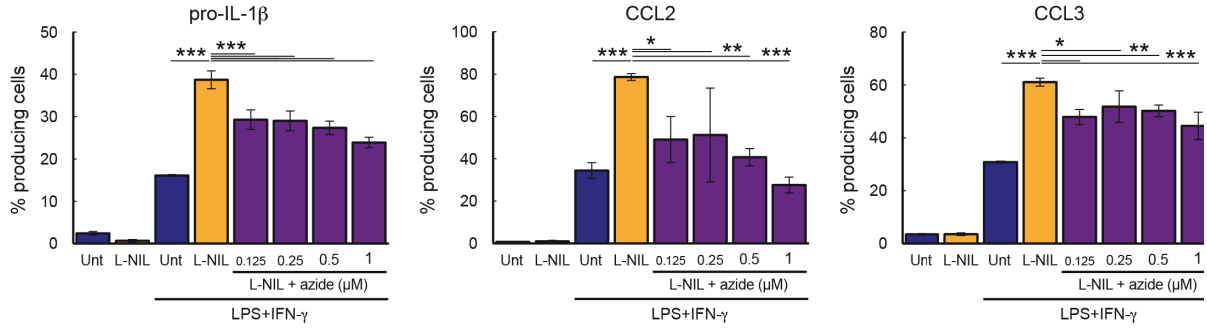

Figure 45. Azide in the absence of NO limits uninfected BMDMs activity

BMDMs were activated 24 h with LPS+IFN-γ in the presence or in the absence of L-NIL or left untreated. When indicated BMDMs were incubated with various concentration of azide for the last 4 h of the culture. Percentages of cytokine-producing cells were assessed by intracellular cytokine staining for pro-IL-1β, CCL2 and CCL3.

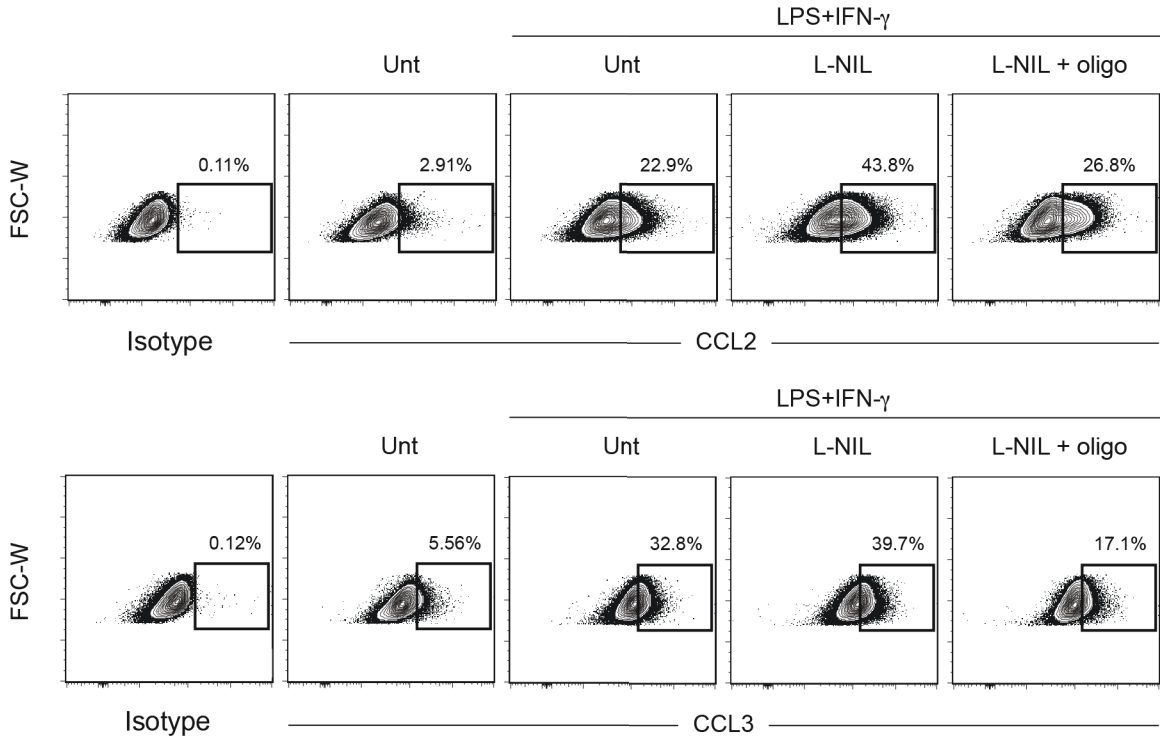

Figure 46. Oligomycin, under hypoxia, without NO, limits uninfected BMDMs activity

WT BMDMs cultivated under hypoxia (pO2=25mmHg) were activated 24 h with LPS+IFN-γ in the presence or absence of L-NIL or left unactivated. When indicated, BMDMs were incubated with oligomycin (1 μM) for the last 4 h of culture. Production of CCL2 (top panel) and CCL3 (bottom panel) was assessed by intracellular cytokine staining. Numbers indicate the percentage of producing cells for each condition.

Together, our results support the idea that NO blockade of mitochondrial respiration rapidly diminishes the cellular energetic resources required for optimal cytokine production.

III.3. NO restricts ATP:ADP ratio in monocyte-derived cells *in vivo*

To test whether NO affect the ATP:ADP ratio *in vivo* during infection, we generated chimeric mice by transducing HSCs with PercevalHR and infected them with *L. major* (**Figure 47**).

Two weeks later, we measured the ATP:ADP ratio in monocyte-derived cells at the infection site in mice treated or not with L-NIL. We observed that iNOS inhibition largely increased cellular ATP:ADP ratio in both P2 and P3 populations (**Figure 48**) supporting the relevance of our model during inflammation *in vivo*.

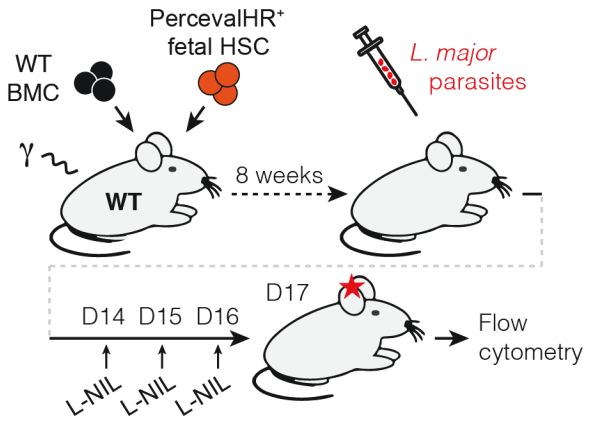

Figure 47. Experimental set-up to study the impact of NO on ATP:ADP ratio in monocyte-derived cells at the site of *L. major* infection

Chimeric mice reconstituted with PercevalHR HSCs were infected with L. major. Two weeks later, some mice were treated with L-NIL for 3 consecutive days. Monocyte-derived cells recovered at the site of infection were analyzed for ATP:ADP ratio (based on PercevalHR fluorescences) by flow cytometry.

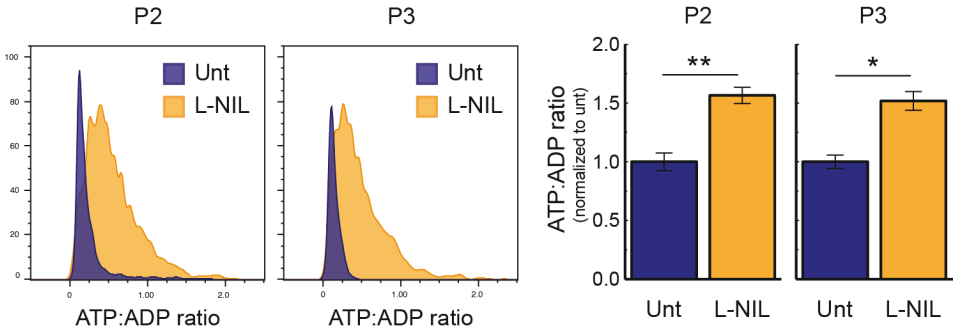

Figure 48. NO lowers ATP:ADP ratio in monocyte-derived cells at the site of *L. major* infection

Representative histograms (left) and bar plot (right) of the ATP:ADP ratio in P2 and P3 populations recovered from infected mice with or without iNOS inhibition. Results were evaluated using a two-tailed unpaired Student's t-test with Welch's correction.

***

IV. Collective NO production provides a quorum-sensing mechanism to dampen chronic inflammation

We next sought to clarify how NO acts in the infected tissue. NO could act in a cell-autonomous manner or act more broadly by diffusing in the tissue. In addition, it was unclear whether NO produced by a single cell has any biological activity or whether the collective production by numerous cells is essential to impact on cellular metabolism.

We first addressed these questions *in vitro* by mixing iNOS competent and deficient macrophages at different ratios to generate distinct densities of NO producing cells at a constant total cell number (**Figure 49**).

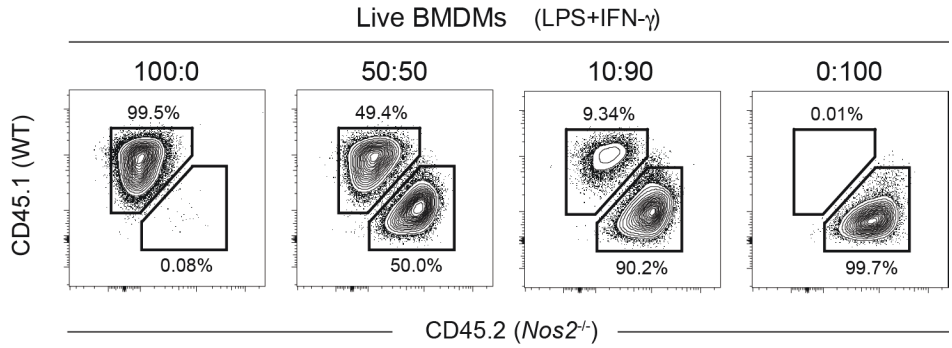

Figure 49. Experimental data showing the ratio obtained *in vitro*

WT or *Nos2*$^{-/-}$ BMDMs were activated 24 h with LPS+IFN-γ either alone (ratios 100:0 and 0:100) or mixed at different ratios (50:50 and 10:90).

We found that the block of cell respiration in macrophages increased with density of NO-producing cells (**Figure 50**). Most importantly, only a modest block in cell respiration was seen in macrophages competent for NO production when these cells were present at low density (10:90 ratio), indicating that the effect on cellular metabolism was by large not cell-intrinsic. Conversely, a block in respiration was detected in *Nos2*$^{-/-}$ macrophages provided that they were surrounded by numerous iNOS competent cells (50:50 ratio) (**Figure 50**).

Importantly, the same rules applied for cytokine and chemokine production (**Figure 51**). Indeed, pro-IL-1β and CCL2 production was suppressed in both WT and *Nos2*$^{-/-}$ macrophages mixed at 50:50 ratio. At lower ratio (10:90), pro-IL-1β and CCL2 production were largely unaffected even in WT macrophages. These results strongly suggest that the density of NO-producing cells plays a crucial role to regulate cell activity.

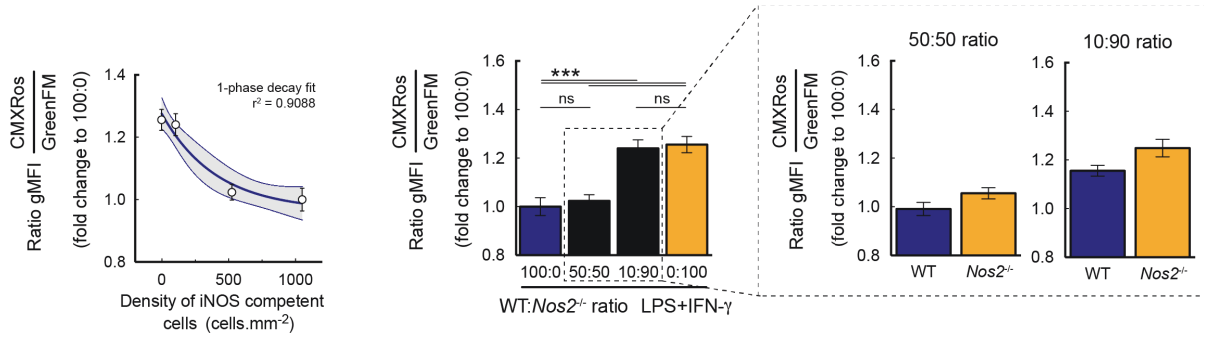

Figure 50. NO acts by diffusion to dampen mitochondria respiration in uninfected BMDMs but only when iNOS competent cells are at high density

WT (CD45.1) or *Nos2*$^{-/-}$ (CD45.2) BMDMs were activated 24 h with LPS+IFN-γ either alone (ratios 100:0 and 0:100) or mixed at different ratios (50:50 and 10:90) and loaded with MitoTracker GreenFM and MitoTracker CMXRos. *Left.* Mitochondrial activity was normalized to the value of activated WT (100:0 ratio) for each group and graphed as a function of the density of iNOS competent cells in the culture. *Right.* Bar plots showing the normalized mitochondrial activity for the different mixed culture conditions. The inset shows the analysis of WT (CD45.1) and *Nos2*$^{-/-}$ (CD45.2) cells in mixed cultures at the indicated ratio.

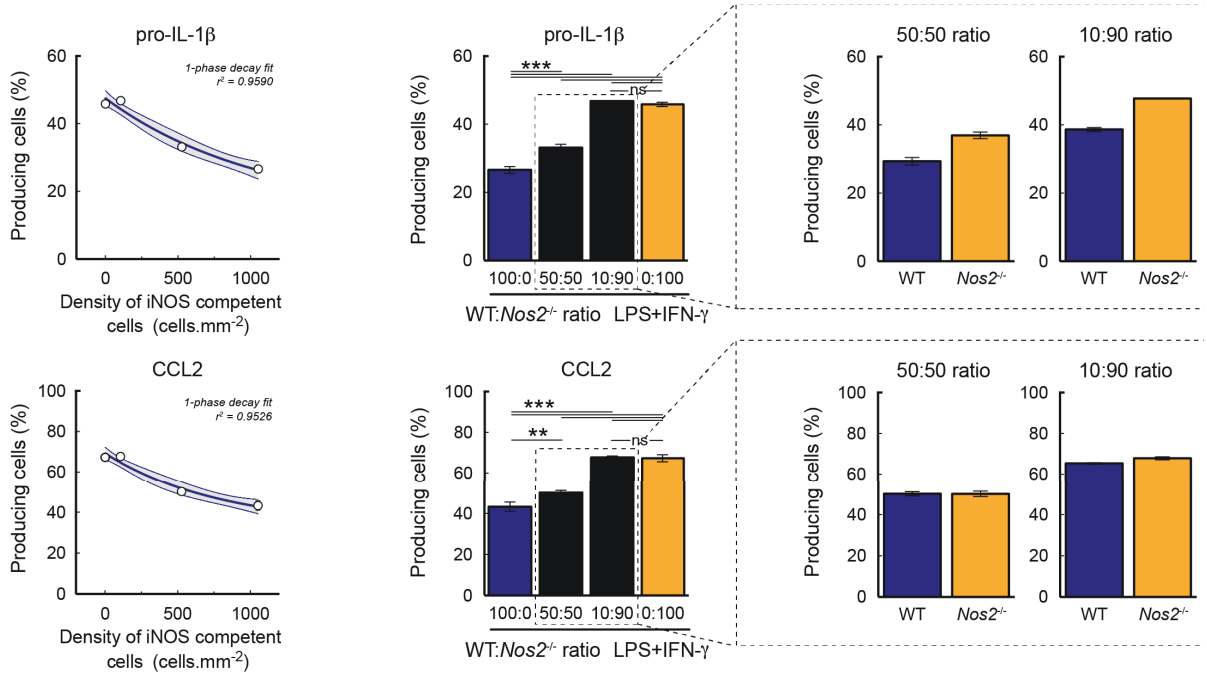

Figure 51. NO acts by diffusion to dampen uninfected BMDM activity but only when iNOS competent cells are at high density

Percentages of cytokine-producing cells were assessed by intracellular cytokine staining for pro-IL-1β and CCL2. *Left.* Percentages of cytokine producing cells were graphed as a function of the density of iNOS competent cells in the culture. *Right.* Bar plots showing the percentages of producing cells for pro-IL-1β (top panel) and CCL2 (bottom panel) for the different mixed culture conditions. The inset shows the analysis of WT (CD45.1) and *Nos2*$^{-/-}$ (CD45.2) cells in mixed cultures at the indicated ratio.

To test this hypothesis *in vivo*, we generated mixed-bone marrow chimeras using various ratios of WT (CD45.1) and *Nos2*$^{-/-}$ (CD45.2) cells for reconstitution (**Figure 52**) in order to establish varying densities of iNOS competent cells at the infection site (**Figure 53**).

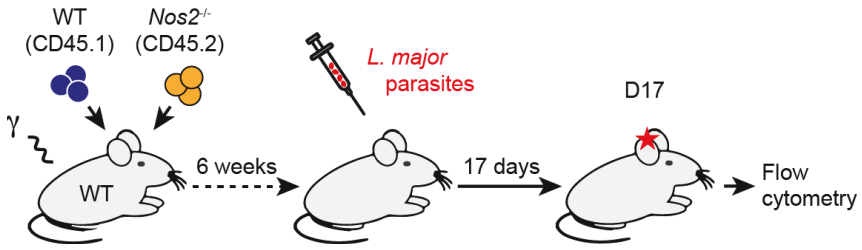

Figure 52. Experimental set-up to study the impact of NO by diffusion at the site of *L. major* infection

Experimental set-up. CD45.1 WT recipient mice were lethally irradiated and reconstituted with CD45.1 WT and CD45.2 Nos2-/- bone marrow cells, mixed at different ratios. Chimeras were infected 6 weeks later with DsRed-expressing *L. major*. Monocyte-derived cells activity was assessed 17 days later by intracellular cytokine staining on extracted ear cells.

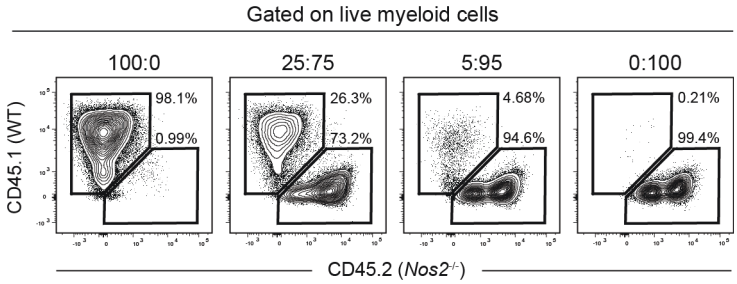

Figure 53. Experimental data showing the ratio obtained at the site of *L. major* infection

Cellular composition in the ear of infected mixed-bone marrow chimeras.

The corresponding cellular densities were estimated by intravital imaging using bone-marrow chimeras reconstituted with various ratios of WT (GFP^{-}) and MAFIA (GFP^{+} monocyte-derived cells) cells (**Figure 54**, **Figure 55**).

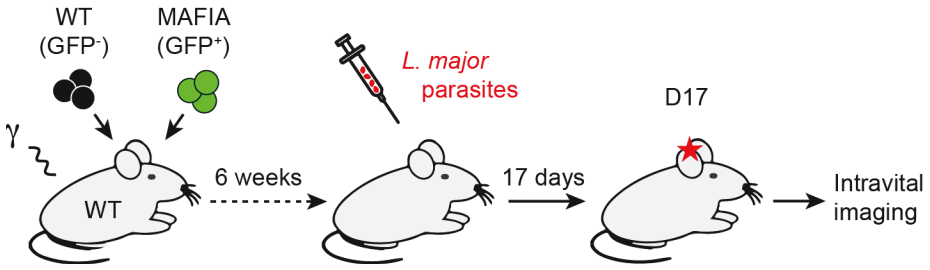

Figure 54. Experimental set-up to establish the correlation at the site of *L. major* infection between the GFP$^+$ cell density and the percentage of GFP$^+$ cell used for reconstitution

Experimental set-up. WT recipient mice were lethally irradiated and reconstituted with WT (GFP$^-$) and MAFIA (GFP$^+$) bone marrow cells, mixed at different ratios. Chimeras were infected 6 weeks later with DsRed-expressing *L. major*. 17 days later, intravital imaging was performed to visualize GFP$^+$ cells in the infected skin.

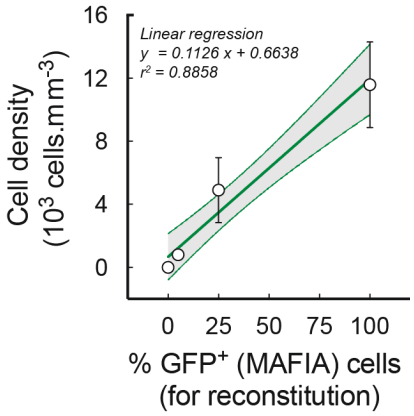

Figure 55. The GFP$^+$ cell density and the percentage of GFP$^+$ cell used for reconstitution are linearly correlated

Left. GFP$^+$ cell density (number of GFP$^+$ cells per mm^3) was correlated with the percentage of GFP$^+$ cells used to reconstitute chimera recipients. *Bottom.* 3D volume reconstruction was used to determine GFP$^+$ cell numbers and the corresponding cell densities at the site of infection.

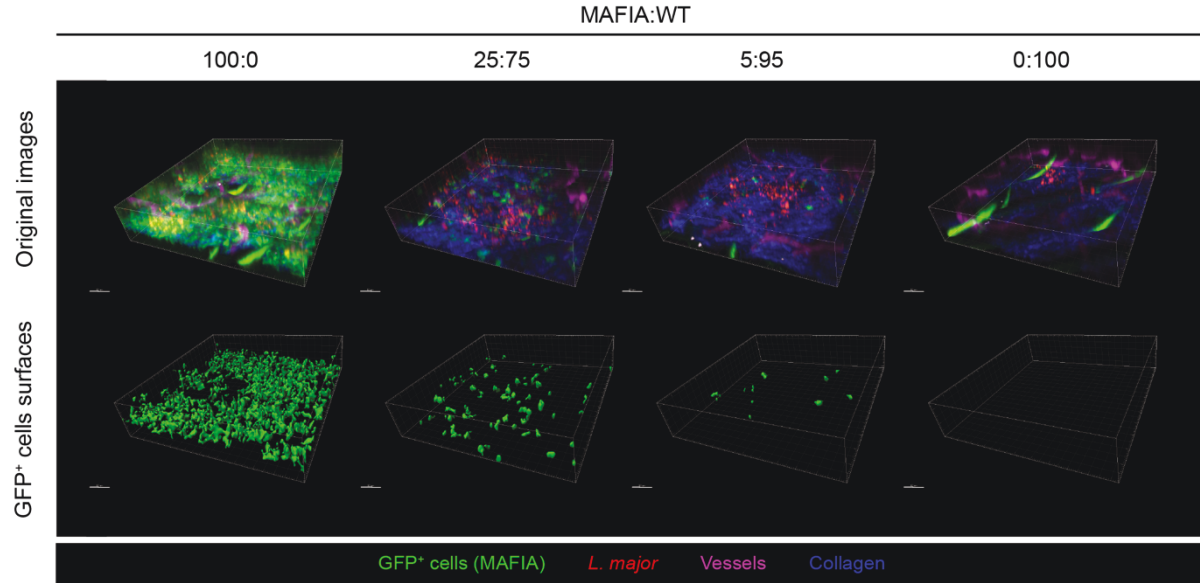

Following infection with *L. major*, we assessed the activity of monocyte-derived cells isolated at the site of infection. Our results revealed that the amount of pro-IL-1β (**Figure 56 top**) produced was regulated by the density of iNOS competent cells. Moreover, the amounts of cytokine production were identical in WT (CD45.1) and *Nos2*$^{-/-}$ (CD45.2) cells analyzed in the same environment, indicating that NO-mediated effect on cytokine production is not cell-intrinsic but instead largely rely on NO diffusion in the tissue. Similar results were obtained analyzing TNF-α (**Figure 56 middle**) and CCL3 (**Figure 56 bottom**) production.

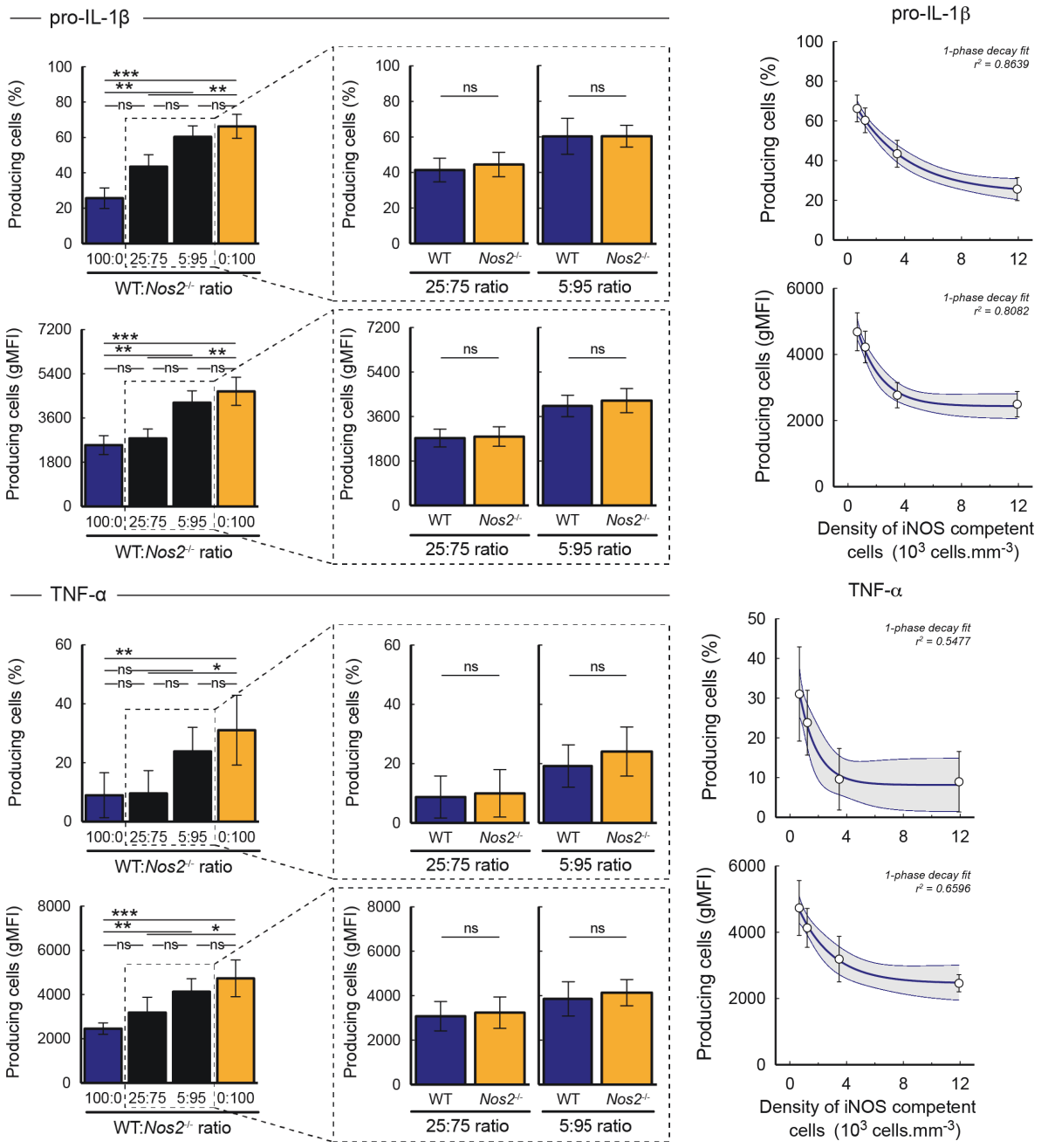

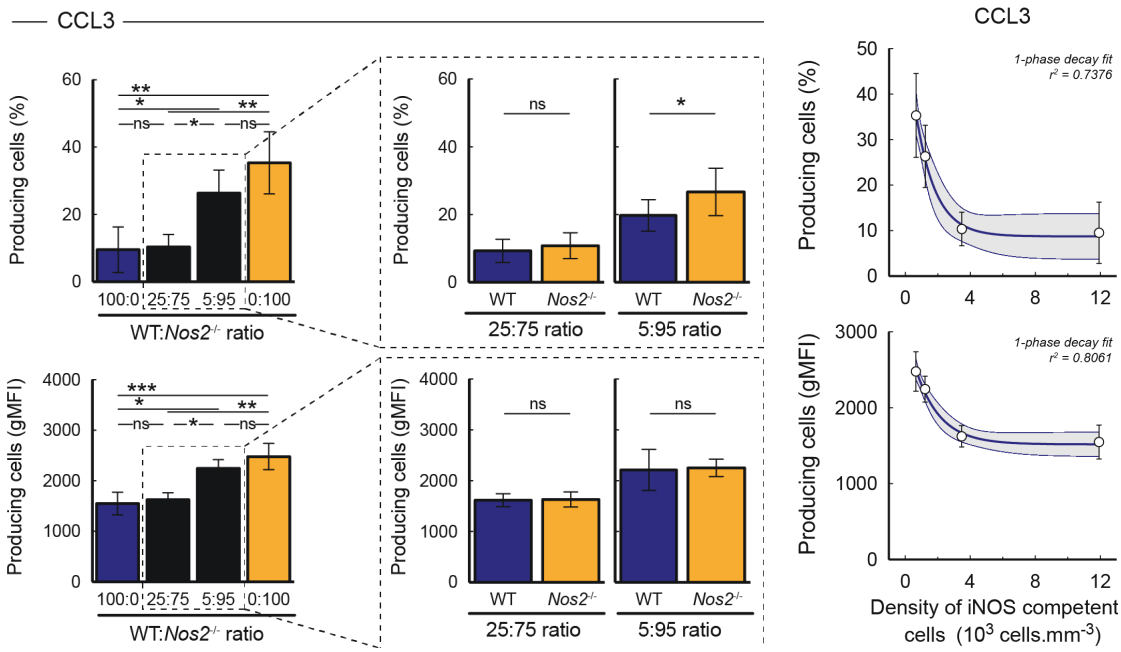

<u>Figure 56.</u> NO acts by diffusion to dampen monocyte-derived cell activity at the site of *L. major* infection but only when a high density of iNOS competent cells is reached

CD45.1 WT recipient mice were lethally irradiated and reconstituted with CD45.1 WT and CD45.2 *Nos2*$^{-/-}$ bone marrow cells, mixed at different ratios to modulate the tissue density of iNOS competent cells. Chimeras were infected 6 weeks later with DsRed-expressing *L. major*. Monocyte-derived cells activity was assessed 17 days later by intracellular cytokine staining on extracted ear cells. *Left.* Percentages (top) and gMFI (bottom) of pro-IL-1β-, TNF-α- and CCL3-producing Ly6C^{+} MHC-II^{+} monocyte-derived cells (P2 gate) among the overall population (100:0 (blue bars), 0:100 (orange bars), mixed chimeras (black bars)) as assessed by intracellular cytokine staining. The inset shows the analysis of WT (CD45.1) and *Nos2*$^{-/-}$ (CD45.2) cells in the same chimeric mice prepared at the indicated WT: *Nos2*$^{-/-}$ ratio. Representative of 7 mice per group in 2 independent experiments. *Right.* Percentages (top) and gMFI (bottom) of pro-IL-1β, TNF-α- and CCL3-producing Ly6C^{+} MHC-II^{+} monocyte-derived cells (P2 gate) were graphed as a function of the estimated density of iNOS competent cells.

Therefore, NO mediates the downregulation of the inflammatory reaction only when a sufficient number of NO-producing cells have accumulated at the site of infection. We estimated that a density of approximately 5000 iNOS competent cells/mm^3 need to be reach to substantially inhibit cytokine production (**<u>Figure 56</u>**). Furthermore, NO acts at the tissue level through diffusion irrespectively of intrinsic iNOS expression.

In sum, monocyte-derived cells that accumulate at the site of infection produce diffusible NO that will progressively inhibit further recruitment and inflammation as cell density increases. Monocyte-derived cells are therefore endowed with a metabolism-based quorum-sensing mechanism to help control and terminate the immune response.

Discussion

Discussion

In the present thesis, we identified a novel mechanism that adjusts the intensity of the inflammatory reaction to the local density of monocyte-derived cells, independently of the pathogen load. Mechanistically we have shown that NO decreases cellular respiration in monocyte-derived cells and consequently limits cellular resources (as measured by a lowered ATP:ADP ratio in the presence of NO). Such restriction dampens cytokine and chemokine production and therefore limits myeloid cell recruitment and overall inflammation. We found that NO acts thereby only when a sufficient number of iNOS-competent cells have accumulated at the site of infection. The property of NO to act on NO-producing cells but only when they are at high density defines a quorum-sensing mechanism for the control and termination of inflammatory reactions.

I. FIGHTING PATHOGENS BY REGULATING INFLAMMATION

Using a model of self-resolving infection with *Leishmania major* parasites, we showed that the role NO extends beyond its well-known antimicrobial properties by profoundly dampening local inflammation independently of the pathogen load. This restriction originates from a defect in monocyte-derived cell to secrete abundance quantities of cytokines and chemokines that fuel myeloid cell recruitment from blood. As a result, immunopathology is avoided as the parasite is eliminated without intense tissue damage. Since iNOS deficiency may affect the initiation and the development of the immune response during *L. major* infection, the effect was revealed using a short pharmacological inhibition of iNOS to specifically reveal the role of NO once the inflammatory reaction was established.

I.1. NO controls parasite load by regulating macrophage activity

Although NO was described to be deleterious to *Leishmania* parasites *in vitro*, its role in direct parasite killing *in vivo* is not clear (see Introduction). Here we confirmed that the role of NO *in vivo* extends beyond its anti-microbial properties by strongly influencing monocyte-derived cell activity. An important finding is that the mechanism described here is independent of the pathogen presence as observations performed in the context of *L. major* were recapitulated *in vitro* on BMDMs as well as *in vivo* in the context of IFA-induced inflammation. In agreement

with previous studies (Bogdan, 2015; Braverman and Stanley, 2017; Eigler et al., 1995; Giustizieri et al., 2002; Speyer et al., 2003; Thomassen et al., 1997), this suggest that the observed effects of NO on the immune reaction are not simply due to indirect changes in the parasite load and that the mechanism described is integral to the inflammation process. We found that NO controls the magnitude of inflammation by altering the cell metabolism of monocyte-derived cells. While this metabolism-based mechanism appears to be critical, NO-mediated suppression of cytokine and chemokine production can results from complementary mechanisms including an alteration of inflammasome assembly (Mishra et al., 2013), a decrease in NF-κB activity (Braverman and Stanley, 2017; Matthews et al., 1996; Mendes et al., 2002) or a defect in macrophage secretory pathway (Machado et al., 2000; Matsushita et al., 2003). Notably, in our model, NO activity diminishes cytokine and chemokine synthesis independently of the parasite (as assessed by intracellular staining) and in a broad manner affecting most type-1, type-2 and suppressive cytokines tested. This supports the idea that the principal mechanism involved may be quite simple and not mediated by a combination of restrictive signaling pathway.

In agreement with various studies (Ariel et al., 2012; Nathan and Ding, 2010; Ortega-Gómez et al., 2013), we showed that macrophages (here $CD64^+$ monocyte-derived cells) are potent regulator of inflammation in addition to their other physiological functions. However, it is important to highlight that while most of the actual knowledge describes macrophage polarity switch as key mechanism to terminate inflammation, here the regulatory mechanism consist in a global dampening of cellular activity rather than a M1 to M2 switch. Such finding raises several questions relative to macrophage biology and inflammation regulation such as:

- is macrophage polarity switch always required for inflammation resolution?
- what bases characterize inflammation that need a polarity switch to be terminated?
- how do we call an immune cell (e.g.: macrophage) that harbor both pro-inflammatory (e.g.: IL-1β, TNF-α…) as well as anti-inflammatory molecules (e.g.: NO, ROS…)?

Further studies will help understand if chronic inflammation can be subdivided in distinct phases that match requirement or not of a macrophage polarity switch and whether we can predict the outcome of inflammation based on its intensity and the macrophage populations present on site. Additionally, the analysis of monocyte-derived cell populations by single cell analysis will be of a great help. Indeed, monocyte-derived cells are highly heterogenous (Guilliams et al., 2016; Menezes et al., 2016) and we cannot exclude that NO induces the differentiation of monocyte-derived cells into a specific subset that we cannot distinguish by

the only use of flow cytometry. Such approach will also be helpful to assess whether our monocyte-derived cells are similar to previously described myeloid cells such as "Tip-DCs" or "MDSCs" that have overlapping phenotypes (Schmid et al., 2012).

I.2. NO avoid immunopathology by diminishing myeloid cell recruitment

As mentioned previously, leishmaniasis is an immunopathology where tissue damage is triggered by an excessive recruitment and activity of immune cells, notably by neutrophils. We suggest that NO restricts excessive recruitment of myeloid cells by diminishing the amount of pro-inflammatory cytokines and chemokines released by monocyte-derived cells. Accordingly, NO may directly or indirectly restrict cytokine and chemokine released by neutrophils as both cell types often act in concert during inflammatory reactions (Dal-Secco et al., 2015; Kreisel et al., 2010; Lämmermann et al., 2013). In addition, NO may act on the vasculature to limit immune cell infiltration from blood, for instance by influencing vessel integrity and modifying vessel leaking as well as adhesion properties. NO-dependent mechanisms that modulate leukocyte adhesion and extravasation have been already described and therefore likely involved in our model (Biffl et al., 1996; Dal Secco et al., 2006; Kubes et al., 1991; Secco et al., 2003).

Furthermore, by performing adoptive transfer of myeloid populations in infected mice, we showed that a sizeable fraction of recruited cells become infected only a few days after transfer. This suggest that the recruitment of new players fuel the infection by providing a new niche for the parasite. This result highlights that dampening inflammation not only reduce tissue scarring but also restrict the size of the *L. major* niche *in vivo*.

I.3. Is this mechanism relevant in other models?

The production of nitric oxide have been shown to be critical to fight *Leishmania major* parasites (Scott and Novais, 2016; Wei et al., 1995) as well as other intracellular parasites as *Toxoplasma gondii* (Scharton-Kersten et al., 1997) or *Trypanosoma cruzi* (Hölscher et al., 1998) but also intracellular bacteria as *Mycobacterium tuberculosis* (Jamaati et al., 2017; MacMicking et al., 1997), *Salmonella enterica* (Alam et al., 2002; Henard and Vázquez-Torres, 2011) or *Listeria monocytogenes* (MacMicking et al., 1995). For each infection, deficiency in NO synthesis favors pathogen growth and immunopathology, suggesting that our mechanism may be relevant in these models. Further work is needed to answer these questions as the answer

may not be trivial. For instance a critical point is the requirement of a high iNOS-competent cell density as well as a powerful iNOS induction.

During *L. major* infection, T cell-derived IFN-γ is the main driver of full monocyte-derived cell activation that allows a high iNOS expression and a massive recruitment of iNOS-competent cells (by macrophage-derived chemokine release). This T cell response develops during the silent phase of the disease and is operational while the pathogen load is still low. Therefore our model may apply to slowly developing diseases such as *M. tuberculosis* or *T. cruzi* infections but possibly not in the case of acute infection as with *L. monocytogenes*, where monocytes are recruited very fast (Serbina et al., 2008). In the latter case, while a high cell density can be easily reached, iNOS induction may not be sufficient due to the lack of large amounts of T cell-derived IFN-γ and NO may not be enough concentrated to mediate its anti-inflammatory effect.

Aside from infectious diseases, inflammation is also integral to tumorigenesis and its intensity during the different stages of tumor development may favor or delay tumor growth (Grivennikov et al., 2010; Shalapour and Karin, 2015). Numerous molecules that are currently tested in clinics to treat patients with cancer target inflammatory cytokines (e.g. TNF-α with Infliximab or Etanercept, IL-6 with Siltuximab or Tocilizumab) as well as inflammatory transcription factors (e.g. JAK1/2 with Ruxolitinib or Pacritinib) and inflammatory cells (e.g. TAMs with Trabectedin, MDSCs with Tasquinimod) (Crusz and Balkwill, 2015). Hence, boosting NO production to dampen inflammation during cancer development may be relevant to complement current therapies. The specific role of NO during tumorigenesis have been investigated and current paradigm attributes anti-tumor effects to high NO concentrations but also pro-tumor effects to low NO concentrations (Rapozzi et al., 2015; Vannini et al., 2015; Xu et al., 2002). Such findings are consistent with our model where NO restricts inflammation that causes tissue damage only when a sufficient amount of iNOS-competent cells has been reached. However, many studies in the cancer field still focus on the direct effects of NO on tumor cells as many studies have been focused on direct effects of NO on *Leishmania major* parasites. It is important to highlight that NO could possibly impact tumor growth in a tumor-independent manner for instance by acting on the tumor microenvironment (Rizi et al., 2017). Also, investigate how NO acts on tumor metabolism and on the tumor microenvironment *in vivo* may help better understand the complexity of tumorigenesis and support a better treatment design. Additionally, it will be important to assess to role of NO on T cells during tumor elimination.

As NO suppresses inflammation, it may directly or indirectly inhibit T cell function as well, which could be detrimental to patients (Ekmekcioglu et al., 2017). Interestingly, we did not find in our model of leishmaniasis that IFN-γ production by $CD4^+$ T cells was dampened by high levels of NO (data not shown), raising the possibility that NO would not negatively impact T cell function during tumor fighting.

I.4. The influence of hypoxia

Hypoxia is a feature of inflammation and its influence on immune reactions can vary depending on the microenvironment and the type of response elicited. Hypoxia controls immune responses by activating transcriptional regulators such as the hypoxia-inducible factor 1α (HIF-1α) and is often driving immune cell dysfunction, contributing to disease progression (Taylor and Colgan, 2017; Taylor et al., 2016). Dissecting the influence of hypoxia on NO biology during leishmaniasis is very difficult because of the lack of proper tools to measure oxygen and NO levels *in vivo*. Numerous studies showed that HIF-1α expression is necessary for optimal innate immune response against *Leishmania* parasites but can also have anti-inflammatory effects that promote parasite growth (Charpentier et al., 2016; Mahnke et al., 2014; Schatz et al., 2016, 2018). Additionally, it appears that *Leishmania* parasite can triggers HIF-1α stabilization as an escape mechanism, but there is no shared consensus about it (Schatz et al., 2018). Also, HIF-1α can be induced by signals activating macrophages independently of hypoxia by itself, so the specific impact of lack of oxygen needs further investigation. Mahnke *et al.* showed that decreased oxygen tension that occurs at the site of leishmania infection reduces iNOS protein levels and impairs the NO-dependent killing of the parasite by activated macrophages (Mahnke et al., 2014). The molecular mechanism explaining such effect is still unclear, but it could be simply due to a lack of substrate for iNOS as O_2 is needed for NO synthesis. Interestingly, reoxygenation of the tissue quickly reverse the demonstrated effect (Mahnke et al., 2014). Therefore, hypoxia seems detrimental to the immune response against *Leishmania* parasites. In our study, we confirmed that NO blockade of macrophage activity by metabolism repression also occurs under hypoxic conditions. However, the effect was less important than under normoxia and one explanation could be that NO was synthetized in less important quantities due to the lack of O_2 as a substrate. Also, we cannot exclude that the mechanism under normoxic conditions partly rely on the formation of RNS such as peroxynitrite that only happens in the presence of O_2. Finally, NO inhibition of ETC components occurs at nanomolar concentrations

and is reversed by O_2 at high concentrations (Brown, 2007). The development of new tools to study hypoxia *in vivo* would be of a great help to address these concerns.

***

II. NO ACTS ON METABOLISM TO REGULATE INFLAMMATION

While establishing the suppression of cytokine and chemokine production in monocyte-derived cells by NO, we observed that the effect was not restricted to some cytokines but was rather very broad, affecting most type-1 cytokines as well as type-2 and suppressive cytokines tested. Such findings suggest that the underlying mechanism originates from an effect either on broad signaling pathways or on physiological processes. We choose to investigate the latter option and ask whether NO effects originated from a change in cellular metabolism. We established *in vivo* that NO dampens monocyte-derived cellular respiration that result in a severe drop in the ATP:ADP ratio, mirror of cell energetic resources. We further showed that such restriction in respiration was sufficient to limit monocyte-derived cell activity and explained the broad suppression of cytokine production.

II.1. NO blocks mitochondrial respiration to limit macrophage activity

Our findings are in accordance with numerous studies showing that NO is able to dampen the respiration of macrophage and DCs *in vitro* and inflammatory DCs restimulated *ex vivo* (Biswas and Mantovani, 2012; Everts et al., 2012; Na et al., 2018; Sancho et al., 2017; Van den Bossche et al., 2016) by targeting mitochondrial components such as mitochondrial complexes or metabolic enzymes (Brown, 1999, 2007; Clementi et al., 1998; Nisoli and Carruba, 2006). In addition to this knowledge, we now provide evidence that NO dampens monocyte-derived cells respiration and energetic resources (ATP:ADP ratio) during a complex ongoing immune response *in vivo*. This was performed by directly analyzing the metabolism of sorted monocyte-derived cells from the site of *L. major* infection without *ex vivo* stimulation and the analysis of PercevalHR$^+$ monocyte-derived cells at the site of infection. Such observations establish the physiological relevance of NO-mediated alteration of cell metabolism in the context of a chronic inflammation with an intracellular pathogen. Additionally, we bring evidence that respiration blockade and decrease in ATP:ADP ratio are by themselves sufficient to limit cytokine and chemokine production suggesting a causal link between NO-mediated respiration

blockade and dampening of monocyte-derived cell activity. Collectively, results from this work and from other studies (Amiel et al., 2014; Everts et al., 2012; Van den Bossche et al., 2016) highlight the diverse effects of respiration blockade by NO on monocyte-derived cell biology, including alteration of survival capacity, plasticity and inflammatory activity.

A causal link between respiration blockade and limited cell activity

Several hypotheses can be proposed to explain the causal link between the cellular respiration inhibition respiration and the decreased cellular activity. First, by depleting the ATP:ADP ratio, NO can dampen numerous physiological processes needed for cell activity. Notably, a lack of ATP could globally restrict protein translation and therefore result in a decreased cytokine synthesis. Such hypothesis could be tested by measuring total protein content in cells exposed or not to NO and by measuring the translation rate in the same settings. Decreased ATP:ADP ratio could also affect the trafficking of intracellular vesicles, leading to defect in cytokine secretion. Additionally, ATP, ADP and AMP levels are directly correlated in the cell, for instance by the action of the adenylate kinase that converts one ATP and one AMP to 2 ADP molecules, and it was shown that the AMP:ATP ratio tends to vary as the square of the ATP:ADP ratio (Hardie et al., 2003). Therefore, NO could act on cell activity by regulating the AMP:ATP ratio that is sensed by the AMP-activated protein kinase (AMPK) that in turn regulates mTOR activity. Other additional mechanisms are discussed later in the discussion.

Differential sensitivity to NO?

Our work revealed that NO represses macrophage metabolism and thus its activity. Importantly, previous work of the laboratory showed that *Leishmania* parasites are repressed in their protein metabolism *in vivo* at the site of infection, using a different readout (Müller et al., 2013). As mentioned just above, it is possible that NO dampens protein metabolism in the parasite by dampening it mitochondrial respiration. However, we still don't appreciate the relative sensitivity of *Leishmania* and macrophages to NO. This raises several questions including:

- Are parasites more sensitive to NO than macrophages?
- Is there a threshold of NO that completely asphyxiate the parasite while leaving the macrophage still able to be functional?
- Do macrophages have specific repair mechanisms to protect from NO?
- …

Further work implementing PercevalHR in *Leishmania* parasites and macrophages before treating them simultaneously with increasing doses of NO will help answer these questions.

II.2. NO may additionally act on other cell types

In this study we focused on monocyte-derived cells, the major population of myeloid cells at the site of infection and also the major infected population. We analyzed cytokine and chemokine production at the single cell level to reveal that NO dampens such production, in accordance with previous studies (Bogdan, 2015; Braverman and Stanley, 2017; Eigler et al., 1995; Giustizieri et al., 2002; Speyer et al., 2003; Thomassen et al., 1997). We showed that such effect originated from a block in mitochondrial respiration. Additionally, we demonstrated that NO acts at the tissue level by diffusion rather than by a cell-intrinsic manner. As the mitochondria is a well conserved organelle between cell types, our findings raise the question whether NO can act on other immune cells such as neutrophils or T cells in a similar manner. Furthermore, NO could as well act on stromal cells (e.g. fibroblasts) to mediate changes in the immune reaction. While investigating IFN-γ production by T cells at the site of *L. major* infection, we did not see differences upon L-NIL treatment (data not shown). Such result also raises the question of whether T cells can be insensitive to NO or whether they can engage specific mechanisms reducing NO effects. In addition, studying NO impact with appropriate readouts should be performed for each cell type of interest.

II.3. Further mechanisms can contribute to limit inflammation

Our study emphasizes a role for NO in reducing cytokine and chemokine production in monocyte-derived cells by altering cellular respiration and energetic yield. However, many additional mitochondria-dependent or mitochondria-independent mechanisms can also contribute to limit inflammation.

ROS

Reactive oxygen species are highly reactive molecules and causing agents of oxidative stress. By this mean they act both as anti-microbial compound and signaling molecule in eukaryotic cells (Fang, 2004). In activated macrophages, ROS can be produced both by the NADPH oxidase localized in the phagosomes and by the complexes I and III of the respiratory chain

(Bedard and Krause, 2007; Murphy, 2009). Similarly to NO, the precise contribution of macrophage-derived ROS as immunomodulatory molecule during inflammation needs to be further characterized. ROS can have pro-inflammatory properties for instance by stabilizing HIF-1α to drive sustained IL-1β synthesis (Calvani et al., 2012; Mills et al., 2016) as well as anti-inflammatory properties for instance by limiting the intensity of acute inflammation in mice in a model of fungal infection with *Aspergillus fumigatus* (Grimm et al., 2013). It appears that the source of ROS, mitochondrial in the former example versus non-mitochondrial in the latter, is critical in influencing inflammation intensity. During *L. major* infection, the interplay between NO and ROS is not understood. As NO can block complexes I and III because of their Fe-S centers (Brown, 1999, 2007), it may suppress excessive mitochondrial ROS generation from these complexes and therefore dampen inflammation. However, while such mechanism could be important for IL-1β production, it is not trivial that ROS can regulates all the cytokines and chemokines affected by NO in our study. Further investigations measuring mitochondrial and cellular ROS in macrophages exposed or not to NO should help answer this question.

Succinate | Itaconate

The metabolic reconversion that occurs during macrophage activation significantly influences the relative proportion of cellular metabolites. Inside the mitochondria, the tricarboxylic acid (TCA) cycle is broken and participate to changes in metabolites concentrations (e.g. succinate) as well as the generation of new metabolites that can have immunomodulatory properties (e.g. itaconate). Succinate was described as a "metabolic signal" during inflammation, which levels are elevated during inflammation to sustain IL-1β production by HIF-1α stabilization and drive mitochondrial ROS production by its oxidation (Mills and O'Neill, 2014; Mills et al., 2016; Tannahill et al., 2013). Itaconate, generated specifically during inflammation by IRG1, is an organic molecule with direct anti-microbial properties as well as anti-inflammatory properties by regulating mitochondrial respiration and succinate levels in activated macrophages (Cordes et al., 2016; Lampropoulou et al., 2016; Michelucci et al., 2013). Recently it has been demonstrated that itaconate mediates its anti-inflammatory properties by acting on Nrf2 to limit inflammation and modulate type I interferons (Mills et al., 2018). Similarly, we have shown that an inflammation-driven metabolite (NO) can block the mitochondrial respiration to mediate anti-inflammatory effects. In addition, we demonstrated that such findings apply *in vivo* during a highly complex chronic inflammation induced by *L. major* infection. While several evidence point out that NO can directly alter mitochondrial complexes by both and Fe-

S centers inactivation and S-nitrosylation (Brown, 2007; Clementi et al., 1998), whether it also mediates its effects by regulating succinate or itaconate levels remains to be clarified. Recent work by Palmieri *et al.* established that NO is the main molecule reprogramming the carbon flux during classic macrophage activation (Palmieri et al., 2018), partly by inhibiting the TCA enzyme aconitase. As aconitase generates cis-aconitate, IRG1 substrate to synthetize itaconate, high NO levels could potentially reduce itaconate levels during inflammation by indirectly inhibiting its production.

Transcription factors

Finally the suppressive effect of NO can originate from changes in broad signaling pathways as mentioned earlier. In a model of infection by *M. tuberculosis*, Braverman and Stanley showed that iNOS was able to regulate macrophage transcriptome during its activation, promoting anti-microbial programs while limiting inflammatory cytokine transcription (Braverman and Stanley, 2017). They showed that iNOS mediates its effect partly by inhibiting the p65/RelA subunit of NF-κB, in agreement with other studies (Kelleher et al., 2007; Matthews et al., 1996). This illustrates that NO is able to target major transcription factors to prevent excessive inflammatory cytokine production. Further studies will help understand the direct effects of NO on NF-κB pathway during *Leishmania* infection. Various modifications induced by *Leishmania* may complicate the interpretation of these studies as the possibility of total NF-κB degradation by the parasite (Cameron et al., 2004) as well as the generation of new NF-κB variants (Gregory et al., 2008) that can have unpredicted effects, for instance repressing iNOS expression (Calegari-Silva et al., 2009). While NO can possibly alter NF-κB activity in our model, the fact that type-2 and suppressive cytokines are affected in a similar manner as type-1 cytokines do not favor this hypothesis as the main mechanism.

Other transcription factors can be targeted to limit inflammation. Peroxisome proliferator-activated receptors (PPARs) are nuclear receptors regulating gene expression in various contexts including cellular differentiation, development, metabolism and inflammation. PPARs have anti-inflammatory properties that originate mainly from their ability to antagonize NF-κB and AP-1 signaling pathways (Daynes and Jones, 2002). NO is able to activate PPARγ in endothelial cells to induce the expression of numerous enzymes as the cyclooxygenase 2 (COX-2) and the heme-oxygenase-1 (HO-1) (Ptasinska et al., 2006). Therefore, NO can during

leishmaniasis activate PPARγ in macrophages to dampen their activity and consequently limit the overall inflammation. Also, NO could lead to the formation of nitro-fatty acids that inhibit NF-κB activity either directly by nitroalkylation or indirectly by activating PPARγ (Buchan et al., 2018; Rom et al., 2018).

Inflammasome

We showed that NO dampens macrophage activity and notably the production of pro-IL-1β production, leading to a decreased secretion of IL-1β as we assessed by multi-analyte profiling. However, other mechanism could further participate in a decreased IL-1β synthesis that we did not investigate. IL-1β is generated from pro-IL-1β by its cleavage by the inflammasome machinery. We mentioned in the introduction that NO was shown to restrict NLRP3 inflammasome activity and consequently reducing IL-1β production in different models (Hernandez-Cuellar et al., 2012; Mao et al., 2013; Mishra et al., 2013). During the infection with *L. major*, NO was equally shown to block NLRP3 inflammasome activity to mediate host protection (Charmoy et al., 2016; Gurung et al., 2015). This raises the possibility that NO could in this study participate in the regulation of IL-1β production by targeting the inflammasome. However, in all of these studies, the model of infection used was not self-resolving, contrary to our model. Indeed, Charmoy *et al.* used the *L. major* Seidman strain that induce a non-healing disease and Gurung *et al.* used mice of the susceptible BALB/c background. When a self-healing stain of *L. major* was used in mice of the resistant C57BL/6 background, Lima-Junior *et al.* showed that NLRP3 inflammasome was in fact dispensable for parasite restriction *in vivo* (Lima-Junior et al., 2013). Therefore, it is unclear whether NO significantly participates to inflammation regulation by targeting the inflammasome machinery in the specific context of an infection by *L. major* parasites.

***

III. DIFFUSION OF A SOLUBLE MEDIATOR

By mixing iNOS competent and deficient cells we confirmed that NO acts *in trans* both *in vitro* and *in vivo*. Furthermore, we demonstrated by varying the density of iNOS competent cells that the effect of NO is closely linked to the density of iNOS competent cells, probably because the

mechanism requires a high NO concentration while diffusing in the extracellular space. We will discuss the two aspects in the following sections.

III.1. NO acts *in trans*

Parameters affecting NO diffusion

NO by its chemical properties is able to diffuse far away from the producing cell and thus can mediate its anti-inflammatory effect on neighboring cells. The impact of NO therefore depends on the parameters affecting its diffusion. NO concentration at the site of production is one of the principal parameter as the higher the concentration is the higher the diffusion rate will be. To increase the production of NO, several mechanisms are possible including an increase in iNOS expression and an increase in the density of iNOS competent cells. In our model of infection by *L. major*, the density of producing cells is increasing over time in the first steps of the disease. Additionally, temperature is a known factor influencing diffusion. At the site of infection, the higher the inflammation is the higher the temperature should increase (as a hallmark of inflammation) (Johnson and Kellogg, 2010; Thepen et al., 2000), thus favoring NO diffusion and its action *in trans*. This could account in a negative feed-forward loop of regulation. Measuring locally the tissue temperature and its effect on the immune cells is very challenging but would be very interesting. Finally, tissue properties as oxygenation levels, edema intensity and cellular composition should as well affect NO diffusion. It is hard to predict the participation of such parameters but we can imagine that a low O_2 tension favors for instance NO diffusion because its stability is increased under hypoxic conditions. Also, it would be very interesting to visualize NO gradients in tissues, as already performed for cytokines (Weber et al., 2013), to get information about its diffusibility and its pattern of expression in the case of an heterogenous production and consumption. The use of theoretical modeling and its possible combination with experimental imaging *in vitro* would be of a great help as it was successfully used for the study of cytokine gradients (Bagnall et al., 2018; Oyler-Yaniv and Krichevsky, 2018; Oyler-Yaniv et al., 2017; Thurley et al., 2015).

NO versus the other non-diffusible anti-inflammatory molecules

As for NO, others molecules such as ROS and itaconate have anti-inflammatory properties but it was never demonstrated that they mediate their effect within a long range. It can be assumed

that some of their chemical properties as charge, polarity, hydrophobicity and molecular weight are incompatible with free diffusion across membranes which can explain that they are retained inside the cell (excluding the existence of dedicated surface transporters). Hence, having similar properties but different physical behavior, all these molecules provide to the immune system complementary cell-intrinsic and cell-extrinsic mechanisms to regulate inflammation. Excluding potential active degradation, it is to highlight that a principal disadvantage of diffusion is that it induces by itself a certain level of dilution that does not occur when considering molecules that are confined inside the cell. However, it allow the communication at distant sites and therefore the existence of quorum-sensing mechanisms as described in bacteria (Miller and Bassler, 2001) and here in the immune system during the reaction against *L. major* parasites. It would be interesting to investigate the relative importance of both mechanisms during an ongoing immune response *in vivo*.

III.2. Quorum-sensing mechanism in immunity

Quorum-sensing mechanisms allow bacteria to sense and react to the density of their population, with the help of a diffusible mediator termed auto-inducer (Miller and Bassler, 2001). Similar mechanisms may exist in the immune system at homeostasis or during immune responses. Previous work of the laboratory showed that $CD4^+$ T cell-derived IFN-γ diffuses away the immunogical synapse, forming a wave able to activate bystander cells (Müller et al., 2012), a mechanism reminiscent of a communication in a "paracrine" manner. Further work showed that NO also diffuses to mediate a tissue-wide *Leishmania* control (Olekhnovitch et al., 2014), leading to the idea that T cell effector function propagates from isolated spots of antigen recognition by a two-wave mechanism relying on IFN-γ and then NO diffusions (Olekhnovitch and Bousso, 2015). Notably, we demonstrated that the effect of NO is dependent on the density of iNOS competent cells, meaning that one NO-producing cell alone cannot be efficient, contrary to a single isolated $CD4^+$ T cell. Thus, NO mediates its effect by a "collective" rather than a "paracrine" mechanism.

Many examples of paracrine signaling exist in the immune system and probably one of the best example would be cytokine signaling as demonstrated for IFN-γ (Müller et al., 2012) or TNF-α (Blasi et al., 1994; Caldwell et al., 2014). In the context of infectious diseases, two recent studies by Moyo *et al.* and Peteranderl *et al.* highlight that paracrine crosstalk between infected

and non-infected macrophages provides mechanisms to dampen inflammation and prevent the development of immunopathology during infection (Moyo et al., 2018; Peteranderl et al., 2016). Interestingly, *M. tuberculosis* is able to hijack paracrine signaling to its own good, by inducing IL-6, IL-10 and GM-CSF production in macrophages that diffuse and induce arginase-1 in neighboring cells, depleting arginine and restricting iNOS activity (Qualls et al., 2010).

We propose that collective mechanisms are integral to immune responses as a way to temporally and locally self-adjust accordingly to the intensity of inflammation without the need for external cues or regulatory cells. Paracrine signaling do not allow such mechanism to exist because it often imply that producing and target cells are of different type and that the signaling molecule is produced "in excess" by isolated cells, meaning that the producing cell can be functional alone. Several collective mechanisms have been revealed recently, showing a gain of interest in this field. For instance, Polonsky *et al.* demonstrated that the $CD4^+$ T cell population regulates its own balance between central memory and effector cell differentiation by a collective mechanism depending the T cell density and molecularly relying on IL-2, IL-6 and SLAMF6 signaling, providing an example of quorum-sensing mechanism among T cells (Polonsky et al., 2018). Also, IgG secreted by activated B cells has been shown to regulate B cell homeostasis (Montaudouin et al., 2013). Interestingly, an advantage of paracrine and quorum sensing mechanisms is to offer the possibility to reduce the level of heterogeneity between cells. For instance, DCs are able to coordinate their activity at later time points after activation by a mechanism depend on an early wave of interferon-mediated paracrine signaling (Shalek et al., 2014). Here, we showed that NO diffusion helps to homogenize cellular metabolism at the tissue level and therefore provide a collective tissue-wide protection against tissue damage, bringing to the field the first evidence of a modification of metabolism by a collective mechanism. Our work extends the work done on the regulation of DC and monocytic cells functions and metabolisms at distance by paracrine signaling via type I interferons (Gautier et al., 2005; Wu et al., 2016).

***

IV. A NEED FOR BETTER IMAGING TOOLS

In this thesis, we showed that NO participates in the regulation of the inflammatory reaction at the site of *L. major* infection by a metabolism-based quorum sensing mechanism. NO produced

by iNOS$^+$ cells diffuses in tissue to dampen mitochondrial respiration in bystander monocyte-derived cells. Yet, we critically lack a precise quantification of NO concentrations and immune cell metabolism in a time and space-resolved manner *in vivo*. Such quantification requires the development of functional fluorescent probes compatible with intravital imaging. We will discuss the current tools available to measure NO and immune cell metabolism and how they can be improved.

IV.1. Descriptive reporters for NO

The measurement of NO is technically difficult as it rapidly reacts with a wide range of molecules and is short-lived. Many tools exists to measure either NO directly or its derivatives (nitrite/nitrate, nitrosothiols, cGMP…) (Csonka et al., 2015; Pluth et al., 2011), with most of the tools being fluorescent sensors. While these tools are functional *in vitro*, none of them have been used successfully *in vivo*. First, most of the fluorescent reporters are organic molecules that are therefore impossible to target to the infected tissue with specificity and correct concentration. To circumvent such problem, we tried to injected a mixture of myeloid cells loaded with 4-Amino-5-Methylamino-2',7'-Difluorofluorescein Diacetate (DAF-FM), a fluorescent reporter that detects NO even at low concentrations. The loading was extremely variable between cell population without NO (excluding a direct comparison between cell types) and no differences in fluorescence was observed when the cells were injected in WT or L-NIL-treated individuals as assessed by flow cytometry. Also, probing NO on histological sections is difficult because of the presence of contaminant as nitrotyrosines and nitrocysteines at basal state (Pacher et al., 2007), but few studies have developed strategies to visualize NO which is encouraging (Hirotatsu et al., 1998; Kashiwagi et al., 2008; Zhang et al., 2014). Second, the specificity of such probes is often poor as reacting with chemically related NO derivatives. Third, the majority of NO tools are not ratiometric, which makes the study of NO concentration variation and diffusion really hard because of the lack of proper controls. Lastly, fluorescent organic molecules are not necessarily compatible with two-photon excitation needed for proper intravital imaging, but several probes have been generated to answer this need (Dai et al., 2017; Liu et al., 2014). Recently, a two-photon excitable and ratiometric reporter for NO was designed (Xie et al., 2017). Most importantly, new genetically-encoded biosensors for imaging NO are developed, which some are FRET based probes and therefore ratiometric (Eroglu et al., 2018). The development of such genetically encoded probes is remarkable because it will probably solve most of the aforementioned issues and open the

possibility of generating a transgenic mouse line reporter for NO. This will complement the current transgenic mouse lines available to detect iNOS expression in tissue (Béchade et al., 2014; Zhang et al., 2003), that allow for instance the quantification of iNOS-competent cell density in tissues. Finally, it is important to highlight that complementary tools are also developed as photoactivable molecules releasing NO upon illumination (Thomsen et al., 2018; Wecksler et al., 2004).

Altogether, the development of such tools will be crucial to answer fundamental questions about the spatiotemporal activity of NO *in vivo* such as:

- How NO concentrations evolve in tissues during inflammation?
- What and where are the principal sources of NO during inflammation?
- Is NO distributed homogenously or in patches in tissues?
- How NO behaves close to vessels in the presence of oxygen?
- How far NO is able to diffuse to mediate its effects?
- Is NO diffusion impaired by physical or chemical barriers in tissues?
- …

IV.2. Dynamics of immune cell metabolism

Immunometabolism is currently under intense investigation and multiple tools participated to this flourishing. Notably, the use of extracellular flux analyzers was of a great help by giving numerous information about mitochondrial functions and glycolysis with a reasonable number of cells and a relatively good throughput. However, such analyses do not give information at the single cell level and rely on isolated cells, preventing the study *in vivo* in their spatial context. Additionally, sample preparation processes are quite slow compared to potential changes in cellular metabolism and must probably impact it, leading to a great risk of misleading results. Finally, we critically lack information about the temporal dynamics of metabolic pathways during immune cell activity. Therefore, the elaboration of tools to image immune cell metabolism during immune reactions *in vivo* with a spatial and temporal resolution is needed. While MALDI-based metabolomics can be an option (Chughtai and Heeren, 2010; Hobson-Gutierrez and Carmona-Fontaine, 2018), some issues aforementioned still remain. To date, the best option would be the use of genetically-encoded fluorescent reporters. The development of such tools is critical to increase our knowledge in immunometabolism for the quantification of:

- The dynamics of metabolic adaptations during immune cell activation
- The plasticity of immune cell metabolism
- The spatial heterogeneity of cellular metabolism in various context (physiological environment, pathogen-induced inflammation, cancer…)
- The fluxes and gradients of metabolites inside and between cells
- …

In this thesis we used the genetically-encoded fluorescent reporter PercevalHR that measures in real time and at the single cell level the cellular ATP:ADP ratio (Tantama et al., 2013). We introduced this reporter in BMDMs to show by time-resolved flow cytometry and real time imaging that NO quickly dampens this ratio, similarly to oligomycin. We showed by flow cytometry that PercevalHR is also operational in complex *in vivo* settings as at the site of *L. major* infection. Further work will help visualize PercevalHR by intravital imaging at the site of *L. major* infection to first map the ATP:ADP ratio landscape at the site of infection and next assess the spatiotemporal activity of NO on energetic resources. Additionally, it would be interesting to introduce PercevalHR into *Leishmania* parasites to further characterize the mode of action of NO at the site of infection, as it has been shown to repress parasite metabolism *in vivo* (Müller et al., 2013). Furthermore, many other genetically-encoded fluorescent reporters have been described in the literature that detect metabolites such as glucose (FLIPglu-…) (Fehr et al., 2003, 2005), pyruvate (Pyronic) (Martín et al., 2014) and lactate (Laconic) (Martín et al., 2013). Their use *in vivo* will be of great help to dissect first the spatial heterogeneity of these metabolites in tissues and second to address the dynamics of metabolic adaptations during immune cell activity. For instance, one could imagine that a cell showing increased lactate production is switching to glycolysis. Further work should address this in the context of *Leishmania* infection but also in other settings as during cancer progression where intense metabolism remodeling occurs. Additionally, the design of tools that can locally modify the concentration of specific metabolites would be appreciated.

Wrap-up

In summary, we have described a metabolism-based quorum sensing mechanisms that acts to limit the inflammatory reaction in the context of *L. major* infection. Future studies will help further understand how immune cells act collectively to regulate immune responses during infection but also during tumorigenesis. The development of new tools to measure cell metabolism in real time and at the single cell level should offer unique opportunities to study the spatiotemporal dynamics of immune cell metabolism *in vivo*.

Methods

I. EXPERIMENTAL MODELS

Mice

C57BL/6J mice were obtained from Charles River France. C57BL/6J-Ptprc[a] (CD45.1), C57BL/6J-Tg(UBC-GFP)30Scha/J (Ubi-GFP), C57BL/6J-*Lyz2*$^{tm1.1Graf[EGFP]}$ (*Lyz2*$^{+/EGFP}$), C57BL/6-Tg(Csf1r-EGFP-NGFR/FKBP1A/TNFRSF6)2Bck/J (MaFIA) and B6.129P2-Nos2tm1Lau/J (*Nos2*$^{-/-}$) transgenic mice were bred in our animal facility. All mice were housed under SPF conditions, sex-matched and aged between 6 and 10 weeks for each experiment. All procedures were performed in agreement with the Institut Pasteur institutional guidelines for animal care. Experimental protocols were approved by the Animal Ethics Committee #1 of the Comité Régional d'Éthique pour l'Expérimentation Animale (CREEA), Ile-de-France (MESR N° 01264).

Parasites

DsRed-expressing *Leishmania major* parasites were grown at 26°C for a maximum of 5 passages in M119 medium supplemented with 10% heat-inactivated fetal bovine serum, 0.1 mM adenine, 1 µg/mL biotin, 5 µg/mL hemin and 2 µg/mL biopterin.

Bone marrow-derived macrophages (BMDMs)

Femurs and tibias were isolated from adult WT or *Nos2*$^{-/-}$ mice, sterilized in 70% ethanol and flushed with PBS. Single cell suspensions were prepared by filtering the marrow through a 30 µm cell strainer. 20×10^6 BMC were cultured in 150 mm non-treated Petri dishes for 7 days, 37°C, 5% CO_2, in 30 mL RPMI medium 1640 - GlutaMAX™ supplemented with 10% heat-inactivated fetal bovine serum, 100 U/mL penicillin, 100 ng/mL streptomycin, 1 mM sodium pyruvate, 1 mM HEPES and 5 mM 2-mercaptoethanol (complete RPMI) and 20% L929-cell conditioned supernatant. 30 mL of fresh medium was added 3 days after plating.

***

II. METHODS

Infection, inflammation model and L-NIL treatment

For infection, stationary-phase promastigotes were resuspended at 10^8 parasites/mL in PBS and 5 µL were injected intradermally into the ear dermis. To induce a non-infectious inflammatory reaction, incomplete Freund's adjuvant was emulsified with an equal volume of saline and 10 µL were injected intradermally into the ear dermis. To inhibit iNOS activity, L-NIL was freshly prepared at 2 mg/mL in PBS and mice were injected with 100 µL i.p. once a day for 3 days, starting 14 days post infection or 4 days post challenge. Age and sex-matched controls were infected or challenged at the same time and did not received L-NIL injection.

Extraction of ear cells

Ears harvested from euthanized mice were separated into dorsal and ventral sheets using tissue forceps before being digested for 45 min, 37°C, 700 rpm, in RPMI medium 1640 supplemented with 100 U/mL penicillin, 100 ng/mL streptomycin, 0.5 mg/mL liberase TL and 50 ng/mL DNase. Single cell suspensions in PBS were prepared by crushing digested ears into a 70 µm cell strainer. After a washing step in PBS and filtration, cells were analyzed by flow cytometry or subjected to extracellular flux analysis.

Adoptive transfer

Bone marrow cells were harvested from Ubi-GFP mice and filtered through a 30 µm cell strainer to generate a single cell suspension. 6×10^7 cells/mice were injected i.v. per mice.

Flow cytometry

In vitro generated BMDMs were washed with cold PBS and incubated for 10 min, 4°C, in 3 mL of Cell Dissociation Buffer to detach the cells. BMDMs were recovered by adding 10 mL of cold PBS and washed before seeding at 10^6 cells/well (6-well non-treated plates) in 2 mL complete RPMI supplemented with 20% L929-cell conditioned supernatant. To vary the density of iNOS competent cells in the culture, we mixed WT and *Nos2*$^{-/-}$ BMDMs at various ratios, keeping the total cell number constant to avoid confounding effects of varying cytokine

and/or nutrients concentrations. The day after seeding, medium was removed and replaced with 2 mL of fresh complete RPMI supplemented with 1 µg/mL LPS + 50 ng/mL IFN-γ for activation. When needed, treatment with 20 µg/mL L-NIL was performed at the time of activation. Treatment with oligomycin or azide was performed 20 h post activation at the indicated doses. To monitor glucose uptake, 20 µM 2-deoxy-2-[(7-nitro-2,1,3-benzoxadiazol-4-yl)amino]-D-glucose (2-NBDG) was incubated with cells during 1 h. 24 h post activation, BMDMs were washed with cold PBS and incubated for 10 min, 4°C, in 300 µL Cell Dissociation Buffer to detach the cells. BMDMs were harvested by adding 1 mL of cold PBS to each well. Cells were stained with Zombie Violet fixable dye diluted at 1:200 in PBS supplemented with 2% FBS and 5 mM EDTA (FACS buffer) for 15 min, 4°C, to assess cell viability. BMDMs were stained for 15 min, 4°C, in FACS buffer supplemented with 10 µg/mL anti-mouse CD16/32 (Fc-block) using a combination of fluorescently-labeled monoclonal antibodies among: PerCP-Cy5.5 anti-CD11b, APC-eFluor® 780 anti-MHC II (I-A/I-E). For intracellular staining, prior harvesting the cells, BD GolgiPlug diluted at 1:1000 was added to every well without volume variation, 20 h post activation. Cells were harvested and stained as described above. BMDMs were fixed for 30 min, 4°C, using formaldehyde solution diluted at 2% in PBS. Cells were permeabilized using PermWash buffer following manufacturer's instructions and stained for 45 min, 4°C, using a combination of fluorescently-labeled monoclonal antibodies among: PE anti-mouse CCL2, PE anti-mouse CCL3, APC anti-mouse IL-1β Pro-form.

For *ex vivo* analyses, extracted ear cells were stained with Zombie Violet fixable dye diluted at 1:200 or LIVE/DEAD blue fixable dye diluted at 1:500 in FACS buffer for 15 min, 4°C, to assess cell viability. Cells were then fixed for 30 min, 4°C, using formaldehyde solution diluted to 2% in PBS. Surface staining of cells was performed for 15 min, 4°C, in FACS buffer supplemented with 10 µg/mL anti-mouse CD16/32 (Fc-block) using a combination of fluorescently-labeled monoclonal antibodies among: BUV395 anti-CD45, BV421 anti-MHC II (I-A/I-E), BV510 anti-Gr-1, BV510 anti-Ly-6G, BV605 anti-Ly-6C, PerCP-Cy5.5 anti-CD11b, PE-Cy7 anti-CD45.1, APC anti-CD11c, APC-eFluor® 780 anti-CD45.2, APC-eFluor® 780 anti-MHC II (I-A/I-E). For intracellular staining, extracted cells were plated in 48-well plates in 1 mL complete RPMI supplemented with BD GolgiPlug (diluted at 1:1000) for 4 h, 37°C. iNOS inhibition was maintained adding 20 µg/mL L-NIL to dedicated wells. Cells were harvested by flushing all wells and submitted to staining as described above. After surface staining, cells were permeabilized using PermWash buffer following manufacturer's

instructions and stained 45 min, 4°C, using a combination of fluorescently-labeled monoclonal antibodies among: Alexa Fluor® 488 anti-mouse TNF-α, eFluor® 660 anti-CCL3, APC anti-mouse IL-1β Pro-form. Samples were analyzed using a BD CantoII or a BD Fortessa flow cytometer equipped with FACSDiva software (BD Bioscience) or a CytoFLEX LX flow cytometer equipped with CytExpert software (Beckman Coulter).

For analysis of PercevalHR-expressing cells, two fluorescence signals were acquired. F_{low} was collected by exciting PercevalHR with a violet laser (λ_{low} = 405 nm) and filtering the signal through a 525/40 filter. F_{high} was collected by exciting PercevalHR with a blue laser (λ_{high} = 488 nm) and filtering the signal through a 510/20+OD1 filter. Cellular ATP:ADP ratio was determined by calculating F_{high}:F_{low} ratio for each acquired cell. For time-resolved (kinetic) flow cytometry, ATP:ADP ratio was normalized to the first value acquired (t_0). Data analysis was performed using FlowJo 10.2 software.

MitoTracker staining

After activation, cells were loaded with MitoTracker® dyes using 40 nM MitoTracker® GreenFM and 50 nM MitoTracker® Red CMXRos during 30 min, 37°C, 5% CO_2. Cells were washed with cold PBS before flow cytometry analysis.

Hypoxic culture

Hypoxic cultures were conducted using PetakaG3 FLAT hypoxic devices (balancing the partial pressure of dissolved oxygen in the media at 25 mmHg). 15×10^6 BMDMs were loaded into each chamber in 20 mL complete RPMI supplemented with 20% L929-cell conditioned medium and cultivated horizontally overnight to allow cell seeding. The day after, medium was replaced for activation. Cell treatments and flow cytometry were performed as described earlier.

Extracellular flux analysis

BMDMs were analyzed using an XF^{e}96 Extracellular Flux Analyzer (Seahorse Bioscience). BMDMs were plated in XF^{e}96 cell culture microplates (10^5 cells/well in 200 µL final) and either left untreated or activated with 1 µg/mL LPS + 50 ng/mL IFN-γ, 37°C, 5% CO_2. 24 h

post activation, cells were washed with XF Base medium supplemented with 10 mM glucose, 2 mM glutamine and 1 mM sodium pyruvate (MitoStress XF running buffer, pH adjusted to 7.4) or supplemented with 2 mM glutamine (GlycoStress XF running buffer, pH adjusted to 7.4), and 175 µL of appropriate XF running buffer was added as final volume. BMDMs were stored 1 h at 37°C in a non-CO_2 incubator before starting the analysis. Following manufacturer's instruction, OCR and ECAR were measured in response to 1 µM oligomycin, 1.5 µM Carbonyl cyanide-*4*-(trifluoromethoxy)phenylhydrazone (FCCP) and 0.5 µM rotenone and antimycin A (MitoStress Test Kit) or in response to 10 mM glucose, 1 µM oligomycin and 50 mM 2-deoxy-glucose (2-DG) (GlycoStress Test Kit).

For *ex vivo* isolation of mononuclear phagocytes from infected ears, we relied on the expression of the CD11c marker on both P2 and P3 populations (Olekhnovitch et al., 2014). $CD11c^+$ cells were isolated from infected ears using positive selection on MACS columns. The isolated population contained at least 90% of $CD11b^+MHC\text{-}II^+$ monocyte-derived cells. Cells were washed and plated at 10^5 cells/well in 175 µL of MitoStress XF running buffer and treated with 20 µg/mL L-NIL or left untreated during 2 h, 37°C, non-CO_2 incubator. Following manufacturer's instruction, OCR and ECAR were measured in response to 1 µM oligomycin, 1.5 µM FCCP and 0.5 µM rotenone and antimycin A (MitoStress Test Kit). Data analysis was performed using Wave software.

Multiplex assay for cytokine and chemokine quantification

Ears harvested from euthanized mice were separated into dorsal and ventral sheets and snap frozen before storage at -80°C. For tissue lysates preparation, ears were thawed out and chopped in 1 mL RIPA buffer on ice. After 20 min incubation, samples were grounded during 2 min with a Potter-Elvehjem PTFE pestle into an appropriate glass tube. Lysates were subsequently clarified by centrifugation for 15 min at 4°C, 15.000 rcf. Multiplex assay was performed following manufacturer's instructions. Lysates were diluted at 1:2 in assay diluent. Standards were reconstituted with RIPA buffer diluted at 1:2 in assay diluent. For analyte capture, the plate was incubated overnight at 4°C under agitation on an orbital shaker. Plate reading was performed using a Bio-Plex 200 system equipped with Bio-Plex Manager software (Bio-Rad).

For *in vitro* analyses, BMDMs were cultivated and activated as indicated during 24 h. Supernatants were harvested and cleared by centrifugation before being snap frozen and stored

at -80°C until analysis. The day of analysis, supernatants were diluted 1:4 in assay diluent and multiplex assay was performed as described previously.

PercevalHR probe and virus generation

The original PercevalHR construct was cloned into a murine stem cell viral (MSCV) vector. HEK 293 cells were co-transfected with 6 µg pMSCV-PercevalHR and 4 µg pCL-Eco plasmids using JetPRIME reagent following manufacturer instructions. Medium was changed 4 h after with complete RPMI. 48 h after transfection, retrovirus containing supernatant was harvested from HEK 293 cells, 0.45 µm-filtered and supplemented with 10 µg/mL polybrene to generate retroviral-conditioned medium.

Retroviral transduction of BMDMs

BMDMs were retrovirally transduced during their differentiation. On day 3, differentiation medium was exchanged with 25 mL retroviral-conditioned medium supplemented with 20% L929-cell conditioned medium for an overnight incubation. On day 4, retroviral medium was replaced with complete RPMI supplemented with 20% L929-cell conditioned supernatant for an additional 3 days. Transduction efficiencies of >60% were routinely achieved.

Generation of mixed-bone marrow chimeras

WT CD45.1 recipient mice were γ-irradiated with a single lethal dose of 9 *Gy*. Femurs and tibias were isolated from adult WT CD45.1 or *Nos2*$^{-/-}$ CD45.2 mice, sterilized in 70% ethanol and flushed with PBS. Single cell suspensions were prepared by filtering the marrow through a 30 µm cell strainer. Mice were anaesthetized 2 hours post irradiation and reconstituted with a total of 5×10^7 bone marrow cells (WT, *Nos2*$^{-/-}$ or a mixture of both) by retro-orbital i.v. injection. Chimeras were infected 6 to 8 weeks after reconstitution. The same protocol was used to generate mixed-bone marrow chimeras using WT and MAFIA cells.

Generation of PercevalHR-expressing fetal liver chimeras

WT recipient mice were γ-irradiated with a single lethal dose of 9 *Gy*. Mice were anaesthetized 2 hours post irradiation and reconstituted with a total of 1×10^6 PercevalHR-expressing fetal

HSCs plus 5×10^5 WT bone marrow cells by retro-orbital i.v. injection. For PercevalHR-expressing HSC generation, fetal liver of E14.5 embryos were harvested and multipotent HSCs were isolated by negative selection on MACS columns using biotin anti-mouse TER-119 antibody. Isolated HSCs were cultivated overnight in complete RPMI supplemented with 200 ng/mL rmSCF, 200 ng/mL rmFlt3-L and 200 ng/mL rmIL-3 at a density of 1×10^6 cells/mL. The day after, 1×10^6 HSCs in 2 mL retroviral-conditioned medium were retrovirally transduced by spin infection (800 *g*, 2 h, 32°C). After the spin infection, medium was replaced with complete RPMI supplemented with the same cytokine cocktail for an overnight incubation before injection into irradiated recipients. Chimeras were infected 8 weeks after reconstitution.

Intravital imaging

Mice were anaesthetized and prepared for intravital two-photon imaging. Each mouse was placed on a custom-designed heated stage, one ear was placed onto a metal piece and immobilized with double sided tape. The ear was kept moisturized using ophthalmic gel covered by a coverslip. Two-photon imaging was performed using a 25X/1.05 NA objective (Olympus) immerged in deionized water and installed into a DM6000 upright microscope equipped with a SP5 confocal head (Leica Microsystem) and a Chameleon Ultra Ti::Sapphire Laser (Coherent) tuned at 920 nm. Emitted fluorescence was split with dichroic mirrors (Semrock) and filtered with appropriate filters (Semrock) for each channel before collection with nondescanned detectors. Typically, images from 15 to 20 z planes spaced by 5 µm were collected every 2 minutes for up to 3 hours. For *in vitro* analysis of PercevalHR-expressing BMDMs, two-photon imaging was performed using a 25X/1.05 NA objective (Olympus) installed into a FVMPE-RS upright microscope (Olympus) equipped with an Insight deep see dual laser (Spectra physics) and a resonant scanner. PercevalHR excitation was achieved using λ_{low} = 830 nm and λ_{high} = 1040 nm. Emitted fluorescence, collected sequentially for each λ, was split with dichroic mirrors (Semrock) and filtered with a 520/35 filter (PercevalHR signal) and a 483/32 filter (background) before collection with GaAsP detectors. Images in a single plan were collected every 15 s for 5 to 10 min. Data collected were analyzed and processed using Fiji (ImageJ) and Imaris software.

***

III. QUANTIFICATION AND STATISTICAL ANALYSIS

Data are reported as the mean ± SD, and numbers of experiments are reported in figure legends. For *in vitro* analyses, statistical differences between two groups were evaluated using a two-tailed unpaired Student's t-test with Welch's correction or using an ordinary one-way ANOVA with post hoc Holm-Sidak test for multiple comparison. For *in vivo* analyses, unless indicated otherwise, statistical differences between two groups were evaluated using a Mann-Whitney U test. Correlation between the density of iNOS competent cell and cellular respiration and cytokine production was further analyzed *in vitro* and *in vivo* by exponential one-phase decay regression. Significance was defined by a p-value<0.05. All statistical tests were performed using GraphPad Prism 6.0a software. p-values were reported as stars: * $p<0.05$; ** $p<0.01$; *** $p<0.005$

References

References

Abdel-Haleem, A.M., Lewis, N.E., Jamshidi, N., Mineta, K., Gao, X., and Gojobori, T. (2017). The Emerging Facets of Non-Cancerous Warburg Effect. Front. Endocrinol. *8*.

Afonina, I.S., Zhong, Z., Karin, M., and Beyaert, R. (2017). Limiting inflammation—the negative regulation of NF-κB and the NLRP3 inflammasome. Nat. Immunol. *18*, 861–869.

Aktan, F. (2004). iNOS-mediated nitric oxide production and its regulation. Life Sci. *75*, 639–653.

Alam, M.S., Akaike, T., Okamoto, S., Kubota, T., Yoshitake, J., Sawa, T., Miyamoto, Y., Tamura, F., and Maeda, H. (2002). Role of Nitric Oxide in Host Defense in Murine Salmonellosis as a Function of Its Antibacterial and Antiapoptotic Activities. Infect. Immun. *70*, 3130–3142.

Alexander, J., and Brombacher, F. (2012). T Helper1/T Helper2 Cells and Resistance/Susceptibility to Leishmania Infection: Is This Paradigm Still Relevant? Front. Immunol. *3*.

Amiel, E., Everts, B., Fritz, D., Beauchamp, S., Ge, B., Pearce, E.L., and Pearce, E.J. (2014). Mechanistic Target of Rapamycin Inhibition Extends Cellular Lifespan in Dendritic Cells by Preserving Mitochondrial Function. J. Immunol. *193*, 2821–2830.

Arango Duque, G., and Descoteaux, A. (2014). Macrophage Cytokines: Involvement in Immunity and Infectious Diseases. Front. Immunol. *5*.

Arend, W.P. (2002). The balance between IL-1 and IL-1Ra in disease. Cytokine Growth Factor Rev. *13*, 323–340.

Ariel, A., Maridonneau-Parini, I., Rovere-Querini, P., Levine, J.S., and Mühl, H. (2012). Macrophages in inflammation and its resolution. Front. Immunol. *3*.

Arita, M., Ohira, T., Sun, Y.-P., Elangovan, S., Chiang, N., and Serhan, C.N. (2007). Resolvin E1 Selectively Interacts with Leukotriene B4 Receptor BLT1 and ChemR23 to Regulate Inflammation. J. Immunol. *178*, 3912–3917.

Arts, R.J.W., Joosten, L.A.B., and Netea, M.G. (2016). Immunometabolic circuits in trained immunity. Semin. Immunol. *28*, 425–430.

Ashley, N.T., Weil, Z.M., and Nelson, R.J. (2012). Inflammation: Mechanisms, Costs, and Natural Variation. Annu. Rev. Ecol. Evol. Syst. *43*, 385–406.

Assreuy, J., Cunha, F.Q., Epperlein, M., Noronha-Dutra, A., O'Donnell, C.A., Liew, F.Y., and Moncada, S. (1994). Production of nitric oxide and superoxide by activated macrophages and killing of Leishmania major. Eur. J. Immunol. *24*, 672–676.

Badirzadeh, A., Taheri, T., Taslimi, Y., Abdossamadi, Z., Heidari-Kharaji, M., Gholami, E., Sedaghat, B., Niyyati, M., and Rafati, S. (2017). Arginase activity in pathogenic and non-pathogenic species of Leishmania parasites. PLoS Negl. Trop. Dis. *11*, e0005774.

Bagnall, J., Boddington, C., England, H., Brignall, R., Downton, P., Alsoufi, Z., Boyd, J., Rowe, W., Bennett, A., Walker, C., et al. (2018). Quantitative analysis of competitive cytokine signaling predicts tissue thresholds for the propagation of macrophage activation. Sci Signal *11*, eaaf3998.

Bambouskova, M., Gorvel, L., Lampropoulou, V., Sergushichev, A., Loginicheva, E., Johnson, K., Korenfeld, D., Mathyer, M.E., Kim, H., Huang, L.-H., et al. (2018). Electrophilic properties of itaconate and derivatives regulate the IκBζ–ATF3 inflammatory axis. Nature *556*, 501–504.

Barak, E., Amin-Spector, S., Gerliak, E., Goyard, S., Holland, N., and Zilberstein, D. (2005). Differentiation of Leishmania donovani in host-free system: analysis of signal perception and response. Mol. Biochem. Parasitol. *141*, 99–108.

Basil, M.C., and Levy, B.D. (2016). Specialized pro-resolving mediators: endogenous regulators of infection and inflammation. Nat. Rev. Immunol. *16*, 51–67.

Bazzan, E., Saetta, M., Turato, G., Borroni, E.M., Cancellieri, C., Baraldo, S., Savino, B., Calabrese, F., Ballarin, A., Balestro, E., et al. (2013). Expression of the Atypical Chemokine Receptor D6 in Human Alveolar Macrophages in COPD. Chest *143*, 98–106.

Béchade, C., Colasse, S., Diana, M.A., Rouault, M., and Bessis, A. (2014). NOS2 expression is restricted to neurons in the healthy brain but is triggered in microglia upon inflammation. Glia *62*, 956–963.

Bedard, K., and Krause, K.-H. (2007). The NOX family of ROS-generating NADPH oxidases: physiology and pathophysiology. Physiol. Rev. *87*, 245–313.

Belkaid, Y., Butcher, B., and Sacks, D.L. (1998). Analysis of cytokine production by inflammatory mouse macrophages at the single-cell level: selective impairment of IL-12 induction in Leishmania-infected cells. Eur. J. Immunol. *28*, 1389–1400.

Belkaid, Y., Mendez, S., Lira, R., Kadambi, N., Milon, G., and Sacks, D. (2000). A Natural Model of Leishmania major Infection Reveals a Prolonged "Silent" Phase of Parasite Amplification in the Skin Before the Onset of Lesion Formation and Immunity. J. Immunol. *165*, 969–977.

Belkaid, Y., Hoffmann, K.F., Mendez, S., Kamhawi, S., Udey, M.C., Wynn, T.A., and Sacks, D.L. (2001). The Role of Interleukin (IL)-10 in the Persistence of Leishmania major in the Skin after Healing and the Therapeutic Potential of Anti–IL-10 Receptor Antibody for Sterile Cure. J. Exp. Med. *194*, 1497–1506.

Belkaid, Y., Stebut, E.V., Mendez, S., Lira, R., Caler, E., Bertholet, S., Udey, M.C., and Sacks, D. (2002a). CD8+ T Cells Are Required for Primary Immunity in C57BL/6 Mice Following Low-Dose, Intradermal Challenge with Leishmania major. J. Immunol. *168*, 3992–4000.

Belkaid, Y., Piccirillo, C.A., Mendez, S., Shevach, E.M., and Sacks, D.L. (2002b). $CD4^+CD25^+$ regulatory T cells control *Leishmania major* persistence and immunity. Nature *420*, 502–507.

Berg, J.M., Tymoczko, J.L., Stryer, L., Berg, J.M., Tymoczko, J.L., and Stryer, L. (2002). Biochemistry (W H Freeman).

Biffl, W.L., Moore, E.E., Moore, F.A., and Barnett, J., Carlton C. (1996). Nitric Oxide Reduces Endothelial Expression of Intercellular Adhesion Molecule (ICAM)-1. J. Surg. Res. *63*, 328–332.

Bingisser, R.M., Tilbrook, P.A., Holt, P.G., and Kees, U.R. (1998). Macrophage-Derived Nitric Oxide Regulates T Cell Activation via Reversible Disruption of the Jak3/STAT5 Signaling Pathway. J. Immunol. *160*, 5729–5734.

Biswas, S.K., and Mantovani, A. (2012). Orchestration of metabolism by macrophages. Cell Metab. *15*, 432–437.

Blanchette, J., Abu-Dayyeh, I., Hassani, K., Whitcombe, L., and Olivier, M. (2009). Regulation of macrophage nitric oxide production by the protein tyrosine phosphatase Src homology 2 domain phosphotyrosine phosphatase 1 (SHP-1). Immunology *127*, 123–133.

Blasi, E., Pitzurra, L., Bartoli, A., Puliti, M., and Bistoni, F. (1994). Tumor necrosis factor as an autocrine and paracrine signal controlling the macrophage secretory response to Candida albicans. Infect. Immun. *62*, 1199–1206.

Bogdan, C. (2008). Mechanisms and consequences of persistence of intracellular pathogens: leishmaniasis as an example. Cell. Microbiol. *10*, 1221–1234.

Bogdan, C. (2012). Natural killer cells in experimental and human leishmaniasis. Front. Cell. Infect. Microbiol. *2*.

Bogdan, C. (2015). Nitric oxide synthase in innate and adaptive immunity: an update. Trends Immunol. *36*, 161–178.

Bogdan, C., and Röllinghoff, M. (1998). The immune response to Leishmania: mechanisms of parasite control and evasion. Int. J. Parasitol. *28*, 121–134.

Bonecchi, R., and Graham, G.J. (2016). Atypical Chemokine Receptors and Their Roles in the Resolution of the Inflammatory Response. Front. Immunol. *7*.

Braverman, J., and Stanley, S.A. (2017). Nitric Oxide Modulates Macrophage Responses to Mycobacterium tuberculosis Infection through Activation of HIF-1α and Repression of NF-κB. J. Immunol. Baltim. Md 1950 *199*, 1805–1816.

Brewig, N., Kissenpfennig, A., Malissen, B., Veit, A., Bickert, T., Fleischer, B., Mostböck, S., and Ritter, U. (2009). Priming of CD8+ and CD4+ T Cells in Experimental Leishmaniasis Is Initiated by Different Dendritic Cell Subtypes. J. Immunol. *182*, 774–783.

Bromley, S.K., Mempel, T.R., and Luster, A.D. (2008). Orchestrating the orchestrators: chemokines in control of T cell traffic. Nat. Immunol. *9*, 970–980.

Brown, G.C. (1999). Nitric oxide and mitochondrial respiration. Biochim. Biophys. Acta BBA - Bioenerg. *1411*, 351–369.

Brown, G.C. (2007). Nitric oxide and mitochondria. Front. Biosci. J. Virtual Libr. *12*, 1024–1033.

Broz, P., and Dixit, V.M. (2016). Inflammasomes: mechanism of assembly, regulation and signalling. Nat. Rev. Immunol. *16*, 407–420.

Buchan, G.J., Bonacci, G., Fazzari, M., Salvatore, S.R., and Gelhaus Wendell, S. (2018). Nitro-fatty acid formation and metabolism. Nitric Oxide *79*, 38–44.

Caldwell, A.B., Cheng, Z., Vargas, J.D., Birnbaum, H.A., and Hoffmann, A. (2014). Network dynamics determine the autocrine and paracrine signaling functions of TNF. Genes Dev. *28*, 2120–2133.

Calegari-Silva, T.C., Pereira, R.M.S., De-Melo, L.D.B., Saraiva, E.M., Soares, D.C., Bellio, M., and Lopes, U.G. (2009). NF-κB-mediated repression of iNOS expression in Leishmania amazonensis macrophage infection. Immunol. Lett. *127*, 19–26.

Calvani, M., Comito, G., Giannoni, E., and Chiarugi, P. (2012). Time-Dependent Stabilization of Hypoxia Inducible Factor-1α by Different Intracellular Sources of Reactive Oxygen Species. PLOS ONE *7*, e38388.

Cameron, P., McGachy, A., Anderson, M., Paul, A., Coombs, G.H., Mottram, J.C., Alexander, J., and Plevin, R. (2004). Inhibition of Lipopolysaccharide-Induced Macrophage IL-12 Production by Leishmania mexicana Amastigotes: The Role of Cysteine Peptidases and the NF-κB Signaling Pathway. J. Immunol. *173*, 3297–3304.

Carrera, L., Gazzinelli, R.T., Badolato, R., Hieny, S., Muller, W., Kuhn, R., and Sacks, D.L. (1996). Leishmania promastigotes selectively inhibit interleukin 12 induction in bone marrow-derived macrophages from susceptible and resistant mice. J. Exp. Med. *183*, 515–526.

Casgrain, P.-A., Martel, C., McMaster, W.R., Mottram, J.C., Olivier, M., and Descoteaux, A. (2016). Cysteine Peptidase B Regulates Leishmania mexicana Virulence through the Modulation of GP63 Expression. PLOS Pathog. *12*, e1005658.

Chakraborty, D., Banerjee, S., Sen, A., Banerjee, K.K., Das, P., and Roy, S. (2005). Leishmania donovani Affects Antigen Presentation of Macrophage by Disrupting Lipid Rafts. J. Immunol. *175*, 3214–3224.

Chang, K.-P., and McGwire, B.S. (2002). Molecular determinants and regulation of Leishmania virulence. Kinetoplastid Biol. Dis. *1*, 1.

Chang, R.H., Feng, M.H., Liu, W.H., and Lai, M.Z. (1997). Nitric oxide increased interleukin-4 expression in T lymphocytes. Immunology *90*, 364–369.

Charmoy, M., Brunner-Agten, S., Aebischer, D., Auderset, F., Launois, P., Milon, G., Proudfoot, A.E.I., and Tacchini-Cottier, F. (2010). Neutrophil-Derived CCL3 Is Essential for the Rapid Recruitment of Dendritic Cells to the Site of Leishmania major Inoculation in Resistant Mice. PLOS Pathog. *6*, e1000755.

Charmoy, M., Hurrell, B.P., Romano, A., Lee, S.H., Ribeiro-Gomes, F., Riteau, N., Mayer-Barber, K., Tacchini-Cottier, F., and Sacks, D.L. (2016). The Nlrp3 inflammasome, IL-1β, and neutrophil recruitment are required for susceptibility to a non-healing strain of Leishmania major in C57BL/6 mice. Eur. J. Immunol. *46*, 897–911.

Charpentier, T., Hammami, A., and Stäger, S. (2016). Hypoxia inducible factor 1α: A critical factor for the immune response to pathogens and Leishmania. Cell. Immunol. *309*, 42–49.

Cheng, S.-C., Quintin, J., Cramer, R.A., Shepardson, K.M., Saeed, S., Kumar, V., Giamarellos-Bourboulis, E.J., Martens, J.H.A., Rao, N.A., Aghajanirefah, A., et al. (2014). mTOR- and HIF-1α–mediated aerobic glycolysis as metabolic basis for trained immunity. Science *345*, 1250684.

Chiarugi, A., Rovida, E., Dello Sbarba, P., and Moroni, F. (2003). Tryptophan availability selectively limits NO-synthase induction in macrophages. J. Leukoc. Biol. *73*, 172–177.

Chong, S.Z., Evrard, M., and Ng, L.G. (2013). Lights, Camera, and Action: Vertebrate Skin Sets the Stage for Immune Cell Interaction with Arthropod-Vectored Pathogens. Front. Immunol. *4*.

Chughtai, K., and Heeren, R.M.A. (2010). Mass Spectrometric Imaging for Biomedical Tissue Analysis. Chem. Rev. *110*, 3237–3277.

Cleeter, M.W.J., Cooper, J.M., Darley-Usmar, V.M., Moncada, S., and Schapira, A.H.V. (1994). Reversible inhibition of cytochrome c oxidase, the terminal enzyme of the mitochondrial respiratory chain, by nitric oxide. FEBS Lett. *345*, 50–54.

Clementi, E., Brown, G.C., Feelisch, M., and Moncada, S. (1998). Persistent inhibition of cell respiration by nitric oxide: crucial role of S-nitrosylation of mitochondrial complex I and protective action of glutathione. Proc. Natl. Acad. Sci. U. S. A. *95*, 7631–7636.

Comalada, M., Yeramian, A., Modolell, M., Lloberas, J., and Celada, A. (2012). Arginine and Macrophage Activation. In Leucocytes, (Humana Press), pp. 223–235.

Cordes, T., Wallace, M., Michelucci, A., Divakaruni, A.S., Sapcariu, S.C., Sousa, C., Koseki, H., Cabrales, P., Murphy, A.N., Hiller, K., et al. (2016). Immunoresponsive Gene 1 and Itaconate Inhibit Succinate Dehydrogenase to Modulate Intracellular Succinate Levels. J. Biol. Chem. *291*, 14274–14284.

Crusz, S.M., and Balkwill, F.R. (2015). Inflammation and cancer: advances and new agents. Nat. Rev. Clin. Oncol. *12*, 584–596.

Csonka, C., Páli, T., Bencsik, P., Görbe, A., Ferdinandy, P., and Csont, T. (2015). Measurement of NO in biological samples. Br. J. Pharmacol. *172*, 1620–1632.

Daff, S. (2010). NO synthase: Structures and mechanisms. Nitric Oxide *23*, 1–11.

Dai, C.-G., Wang, J.-L., Fu, Y.-L., Zhou, H.-P., and Song, Q.-H. (2017). Selective and Real-Time Detection of Nitric Oxide by a Two-Photon Fluorescent Probe in Live Cells and Tissue Slices. Anal. Chem. *89*, 10511–10519.

Daintith, J. (2008). A Dictionary of Chemistry (Oxford University Press).

Dal Secco, D., Paron, J.A., de Oliveira, S.H.P., Ferreira, S.H., Silva, J.S., and Cunha, F. de Q. (2003). Neutrophil migration in inflammation: nitric oxide inhibits rolling, adhesion and induces apoptosis. Nitric Oxide *9*, 153–164.

Dal Secco, D., Moreira, A.P., Freitas, A., Silva, J.S., Rossi, M.A., Ferreira, S.H., and Cunha, F.Q. (2006). Nitric oxide inhibits neutrophil migration by a mechanism dependent on ICAM-1: Role of soluble guanylate cyclase. Nitric Oxide *15*, 77–86.

Dal Secco, D., Wang, J., Zeng, Z., Kolaczkowska, E., Wong, C.H.Y., Petri, B., Ransohoff, R.M., Charo, I.F., Jenne, C.N., and Kubes, P. (2015). A dynamic spectrum of monocytes arising from the in situ reprogramming of CCR2+ monocytes at a site of sterile injury. J. Exp. Med. *212*, 447–456.

Daynes, R.A., and Jones, D.C. (2002). Emerging roles of PPARS in inflammation and immunity. Nat. Rev. Immunol. *2*, 748–759.

Dean, R.A., Cox, J.H., Bellac, C.L., Doucet, A., Starr, A.E., and Overall, C.M. (2008). Macrophage-specific metalloelastase (MMP-12) truncates and inactivates ELR+ CXC chemokines and generates CCL2, -7, -8, and -13 antagonists: potential role of the macrophage in terminating polymorphonuclear leukocyte influx. Blood *112*, 3455–3464.

Derbyshire, E.R., and Marletta, M.A. (2012). Structure and Regulation of Soluble Guanylate Cyclase. Annu. Rev. Biochem. *81*, 533–559.

Dermine, J.-F., Scianimanico, S., Privé, C., Descoteaux, A., and Desjardins, M. (2000). Leishmania promastigotes require lipophosphoglycan to actively modulate the fusion properties of phagosomes at an early step of phagocytosis. Cell. Microbiol. *2*, 115–126.

Dotiwala, F., Mulik, S., Polidoro, R.B., Ansara, J.A., Burleigh, B.A., Walch, M., Gazzinelli, R.T., and Lieberman, J. (2016). Killer lymphocytes use granulysin, perforin and granzymes to kill intracellular parasites. Nat. Med. *22*, 210–216.

Egen, J.G., Rothfuchs, A.G., Feng, C.G., Horwitz, M.A., Sher, A., and Germain, R.N. (2011). Intravital Imaging Reveals Limited Antigen Presentation and T Cell Effector Function in Mycobacterial Granulomas. Immunity *34*, 807–819.

Eickhoff, S., Brewitz, A., Gerner, M.Y., Klauschen, F., Komander, K., Hemmi, H., Garbi, N., Kaisho, T., Germain, R.N., and Kastenmüller, W. (2015). Robust Anti-viral Immunity Requires Multiple Distinct T Cell-Dendritic Cell Interactions. Cell *162*, 1322–1337.

Eigler, A., Moeller, J., and Endres, S. (1995). Exogenous and endogenous nitric oxide attenuates tumor necrosis factor synthesis in the murine macrophage cell line RAW 264.7. J. Immunol. Baltim. Md 1950 *154*, 4048–4054.

Ekmekcioglu, S., Grimm, E.A., and Roszik, J. (2017). Targeting iNOS to increase efficacy of immunotherapies. Hum. Vaccines Immunother. *13*, 1105–1108.

El Kasmi, K.C., and Stenmark, K.R. (2015). Contribution of Metabolic Reprogramming to Macrophage Plasticity and Function. Semin. Immunol. *27*, 267–275.

El-Hani, C.N., Borges, V.M., Wanderley, J.L.M., and Barcinski, M.A. (2012). Apoptosis and apoptotic mimicry in Leishmania: an evolutionary perspective. Front. Cell. Infect. Microbiol. *2*.

Eroglu, E., Charoensin, S., Bischof, H., Ramadani, J., Gottschalk, B., Depaoli, M.R., Waldeck-Weiermair, M., Graier, W.F., and Malli, R. (2018). Genetic biosensors for imaging nitric oxide in single cells. Free Radic. Biol. Med.

Everts, B., Amiel, E., van der Windt, G.J.W., Freitas, T.C., Chott, R., Yarasheski, K.E., Pearce, E.L., and Pearce, E.J. (2012). Commitment to glycolysis sustains survival of NO-producing inflammatory dendritic cells. Blood *120*, 1422–1431.

Fang, F.C. (2004). Antimicrobial reactive oxygen and nitrogen species: concepts and controversies. Nat. Rev. Microbiol. *2*, 820–832.

Faria, D.R., Souza, P.E.A., Durães, F.V., Carvalho, E.M., Gollob, K.J., Machado, P.R., and Dutra, W.O. (2009). Recruitment of CD8+ T cells expressing granzyme A is associated with lesion progression in human cutaneous leishmaniasis. Parasite Immunol. *31*, 432–439.

Faria, M.S., Reis, F.C.G., and Lima, A.P.C.A. (2012). Toll-Like Receptors in Leishmania Infections: Guardians or Promoters?

Fehr, M., Lalonde, S., Lager, I., Wolff, M.W., and Frommer, W.B. (2003). In Vivo Imaging of the Dynamics of Glucose Uptake in the Cytosol of COS-7 Cells by Fluorescent Nanosensors. J. Biol. Chem. *278*, 19127–19133.

Fehr, M., Takanaga, H., Ehrhardt, D.W., and Frommer, W.B. (2005). Evidence for High-Capacity Bidirectional Glucose Transport across the Endoplasmic Reticulum Membrane by Genetically Encoded Fluorescence Resonance Energy Transfer Nanosensors. Mol. Cell. Biol. *25*, 11102–11112.

Fernandez-de-Cossio-Diaz, J., and Vazquez, A. (2017). Limits of aerobic metabolism in cancer cells. Sci. Rep. *7*.

Figueiredo, A.B., Serafim, T.D., Marques-da-Silva, E.A., Meyer-Fernandes, J.R., and Afonso, L.C.C. (2012). Leishmania amazonensis impairs DC function by inhibiting CD40 expression via A2B adenosine receptor activation. Eur. J. Immunol. *42*, 1203–1215.

Filipe-Santos, O., Pescher, P., Breart, B., Lippuner, C., Aebischer, T., Glaichenhaus, N., Späth, G.F., and Bousso, P. (2009). A Dynamic Map of Antigen Recognition by CD4 T Cells at the Site of Leishmania major Infection. Cell Host Microbe *6*, 23–33.

Filippi, C.M., and Herrath, M. von (2008). IL-10 and the resolution of infections. J. Pathol. *214*, 224–230.

Forestier, C.-L., Gao, Q., and Boons, G.-J. (2015). Leishmania lipophosphoglycan: how to establish structure-activity relationships for this highly complex and multifunctional glycoconjugate? Front. Cell. Infect. Microbiol. *4*.

Forget, G., Gregory, D.J., and Olivier, M. (2005). Proteasome-mediated Degradation of STAT1α following Infection of Macrophages with Leishmania donovani. J. Biol. Chem. *280*, 30542–30549.

Forget, G., Gregory, D.J., Whitcombe, L.A., and Olivier, M. (2006). Role of Host Protein Tyrosine Phosphatase SHP-1 in Leishmania donovani-Induced Inhibition of Nitric Oxide Production. Infect. Immun. *74*, 6272–6279.

Freemerman, A.J., Johnson, A.R., Sacks, G.N., Milner, J.J., Kirk, E.L., Troester, M.A., Macintyre, A.N., Goraksha-Hicks, P., Rathmell, J.C., and Makowski, L. (2014). Metabolic Reprogramming of Macrophages GLUCOSE TRANSPORTER 1 (GLUT1)-MEDIATED GLUCOSE METABOLISM DRIVES A PROINFLAMMATORY PHENOTYPE. J. Biol. Chem. *289*, 7884–7896.

de Freitas Balanco, J.M., Costa Moreira, M.E., Bonomo, A., Bozza, P.T., Amarante-Mendes, G., Pirmez, C., and Barcinski, M.A. (2001). Apoptotic mimicry by an obligate intracellular parasite downregulates macrophage microbicidal activity. Curr. Biol. *11*, 1870–1873.

Fritzsche, C., Schleicher, U., and Bogdan, C. (2010). Endothelial nitric oxide synthase limits the inflammatory response in mouse cutaneous leishmaniasis. Immunobiology *215*, 826–832.

Gabryšová, L., Nicolson, K.S., Streeter, H.B., Verhagen, J., Sabatos-Peyton, C.A., Morgan, D.J., and Wraith, D.C. (2009). Negative feedback control of the autoimmune response through antigen-induced differentiation of IL-10–secreting Th1 cells. J. Exp. Med. *206*, 1755–1767.

Galván-Peña, S., and O'Neill, L.A.J. (2014). Metabolic Reprograming in Macrophage Polarization. Front. Immunol. *5*.

Ganeshan, K., and Chawla, A. (2014). Metabolic Regulation of Immune Responses. Annu. Rev. Immunol. *32*, 609–634.

Gannavaram, S., Bhattacharya, P., Ismail, N., Kaul, A., Singh, R., and Nakhasi, H.L. (2016). Modulation of Innate Immune Mechanisms to Enhance Leishmania Vaccine-Induced Immunity: Role of Coinhibitory Molecules. Front. Immunol. *7*.

Gautier, G., Humbert, M., Deauvieau, F., Scuiller, M., Hiscott, J., Bates, E.E.M., Trinchieri, G., Caux, C., and Garrone, P. (2005). A type I interferon autocrine–paracrine loop is involved in Toll-like receptor-induced interleukin-12p70 secretion by dendritic cells. J. Exp. Med. *201*, 1435–1446.

Geeraerts, X., Bolli, E., Fendt, S.-M., and Van Ginderachter, J.A. (2017). Macrophage Metabolism As Therapeutic Target for Cancer, Atherosclerosis, and Obesity. Front. Immunol. *8*.

Ghosh, S., Bhattacharyya, S., Sirkar, M., Sa, G.S., Das, T., Majumdar, D., Roy, S., and Majumdar, S. (2002). Leishmania donovani suppresses activated protein 1 and NF-kappaB activation in host macrophages via ceramide generation: involvement of extracellular signal-regulated kinase. Infect. Immun. *70*, 6828–6838.

Gillespie, P.M., Beaumier, C.M., Strych, U., Hayward, T., Hotez, P.J., and Bottazzi, M.E. (2016). Status of vaccine research and development of vaccines for leishmaniasis. Vaccine *34*, 2992–2995.

Giustizieri, M.L., Albanesi, C., Scarponi, C., De Pità, O., and Girolomoni, G. (2002). Nitric Oxide Donors Suppress Chemokine Production by Keratinocytes in Vitro and in Vivo. Am. J. Pathol. *161*, 1409–1418.

Glass, C.K., and Natoli, G. (2016). Molecular control of activation and priming in macrophages. Nat. Immunol. *17*, 26–33.

Glennie, N.D., Yeramilli, V.A., Beiting, D.P., Volk, S.W., Weaver, C.T., and Scott, P. (2015). Skin-resident memory CD4+ T cells enhance protection against Leishmania major infection. J. Exp. Med. *212*, 1405–1414.

Glennie, N.D., Volk, S.W., and Scott, P. (2017). Skin-resident CD4+ T cells protect against Leishmania major by recruiting and activating inflammatory monocytes. PLOS Pathog. *13*, e1006349.

Godson, C., Mitchell, S., Harvey, K., Petasis, N.A., Hogg, N., and Brady, H.R. (2000). Cutting Edge: Lipoxins Rapidly Stimulate Nonphlogistic Phagocytosis of Apoptotic Neutrophils by Monocyte-Derived Macrophages. J. Immunol. *164*, 1663–1667.

Gollob, K.J., Antonelli, L.R.V., and Dutra, W.O. (2005). Insights into CD4+ memory T cells following Leishmania infection. Trends Parasitol. *21*, 347–350.

Goncalves, R., Zhang, X., Cohen, H., Debrabant, A., and Mosser, D.M. (2011). Platelet activation attracts a subpopulation of effector monocytes to sites of Leishmania major infection. J. Exp. Med. *208*, 1253–1265.

Greene, E.R., Huang, S., Serhan, C.N., and Panigrahy, D. (2011). Regulation of inflammation in cancer by eicosanoids. Prostaglandins Other Lipid Mediat. *96*, 27–36.

Gregory, D.J., Godbout, M., Contreras, I., Forget, G., and Olivier, M. (2008). A novel form of NF-κB is induced by Leishmania infection: Involvement in macrophage gene expression. Eur. J. Immunol. *38*, 1071–1081.

Griffith, J.W., Sokol, C.L., and Luster, A.D. (2014). Chemokines and Chemokine Receptors: Positioning Cells for Host Defense and Immunity. Annu. Rev. Immunol. *32*, 659–702.

Grimm, M.J., Vethanayagam, R.R., Almyroudis, N.G., Dennis, C.G., Khan, A.N.H., D'Auria, A.C., Singel, K.L., Davidson, B.A., Knight, P.R., Blackwell, T.S., et al. (2013). Monocyte- and macrophage-targeted NADPH oxidase mediates antifungal host defense and regulation of acute inflammation in mice. J. Immunol. Baltim. Md 1950 *190*, 4175–4184.

Grivennikov, S.I., Greten, F.R., and Karin, M. (2010). Immunity, Inflammation, and Cancer. Cell *140*, 883–899.

Guarda, G., Dostert, C., Staehli, F., Cabalzar, K., Castillo, R., Tardivel, A., Schneider, P., and Tschopp, J. (2009). T cells dampen innate immune responses through inhibition of NLRP1 and NLRP3 inflammasomes. Nature *460*, 269–273.

Guarda, G., Braun, M., Staehli, F., Tardivel, A., Mattmann, C., Förster, I., Farlik, M., Decker, T., Du Pasquier, R.A., Romero, P., et al. (2011). Type I Interferon Inhibits Interleukin-1 Production and Inflammasome Activation. Immunity *34*, 213–223.

Guilliams, M., Dutertre, C.-A., Scott, C.L., McGovern, N., Sichien, D., Chakarov, S., Van Gassen, S., Chen, J., Poidinger, M., De Prijck, S., et al. (2016). Unsupervised High-Dimensional Analysis Aligns Dendritic Cells across Tissues and Species. Immunity *45*, 669–684.

Gupta, G., Oghumu, S., and Satoskar, A.R. (2013). Chapter Five - Mechanisms of Immune Evasion in Leishmaniasis. In Advances in Applied Microbiology, S. Sariaslani, and G.M. Gadd, eds. (Academic Press), pp. 155–184.

Gurung, P., Karki, R., Vogel, P., Watanabe, M., Bix, M., Lamkanfi, M., and Kanneganti, T.-D. (2015). An NLRP3 inflammasome–triggered Th2-biased adaptive immune response promotes leishmaniasis. J. Clin. Invest. *125*, 1329–1338.

Harari, O., and Liao, J.K. (2004). Inhibition of MHC II Gene Transcription by Nitric Oxide and Antioxidants. Curr. Pharm. Des. *10*, 893–898.

Hardie, D.G., Scott, J.W., Pan, D.A., and Hudson, E.R. (2003). Management of cellular energy by the AMP-activated protein kinase system. FEBS Lett. *546*, 113–120.

Hartley, M.-A., Drexler, S., Ronet, C., Beverley, S.M., and Fasel, N. (2014). The immunological, environmental, and phylogenetic perpetrators of metastatic leishmaniasis. Trends Parasitol. *30*, 412–422.

Haschemi, A., Kosma, P., Gille, L., Evans, C.R., Burant, C.F., Starkl, P., Knapp, B., Haas, R., Schmid, J.A., Jandl, C., et al. (2012). The Sedoheptulose Kinase CARKL Directs Macrophage Polarization through Control of Glucose Metabolism. Cell Metab. *15*, 813–826.

Hatzigeorgiou, D.E., Geng, J., Zhu, B., Zhang, Y., Liu, K., Rom, W.N., Fenton, M.J., Turco, S.J., and Ho, J.L. (1996). Lipophosphoglycan from Leishmania suppresses agonist-induced interleukin 1 beta gene expression in human monocytes via a unique promoter sequence. Proc. Natl. Acad. Sci. U. S. A. *93*, 14708–14713.

Henard, C.A., and Vázquez-Torres, A. (2011). Nitric Oxide and Salmonella Pathogenesis. Front. Microbiol. *2*.

Herbst, S., Schaible, U.E., and Schneider, B.E. (2011). Interferon Gamma Activated Macrophages Kill Mycobacteria by Nitric Oxide Induced Apoptosis. PLOS ONE *6*, e19105.

Hernández-Chinea, C., Maimone, L., Campos, Y., Mosca, W., and Romero, P.J. (2017). Apparent isocitrate lyase activity in Leishmania amazonensis. Acta Parasitol. *62*, 701–707.

Hernandez-Cuellar, E., Tsuchiya, K., Hara, H., Fang, R., Sakai, S., Kawamura, I., Akira, S., and Mitsuyama, M. (2012). Cutting Edge: Nitric Oxide Inhibits the NLRP3 Inflammasome. J. Immunol. *189*, 5113–5117.

Hess, D.T., Matsumoto, A., Kim, S.-O., Marshall, H.E., and Stamler, J.S. (2005). Protein *S*-nitrosylation: purview and parameters. Nat. Rev. Mol. Cell Biol. *6*, 150–166.

Hickey, M.J. (2001). Role of inducible nitric oxide synthase in the regulation of leucocyte recruitment. Clin. Sci. *100*, 1–12.

Hirotatsu, K., Nakatsubo, N., Kikuchi, K., Urano, Y., Higuchi, T., Tanaka, J., Kudo, Y., and Nagano, T. (1998). Direct evidence of NO production in rat hippocampus and cortex using a new fluorescent indicator: DAF-2 DA. NeuroReport *9*, 3345.

Hobson-Gutierrez, S.A., and Carmona-Fontaine, C. (2018). The metabolic axis of macrophage and immune cell polarization. Dis. Model. Mech. *11*, dmm034462.

Hölscher, C., Köhler, G., Müller, U., Mossmann, H., Schaub, G.A., and Brombacher, F. (1998). Defective Nitric Oxide Effector Functions Lead to Extreme Susceptibility of Trypanosoma cruzi-Infected Mice Deficient in Gamma Interferon Receptor or Inducible Nitric Oxide Synthase. Infect. Immun. *66*, 1208–1215.

Holzmuller, P., Bras-Gonçalves, R., and Lemesre, J.-L. (2006). Phenotypical characteristics, biochemical pathways, molecular targets and putative role of nitric oxide-mediated programmed cell death in Leishmania. Parasitology *132*, S19–S32.

Huang, F.-P., Niedbala, W., Wei, X.-Q., Xu, D., Feng, G., Robinson, J.H., Lam, C., and Liew, F.Y. (1998). Nitric oxide regulates Th1 cell development through the inhibition of IL-12 synthesis by macrophages. Eur. J. Immunol. *28*, 4062–4070.

Ibiza, S., and Serrador, J.M. (2008). The role of nitric oxide in the regulation of adaptive immune responses. Inmunología *27*, 103–117.

Ibiza, S., Víctor, V.M., Boscá, I., Ortega, A., Urzainqui, A., O'Connor, J.E., Sánchez-Madrid, F., Esplugues, J.V., and Serrador, J.M. (2006). Endothelial Nitric Oxide Synthase Regulates T Cell Receptor Signaling at the Immunological Synapse. Immunity *24*, 753–765.

Inbar, E., Hughitt, V.K., Dillon, L.A.L., Ghosh, K., El-Sayed, N.M., and Sacks, D.L. (2017). The Transcriptome of Leishmania major Developmental Stages in Their Natural Sand Fly Vector. MBio *8*, e00029-17.

Infantino, V., Convertini, P., Cucci, L., Panaro, M.A., Di Noia, M.A., Calvello, R., Palmieri, F., and Iacobazzi, V. (2011). The mitochondrial citrate carrier: a new player in inflammation. Biochem. J. *438*, 433–436.

Iniesta, V., Gómez-Nieto, L.C., and Corraliza, I. (2001). The inhibition of arginase by N(omega)-hydroxy-l-arginine controls the growth of Leishmania inside macrophages. J. Exp. Med. *193*, 777–784.

Ip, W.K.E., Hoshi, N., Shouval, D.S., Snapper, S., and Medzhitov, R. (2017). Anti-inflammatory effect of IL-10 mediated by metabolic reprogramming of macrophages. Science *356*, 513–519.

Ito, C., Saito, Y., Nozawa, T., Fujii, S., Sawa, T., Inoue, H., Matsunaga, T., Khan, S., Akashi, S., Hashimoto, R., et al. (2013). Endogenous Nitrated Nucleotide Is a Key Mediator of Autophagy and Innate Defense against Bacteria. Mol. Cell *52*, 794–804.

Jamaati, H., Mortaz, E., Pajouhi, Z., Folkerts, G., Movassaghi, M., Moloudizargari, M., Adcock, I.M., and Garssen, J. (2017). Nitric Oxide in the Pathogenesis and Treatment of Tuberculosis. Front. Microbiol. *8*.

Jantsch, J., Schatz, V., Friedrich, D., Schröder, A., Kopp, C., Siegert, I., Maronna, A., Wendelborn, D., Linz, P., Binger, K.J., et al. (2015). Cutaneous Na+ Storage Strengthens the Antimicrobial Barrier Function of the Skin and Boosts Macrophage-Driven Host Defense. Cell Metab. *21*, 493–501.

Jaramillo, M., Gomez, M.A., Larsson, O., Shio, M.T., Topisirovic, I., Contreras, I., Luxenburg, R., Rosenfeld, A., Colina, R., McMaster, R.W., et al. (2011). Leishmania Repression of Host

Translation through mTOR Cleavage Is Required for Parasite Survival and Infection. Cell Host Microbe *9*, 331–341.

Jha, A.K., Huang, S.C.-C., Sergushichev, A., Lampropoulou, V., Ivanova, Y., Loginicheva, E., Chmielewski, K., Stewart, K.M., Ashall, J., Everts, B., et al. (2015). Network Integration of Parallel Metabolic and Transcriptional Data Reveals Metabolic Modules that Regulate Macrophage Polarization. Immunity *42*, 419–430.

Johnson, J.M., and Kellogg, D.L. (2010). Local thermal control of the human cutaneous circulation. J. Appl. Physiol. *109*, 1229–1238.

Jones, H.R., Robb, C.T., Perretti, M., and Rossi, A.G. (2016). The role of neutrophils in inflammation resolution. Semin. Immunol. *28*, 137–145.

Kashem, S.W., Haniffa, M., and Kaplan, D.H. (2017). Antigen-Presenting Cells in the Skin. Annu. Rev. Immunol. *35*, 469–499.

Kashiwagi, S., Tsukada, K., Xu, L., Miyazaki, J., Kozin, S.V., Tyrrell, J.A., Sessa, W.C., Gerweck, L.E., Jain, R.K., and Fukumura, D. (2008). Perivascular nitric oxide gradients normalize tumor vasculature. Nat. Med. *14*, 255–257.

Kaye, P., and Scott, P. (2011). Leishmaniasis: complexity at the host–pathogen interface. Nat. Rev. Microbiol. *9*, 604–615.

Kelleher, Z.T., Matsumoto, A., Stamler, J.S., and Marshall, H.E. (2007). NOS2 Regulation of NF-κB by S-Nitrosylation of p65. J. Biol. Chem. *282*, 30667–30672.

Kelly, B., and O'Neill, L.A. (2015). Metabolic reprogramming in macrophages and dendritic cells in innate immunity. Cell Res. *25*, 771–784.

Kelm, M. (1999). Nitric oxide metabolism and breakdown. Biochim. Biophys. Acta BBA - Bioenerg. *1411*, 273–289.

Kima, P.E., and Soong, L. (2013). Interferon Gamma in Leishmaniasis. Front. Immunol. *4*.

Kima, P.E., Soong, L., Chicharro, C., Ruddle, N.H., and McMahon-Pratt, D. (1996). Leishmania-infected macrophages sequester endogenously synthesized parasite antigens from presentation to CD4+ T cells. Eur. J. Immunol. *26*, 3163–3169.

Kobayashi, Y. (2010). The regulatory role of nitric oxide in proinflammatory cytokine expression during the induction and resolution of inflammation. J. Leukoc. Biol. *88*, 1157–1162.

Kone, B.C., Kuncewicz, T., Zhang, W., and Yu, Z.-Y. (2003). Protein interactions with nitric oxide synthases: controlling the right time, the right place, and the right amount of nitric oxide. Am. J. Physiol.-Ren. Physiol. *285*, F178–F190.

Kreisel, D., Nava, R.G., Li, W., Zinselmeyer, B.H., Wang, B., Lai, J., Pless, R., Gelman, A.E., Krupnick, A.S., and Miller, M.J. (2010). In vivo two-photon imaging reveals monocyte-dependent neutrophil extravasation during pulmonary inflammation. Proc. Natl. Acad. Sci. *107*, 18073–18078.

Kubes, P., Suzuki, M., and Granger, D.N. (1991). Nitric oxide: an endogenous modulator of leukocyte adhesion. Proc. Natl. Acad. Sci. *88*, 4651–4655.

Kumar, R., and Engwerda, C. (2014). Vaccines to prevent leishmaniasis. Clin. Transl. Immunol. *3*, e13.

La Flamme, A.C., Kharkrang, M., Stone, S., Mirmoeini, S., Chuluundorj, D., and Kyle, R. (2012). Type II-Activated Murine Macrophages Produce IL-4. PLoS ONE *7*.

Lamkanfi, M., and Dixit, V.M. (2014). Mechanisms and Functions of Inflammasomes. Cell *157*, 1013–1022.

Lämmermann, T., Afonso, P.V., Angermann, B.R., Wang, J.M., Kastenmüller, W., Parent, C.A., and Germain, R.N. (2013). Neutrophil swarms require LTB4 and integrins at sites of cell death *in vivo* . Nature *498*, 371–375.

Lampropoulou, V., Sergushichev, A., Bambouskova, M., Nair, S., Vincent, E.E., Loginicheva, E., Cervantes-Barragan, L., Ma, X., Huang, S.C.-C., Griss, T., et al. (2016). Itaconate Links Inhibition of Succinate Dehydrogenase with Macrophage Metabolic Remodeling and Regulation of Inflammation. Cell Metab. *24*, 158–166.

Lancaster, J.R. (1997). A Tutorial on the Diffusibility and Reactivity of Free Nitric Oxide. Nitric Oxide *1*, 18–30.

Langlet, C., Tamoutounour, S., Henri, S., Luche, H., Ardouin, L., Grégoire, C., Malissen, B., and Guilliams, M. (2012). CD64 Expression Distinguishes Monocyte-Derived and Conventional Dendritic Cells and Reveals Their Distinct Role during Intramuscular Immunization. J. Immunol. *188*, 1751–1760.

Langston, P.K., Shibata, M., and Horng, T. (2017). Metabolism Supports Macrophage Activation. Front. Immunol. *8*.

Laskay, T., Zandbergen, G. van, and Solbach, W. (2003). Neutrophil granulocytes – Trojan horses for Leishmania major and other intracellular microbes? Trends Microbiol. *11*, 210–214.

Laskay, T., van Zandbergen, G., and Solbach, W. (2008). Neutrophil granulocytes as host cells and transport vehicles for intracellular pathogens: Apoptosis as infection-promoting factor. Immunobiology *213*, 183–191.

Lawless, S.J., Kedia-Mehta, N., Walls, J.F., McGarrigle, R., Convery, O., Sinclair, L.V., Navarro, M.N., Murray, J., and Finlay, D.K. (2017). Glucose represses dendritic cell-induced T cell responses. Nat. Commun. *8*, 15620.

Lee, S.-W., Choi, H., Eun, S.-Y., Fukuyama, S., and Croft, M. (2011). Nitric Oxide Modulates TGF-β–Directive Signals To Suppress Foxp3+ Regulatory T Cell Differentiation and Potentiate Th1 Development. J. Immunol. Baltim. Md 1950 *186*, 6972–6980.

Lefer, D.J., Jones, S.P., Girod, W.G., Baines, A., Grisham, M.B., Cockrell, A.S., Huang, P.L., and Scalia, R. (1999). Leukocyte-endothelial cell interactions in nitric oxide synthase-deficient mice. Am. J. Physiol. *276*, H1943-1950.

Lemesre, J.-L., Sereno, D., Daulouède, S., Veyret, B., Brajon, N., and Vincendeau, P. (1997). Leishmaniaspp.: Nitric Oxide-Mediated Metabolic Inhibition of Promastigote and Axenically Grown Amastigote Forms. Exp. Parasitol. *86*, 58–68.

León, B., López-Bravo, M., and Ardavín, C. (2007). Monocyte-Derived Dendritic Cells Formed at the Infection Site Control the Induction of Protective T Helper 1 Responses against Leishmania. Immunity *26*, 519–531.

Letterio, J.J., and Roberts, A.B. (1998). REGULATION OF IMMUNE RESPONSES BY TGF-β. Annu. Rev. Immunol. *16*, 137–161.

Liberti, M.V., and Locasale, J.W. (2016). The Warburg Effect: How Does it Benefit Cancer Cells? Trends Biochem. Sci. *41*, 211–218.

Liew, F.Y., Millott, S., Parkinson, C., Palmer, R.M., and Moncada, S. (1990). Macrophage killing of Leishmania parasite in vivo is mediated by nitric oxide from L-arginine. J. Immunol. *144*, 4794–4797.

Lima-Junior, D.S., Costa, D.L., Carregaro, V., Cunha, L.D., Silva, A.L.N., Mineo, T.W.P., Gutierrez, F.R.S., Bellio, M., Bortoluci, K.R., Flavell, R.A., et al. (2013). Inflammasome-derived IL-1β production induces nitric oxide–mediated resistance to *Leishmania*. Nat. Med. *19*, 909–915.

Liu, D., and Uzonna, J.E. (2012). The early interaction of Leishmania with macrophages and dendritic cells and its influence on the host immune response. Front. Cell. Infect. Microbiol. *2*.

Liu, L., Lu, Y., Martinez, J., Bi, Y., Lian, G., Wang, T., Milasta, S., Wang, J., Yang, M., Liu, G., et al. (2016). Proinflammatory signal suppresses proliferation and shifts macrophage metabolism from Myc-dependent to HIF1α-dependent. Proc. Natl. Acad. Sci. U. S. A. *113*, 1564–1569.

Liu, Q., Xue, L., Zhu, D.-J., Li, G.-P., and Jiang, H. (2014). Highly selective two-photon fluorescent probe for imaging of nitric oxide in living cells. Chin. Chem. Lett. *25*, 19–23.

Llovera, M., Pearson, J.D., Moreno, C., and Riveros-Moreno, V. (2001). Impaired response to interferon-γ in activated macrophages due to tyrosine nitration of STAT1 by endogenous nitric oxide. Br. J. Pharmacol. *132*, 419–426.

Lo, S.K., Bovis, L., Matura, R., Zhu, B., He, S., Lum, H., Turco, S.J., and Ho, J.L. (1998). Leishmania lipophosphoglycan reduces monocyte transendothelial migration: Modulation of cell adhesion molecules, intercellular junctional proteins, and chemoattractants. J. Immunol. *160*, 1857–1865.

Lodge, R., Diallo, T.O., and Descoteaux, A. (2006). Leishmania donovani lipophosphoglycan blocks NADPH oxidase assembly at the phagosome membrane. Cell. Microbiol. *8*, 1922–1931.

Loeuillet, C., Bañuls, A.-L., and Hide, M. (2016). Study of Leishmania pathogenesis in mice: experimental considerations. Parasit. Vectors *9*.

Lorenz, M.C., and Fink, G.R. (2002). Life and Death in a Macrophage: Role of the Glyoxylate Cycle in Virulence. Eukaryot. Cell *1*, 657–662.

Lowenstein, C.J., and Padalko, E. (2004). iNOS (NOS2) at a glance. J. Cell Sci. *117*, 2865–2867.

Lu, G., Zhang, R., Geng, S., Peng, L., Jayaraman, P., Chen, C., Xu, F., Yang, J., Li, Q., Zheng, H., et al. (2015). Myeloid cell-derived inducible nitric oxide synthase suppresses M1 macrophage polarization. Nat. Commun. *6*, 6676.

Lukacs-Kornek, V., Malhotra, D., Fletcher, A.L., Acton, S.E., Elpek, K.G., Tayalia, P., Collier, A., and Turley, S.J. (2011). Regulated release of nitric oxide by nonhematopoietic stroma controls expansion of the activated T cell pool in lymph nodes. Nat. Immunol. *12*, 1096–1104.

Lunt, S.Y., and Vander Heiden, M.G. (2011). Aerobic Glycolysis: Meeting the Metabolic Requirements of Cell Proliferation. Annu. Rev. Cell Dev. Biol. *27*, 441–464.

Maarsingh, H., Zaagsma, J., and Meurs, H. (2009). Arginase: a key enzyme in the pathophysiology of allergic asthma opening novel therapeutic perspectives. Br. J. Pharmacol. *158*, 652–664.

Machado, J.D., Segura, F., Brioso, M.A., and Borges, R. (2000). Nitric Oxide Modulates a Late Step of Exocytosis. J. Biol. Chem. *275*, 20274–20279.

MacMicking, J.D. (2012). Interferon-inducible effector mechanisms in cell-autonomous immunity. Nat. Rev. Immunol. *12*, 367–382.

MacMicking, J.D., Nathan, C., Hom, G., Chartrain, N., Fletcher, D.S., Trumbauer, M., Stevens, K., Xie, Q., Sokol, K., Hutchinson, N., et al. (1995). Altered responses to bacterial infection and endotoxic shock in mice lacking inducible nitric oxide synthase. Cell *81*, 641–650.

MacMicking, J.D., North, R.J., LaCourse, R., Mudgett, J.S., Shah, S.K., and Nathan, C.F. (1997). Identification of nitric oxide synthase as a protective locus against tuberculosis. Proc. Natl. Acad. Sci. *94*, 5243–5248.

Mahnke, A., Meier, R.J., Schatz, V., Hofmann, J., Castiglione, K., Schleicher, U., Wolfbeis, O.S., Bogdan, C., and Jantsch, J. (2014). Hypoxia in Leishmania major Skin Lesions Impairs the NO-Dependent Leishmanicidal Activity of Macrophages. J. Invest. Dermatol. *134*, 2339–2346.

Malherbe, L., Filippi, C., Julia, V., Foucras, G., Moro, M., Appel, H., Wucherpfennig, K., Guéry, J.-C., and Glaichenhaus, N. (2000). Selective Activation and Expansion of High-Affinity CD4+ T Cells in Resistant Mice upon Infection with Leishmania major. Immunity *13*, 771–782.

Malissen, B., Tamoutounour, S., and Henri, S. (2014). The origins and functions of dendritic cells and macrophages in the skin. Nat. Rev. Immunol. *14*, 417–428.

Mandell, M.A., and Beverley, S.M. (2017). Continual renewal and replication of persistent Leishmania major parasites in concomitantly immune hosts. Proc. Natl. Acad. Sci. *114*, E801–E810.

Mantovani, A., Bonecchi, R., and Locati, M. (2006). Tuning inflammation and immunity by chemokine sequestration: decoys and more. Nat. Rev. Immunol. *6*, 907–918.

Mao, K., Chen, S., Chen, M., Ma, Y., Wang, Y., Huang, B., He, Z., Zeng, Y., Hu, Y., Sun, S., et al. (2013). Nitric oxide suppresses NLRP3 inflammasome activation and protects against LPS-induced septic shock. Cell Res. *23*, 201–212.

Marth, T., and Kelsall, B.L. (1997). Regulation of Interleukin-12 by Complement Receptor 3 Signaling. J. Exp. Med. *185*, 1987–1995.

Martín, A.S., Ceballo, S., Ruminot, I., Lerchundi, R., Frommer, W.B., and Barros, L.F. (2013). A Genetically Encoded FRET Lactate Sensor and Its Use To Detect the Warburg Effect in Single Cancer Cells. PLOS ONE *8*, e57712.

Martín, A.S., Ceballo, S., Baeza-Lehnert, F., Lerchundi, R., Valdebenito, R., Contreras-Baeza, Y., Alegría, K., and Barros, L.F. (2014). Imaging Mitochondrial Flux in Single Cells with a FRET Sensor for Pyruvate. PLOS ONE *9*, e85780.

Martinez, F.O., and Gordon, S. (2014). The M1 and M2 paradigm of macrophage activation: time for reassessment. F1000Prime Rep *6*.

Martínez-López, M., Soto, M., Iborra, S., and Sancho, D. (2018). Leishmania Hijacks Myeloid Cells for Immune Escape. Front. Microbiol. *9*.

Martiny, A., Meyer-Fernandes, J.R., de Souza, W., and Vannier-Santos, M.A. (1999). Altered tyrosine phosphorylation of ERK1 MAP kinase and other macrophage molecules caused by Leishmania amastigotes. Mol. Biochem. Parasitol. *102*, 1–12.

Matheoud, D., Moradin, N., Bellemare-Pelletier, A., Shio, M.T., Hong, W.J., Olivier, M., Gagnon, É., Desjardins, M., and Descoteaux, A. (2013). Leishmania Evades Host Immunity by Inhibiting Antigen Cross-Presentation through Direct Cleavage of the SNARE VAMP8. Cell Host Microbe *14*, 15–25.

Matsushita, K., Morrell, C.N., Cambien, B., Yang, S.-X., Yamakuchi, M., Bao, C., Hara, M.R., Quick, R.A., Cao, W., O'Rourke, B., et al. (2003). Nitric Oxide Regulates Exocytosis by S-Nitrosylation of N-ethylmaleimide-Sensitive Factor. Cell *115*, 139–150.

Matte, C., Maion, G., Mourad, W., and Olivier, M. (2001). Leishmania donovani-induced macrophages cyclooxygenase-2 and prostaglandin E2 synthesis. Parasite Immunol. *23*, 177–184.

Matthews, J.R., Botting, C.H., Panico, M., Morris, H.R., and Hay, R.T. (1996). Inhibition of NF-kappaB DNA binding by nitric oxide. Nucleic Acids Res. *24*, 2236–2242.

Mauël, J., and Ransijn, A. (1997). Leishmaniaspp.: Mechanisms of Toxicity of Nitrogen Oxidation Products. Exp. Parasitol. *87*, 98–111.

Mazzoni, A., Bronte, V., Visintin, A., Spitzer, J.H., Apolloni, E., Serafini, P., Zanovello, P., and Segal, D.M. (2002). Myeloid Suppressor Lines Inhibit T Cell Responses by an NO-Dependent Mechanism. J. Immunol. *168*, 689–695.

McConville, M.J., and Naderer, T. (2011). Metabolic Pathways Required for the Intracellular Survival of Leishmania. Annu. Rev. Microbiol. *65*, 543–561.

McConville, M.J., de Souza, D., Saunders, E., Likic, V.A., and Naderer, T. (2007). Living in a phagolysosome; metabolism of Leishmania amastigotes. Trends Parasitol. *23*, 368–375.

McQuibban, G.A., Gong, J.-H., Wong, J.P., Wallace, J.L., Clark-Lewis, I., and Overall, C.M. (2002). Matrix metalloproteinase processing of monocyte chemoattractant proteins generates CC chemokine receptor antagonists with anti-inflammatory properties in vivo. Blood *100*, 1160–1167.

Medzhitov, R. (2008). Origin and physiological roles of inflammation.

Meier, C.L., Svensson, M., and Kaye, P.M. (2003). Leishmania-Induced Inhibition of Macrophage Antigen Presentation Analyzed at the Single-Cell Level. J. Immunol. *171*, 6706–6713.

Mendes, A.F., Carvalho, A.P., Caramona, M.M., and Lopes, M.C. (2002). Role of nitric oxide in the activation of NF-κB, AP-1 and NOS II expression in articular chondrocytes. Inflamm. Res. *51*, 369–375.

Mendez, S., Reckling, S.K., Piccirillo, C.A., Sacks, D., and Belkaid, Y. (2004). Role for CD4+ CD25+ Regulatory T Cells in Reactivation of Persistent Leishmaniasis and Control of Concomitant Immunity. J. Exp. Med. *200*, 201–210.

Menezes, S., Melandri, D., Anselmi, G., Perchet, T., Loschko, J., Dubrot, J., Patel, R., Gautier, E.L., Hugues, S., Longhi, M.P., et al. (2016). The Heterogeneity of Ly6Chi Monocytes Controls Their Differentiation into iNOS+ Macrophages or Monocyte-Derived Dendritic Cells. Immunity *45*, 1205–1218.

Meredith, M.M., Liu, K., Darrasse-Jeze, G., Kamphorst, A.O., Schreiber, H.A., Guermonprez, P., Idoyaga, J., Cheong, C., Yao, K.-H., Niec, R.E., et al. (2012). Expression of the zinc finger transcription factor zDC (Zbtb46, Btbd4) defines the classical dendritic cell lineage. J. Exp. Med. *209*, 1153–1165.

Michelucci, A., Cordes, T., Ghelfi, J., Pailot, A., Reiling, N., Goldmann, O., Binz, T., Wegner, A., Tallam, A., Rausell, A., et al. (2013). Immune-responsive gene 1 protein links metabolism to immunity by catalyzing itaconic acid production. Proc. Natl. Acad. Sci. U. S. A. *110*, 7820–7825.

Mildner, A., and Jung, S. (2014). Development and Function of Dendritic Cell Subsets. Immunity *40*, 642–656.

Mildner, A., Marinkovic, G., and Jung, S. (2016). Murine Monocytes: Origins, Subsets, Fates, and Functions. Microbiol. Spectr. *4*.

Miller, M.B., and Bassler, B.L. (2001). Quorum Sensing in Bacteria. Annu. Rev. Microbiol. *55*, 165–199.

Millet, P., Vachharajani, V., McPhail, L., Yoza, B., and McCall, C.E. (2016). GAPDH Binding to TNF-α mRNA Contributes to Posttranscriptional Repression in Monocytes: A Novel Mechanism of Communication between Inflammation and Metabolism. J. Immunol. *196*, 2541–2551.

Mills, E., and O'Neill, L.A.J. (2014). Succinate: a metabolic signal in inflammation. Trends Cell Biol. *24*, 313–320.

Mills, E.L., Kelly, B., Logan, A., Costa, A.S.H., Varma, M., Bryant, C.E., Tourlomousis, P., Däbritz, J.H.M., Gottlieb, E., Latorre, I., et al. (2016). Succinate Dehydrogenase Supports Metabolic Repurposing of Mitochondria to Drive Inflammatory Macrophages. Cell *167*, 457-470.e13.

Mills, E.L., Ryan, D.G., Prag, H.A., Dikovskaya, D., Menon, D., Zaslona, Z., Jedrychowski, M.P., Costa, A.S.H., Higgins, M., Hams, E., et al. (2018). Itaconate is an anti-inflammatory metabolite that activates Nrf2 via alkylation of KEAP1. Nature *556*, 113–117.

Mishra, B.B., Rathinam, V.A.K., Martens, G.W., Martinot, A.J., Kornfeld, H., Fitzgerald, K.A., and Sassetti, C.M. (2013). Nitric oxide controls the immunopathology of tuberculosis by inhibiting NLRP3 inflammasome–dependent processing of IL-1β. Nat. Immunol. *14*, 52–60.

Mishra, B.B., Lovewell, R.R., Olive, A.J., Zhang, G., Wang, W., Eugenin, E., Smith, C.M., Phuah, J.Y., Long, J.E., Dubuke, M.L., et al. (2017). Nitric oxide prevents a pathogen-permissive granulocytic inflammation during tuberculosis. Nat. Microbiol. *2*, 17072.

Montaudouin, C., Anson, M., Hao, Y., Duncker, S.V., Fernandez, T., Gaudin, E., Ehrenstein, M., Kerr, W.G., Colle, J.-H., Bruhns, P., et al. (2013). Quorum Sensing Contributes to Activated IgM-Secreting B Cell Homeostasis. J. Immunol. *190*, 106–114.

Moore, K.W., de Waal Malefyt, R., Coffman, R.L., and O'Garra, A. (2001). Interleukin-10 and the Interleukin-10 Receptor. Annu. Rev. Immunol. *19*, 683–765.

Moore, W.M., Webber, R.K., Jerome, G.M., Tjoeng, F.S., Misko, T.P., and Currie, M.G. (1994). L-N6-(1-Iminoethyl)lysine: A Selective Inhibitor of Inducible Nitric Oxide Synthase. J. Med. Chem. *37*, 3886–3888.

Moradin, N., and Descoteaux, A. (2012). Leishmania promastigotes: building a safe niche within macrophages. Front. Cell. Infect. Microbiol. *2*.

Mosser, D.M., and Edwards, J.P. (2008). Exploring the full spectrum of macrophage activation. Nat. Rev. Immunol. *8*, 958–969.

Mosser, D.M., and Zhang, X. (2008). Interleukin-10: new perspectives on an old cytokine. Immunol. Rev. *226*, 205–218.

Mougneau, E., Bihl, F., and Glaichenhaus, N. (2011). Cell biology and immunology of Leishmania. Immunol. Rev. *240*, 286–296.

Moyo, D., Beattie, L., Andrews, P.S., Moore, J.W.J., Timmis, J., Sawtell, A., Hoehme, S., Sampson, A.T., and Kaye, P.M. (2018). Macrophage Transactivation for Chemokine Production Identified as a Negative Regulator of Granulomatous Inflammation Using Agent-Based Modeling. Front. Immunol. *9*.

Muleme, H.M., Reguera, R.M., Berard, A., Azinwi, R., Jia, P., Okwor, I.B., Beverley, S., and Uzonna, J.E. (2009). Infection with Arginase-Deficient Leishmania major Reveals a Parasite Number-Dependent and Cytokine-Independent Regulation of Host Cellular Arginase Activity and Disease Pathogenesis. J. Immunol. *183*, 8068–8076.

Müller, A.J., Filipe-Santos, O., Eberl, G., Aebischer, T., Späth, G.F., and Bousso, P. (2012). CD4+ T Cells Rely on a Cytokine Gradient to Control Intracellular Pathogens beyond Sites of Antigen Presentation. Immunity *37*, 147–157.

Müller, A.J., Aeschlimann, S., Olekhnovitch, R., Dacher, M., Späth, G.F., and Bousso, P. (2013). Photoconvertible Pathogen Labeling Reveals Nitric Oxide Control of Leishmania major Infection In Vivo via Dampening of Parasite Metabolism. Cell Host Microbe *14*, 460–467.

Munn, D.H., Shafizadeh, E., Attwood, J.T., Bondarev, I., Pashine, A., and Mellor, A.L. (1999). Inhibition of T cell proliferation by macrophage tryptophan catabolism. J. Exp. Med. *189*, 1363–1372.

Murphy, M.P. (2009). How mitochondria produce reactive oxygen species. Biochem. J. *417*, 1–13.

Murray, P.J. (2017). Macrophage Polarization. Annu. Rev. Physiol. *79*, 541–566.

Murray, P.J., and Wynn, T.A. (2011). Protective and pathogenic functions of macrophage subsets. Nat. Rev. Immunol. *11*, 723–737.

Murray, P.J., Allen, J.E., Biswas, S.K., Fisher, E.A., Gilroy, D.W., Goerdt, S., Gordon, S., Hamilton, J.A., Ivashkiv, L.B., Lawrence, T., et al. (2014). Macrophage Activation and Polarization: Nomenclature and Experimental Guidelines. Immunity *41*, 14–20.

Na, Y.R., Je, S., and Seok, S.H. (2018). Metabolic features of macrophages in inflammatory diseases and cancer. Cancer Lett. *413*, 46–58.

Nagaraj, S., Gupta, K., Pisarev, V., Kinarsky, L., Sherman, S., Kang, L., Herber, D., Schneck, J., and Gabrilovich, D.I. (2007). Altered recognition of antigen is a novel mechanism of CD8+ T cell tolerance in cancer. Nat. Med. *13*, 828–835.

Nagy, G., Koncz, A., and Perl, A. (2003). T Cell Activation-Induced Mitochondrial Hyperpolarization Is Mediated by Ca2+- and Redox-Dependent Production of Nitric Oxide. J. Immunol. Baltim. Md 1950 *171*, 5188–5197.

Naik, S., Bouladoux, N., Wilhelm, C., Molloy, M.J., Salcedo, R., Kastenmuller, W., Deming, C., Quinones, M., Koo, L., Conlan, S., et al. (2012). Compartmentalized Control of Skin Immunity by Resident Commensals. Science *337*, 1115–1119.

Nathan, C., and Ding, A. (2010). Nonresolving Inflammation. Cell *140*, 871–882.

Netea, M.G., Balkwill, F., Chonchol, M., Cominelli, F., Donath, M.Y., Giamarellos-Bourboulis, E.J., Golenbock, D., Gresnigt, M.S., Heneka, M.T., Hoffman, H.M., et al. (2017). A guiding map for inflammation.

Neves, B.M., Silvestre, R., Resende, M., Ouaissi, A., Cunha, J., Tavares, J., Loureiro, I., Santarém, N., Silva, A.M., Lopes, M.C., et al. (2010). Activation of Phosphatidylinositol 3-Kinase/Akt and Impairment of Nuclear Factor-κB: Molecular Mechanisms Behind the Arrested Maturation/Activation State of Leishmania infantum-Infected Dendritic Cells. Am. J. Pathol. *177*, 2898–2911.

Ng, L.G., Hsu, A., Mandell, M.A., Roediger, B., Hoeller, C., Mrass, P., Iparraguirre, A., Cavanagh, L.L., Triccas, J.A., Beverley, S.M., et al. (2008). Migratory Dermal Dendritic Cells Act as Rapid Sensors of Protozoan Parasites. PLOS Pathog. *4*, e1000222.

Ng, T.H.S., Britton, G.J., Hill, E.V., Verhagen, J., Burton, B.R., and Wraith, D.C. (2013). Regulation of Adaptive Immunity; The Role of Interleukin-10. Front. Immunol. *4*.

Niedbala, W., Wei, X.-Q., Piedrafita, D., Xu, D., and Liew, F.Y. (1999). Effects of nitric oxide on the induction and differentiation of Th1 cells. Eur. J. Immunol. *29*, 2498–2505.

Niedbala, W., Wei, X., Campbell, C., Thomson, D., Komai-Koma, M., and Liew, F.Y. (2002). Nitric oxide preferentially induces type 1 T cell differentiation by selectively up-regulating IL-12 receptor β2 expression via cGMP. Proc. Natl. Acad. Sci. *99*, 16186–16191.

Niedbala, W., Cai, B., and Liew, F.Y. (2006). Role of nitric oxide in the regulation of T cell functions. Ann. Rheum. Dis. *65*, iii37–iii40.

Niedbala, W., Cai, B., Liu, H., Pitman, N., Chang, L., and Liew, F.Y. (2007). Nitric oxide induces CD4+CD25+ Foxp3− regulatory T cells from CD4+CD25− T cells via p53, IL-2, and OX40. Proc. Natl. Acad. Sci. U. S. A. *104*, 15478–15483.

Niiro, H., Otsuka, T., Kuga, S., Nemoto, Y., Abe, M., Hara, N., Nakano, T., Ogo, T., and Niho, Y. (1994). IL-10 inhibits prostaglandin E2 production by lipopolysaccharide-stimulated monocytes. Int. Immunol. *6*, 661–664.

Niiro, H., Otsuka, T., Tanabe, T., Hara, S., Kuga, S., Nemoto, Y., Tanaka, Y., Nakashima, H., Kitajima, S., and Abe, M. (1995). Inhibition by interleukin-10 of inducible cyclooxygenase expression in lipopolysaccharide-stimulated monocytes: its underlying mechanism in comparison with interleukin-4. Blood *85*, 3736–3745.

Nisoli, E., and Carruba, M.O. (2006). Nitric oxide and mitochondrial biogenesis. J Cell Sci *119*, 2855–2862.

Nomura, M., Liu, J., Rovira, I.I., Gonzalez-Hurtado, E., Lee, J., Wolfgang, M.J., and Finkel, T. (2016). Fatty acid oxidation in macrophage polarization. Nat. Immunol. *17*, 216–217.

Nylén, S., and Eidsmo, L. (2012). Tissue damage and immunity in cutaneous leishmaniasis. Parasite Immunol. *34*, 551–561.

Oburoglu, L., Tardito, S., Fritz, V., de Barros, S.C., Merida, P., Craveiro, M., Mamede, J., Cretenet, G., Mongellaz, C., An, X., et al. (2014). Glucose and Glutamine Metabolism Regulate Human Hematopoietic Stem Cell Lineage Specification. Cell Stem Cell *15*, 169–184.

Olekhnovitch, R., and Bousso, P. (2015). Induction, Propagation, and Activity of Host Nitric Oxide: Lessons from Leishmania Infection. Trends Parasitol. *31*, 653–664.

Olekhnovitch, R., Ryffel, B., Müller, A.J., and Bousso, P. (2014). Collective nitric oxide production provides tissue-wide immunity during *Leishmania* infection. J. Clin. Invest. *124*, 1711–1722.

Olivier, M., Gregory, D.J., and Forget, G. (2005). Subversion Mechanisms by Which Leishmania Parasites Can Escape the Host Immune Response: a Signaling Point of View. Clin. Microbiol. Rev. *18*, 293–305.

Olivier, M., Atayde, V.D., Isnard, A., Hassani, K., and Shio, M.T. (2012). Leishmania virulence factors: focus on the metalloprotease GP63. Microbes Infect. *14*, 1377–1389.

O'Neill, L.A.J. (2011). A critical role for citrate metabolism in LPS signalling. Biochem. J. *438*, e5–e6.

O'Neill, L.A.J., and Pearce, E.J. (2016). Immunometabolism governs dendritic cell and macrophage function. J. Exp. Med. *213*, 15–23.

O'Neill, L.A.J., Kishton, R.J., and Rathmell, J. (2016). A guide to immunometabolism for immunologists. Nat. Rev. Immunol. *16*, 553–565.

Ortega-Gómez, A., Perretti, M., and Soehnlein, O. (2013). Resolution of inflammation: an integrated view. EMBO Mol. Med. *5*, 661–674.

Osman, M., Mistry, A., Keding, A., Gabe, R., Cook, E., Forrester, S., Wiggins, R., Marco, S.D., Colloca, S., Siani, L., et al. (2017). A third generation vaccine for human visceral leishmaniasis and post kala azar dermal leishmaniasis: First-in-human trial of ChAd63-KH. PLoS Negl. Trop. Dis. *11*, e0005527.

Ouimet, M., Ediriweera, H.N., Gundra, U.M., Sheedy, F.J., Ramkhelawon, B., Hutchison, S.B., Rinehold, K., Solingen, C. van, Fullerton, M.D., Cecchini, K., et al. (2015). MicroRNA-33–dependent regulation of macrophage metabolism directs immune cell polarization in atherosclerosis. J. Clin. Invest. *125*, 4334–4348.

Ouimet, M., Koster, S., Sakowski, E., Ramkhelawon, B., Solingen, C. van, Oldebeken, S., Karunakaran, D., Portal-Celhay, C., Sheedy, F.J., Ray, T.D., et al. (2016). *Mycobacterium tuberculosis* induces the miR-33 locus to reprogram autophagy and host lipid metabolism. Nat. Immunol. *17*, 677–686.

Ouyang, W., Rutz, S., Crellin, N.K., Valdez, P.A., and Hymowitz, S.G. (2011). Regulation and Functions of the IL-10 Family of Cytokines in Inflammation and Disease. Annu. Rev. Immunol. *29*, 71–109.

Oyler-Yaniv, A., and Krichevsky, O. (2018). Imaging Cytokine Concentration Fields Using PlaneView Imaging Devices. BIO-Protoc. *8*.

Oyler-Yaniv, A., Oyler-Yaniv, J., Whitlock, B.M., Liu, Z., Germain, R.N., Huse, M., Altan-Bonnet, G., and Krichevsky, O. (2017). A Tunable Diffusion-Consumption Mechanism of Cytokine Propagation Enables Plasticity in Cell-to-Cell Communication in the Immune System. Immunity *46*, 609–620.

Pacher, P., Beckman, J.S., and Liaudet, L. (2007). Nitric Oxide and Peroxynitrite in Health and Disease. Physiol. Rev. *87*, 315–424.

Palmieri, E.M., Baseler, W.A., Davies, L.C., Gonzalez-Cotto, M., Ghesquiere, B., Fan, T.W.M., Lane, A.N., Wink, D.A., and McVicar, D.W. (2018). Nitric oxide dictates the

reprogramming of carbon flux during M1 macrophage polarization. J. Immunol. *200*, 170.18-170.18.

Palsson-McDermott, E.M., Curtis, A.M., Goel, G., Lauterbach, M.A.R., Sheedy, F.J., Gleeson, L.E., van den Bosch, M.W.M., Quinn, S.R., Domingo-Fernandez, R., Johnston, D.G.W., et al. (2015). Pyruvate Kinase M2 Regulates Hif-1α Activity and IL-1β Induction and Is a Critical Determinant of the Warburg Effect in LPS-Activated Macrophages. Cell Metab. *21*, 65–80.

Pautz, A., Art, J., Hahn, S., Nowag, S., Voss, C., and Kleinert, H. (2010). Regulation of the expression of inducible nitric oxide synthase. Nitric Oxide *23*, 75–93.

Pearce, E.L., and Pearce, E.J. (2013). Metabolic Pathways in Immune Cell Activation and Quiescence. Immunity *38*, 633–643.

Peniche, A.G., Bonilla, D.L., Palma, G.I., Melby, P.C., Travi, B.L., and Osorio, E.Y. (2017). A secondary wave of neutrophil infiltration causes necrosis and ulceration in lesions of experimental American cutaneous leishmaniasis. PLOS ONE *12*, e0179084.

Peteranderl, C., Morales-Nebreda, L., Selvakumar, B., Lecuona, E., Vadász, I., Morty, R.E., Schmoldt, C., Bespalowa, J., Wolff, T., Pleschka, S., et al. (2016). Macrophage-epithelial paracrine crosstalk inhibits lung edema clearance during influenza infection. J. Clin. Invest. *126*, 1566–1580.

Peters, N.C., Egen, J.G., Secundino, N., Debrabant, A., Kimblin, N., Kamhawi, S., Lawyer, P., Fay, M.P., Germain, R.N., and Sacks, D. (2008). In Vivo Imaging Reveals an Essential Role for Neutrophils in Leishmaniasis Transmitted by Sand Flies. Science *321*, 970–974.

Peters, N.C., Pagán, A.J., Lawyer, P.G., Hand, T.W., Roma, E.H., Stamper, L.W., Romano, A., and Sacks, D.L. (2014). Chronic Parasitic Infection Maintains High Frequencies of Short-Lived Ly6C+CD4+ Effector T Cells That Are Required for Protection against Re-infection. PLOS Pathog. *10*, e1004538.

Piedrafita, D., Proudfoot, L., Nikolaev, A.V., Xu, D., Sands, W., Feng, G.J., Thomas, E., Brewer, J., Ferguson, M.A., Alexander, J., et al. (1999). Regulation of macrophage IL-12 synthesis by Leishmania phosphoglycans. Eur. J. Immunol. *29*, 235–244.

Pluth, M.D., Tomat, E., and Lippard, S.J. (2011). Biochemistry of Mobile Zinc and Nitric Oxide Revealed by Fluorescent Sensors. Annu. Rev. Biochem. *80*, 333–355.

Polonsky, M., Rimer, J., Kern-Perets, A., Zaretsky, I., Miller, S., Bornstein, C., David, E., Kopelman, N.M., Stelzer, G., Porat, Z., et al. (2018). Induction of CD4 T cell memory by local cellular collectivity. Science *360*, eaaj1853.

Privé, C., and Descoteaux, A. (2000). Leishmania donovani promastigotes evade the activation of mitogen-activated protein kinases p38, c-Jun N-terminal kinase, and extracellular signal-regulated kinase-1/2 during infection of naive macrophages. Eur. J. Immunol. *30*, 2235–2244.

Ptasinska, A., Wang, S., Zhang, J., Wesley, R.A., and Danner, R.L. (2006). Nitric oxide activation of peroxisome proliferator-activated receptor gamma through a p38 MAPK signaling pathway. FASEB J. *21*, 950–961.

Qualls, J.E., Neale, G., Smith, A.M., Koo, M.-S., DeFreitas, A.A., Zhang, H., Kaplan, G., Watowich, S.S., and Murray, P.J. (2010). Arginine Usage in Mycobacteria-Infected Macrophages Depends on Autocrine-Paracrine Cytokine Signaling. Sci Signal *3*, ra62–ra62.

Rapozzi, V., Della Pietra, E., and Bonavida, B. (2015). Dual roles of nitric oxide in the regulation of tumor cell response and resistance to photodynamic therapy. Redox Biol. *6*, 311–317.

Rayner, K.J., Esau, C.C., Hussain, F.N., McDaniel, A.L., Marshall, S.M., Gils, J.M. van, Ray, T.D., Sheedy, F.J., Goedeke, L., Liu, X., et al. (2011). Inhibition of miR-33a/b in non-human primates raises plasma HDL and lowers VLDL triglycerides. Nature *478*, 404–407.

Reboldi, A., Dang, E.V., McDonald, J.G., Liang, G., Russell, D.W., and Cyster, J.G. (2014). 25-Hydroxycholesterol suppresses interleukin-1–driven inflammation downstream of type I interferon. Science *345*, 679–684.

Reithinger, R., Dujardin, J.-C., Louzir, H., Pirmez, C., Alexander, B., and Brooker, S. (2007). Cutaneous leishmaniasis. Lancet Infect. Dis. *7*, 581–596.

Ren, G., Zhang, L., Zhao, X., Xu, G., Zhang, Y., Roberts, A.I., Zhao, R.C., and Shi, Y. (2008). Mesenchymal Stem Cell-Mediated Immunosuppression Occurs via Concerted Action of Chemokines and Nitric Oxide. Cell Stem Cell *2*, 141–150.

Rethi, B., and Eidsmo, L. (2012). FasL and TRAIL signaling in the skin during cutaneous leishmaniasis - implications for tissue immunopathology and infectious control. Front. Immunol. *3*.

Ribeiro-Gomes, F.L., Peters, N.C., Debrabant, A., and Sacks, D.L. (2012). Efficient Capture of Infected Neutrophils by Dendritic Cells in the Skin Inhibits the Early Anti-Leishmania Response. PLOS Pathog. *8*, e1002536.

Ribeiro-Gomes, F.L., Roma, E.H., Carneiro, M.B.H., Doria, N.A., Sacks, D.L., and Peters, N.C. (2014). Site-Dependent Recruitment of Inflammatory Cells Determines the Effective Dose of Leishmania major. Infect. Immun. *82*, 2713–2727.

Ritter, U., Moll, H., Laskay, T., Bröcker, E.-B., Velazco, O., Becker, I., and Gillitzer, R. (1996). Differential Expression of Chemokines in Patients with Localized and Diffuse Cutaneous American Leishmaniasis. J. Infect. Dis. *173*, 699–709.

Ritter, U., Meißner, A., Scheidig, C., and Körner, H. (2004). CD8α- and Langerin-negative dendritic cells, but not Langerhans cells, act as principal antigen-presenting cells in leishmaniasis. Eur. J. Immunol. *34*, 1542–1550.

Ritter, U., Frischknecht, F., and van Zandbergen, G. (2009). Are neutrophils important host cells for Leishmania parasites? Trends Parasitol. *25*, 505–510.

Rizi, B.S., Achreja, A., and Nagrath, D. (2017). Nitric Oxide: The Forgotten Child of Tumor Metabolism. Trends Cancer *3*, 659–672.

Rodriguez, P.C., Zea, A.H., Culotta, K.S., Zabaleta, J., Ochoa, J.B., and Ochoa, A.C. (2002). Regulation of T Cell Receptor CD3ζ Chain Expression byl-Arginine. J. Biol. Chem. *277*, 21123–21129.

Rodriguez, P.C., Zea, A.H., DeSalvo, J., Culotta, K.S., Zabaleta, J., Quiceno, D.G., Ochoa, J.B., and Ochoa, A.C. (2003). l-Arginine Consumption by Macrophages Modulates the Expression of CD3ζ Chain in T Lymphocytes. J. Immunol. *171*, 1232–1239.

Rodriguez, P.C., Quiceno, D.G., and Ochoa, A.C. (2007). l-arginine availability regulates T-lymphocyte cell-cycle progression. Blood *109*, 1568–1573.

Rodríguez-Prados, J.-C., Través, P.G., Cuenca, J., Rico, D., Aragonés, J., Martín-Sanz, P., Cascante, M., and Boscá, L. (2010). Substrate Fate in Activated Macrophages: A Comparison between Innate, Classic, and Alternative Activation. J. Immunol. *185*, 605–614.

Rom, O., Khoo, N.K.H., Chen, Y.E., and Villacorta, L. (2018). Inflammatory signaling and metabolic regulation by nitro-fatty acids. Nitric Oxide *78*, 140–145.

Romano, A., Carneiro, M.B.H., Doria, N.A., Roma, E.H., Ribeiro-Gomes, F.L., Inbar, E., Lee, S.H., Mendez, J., Paun, A., Sacks, D.L., et al. (2017). Divergent roles for Ly6C+CCR2+CX3CR1+ inflammatory monocytes during primary or secondary infection of the skin with the intra-phagosomal pathogen Leishmania major. PLOS Pathog. *13*, e1006479.

Roncarolo, M.-G., and Gregori, S. (2008). Is FOXP3 a bona fide marker for human regulatory T cells? Eur. J. Immunol. *38*, 925–927.

Rosales, C., and Uribe-Querol, E. (2017). Phagocytosis: A Fundamental Process in Immunity. BioMed Res. Int. *2017*.

Sacks, D., and Kamhawi, and S. (2001). Molecular Aspects of Parasite-Vector and Vector-Host Interactions in Leishmaniasis. Annu. Rev. Microbiol. *55*, 453–483.

Sacks, D., and Noben-Trauth, N. (2002). The immunology of susceptibility and resistance to *Leishmania major* in mice. Nat. Rev. Immunol. *2*, 845–858.

Saeed, S., Quintin, J., Kerstens, H.H.D., Rao, N.A., Aghajanirefah, A., Matarese, F., Cheng, S.-C., Ratter, J., Berentsen, K., Ent, M.A. van der, et al. (2014). Epigenetic programming of monocyte-to-macrophage differentiation and trained innate immunity. Science *345*, 1251086.

Saha, S., Shalova, I.N., and Biswas, S.K. (2017). Metabolic regulation of macrophage phenotype and function. Immunol. Rev. *280*, 102–111.

Sancho, D., Enamorado, M., and Garaude, J. (2017). Innate Immune Function of Mitochondrial Metabolism. Front. Immunol. *8*.

Santos, C. da S., Boaventura, V., Ribeiro Cardoso, C., Tavares, N., Lordelo, M.J., Noronha, A., Costa, J., Borges, V.M., de Oliveira, C.I., Van Weyenbergh, J., et al. (2013). CD8+ Granzyme B+–Mediated Tissue Injury vs. CD4+IFNγ+–Mediated Parasite Killing in Human Cutaneous Leishmaniasis. J. Invest. Dermatol. *133*, 1533–1540.

Scharton, T.M., and Scott, P. (1993). Natural killer cells are a source of interferon gamma that drives differentiation of CD4+ T cell subsets and induces early resistance to Leishmania major in mice. J. Exp. Med. *178*, 567–577.

Scharton-Kersten, T.M., Yap, G., Magram, J., and Sher, A. (1997). Inducible Nitric Oxide Is Essential for Host Control of Persistent but Not Acute Infection with the Intracellular Pathogen Toxoplasma gondii. J. Exp. Med. *185*, 1261–1274.

Schatz, V., Strüssmann, Y., Mahnke, A., Schley, G., Waldner, M., Ritter, U., Wild, J., Willam, C., Dehne, N., Brüne, B., et al. (2016). Myeloid Cell–Derived HIF-1α Promotes Control of *Leishmania major*. J. Immunol. *197*, 4034–4041.

Schatz, V., Neubert, P., Rieger, F., and Jantsch, J. (2018). Hypoxia, Hypoxia-Inducible Factor-1α, and Innate Antileishmanial Immune Responses. Front. Immunol. *9*.

Schleicher, U., Paduch, K., Debus, A., Obermeyer, S., König, T., Kling, J.C., Ribechini, E., Dudziak, D., Mougiakakos, D., Murray, P.J., et al. (2016). TNF-Mediated Restriction of Arginase 1 Expression in Myeloid Cells Triggers Type 2 NO Synthase Activity at the Site of Infection. Cell Rep. *15*, 1062–1075.

Schmid, M., Wege, A.K., and Ritter, U. (2012). Characteristics of "Tip-DCs and MDSCs" and Their Potential Role in Leishmaniasis. Front. Microbiol. *3*.

Scialò, F., Fernández-Ayala, D.J., and Sanz, A. (2017). Role of Mitochondrial Reverse Electron Transport in ROS Signaling: Potential Roles in Health and Disease. Front. Physiol. *8*.

Scott, P., and Novais, F.O. (2016). Cutaneous leishmaniasis: immune responses in protection and pathogenesis. Nat. Rev. Immunol. *16*, 581–592.

Segura, E., and Amigorena, S. (2013). Inflammatory dendritic cells in mice and humans. Trends Immunol. *34*, 440–445.

Sektioglu, I.M., Carretero, R., Bender, N., Bogdan, C., Garbi, N., Umansky, V., Umansky, L., Urban, K., von Knebel-Döberitz, M., Somasundaram, V., et al. (2016). Macrophage-derived nitric oxide initiates T-cell diapedesis and tumor rejection. Oncoimmunology *5*.

Senyilmaz, D., and Teleman, A.A. (2015). Chicken or the egg: Warburg effect and mitochondrial dysfunction. F1000Prime Rep. *7*.

Serbina, N.V., and Pamer, E.G. (2006). Monocyte emigration from bone marrow during bacterial infection requires signals mediated by chemokine receptor CCR2. Nat. Immunol. *7*, 311–317.

Serbina, N.V., Salazar-Mather, T.P., Biron, C.A., Kuziel, W.A., and Pamer, E.G. (2003). TNF/iNOS-Producing Dendritic Cells Mediate Innate Immune Defense against Bacterial Infection. Immunity *19*, 59–70.

Serbina, N.V., Jia, T., Hohl, T.M., and Pamer, E.G. (2008). Monocyte-Mediated Defense Against Microbial Pathogens. Annu. Rev. Immunol. *26*, 421–452.

Serhan, C.N. (2014). Pro-resolving lipid mediators are leads for resolution physiology. Nature *510*, 92–101.

Serhan, C.N., and Savill, J. (2005). Resolution of inflammation: the beginning programs the end. Nat. Immunol. *6*, 1191–1197.

Shalapour, S., and Karin, M. (2015). Immunity, inflammation, and cancer: an eternal fight between good and evil. J. Clin. Invest. *125*, 3347–3355.

Shalek, A.K., Satija, R., Shuga, J., Trombetta, J.J., Gennert, D., Lu, D., Chen, P., Gertner, R.S., Gaublomme, J.T., Yosef, N., et al. (2014). Single-cell RNA-seq reveals dynamic paracrine control of cellular variation. Nature *510*, 363–369.

Shi, C., and Pamer, E.G. (2011). Monocyte recruitment during infection and inflammation. Nat. Rev. Immunol. *11*, 762–774.

Siegert, S., Huang, H.-Y., Yang, C.-Y., Scarpellino, L., Carrie, L., Essex, S., Nelson, P.J., Heikenwalder, M., Acha-Orbea, H., Buckley, C.D., et al. (2011). Fibroblastic Reticular Cells From Lymph Nodes Attenuate T Cell Expansion by Producing Nitric Oxide. PLOS ONE *6*, e27618.

Simon, M.W., Martin, E., and Mukkada, A.J. (1978). Evidence for a functional glyoxylate cycle in the leishmaniae. J. Bacteriol. *135*, 895–899.

Soehnlein, O., Lindbom, L., and Weber, C. (2009). Mechanisms underlying neutrophil-mediated monocyte recruitment. Blood *114*, 4613–4623.

Soehnlein, O., Steffens, S., Hidalgo, A., and Weber, C. (2017). Neutrophils as protagonists and targets in chronic inflammation. Nat. Rev. Immunol. *17*, 248–261.

de Souza Leao, S., Lang, T., Prina, E., Hellio, R., and Antoine, J.C. (1995). Intracellular Leishmania amazonensis amastigotes internalize and degrade MHC class II molecules of their host cells. J. Cell Sci. *108*, 3219–3231.

Späth, G.F., Garraway, L.A., Turco, S.J., and Beverley, S.M. (2003). The role(s) of lipophosphoglycan (LPG) in the establishment of Leishmania major infections in mammalian hosts. Proc. Natl. Acad. Sci. *100*, 9536–9541.

Speyer, C.L., Neff, T.A., Warner, R.L., Guo, R.-F., Sarma, J.V., Riedemann, N.C., Murphy, M.E., Murphy, H.S., and Ward, P.A. (2003). Regulatory effects of iNOS on acute lung inflammatory responses in mice. Am. J. Pathol. *163*, 2319–2328.

Srivastav, S., Kar, S., Chande, A.G., Mukhopadhyaya, R., and Das, P.K. (2012). Leishmania donovani Exploits Host Deubiquitinating Enzyme A20, a Negative Regulator of TLR Signaling, To Subvert Host Immune Response. J. Immunol. *189*, 924–934.

Stäger, S., and Rafati, S. (2012). CD8+ T Cells in Leishmania Infections: Friends or Foes? Front. Immunol. *3*.

Stamler, J.S., Lamas, S., and Fang, F.C. (2001). Nitrosylation: The Prototypic Redox-Based Signaling Mechanism. Cell *106*, 675–683.

Stebut, E. von, Belkaid, Y., Jakob, T., Sacks, D.L., and Udey, M.C. (1998). Uptake of Leishmania major Amastigotes Results in Activation and Interleukin 12 Release from Murine Skin–derived Dendritic Cells: Implications for the Initiation of Anti-Leishmania Immunity. J. Exp. Med. *188*, 1547–1552.

von Stebut, E., and Tenzer, S. (2018). Cutaneous leishmaniasis: Distinct functions of dendritic cells and macrophages in the interaction of the host immune system with Leishmania major. Int. J. Med. Microbiol. *308*, 206–214.

Stenger, S., Thüring, H., Röllinghoff, M., and Bogdan, C. (1994). Tissue expression of inducible nitric oxide synthase is closely associated with resistance to Leishmania major. J. Exp. Med. *180*, 783–793.

Stenger, S., Donhauser, N., Thüring, H., Röllinghoff, M., and Bogdan, C. (1996). Reactivation of latent leishmaniasis by inhibition of inducible nitric oxide synthase. J. Exp. Med. *183*, 1501–1514.

Sugimoto, M.A., Sousa, L.P., Pinho, V., Perretti, M., and Teixeira, M.M. (2016). Resolution of Inflammation: What Controls Its Onset? Front. Immunol. *7*.

Surh, Y.-J., Na, H.-K., Park, J.-M., Lee, H.-N., Kim, W., Yoon, I.-S., and Kim, D.-D. (2011). 15-Deoxy-Δ12,14-prostaglandin J2, an electrophilic lipid mediator of anti-inflammatory and pro-resolving signaling. Biochem. Pharmacol. *82*, 1335–1351.

Sutterwala, F.S., Noel, G.J., Salgame, P., and Mosser, D.M. (1998). Reversal of Proinflammatory Responses by Ligating the Macrophage Fcγ Receptor Type I. J. Exp. Med. *188*, 217–222.

Sypek, J.P., Chung, C.L., Mayor, S.E., Subramanyam, J.M., Goldman, S.J., Sieburth, D.S., Wolf, S.F., and Schaub, R.G. (1993). Resolution of cutaneous leishmaniasis: interleukin 12 initiates a protective T helper type 1 immune response. J. Exp. Med. *177*, 1797–1802.

Szabó, C., Ischiropoulos, H., and Radi, R. (2007). Peroxynitrite: biochemistry, pathophysiology and development of therapeutics. Nat. Rev. Drug Discov. *6*, 662–680.

Tannahill, G.M., Curtis, A.M., Adamik, J., Palsson-McDermott, E.M., McGettrick, A.F., Goel, G., Frezza, C., Bernard, N.J., Kelly, B., Foley, N.H., et al. (2013). Succinate is an inflammatory signal that induces IL-1β through HIF-1α. Nature *496*, 238–242.

Tantama, M., Martínez-François, J.R., Mongeon, R., and Yellen, G. (2013). Imaging energy status in live cells with a fluorescent biosensor of the intracellular ATP-to-ADP ratio. Nat. Commun. *4*, 2550.

Taylor, C.T., and Colgan, S.P. (2017). Regulation of immunity and inflammation by hypoxia in immunological niches. Nat. Rev. Immunol. *17*, 774–785.

Taylor, C.T., Doherty, G., Fallon, P.G., and Cummins, E.P. (2016). Hypoxia-dependent regulation of inflammatory pathways in immune cells. J. Clin. Invest. *126*, 3716–3724.

Taylor-Robinson, A.W. (1997). Inhibition of IL-2 production by nitric oxide: A novel self-regulatory mechanism for Th1 cell proliferation. Immunol. Cell Biol. *75*, 167–175.

Thepen, T., Vuuren, A.J.H. van, Kiekens, R.C.M., Damen, C.A., Vooijs, W.C., and Winkel, J.G.J. van de (2000). Resolution of cutaneous inflammation after local elimination of macrophages. Nat. Biotechnol. *18*, 48–51.

Thomas, D.D. (2015). Breathing new life into nitric oxide signaling: A brief overview of the interplay between oxygen and nitric oxide. Redox Biol. *5*, 225–233.

Thomas, D.D., Liu, X., Kantrow, S.P., and Lancaster, J.R. (2001). The biological lifetime of nitric oxide: Implications for the perivascular dynamics of NO and O2. Proc. Natl. Acad. Sci. U. S. A. *98*, 355–360.

Thomassen, M.J., Buhrow, L.T., Connors, M.J., Kaneko, F.T., Erzurum, S.C., and Kavuru, M.S. (1997). Nitric oxide inhibits inflammatory cytokine production by human alveolar macrophages. Am. J. Respir. Cell Mol. Biol. *17*, 279–283.

Thomsen, H., Marino, N., Conoci, S., Sortino, S., and Ericson, M.B. (2018). Confined photo-release of nitric oxide with simultaneous two-photon fluorescence tracking in a cellular system. Sci. Rep. *8*, 9753.

Thurley, K., Gerecht, D., Friedmann, E., and Höfer, T. (2015). Three-Dimensional Gradients of Cytokine Signaling between T Cells. PLOS Comput. Biol. *11*, e1004206.

Thwe, P.M., and Amiel, E. (2018). The role of nitric oxide in metabolic regulation of Dendritic cell immune function. Cancer Lett. *412*, 236–242.

Torres-Guerrero, E., Quintanilla-Cedillo, M.R., Ruiz-Esmenjaud, J., and Arenas, R. (2017). Leishmaniasis: a review. F1000Research *6*, 750.

Travis, M.A., and Sheppard, D. (2014). TGF-β Activation and Function in Immunity. Annu. Rev. Immunol. *32*, 51–82.

Trez, C.D., Magez, S., Akira, S., Ryffel, B., Carlier, Y., and Muraille, E. (2009). iNOS-Producing Inflammatory Dendritic Cells Constitute the Major Infected Cell Type during the Chronic Leishmania major Infection Phase of C57BL/6 Resistant Mice. PLOS Pathog. *5*, e1000494.

Tsunawaki, S., Sporn, M., Ding, A., and Nathan, C. (1988). Deactivation of macrophages by transforming growth factor-β. Nature *334*, 260–262.

Tsunawaki, S., Sporn, M., and Nathan, C. (1989). Comparison of transforming growth factor-beta and a macrophage- deactivating polypeptide from tumor cells. Differences in antigenicity and mechanism of action. J. Immunol. *142*, 3462–3468.

Uzonna, J.E., Joyce, K.L., and Scott, P. (2004). Low Dose Leishmania major Promotes a Transient T Helper Cell Type 2 Response That Is Down-regulated by Interferon γ–producing CD8+ T Cells. J. Exp. Med. *199*, 1559–1566.

Vacchini, A., Locati, M., and Borroni, E.M. (2016). Overview and potential unifying themes of the atypical chemokine receptor family. J. Leukoc. Biol. *99*, 883–892.

Van den Bossche, J., Baardman, J., and Winther, M.P.J. de (2015). Metabolic Characterization of Polarized M1 and M2 Bone Marrow-derived Macrophages Using Real-time Extracellular Flux Analysis. JoVE J. Vis. Exp. e53424–e53424.

Van den Bossche, J., Baardman, J., Otto, N.A., van der Velden, S., Neele, A.E., van den Berg, S.M., Luque-Martin, R., Chen, H.-J., Boshuizen, M.C.S., Ahmed, M., et al. (2016).

Mitochondrial Dysfunction Prevents Repolarization of Inflammatory Macrophages. Cell Rep. *17*, 684–696.

Van den Bossche, J., O'Neill, L.A., and Menon, D. (2017). Macrophage Immunometabolism: Where Are We (Going)? Trends Immunol. *38*, 395–406.

Vannini, F., Kashfi, K., and Nath, N. (2015). The dual role of iNOS in cancer. Redox Biol. *6*, 334–343.

Veer, M.J. de, Curtis, J.M., Baldwin, T.M., DiDonato, J.A., Sexton, A., McConville, M.J., Handman, E., and Schofield, L. (2003). MyD88 is essential for clearance of Leishmania major: possible role for lipophosphoglycan and Toll-like receptor 2 signaling. Eur. J. Immunol. *33*, 2822–2831.

Veglia, F., Perego, M., and Gabrilovich, D. (2018). Myeloid-derived suppressor cells coming of age. Nat. Immunol. *19*, 108–119.

Verma, J.K., Rastogi, R., and Mukhopadhyay, A. (2017). Leishmania donovani resides in modified early endosomes by upregulating Rab5a expression via the downregulation of miR-494. PLOS Pathog. *13*, e1006459.

Vig, M., Srivastava, S., Kandpal, U., Sade, H., Lewis, V., Sarin, A., George, A., Bal, V., Durdik, J.M., and Rath, S. (2004). Inducible nitric oxide synthase in T cells regulates T cell death and immune memory. J. Clin. Invest. *113*, 1734–1742.

Voet, D., and Voet, J.G. (2010). Biochemistry, 4th Edition.

Von Stebut, E. (2007). Immunology of cutaneous leishmaniasis: the role of mast cells, phagocytes and dendritic cells for protective immunity. Eur. J. Dermatol. EJD *17*, 115–122.

Wanderley, J.L.M., Moreira, M.E.C., Benjamin, A., Bonomo, A.C., and Barcinski, M.A. (2006). Mimicry of apoptotic cells by exposing phosphatidylserine participates in the establishment of amastigotes of Leishmania (L) amazonensis in mammalian hosts. J. Immunol. Baltim. Md 1950 *176*, 1834–1839.

Weber, M., Hauschild, R., Schwarz, J., Moussion, C., Vries, I. de, Legler, D.F., Luther, S.A., Bollenbach, T., and Sixt, M. (2013). Interstitial Dendritic Cell Guidance by Haptotactic Chemokine Gradients. Science *339*, 328–332.

Wecksler, S., Mikhailovsky, A., and Ford, P.C. (2004). Photochemical Production of Nitric Oxide via Two-Photon Excitation with NIR Light. J. Am. Chem. Soc. *126*, 13566–13567.

Wei, X., Charles, I.G., Smith, A., Ure, J., Feng, G., Huang, F., Xu, D., Mullers, W., Moncada, S., and Liew, F.Y. (1995). Altered immune responses in mice lacking inducible nitric oxide synthase. Nature *375*, 408–411.

Werner, F., Jain, M.K., Feinberg, M.W., Sibinga, N.E.S., Pellacani, A., Wiesel, P., Chin, M.T., Topper, J.N., Perrella, M.A., and Lee, M.-E. (2000). Transforming Growth Factor-β1 Inhibition of Macrophage Activation Is Mediated via Smad3. J. Biol. Chem. *275*, 36653–36658.

Williams, N.C., and O'Neill, L.A.J. (2018). A Role for the Krebs Cycle Intermediate Citrate in Metabolic Reprogramming in Innate Immunity and Inflammation. Front. Immunol. *9*.

Wolf, A.J., Reyes, C.N., Liang, W., Becker, C., Shimada, K., Wheeler, M.L., Cho, H.C., Popescu, N.I., Coggeshall, K.M., Arditi, M., et al. (2016). Hexokinase Is an Innate Immune Receptor for the Detection of Bacterial Peptidoglycan. Cell *166*, 624–636.

Wu, D., Sanin, D.E., Everts, B., Chen, Q., Qiu, J., Buck, M.D., Patterson, A., Smith, A.M., Chang, C.-H., Liu, Z., et al. (2016). Type 1 Interferons Induce Changes in Core Metabolism that Are Critical for Immune Function. Immunity *44*, 1325–1336.

Xie, X., Fan, J., Liang, M., Li, Y., Jiao, X., Wang, X., and Tang, B. (2017). A two-photon excitable and ratiometric fluorogenic nitric oxide photoreleaser and its biological applications. Chem. Commun. *53*, 11941–11944.

Xiong, H., and Pamer, E.G. (2015). Monocytes and infection: Modulator, messenger and effector. Immunobiology *220*, 210–214.

Xu, W., Liu, L.Z., Loizidou, M., Ahmed, M., and Charles, I.G. (2002). The role of nitric oxide in cancer. Cell Res. *12*, 311–320.

Yao, Q., Song, Z., Wang, B., and Zhang, J. (2018). Emerging roles of microRNAs in the metabolic control of immune cells. Cancer Lett. *433*, 10–17.

Yau, W.-L., Blisnick, T., Taly, J.-F., Helmer-Citterich, M., Schiene-Fischer, C., Leclercq, O., Li, J., Schmidt-Arras, D., Morales, M.A., Notredame, C., et al. (2010). Cyclosporin A Treatment of Leishmania donovani Reveals Stage-Specific Functions of Cyclophilins in Parasite Proliferation and Viability. PLoS Negl. Trop. Dis. *4*, e729.

Yeramian, A., Martin, L., Arpa, L., Bertran, J., Soler, C., McLeod, C., Modolell, M., Palacín, M., Lloberas, J., and Celada, A. (2006). Macrophages require distinct arginine catabolism and transport systems for proliferation and for activation. Eur. J. Immunol. *36*, 1516–1526.

Zaph, C., Uzonna, J., Beverley, S.M., and Scott, P. (2004). Central memory T cells mediate long-term immunity to *Leishmania major* in the absence of persistent parasites. Nat. Med. *10*, 1104–1110.

Zhang, H.-X., Chen, J.-B., Guo, X.-F., Wang, H., and Zhang, H.-S. (2014). Highly Sensitive Low-Background Fluorescent Probes for Imaging of Nitric Oxide in Cells and Tissues. Anal. Chem. *86*, 3115–3123.

Zhang, N., Weber, A., Li, B., Lyons, R., Contag, P.R., Purchio, A.F., and West, D.B. (2003). An Inducible Nitric Oxide Synthase-Luciferase Reporter System for In Vivo Testing of Anti-inflammatory Compounds in Transgenic Mice. J. Immunol. *170*, 6307–6319.

Zigmond, E., Varol, C., Farache, J., Elmaliah, E., Satpathy, A.T., Friedlander, G., Mack, M., Shpigel, N., Boneca, I.G., Murphy, K.M., et al. (2012). Ly6Chi Monocytes in the Inflamed Colon Give Rise to Proinflammatory Effector Cells and Migratory Antigen-Presenting Cells. Immunity *37*, 1076–1090.

Manuscript accepted and in production

A metabolism-based quorum sensing mechanism contributes to termination of inflammatory responses

Jérémy Postat[1,2,3], Romain Olekhnovitch[1,2,3], Fabrice Lemaître[1,2] and Philippe Bousso[1,2,4,*]

[1] Dynamics of Immune Responses Unit, Institut Pasteur, 75015 Paris, France
[2] INSERM U1223, 75015 Paris, France
[3] University Paris Diderot, Sorbonne Paris Cité, Cellule Pasteur, rue du Dr Roux, 75015 Paris, France
[4] Lead Contact

[*] Correspondence to: philippe.bousso@pasteur.fr

Summary

Recruitment of immune cells with antimicrobial activities is essential to fight local infections but has the potential to trigger immunopathology. Whether the immune system has the ability to sense inflammation intensity and self-adjust accordingly to limit tissue damage remains to be fully established. During local infection with an intracellular pathogen, we have shown that nitric oxide (NO) produced by recruited monocyte-derived cells was essential to limit inflammation and cell recruitment. Mechanistically, we have provided evidence that NO dampened monocyte-derived cell cytokine and chemokine production by inhibiting cellular respiration and reducing cellular ATP:ADP ratio. Such metabolic control operated at the tissue level but only when a sufficient number of NO producing cells reached the site of infection. Thus, NO production and activity act as a quorum sensing mechanism to help terminate the inflammatory response.

Graphical abstract

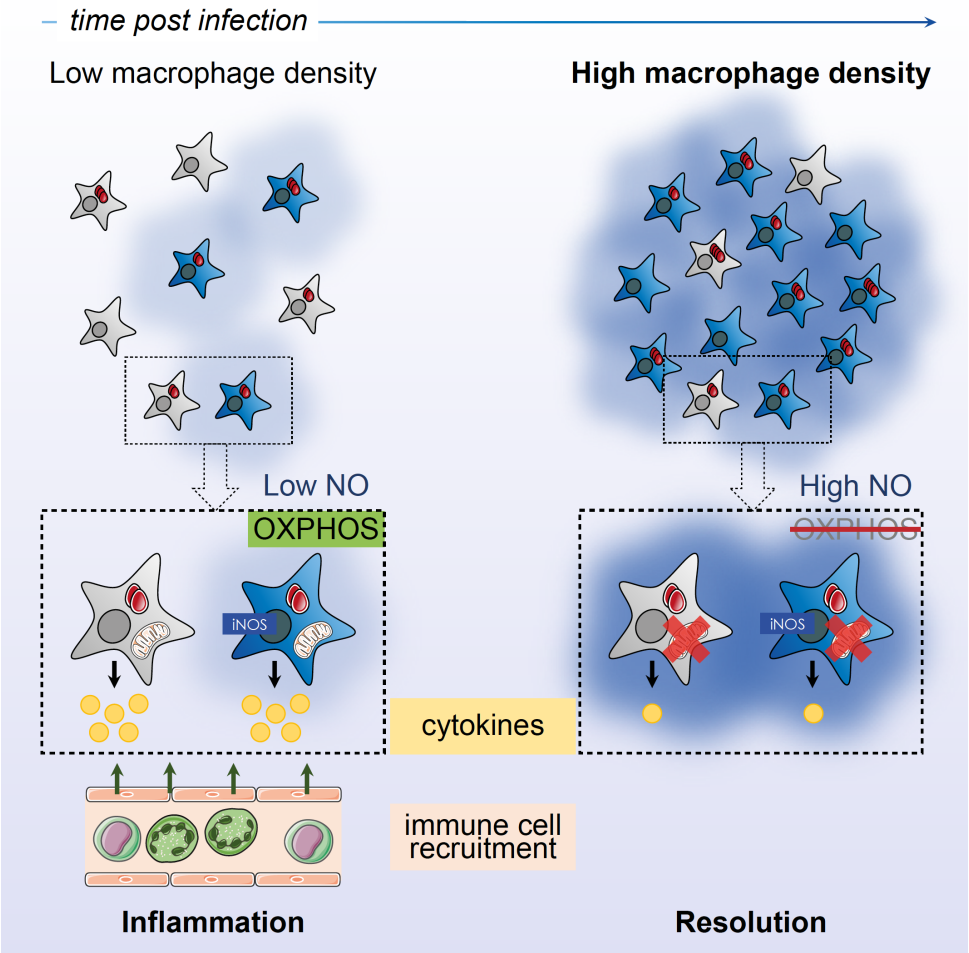

Highlights

- NO limits cytokine production by monocyte-derived cells during *L. major* infection
- NO reduces mitochondrial respiration and cellular ATP:ADP ratio *in vivo*
- The density of NO producing cells controls immune cell activity at the tissue level
- NO production acts as a quorum sensing mechanism to help terminate inflammation

eTOC Blurb

Mechanisms sensing when a sufficient number of immune cells have accumulated in tissues to terminate inflammation are incompletely understood. Here, Postat *et al.* establish that NO produced at inflammatory sites acts as a quorum sensing mechanism to adjust monocyte-derived cell respiration and cytokine production to their density in the tissue.

Introduction

Infection with pathogens and tissue damage triggers inflammation, a dynamic process aimed at protecting the injured host. Soluble mediators produced in particular by macrophages and mast cells actively increase vascular permeability and attract immune cells with antimicrobial properties (Medzhitov, 2008). However, overwhelming inflammation may be responsible for severe immunopathology often due to excessive neutrophil accumulation. Mechanisms to terminate inflammation are therefore essential for balancing antimicrobial activity and tissue damage.

While the decrease in pathogen load or injury may help limit inflammation, active mechanisms implicating immune cells and mediators have also been shown to suppress the inflammatory reaction (Ortega-Gomez et al., 2013; Sugimoto et al., 2016). These include processes to decrease neutrophil activity and numbers through induction of apoptosis and increased clearance, mechanisms to regulate cytokine and chemokine activity by reactive oxygen species (ROS) generation or through truncation and sequestration by decoy receptors. Additionally, macrophage transition from a pro-inflammatory to a pro-resolving state represents an important step for terminating immune responses. Despite this important knowledge, mechanisms that select the appropriate time for inflammation resolution are poorly understood. Specifically, whether a mechanism exists to sense when a sufficient number of immune cells have accumulated to elicit the termination of inflammation remains unknown.

To address these questions, we took advantage of the self-resolving cutaneous infection with *Leishmania major* parasites (Sacks and Noben-Trauth, 2002; Scott and Novais, 2016) as a physiological model to study inflammation termination. Local infection with this intracellular pathogen triggers the massive recruitment of monocyte-derived mononuclear phagocytes (thereafter referred to as monocyte-derived cells), that not only represents the major populations of infected cells but are also actively involved in fighting the infection (De Trez et al., 2009; Leon et al., 2007; Olekhnovitch et al., 2014). Efficient immune responses indeed rely on inducible nitric oxide synthase (iNOS, NOS2)-mediated nitric oxide (NO) production by monocyte-derived cells, promoted by interferon-γ (IFN-γ) producing $CD4^+$ T cells (Olekhnovitch and Bousso, 2015; Sacks and Noben-Trauth, 2002; Scott and Novais, 2016). NO production has a direct effect on the parasite, limiting its proliferation and survival (Liew et al., 1990; Muller et al., 2013). However, decreasing parasite load may not be sufficient to stop the inflammatory reaction raising the possibility that additional mechanisms acting on immune cells are important to terminate the response. Notably, NO displays immunoregulatory properties (Bogdan, 2001; Giustizieri et al., 2002; Kobayashi, 2010; Lu et al., 2015; Mishra et al., 2013; Speyer et al., 2003; Thomassen et al., 1997) suggesting that it can act not only on the pathogen but also on inflammatory cells at the site of infection. In addition, recent studies have indicated that NO can modify cellular metabolism in *in vitro* settings (Everts et al., 2012; Van den Bossche et al., 2016). However, by which mechanisms NO could influence the inflammatory response *in vivo* remains to be fully established. In particular, the relevance of NO impact on metabolism *in vivo* has yet to be demonstrated. Finally, the spatiotemporal activity of NO in tissues is largely unknown.

Here, we have shown that NO production acts to adjust and limit the intensity of the inflammatory response. We have established that NO suppresses monocyte-derived cell accumulation as well as cytokine and chemokine production by blocking cellular respiration and decreasing ATP:ADP ratio. Such mechanism required a high density of recruited iNOS-expressing cells and acted at the tissue level through NO diffusion. Thus, monocyte-derived cells not only produce NO but are also regulated in number and activity by the amount of this molecule in the environment, establishing a quorum sensing mechanism for the control of inflammatory responses.

Results

NO dampens the inflammatory reaction at the site of *L. major* infection

During infection with intracellular pathogens, host NO can exert pleiotropic effects influencing immune responses at multiple stages (Bogdan, 2015; Olekhnovitch and Bousso, 2015). To specifically evaluate the impact of NO production on an established inflammatory reaction, we assessed the consequence of a short period of iNOS inhibition in *L. major* infected mice (**Figure 1A**). We used the specific iNOS chemical inhibitor L-NIL and treated mice 2 weeks post infection for 3 days. We found that iNOS inhibition profoundly increased myeloid cell numbers at the site of infection, with a major effect on neutrophils and monocyte-derived cells (**Figure 1B**). We and others have previously shown that Ly6C^{+}MHC-II^{-} monocytes (P1 population) are massively recruited at the site of infection and further differentiate into Ly6C^{+}MHC-II^{+} (P2 population) and subsequently into Ly6C^{-}MHC-II^{+} cells (P3 population) (Leon et al., 2007; Olekhnovitch et al., 2014). All three populations of mononuclear phagocytes were substantially increased upon a short inhibition of iNOS (**Figure 1B**). To extend these results, we used *Lyz2*$^{+/EGFP}$ mice (in which both neutrophils and macrophages are labeled with GFP) to visualize the effect of iNOS inhibition on myeloid cell density at the site of infection. Consistent with our flow cytometric analysis, two-photon imaging of the ear dermis revealed a significant increase in the density of myeloid cells (GFP^{+}) upon transient iNOS inhibition (**Figure 1C**). We next investigated the effect of iNOS inhibition on the inflammatory milieu at the site of infection by analyzing cytokine and chemokine concentrations in total ear tissue. We observed an overall increase in cytokine concentrations when iNOS activity was blocked. The effect appeared very broad and concerned most of the cytokines tested, including IL-1α, IL-1β, TNF-α, IL-6, IL-12 (p40 and p70), IL-10, IL-5, IL-4 (**Figure 1D**). Similarly, iNOS inhibition led to a dramatic increase in chemokine concentrations in the ear tissue, including CXCL1, CXCL10, CCL2, CCL3 (**Figure 1D**). Altogether, our results indicate that NO production at the site of *L. major* infection controls, either directly (acting on cells) or indirectly (acting on the pathogen), the inflammatory reaction, limiting immune cell infiltrates together with cytokine and chemokine concentrations.

NO impacts myeloid cell recruitment at the site of *L. major* infection

To specifically assess the role of NO on immune cell recruitment at the site of infection, we performed adoptive transfer of myeloid populations by injecting fluorescently-labeled bone marrow cells in infected mice. Cell recruitment in the infected ear was assessed in the presence or absence of iNOS inhibition (**Figure 2A**). Using intravital imaging, we detected the recruitment of transferred cells at the site of infection with a marked increase in GFP^{+} cell numbers upon suppression of iNOS activity (**Figure 2B**). We confirmed this result using flow cytometry with a significant enhancement of myeloid cell (including neutrophils) recruitment upon iNOS inhibition (**Figure 2C**). Notably, a sizable fraction (~6%) of newly recruited cells including neutrophils and monocyte-derived cells became infected in wild-type mice during this short window of time (**Figure 2D**). Our results suggest that the constant recruitment of myeloid cells contributes to fuel *L. major* infection and, most importantly, that iNOS activity limits such a self-sustained process.

NO restricts monocyte-derived cells function *in vivo* at the single cell level

Having shown that NO limits the overall cytokine production in the infected tissue, we asked whether this effect was uniquely due to a reduced accumulation of cytokine-producing immune cells or whether NO exerted an additional effect on immune cell activity. We focused on monocyte-derived cells, the major population of myeloid cells at the site of infection and analyzed cytokine production at the single cell level, in infected mice upon transient inhibition of iNOS (**Figure 3A**). As shown in **Figure 3B-C**, we observed an increased percentage of TNF-α-producing cells as well as an increased cytokine production on a per cell basis in infected mice in which iNOS activity was suppressed. This

effect was not specific to TNF-α since we obtained similar results by analyzing the production of two other cytokines: pro-IL-1β and CCL3 (**Figure 3C**). Similar effects were observed when either total or infected cells were analyzed (**Figure S1A-B**). These results indicate that NO produced by monocyte-derived cells at the site of infection dampens their ability to produce cytokines and chemokines. When assessing the effects of L-NIL treatment, we found that a 3-days inhibition of iNOS also increased the percentage of infected monocyte-derived cells (**Figure S1C-D**). While this could be the result of the increased immune cell recruitment at the site of infection, it could also reflect NO antimicrobial activity. Therefore, it was important to test whether NO mediated its effects indirectly by influencing pathogen load or by direct alteration of cellular activity. To test the latter possibility, we analyzed how NO affects monocyte-derived cell activity in a non-infectious model of inflammation using emulsified incomplete Freund's adjuvant (**Figure S2A**). In this model, we observed massive recruitment of myeloid cells including the three aforementioned mononuclear phagocytes populations (P1, P2, P3) and a robust induction of iNOS (**Figure S2B-C**). Importantly, treatment with L-NIL increased monocyte-derived cell activity as measured by TNF-α, CCL2 and CCL3 production (**Figure S2D**). These results suggest that NO can restrict monocyte-derived cell activity independently of any potential effect on pathogen burden

NO broadly restricts bone marrow-derived macrophages functions *in vitro*

To further confirm and dissect the direct effect of NO on immune cells, we activated WT or *Nos2*$^{-/-}$ bone marrow-derived macrophages *in vitro* and in the absence of pathogen with LPS+IFN-γ, a treatment that induces iNOS expression in WT cells. As shown in **Figure 4A**, LPS+IFN-γ treatment induced the intracellular production of the tested cytokines (pro-IL-1β and CCL2) in both WT and *Nos2*$^{-/-}$ macrophages. However, cytokine production was significantly higher in *Nos2*$^{-/-}$ macrophages. We repeated these experiments by treating WT macrophages with L-NIL to suppress NO production in order to exclude any potential additional defect of cells isolated from *Nos2*$^{-/-}$ mice. Consistently, we observed higher production of pro-IL-1β and CCL2 in the presence of iNOS inhibition (**Figure 4B**). As expected, L-NIL had no effects on *Nos2*$^{-/-}$ macrophages or on WT unactivated macrophages (**Figure S3**). We extended the aforementioned results obtained with intracellular cytokine staining by performing multi-analyte cytokine profiling on macrophage supernatants. Reflecting the effect of iNOS inhibition during *L. major* infection, *Nos2*$^{-/-}$ macrophages exhibited an overall increased production of inflammatory cytokines and chemokines, including IL-1α, IL-1β, IL-6, CXCL10, CCL2, CCL3 (**Figure 4C**). These results suggest that NO acts on macrophages to limit cytokine and chemokine production both *in vitro* and *in vivo*.

NO blockade of mitochondrial respiration restricts ATP:ADP ratio and macrophage activity

Given the broad suppression of cytokine production by NO, we asked whether this effect could originate from a change in cellular metabolism (Biswas and Mantovani, 2012; Everts et al., 2012; Lu et al., 2015; Na et al., 2018; Sancho et al., 2017; Thwe and Amiel, 2018; Van den Bossche et al., 2016; Van den Bossche et al., 2017). Consistent with this idea, we observed that WT macrophages engage glycolysis but stop relying on oxidative phosphorylation upon activation as measured by decreased basal respiration and ATP synthesis (**Figure 5A-B**). By contrast, *Nos2*$^{-/-}$ macrophages used both respiration and glycolysis upon activation (**Figure 5A-B**). Overall, glycolytic activity and glucose uptake were not affected by iNOS activity (**Figure S4**). Similarly, blocking iNOS activity with L-NIL in WT macrophages restored their respiratory capacity when activated (**Figure 5C**). To confirm these findings at the single cell level, we used a combination of dyes to measure total (MitoTracker GreenFM) and respiring (MitoTracker Red CMXRos) mitochondria by flow cytometry. A drop in cell respiration was seen upon activation of WT but not *Nos2*$^{-/-}$ macrophages (**Figure S5A**). Again, blocking iNOS activity in WT macrophages was sufficient to restore respiration (**Figure S5B**). To test whether these findings pertain to monocyte-derived cells *in vivo* at the site of *L. major* infection, we sorted monocyte-derived cells from the ears of infected WT mice and subjected them

to metabolic flux analysis in the presence or absence of L-NIL. As observed with *in vitro* macrophages, *ex vivo*-isolated WT monocyte-derived cells displayed a block in respiration that was relieved by a short incubation (2h) with L-NIL (**Figure 5D**). These results demonstrate that NO production by macrophages drastically suppresses their respiratory capacity, in both bone marrow-derived macrophages and monocyte-derived cells at the site of infection.

To further characterized the impact of NO on cellular metabolism, we relied on PercevalHR, a genetically-encoded fluorescent probe for monitoring ATP:ADP ratio hence providing a readout for the energetic status of individual cells in real-time (Tantama et al., 2013). Upon NO exposure, we observed a drop in ATP:ADP ratio in activated and L-NIL-treated PercevalHR-expressing macrophages within less than 10 minutes, as measured by time-resolved flow cytometry (**Figure 6A**). These findings were confirmed by following individual PercevalHR-expressing macrophages using live-imaging (**Figure 6B**). Thus, one important consequence of NO targeting of mitochondrial respiration is the rapid and substantial reduction in the cellular ATP:ADP ratio. We next ask whether such energetic changes could explain the reduced cytokine production in macrophages exposed to NO. We therefore specifically inhibited the ATP synthase using oligomycin (that targets the F0 subunit of the ATP synthase). We noted that oligomycin treatment induced a drop in ATP:ADP ratio similar to that observed with NO (**Figure 6C-D**). Most importantly, a short term (4 h) inhibition of ATP synthase in macrophages was sufficient to reduce cytokine and chemokine production as measured by intracellular cytokine staining (**Figure 6E**) and multi-analyte cytokine profiling (**Figure 6F**). Similar results were observed by performing the experiment in hypoxic condition **(Figure S6A**) or by blocking respiration with azide that targets complex IV of the mitochondrial respiratory chain, which activity precedes that of the ATP synthase **(Figure S6B**). Together, our results support the idea that NO blockade of mitochondrial respiration rapidly diminishes the cellular energetic resources required for optimal cytokine production. To test whether NO also affect the ATP:ADP ratio *in vivo* during infection, we generated chimeric mice by transducing HSCs with PercevalHR and infected them with *L. major* (**Figure 6G**). Two weeks later, we measured the ATP:ADP ratio in monocyte-derived cells at the infection site in mice treated or not with L-NIL. We observed that iNOS inhibition largely increased cellular ATP:ADP ratio in both P2 and P3 populations (**Figure 6H**) supporting the relevance of our model during inflammation *in vivo*.

Collective NO production provides a quorum-sensing mechanism to dampen chronic inflammation

We next sought to clarify how NO acts in the infected tissue. NO could act in a cell-autonomous manner, suppressing the respiration of individual NO-producing cells or act more broadly by diffusing in the tissue. In addition, it was unclear whether NO produced by a single cell has any biological activity or whether the collective production by numerous cells is essential to impact on cellular metabolism.

We first addressed these questions *in vitro* by mixing iNOS competent and deficient macrophages at different ratios to generate distinct densities of NO producing cells at a constant total cell number. We found that the block of cell respiration in macrophages increased with density of NO-producing cells (**Figure S5C-E**). Most importantly, only a modest block in cell respiration was seen in macrophages competent for NO production when these cells were present at low density (10:90 ratio), indicating that the effect on cellular metabolism was by large not cell-intrinsic. Conversely, a block in respiration was detected in *Nos2*$^{-/-}$ macrophages provided that they were surrounded by numerous iNOS competent cells (50:50 ratio) (**Figure S5C-E**). Importantly, the same rules applied for cytokine and chemokine production (**Figure S5F-G**). Indeed, pro-IL-1β and CCL2 production was suppressed in both WT and *Nos2*$^{-/-}$ macrophages mixed at 50:50 ratio. At lower ratio (10:90), pro-IL-1β and CCL2 production were largely unaffected even in WT macrophages. These results strongly suggest that the density of NO-producing cells plays a crucial role to regulate cell activity (**Figure S5**).

To test this hypothesis *in vivo*, we generated mixed-bone marrow chimeras using various ratios of WT (CD45.1) and *Nos2*$^{-/-}$ (CD45.2) cells for reconstitution (**Figure 7A-B**) in order to establish varying densities of iNOS competent cells at the infection site. The corresponding cellular densities were estimated by intravital imaging (**Figure S7A-C**). Following infection with *L. major*, we assessed the activity of monocyte-derived cells isolated at the site of infection. Our results revealed that the amount of pro-IL-1β (**Figure 7C, Figure S7D**) produced was regulated by the density of iNOS competent cells. Moreover, the amounts of cytokine production were identical in WT (CD45.1) and *Nos2*$^{-/-}$ (CD45.2) cells analyzed in the same environment, indicating that NO-mediated effect on cytokine production is not cell-intrinsic but instead largely rely on NO diffusion in the tissue. Similar results were obtained analyzing TNF-α (**Figure 7D, Figure S7D**) and CCL3 (**Figure 7E, Figure S7D**) production. Therefore, NO mediates the downregulation of the inflammatory reaction only when a sufficient number of NO-producing cells have accumulated at the site of infection. We estimated that a density of approximately 5000 iNOS competent cells/mm^3 need to be reach to substantially inhibit cytokine production (**Figure S7D**). Furthermore, NO acts at the tissue level through diffusion irrespectively of intrinsic iNOS expression.

In sum, monocyte-derived cells that accumulate at the site of infection produce diffusible NO that will progressively inhibit further recruitment and inflammation as cell density increases. Monocyte-derived cells are therefore endowed with a metabolism-based quorum-sensing mechanism to help control and terminate the immune response.

Discussion

In the present report, we identified a novel mechanism that adjusts the intensity of the inflammatory reaction to the local density of monocyte-derived cells. Mechanistically, we have shown that nitric oxide decreased cellular respiration, ATP:ADP ratio and cytokine and chemokine production, dampening myeloid cell recruitment and overall inflammation. Since NO was found to act only when a sufficient number of NO-producing cells have accumulated, these properties define a quorum-sensing mechanism for the control and termination of inflammatory reactions.

In the context of infection with an intracellular pathogen, we confirmed that the role of NO extends beyond its well-known antimicrobial properties by profoundly influencing immune cell activity *in vivo*. *Nos2*$^{-/-}$ mice have been previously shown to exhibit exacerbated immunopathology in response to infection with *L. major* or *M. tuberculosis* (Belkaid et al., 2000; Mishra et al., 2017; Mishra et al., 2013; Wei et al., 1995). Since iNOS deficiency may affect the initiation and development of the immune response, we used a short pharmacological inhibition of iNOS to reveal the role of NO specifically once the inflammatory reaction is established. Blocking NO production for 3 days was sufficient to boost monocyte-derived cell ability to secrete cytokines and chemokines at the single cell level and to increase myeloid cell recruitment and accumulation. Such an enhanced recruitment of myeloid cells could possibly originate from factors derived from monocytes and/or neutrophils, two cell types that that act in concert during inflammation (Dal-Secco et al., 2015; Kreisel et al., 2010; Lammermann et al., 2013). In addition, NO could influence cell recruitment by modulating leukocyte adhesion and extravasation (Banick et al., 1997; Kubes et al., 1991). In agreement with previous studies (Bogdan, 2001; Braverman and Stanley, 2017; Eigler et al., 1995; Giustizieri et al., 2002; Speyer et al., 2003; Thomassen et al., 1997), these observations were recapitulated on *in vitro* derived-macrophages in the absence of pathogen, suggesting that the observed effects of NO on the immune reaction were not simply due to indirect changes in the parasite. NO-mediated suppression of cytokine production can result from an alteration of inflammasome assembly (Mishra et al., 2013) or a decrease in NF-κB activity (Braverman and Stanley, 2017; Matthews et al., 1996). Notably, in our model, NO appeared to decrease cytokine and chemokine production very broadly, affecting most type-1, type-2 and suppressive cytokines tested.

The wide range of cytokines and chemokines downregulated by NO prompted us to investigate a global effect on cellular metabolism. NO has the ability to block the respiratory chain (Brown, 1999, 2001; Clementi et al., 1998) and iNOS induction has been shown to block respiration in dendritic cells and macrophages cultured *in vitro* (Van den Bossche et al., 2016) or in inflammatory dendritic cells stimulated *ex vivo* (Everts et al., 2012). To extend these findings, we sought to determine whether blockade of respiration by NO could be observed in an ongoing immune response. By directly analyzing the metabolism of sorted monocyte-derived cells from the site of *L. major* infection, we showed that these cells exhibited a profound block in cell respiration that could be reversed by a short inhibition of iNOS. Using a genetically-encoded reporter for ATP:ADP ratio (PercevalHR), we noted that NO decreased the cellular energetic yield both *in vitro* and *in vivo*. These observations establish the physiological relevance of NO-mediated alteration of cell metabolism in the context of a chronic inflammation with an intracellular pathogen. Importantly, we provide evidence that respiration blockade and decrease in ATP production are by themselves sufficient to limit cytokine and chemokine production suggesting a causal link between NO-mediated respiration blockade and dampening of monocyte-derived cell activity. While our data support a role for NO in reducing cytokine production by altering respiration and energetic yield, additional mechanisms could also contribute to limit inflammation. These include mitochondria-dependent mechanisms such as modulation of mitochondrial ROS (Mills et al., 2016) and/or concentrations of specific metabolites (e.g succinate (Mills et al., 2016; Tannahill et al., 2013) and itaconate (Cordes et al., 2016;

Lampropoulou et al., 2016; Michelucci et al., 2013)) but also mitochondria-independent mechanisms such as modulation of NADPH oxidase-derived ROS (Bagaitkar et al., 2015; Harbort et al., 2015; Meissner et al., 2008; Morgenstern et al., 1997; Warnatsch et al., 2017) and/or alteration of the NF-κB pathway (Braverman and Stanley, 2017; Matthews et al., 1996). Collectively, results from this work and from other studies (Amiel et al., 2014; Everts et al., 2012; Van den Bossche et al., 2016) highlight the diverse effects of respiration blockade by NO on monocyte-derived cell biology, including alteration of survival capacity, plasticity and inflammatory activity.

One key result of our study is that the impact of NO on monocyte-derived cell metabolism is not a cell-autonomous mechanism requiring intrinsic iNOS expression. Instead, it is the number of NO-producing cells in the microenvironment that determines the respiratory capacity of monocyte-derived cells at the tissue level, affecting similarly NO-producing and non-producing cells, most likely through diffusion. In other contexts, cytokine may similarly act both on producing and non-producing cells to coordinate heterogeneous populations in a given environment (Shalek et al., 2014). We have previously observed such a dependency on collective NO production and NO diffusion to mediate antimicrobial activity (Olekhnovitch et al., 2014). *In vitro* experiments have delineated the various impact of iNOS induction on macrophages and dendritic cells (Everts et al., 2012; Lu et al., 2015; Van den Bossche et al., 2016). Our results suggest that it is important to consider that these effects are not necessarily cell-autonomous and can vary drastically *in vivo* based on the density of iNOS-expressing cells in the microenvironment. In this respect, we estimated that the suppressive effects of NO were substantial when the density of monocyte-derived cells reached 5000 cells/mm^3 in the skin.

Quorum-sensing mechanisms allow bacteria to sense and react to the density of their population, with the help of a diffusible mediator termed auto-inducer (Miller and Bassler, 2001). Similar mechanisms may exist in the immune system at homeostasis or during immune responses. For example, IgG secreted by activated B cells has been shown to regulate B cell homeostasis (Montaudouin et al., 2013). Here, we show that monocyte-derived cells can modify their activity and recruitment by sensing their density through the release of the diffusible molecule NO. We therefore propose that quorum-sensing is integral to the inflammatory reaction, allowing to temporally control immune cell numbers and activity for optimal immune responses with limited immunopathology.

Acknowledgments

We thank C. Demangel and members of the Bousso laboratory for critical review of the manuscript. We acknowledge the mouse facility and Technology Core of the Center for Translational Science (CRT) at Institut Pasteur for support in conducting this study and the specific contribution of B. Charbit, T. Stephen, S. Novault and S. Schmutz. The work was supported by Institut Pasteur, Inserm, and by a Starting (Lymphocytecontact) and an Advanced Grant (ENLIGHTEN) from the European Research Council.

Author contributions

J.P. conducted the experiments. F.L. generated reagents, J.P., R.O. and P.B. designed the experiments and analyzed the data. J.P. and P.B. wrote the manuscript.

Competing financial interests

The authors declare no competing financial interest.

References

Amiel, E., Everts, B., Fritz, D., Beauchamp, S., Ge, B., Pearce, E.L., and Pearce, E.J. (2014). Mechanistic target of rapamycin inhibition extends cellular lifespan in dendritic cells by preserving mitochondrial function. J Immunol *193*, 2821-2830.

Bagaitkar, J., Pech, N.K., Ivanov, S., Austin, A., Zeng, M.Y., Pallat, S., Huang, G., Randolph, G.J., and Dinauer, M.C. (2015). NADPH oxidase controls neutrophilic response to sterile inflammation in mice by regulating the IL-1alpha/G-CSF axis. Blood *126*, 2724-2733.

Banick, P.D., Chen, Q., Xu, Y.A., and Thom, S.R. (1997). Nitric oxide inhibits neutrophil beta 2 integrin function by inhibiting membrane-associated cyclic GMP synthesis. J Cell Physiol *172*, 12-24.

Belkaid, Y., Mendez, S., Lira, R., Kadambi, N., Milon, G., and Sacks, D. (2000). A natural model of Leishmania major infection reveals a prolonged "silent" phase of parasite amplification in the skin before the onset of lesion formation and immunity. J Immunol *165*, 969-977.

Biswas, S.K., and Mantovani, A. (2012). Orchestration of metabolism by macrophages. Cell Metab *15*, 432-437.

Bogdan, C. (2001). Nitric oxide and the immune response. Nature immunology *2*, 907-916.
Bogdan, C. (2015). Nitric oxide synthase in innate and adaptive immunity: an update. Trends Immunol *36*, 161-178.

Braverman, J., and Stanley, S.A. (2017). Nitric Oxide Modulates Macrophage Responses to Mycobacterium tuberculosis Infection through Activation of HIF-1alpha and Repression of NF-kappaB. J Immunol *199*, 1805-1816.

Brown, G.C. (1999). Nitric oxide and mitochondrial respiration. Biochim Biophys Acta *1411*, 351-369.

Brown, G.C. (2001). Regulation of mitochondrial respiration by nitric oxide inhibition of cytochrome c oxidase. Biochim Biophys Acta *1504*, 46-57.

Clementi, E., Brown, G.C., Feelisch, M., and Moncada, S. (1998). Persistent inhibition of cell respiration by nitric oxide: crucial role of S-nitrosylation of mitochondrial complex I and protective action of glutathione. Proc Natl Acad Sci U S A *95*, 7631-7636.

Cordes, T., Wallace, M., Michelucci, A., Divakaruni, A.S., Sapcariu, S.C., Sousa, C., Koseki, H., Cabrales, P., Murphy, A.N., Hiller, K.*, et al.* (2016). Immunoresponsive Gene 1 and Itaconate Inhibit Succinate Dehydrogenase to Modulate Intracellular Succinate Levels. J Biol Chem *291*, 14274-14284.

Dal-Secco, D., Wang, J., Zeng, Z., Kolaczkowska, E., Wong, C.H., Petri, B., Ransohoff, R.M., Charo, I.F., Jenne, C.N., and Kubes, P. (2015). A dynamic spectrum of monocytes arising from the in situ reprogramming of CCR2+ monocytes at a site of sterile injury. J Exp Med *212*, 447-456.

De Trez, C., Magez, S., Akira, S., Ryffel, B., Carlier, Y., and Muraille, E. (2009). iNOS-producing inflammatory dendritic cells constitute the major infected cell type during the chronic Leishmania major infection phase of C57BL/6 resistant mice. PLoS pathogens *5*, e1000494.

Eigler, A., Moeller, J., and Endres, S. (1995). Exogenous and endogenous nitric oxide attenuates tumor necrosis factor synthesis in the murine macrophage cell line RAW 264.7. J Immunol *154*, 4048-4054.

Everts, B., Amiel, E., van der Windt, G.J., Freitas, T.C., Chott, R., Yarasheski, K.E., Pearce, E.L., and Pearce, E.J. (2012). Commitment to glycolysis sustains survival of NO-producing inflammatory dendritic cells. Blood *120*, 1422-1431.

Giustizieri, M.L., Albanesi, C., Scarponi, C., De Pita, O., and Girolomoni, G. (2002). Nitric oxide donors suppress chemokine production by keratinocytes in vitro and in vivo. Am J Pathol *161*, 1409-1418.

Harbort, C.J., Soeiro-Pereira, P.V., von Bernuth, H., Kaindl, A.M., Costa-Carvalho, B.T., Condino-Neto, A., Reichenbach, J., Roesler, J., Zychlinsky, A., and Amulic, B. (2015). Neutrophil oxidative burst activates ATM to regulate cytokine production and apoptosis. Blood *126*, 2842-2851.

Kobayashi, Y. (2010). The regulatory role of nitric oxide in proinflammatory cytokine expression during the induction and resolution of inflammation. J Leukoc Biol *88*, 1157-1162.
Kreisel, D., Nava, R.G., Li, W., Zinselmeyer, B.H., Wang, B., Lai, J., Pless, R., Gelman, A.E., Krupnick, A.S., and Miller, M.J. (2010). In vivo two-photon imaging reveals monocyte-dependent neutrophil extravasation during pulmonary inflammation. Proc Natl Acad Sci U S A *107*, 18073-18078.

Kubes, P., Suzuki, M., and Granger, D.N. (1991). Nitric oxide: an endogenous modulator of leukocyte adhesion. Proc Natl Acad Sci U S A *88*, 4651-4655.

Lammermann, T., Afonso, P.V., Angermann, B.R., Wang, J.M., Kastenmuller, W., Parent, C.A., and Germain, R.N. (2013). Neutrophil swarms require LTB4 and integrins at sites of cell death in vivo. Nature *498*, 371-375.

Lampropoulou, V., Sergushichev, A., Bambouskova, M., Nair, S., Vincent, E.E., Loginicheva, E., Cervantes-Barragan, L., Ma, X., Huang, S.C., Griss, T.*, et al.* (2016). Itaconate Links Inhibition of Succinate Dehydrogenase with Macrophage Metabolic Remodeling and Regulation of Inflammation. Cell Metab *24*, 158-166.

Leon, B., Lopez-Bravo, M., and Ardavin, C. (2007). Monocyte-derived dendritic cells formed at the infection site control the induction of protective T helper 1 responses against Leishmania. Immunity *26*, 519-531.

Liew, F.Y., Millott, S., Parkinson, C., Palmer, R.M., and Moncada, S. (1990). Macrophage killing of Leishmania parasite in vivo is mediated by nitric oxide from L-arginine. J Immunol *144*, 4794-4797.

Lu, G., Zhang, R., Geng, S., Peng, L., Jayaraman, P., Chen, C., Xu, F., Yang, J., Li, Q., Zheng, H.*, et al.* (2015). Myeloid cell-derived inducible nitric oxide synthase suppresses M1 macrophage polarization. Nat Commun *6*, 6676.

Matthews, J.R., Botting, C.H., Panico, M., Morris, H.R., and Hay, R.T. (1996). Inhibition of NF-kappaB DNA binding by nitric oxide. Nucleic Acids Res *24*, 2236-2242.

Medzhitov, R. (2008). Origin and physiological roles of inflammation. Nature *454*, 428-435.
Meissner, F., Molawi, K., and Zychlinsky, A. (2008). Superoxide dismutase 1 regulates caspase-1 and endotoxic shock. Nat Immunol *9*, 866-872.

Michelucci, A., Cordes, T., Ghelfi, J., Pailot, A., Reiling, N., Goldmann, O., Binz, T., Wegner, A., Tallam, A., Rausell, A.*, et al.* (2013). Immune-responsive gene 1 protein links metabolism to immunity by catalyzing itaconic acid production. Proc Natl Acad Sci U S A *110*, 7820-7825.
Miller, M.B., and Bassler, B.L. (2001). Quorum sensing in bacteria. Annu Rev Microbiol *55*, 165-199.

Mills, E.L., Kelly, B., Logan, A., Costa, A.S.H., Varma, M., Bryant, C.E., Tourlomousis, P., Dabritz, J.H.M., Gottlieb, E., Latorre, I.*, et al.* (2016). Succinate Dehydrogenase Supports Metabolic Repurposing of Mitochondria to Drive Inflammatory Macrophages. Cell *167*, 457-470 e413.

Mishra, B.B., Lovewell, R.R., Olive, A.J., Zhang, G., Wang, W., Eugenin, E., Smith, C.M., Phuah, J.Y., Long, J.E., Dubuke, M.L.*, et al.* (2017). Nitric oxide prevents a pathogen-permissive granulocytic inflammation during tuberculosis. Nat Microbiol *2*, 17072.

Mishra, B.B., Rathinam, V.A., Martens, G.W., Martinot, A.J., Kornfeld, H., Fitzgerald, K.A., and Sassetti, C.M. (2013). Nitric oxide controls the immunopathology of tuberculosis by inhibiting NLRP3 inflammasome-dependent processing of IL-1beta. Nat Immunol *14*, 52-60.
Montaudouin, C., Anson, M., Hao, Y., Duncker, S.V., Fernandez, T., Gaudin, E., Ehrenstein, M., Kerr, W.G., Colle, J.H., Bruhns, P.*, et al.* (2013). Quorum sensing contributes to activated IgM-secreting B cell homeostasis. J Immunol *190*, 106-114.

Morgenstern, D.E., Gifford, M.A., Li, L.L., Doerschuk, C.M., and Dinauer, M.C. (1997). Absence of respiratory burst in X-linked chronic granulomatous disease mice leads to abnormalities in both host defense and inflammatory response to Aspergillus fumigatus. J Exp Med *185*, 207-218.

Muller, A.J., Aeschlimann, S., Olekhnovitch, R., Dacher, M., Spath, G.F., and Bousso, P. (2013). Photoconvertible pathogen labeling reveals nitric oxide control of Leishmania major infection in vivo via dampening of parasite metabolism. Cell host & microbe *14*, 460-467.

Na, Y.R., Je, S., and Seok, S.H. (2018). Metabolic features of macrophages in inflammatory diseases and cancer. Cancer Lett *413*, 46-58.

Olekhnovitch, R., and Bousso, P. (2015). Induction, Propagation, and Activity of Host Nitric Oxide: Lessons from Leishmania Infection. Trends in parasitology *31*, 653-664.

Olekhnovitch, R., Ryffel, B., Muller, A.J., and Bousso, P. (2014). Collective nitric oxide production provides tissue-wide immunity during Leishmania infection. The Journal of clinical investigation *124*, 1711-1722.

Ortega-Gomez, A., Perretti, M., and Soehnlein, O. (2013). Resolution of inflammation: an integrated view. EMBO Mol Med *5*, 661-674.

Sacks, D., and Noben-Trauth, N. (2002). The immunology of susceptibility and resistance to Leishmania major in mice. Nat Rev Immunol *2*, 845-858.

Sancho, D., Enamorado, M., and Garaude, J. (2017). Innate Immune Function of Mitochondrial Metabolism. Front Immunol *8*, 527.

Scott, P., and Novais, F.O. (2016). Cutaneous leishmaniasis: immune responses in protection and pathogenesis. Nat Rev Immunol *16*, 581-592.

Shalek, A.K., Satija, R., Shuga, J., Trombetta, J.J., Gennert, D., Lu, D., Chen, P., Gertner, R.S., Gaublomme, J.T., Yosef, N.*, et al.* (2014). Single-cell RNA-seq reveals dynamic paracrine control of cellular variation. Nature *510*, 363-369.

Speyer, C.L., Neff, T.A., Warner, R.L., Guo, R.F., Sarma, J.V., Riedemann, N.C., Murphy, M.E., Murphy, H.S., and Ward, P.A. (2003). Regulatory effects of iNOS on acute lung inflammatory responses in mice. Am J Pathol *163*, 2319-2328.

Sugimoto, M.A., Sousa, L.P., Pinho, V., Perretti, M., and Teixeira, M.M. (2016). Resolution of Inflammation: What Controls Its Onset? Front Immunol *7*, 160.

Tannahill, G.M., Curtis, A.M., Adamik, J., Palsson-McDermott, E.M., McGettrick, A.F., Goel, G., Frezza, C., Bernard, N.J., Kelly, B., Foley, N.H.*, et al.* (2013). Succinate is an inflammatory signal that induces IL-1beta through HIF-1alpha. Nature *496*, 238-242.

Tantama, M., Martinez-Francois, J.R., Mongeon, R., and Yellen, G. (2013). Imaging energy status in live cells with a fluorescent biosensor of the intracellular ATP-to-ADP ratio. Nat Commun *4*, 2550.

Thomassen, M.J., Buhrow, L.T., Connors, M.J., Kaneko, F.T., Erzurum, S.C., and Kavuru, M.S. (1997). Nitric oxide inhibits inflammatory cytokine production by human alveolar macrophages. Am J Respir Cell Mol Biol *17*, 279-283.

Thwe, P.M., and Amiel, E. (2018). The role of nitric oxide in metabolic regulation of Dendritic cell immune function. Cancer Lett *412*, 236-242.

Van den Bossche, J., Baardman, J., Otto, N.A., van der Velden, S., Neele, A.E., van den Berg, S.M., Luque-Martin, R., Chen, H.J., Boshuizen, M.C., Ahmed, M.*, et al.* (2016). Mitochondrial Dysfunction Prevents Repolarization of Inflammatory Macrophages. Cell Rep *17*, 684-696.

Van den Bossche, J., O'Neill, L.A., and Menon, D. (2017). Macrophage Immunometabolism: Where Are We (Going)? Trends Immunol *38*, 395-406.

Warnatsch, A., Tsourouktsoglou, T.D., Branzk, N., Wang, Q., Reincke, S., Herbst, S., Gutierrez, M., and Papayannopoulos, V. (2017). Reactive Oxygen Species Localization Programs Inflammation to Clear Microbes of Different Size. Immunity *46*, 421-432.

Wei, X.Q., Charles, I.G., Smith, A., Ure, J., Feng, G.J., Huang, F.P., Xu, D., Muller, W., Moncada, S., and Liew, F.Y. (1995). Altered immune responses in mice lacking inducible nitric oxide synthase. Nature *375*, 408-411.

Figures

Postat et al.
Figure 1

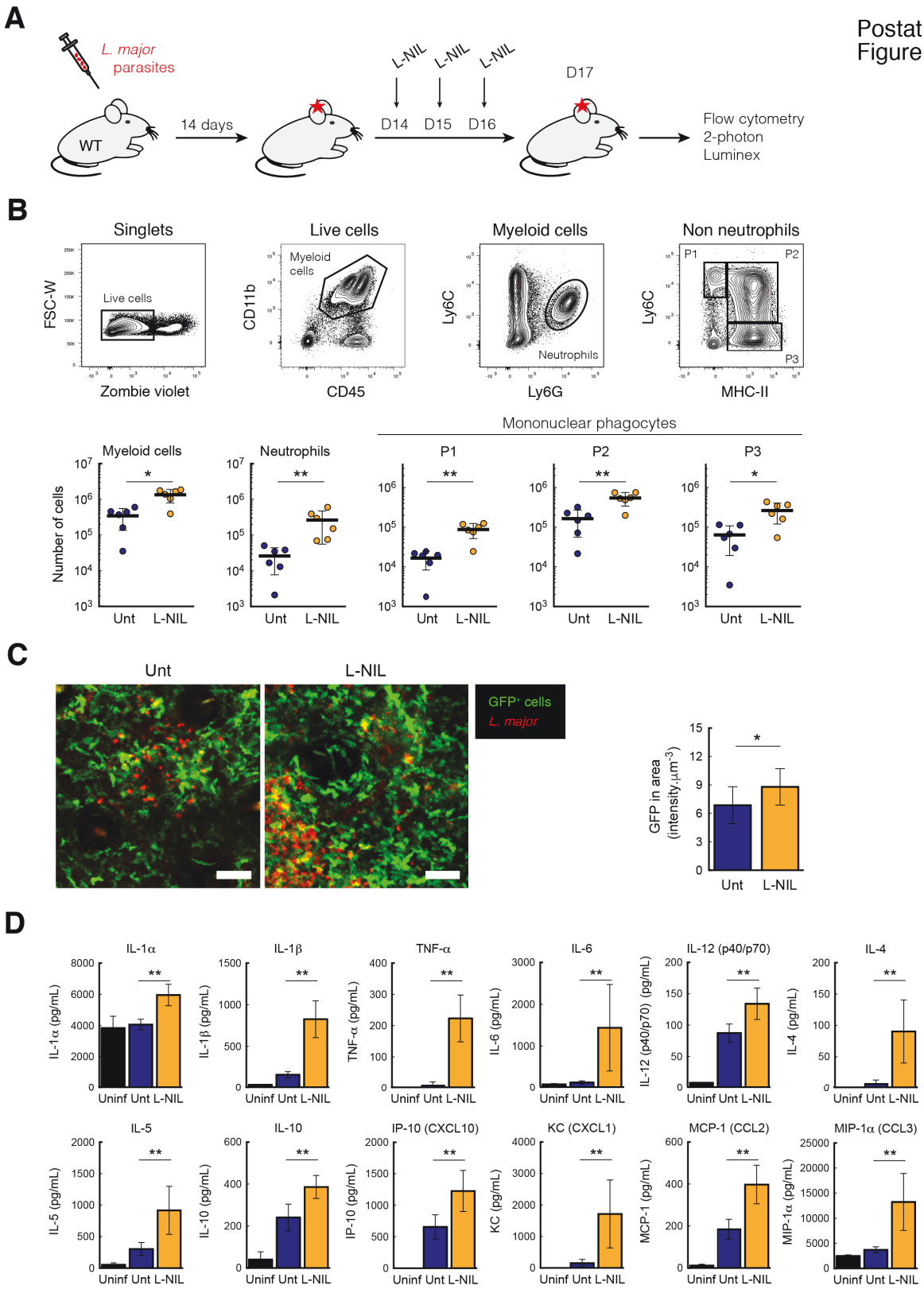

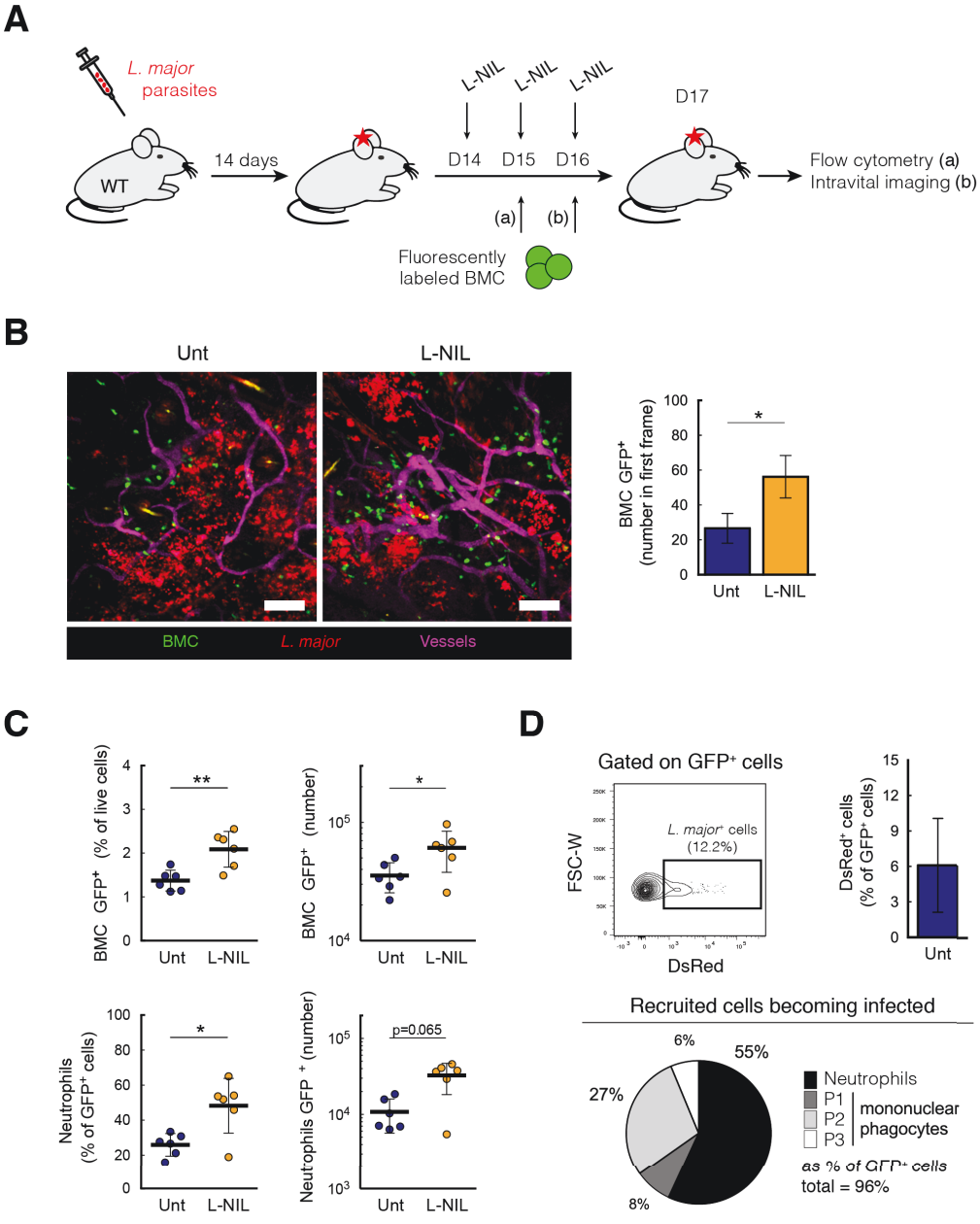
A
L. major parasites
WT
14 days
L-NIL
L-NIL
L-NIL
D14
D15
D16
D17
(a)
(b)
Flow cytometry (a)
Intravital imaging (b)
Fluorescently labeled BMC
B
Unt
L-NIL
BMC
L. major
Vessels
BMC GFP+ (number in first frame)
Unt
L-NIL
C
BMC GFP+ (% of live cells)
BMC GFP+ (number)
Neutrophils (% of GFP+ cells)
Neutrophils GFP+ (number)
p=0.065
D
Gated on GFP+ cells
L. major+ cells (12.2%)
FSC-W
DsRed
DsRed+ cells (% of GFP+ cells)
Recruited cells becoming infected
6%
55%
27%
8%
Neutrophils
P1
P2
P3
mononuclear phagocytes
as % of GFP+ cells
total = 96%

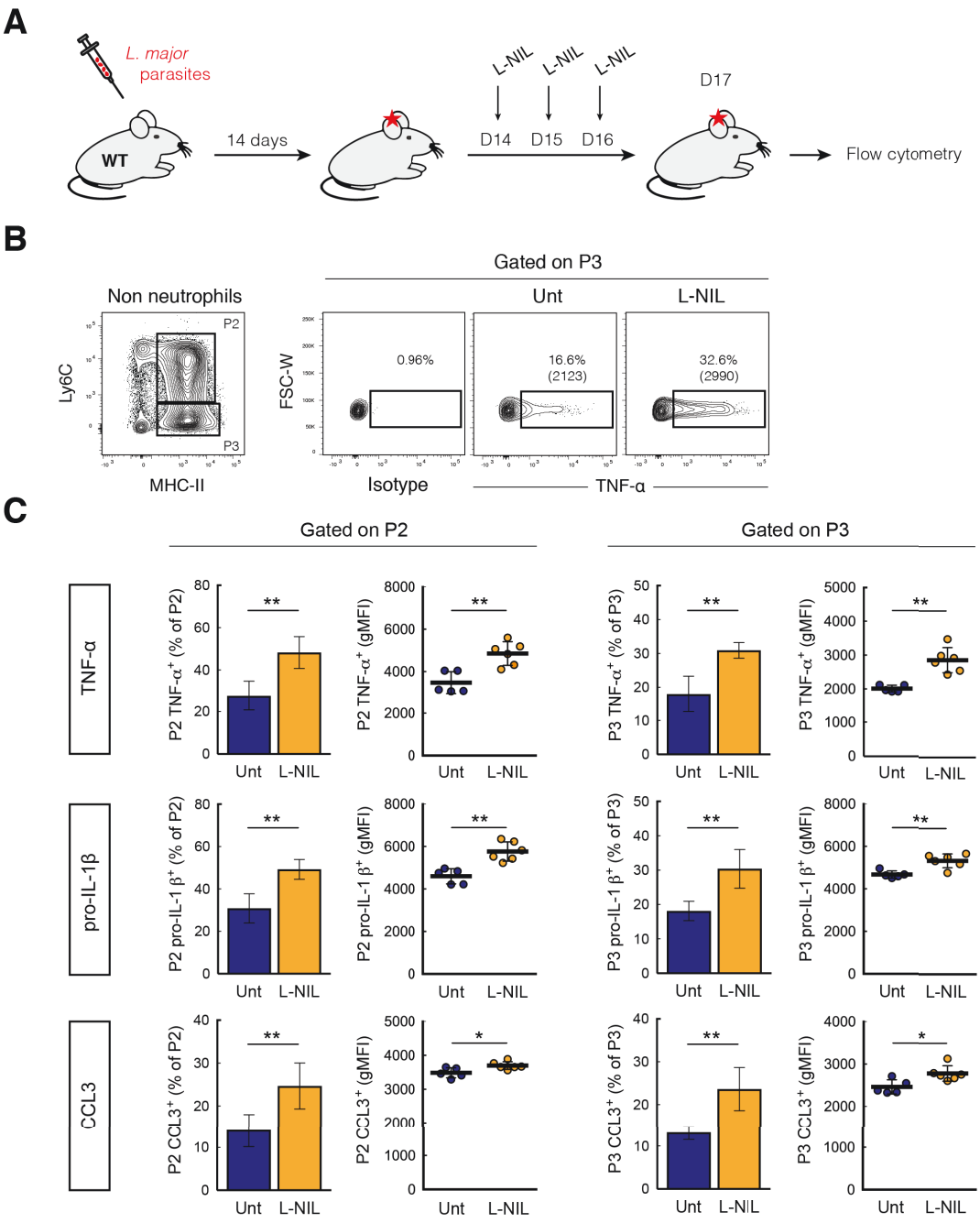
A
L. major parasites
WT
14 days
L-NIL
L-NIL
L-NIL
D14
D15
D16
D17
Flow cytometry
B
Non neutrophils
P2
P3
Ly6C
MHC-II
Gated on P3
Unt
L-NIL
FSC-W
0.96%
16.6%
(2123)
32.6%
(2990)
Isotype
TNF-α
C
Gated on P2
Gated on P3
TNF-α
pro-IL-1β
CCL3
P2 TNF-α+ (% of P2)
P2 TNF-α+ (gMFI)
P3 TNF-α+ (% of P3)
P3 TNF-α+ (gMFI)
P2 pro-IL-1 β+ (% of P2)
P2 pro-IL-1 β+ (gMFI)
P3 pro-IL-1 β+ (% of P3)
P3 pro-IL-1 β+ (gMFI)
P2 CCL3+ (% of P2)
P2 CCL3+ (gMFI)
P3 CCL3+ (% of P3)
P3 CCL3+ (gMFI)
Unt
L-NIL
**
*

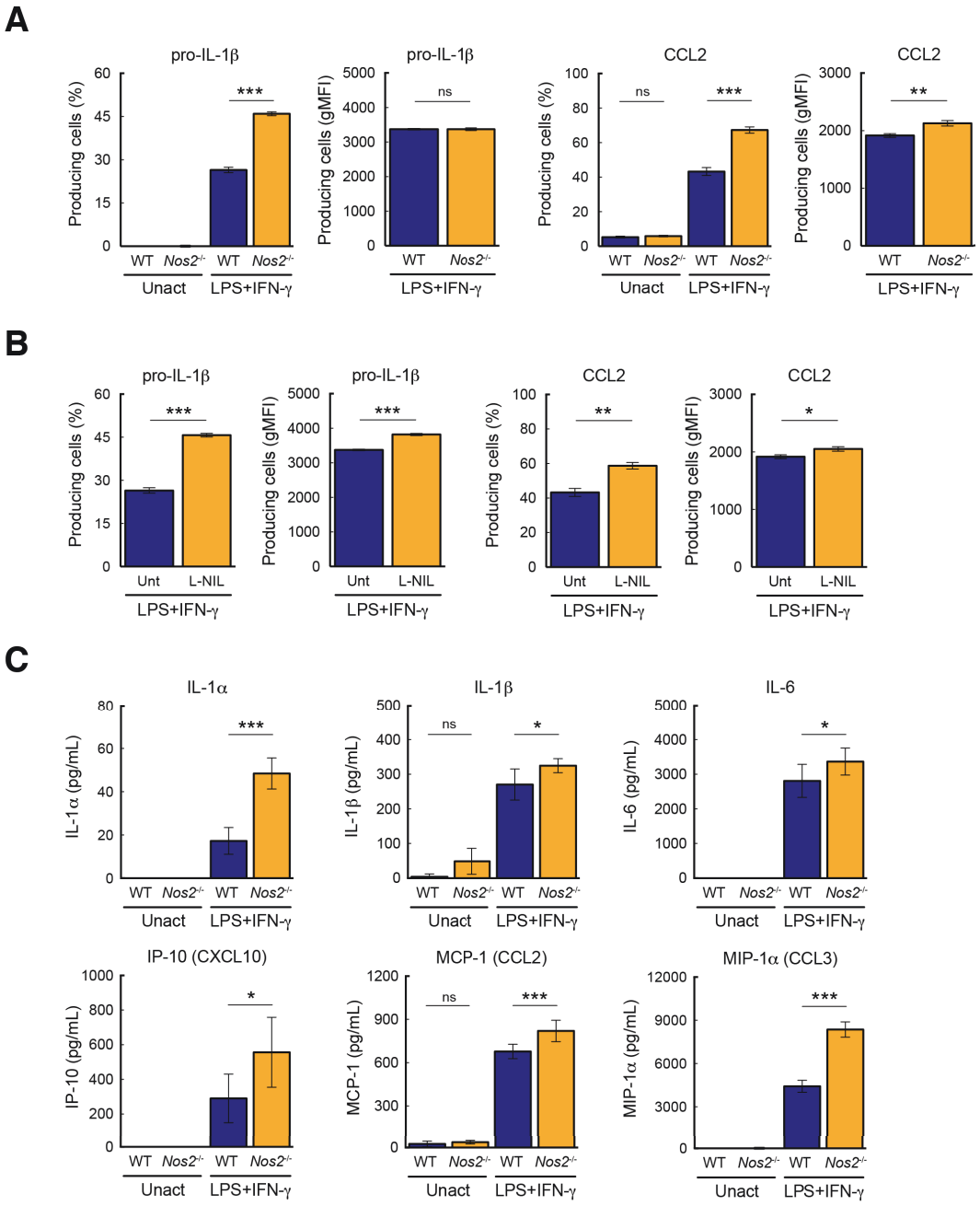
A
pro-IL-1β
Producing cells (%)
***
WT Nos2-/- WT Nos2-/-
Unact LPS+IFN-γ
pro-IL-1β
Producing cells (gMFI)
ns
WT Nos2-/-
LPS+IFN-γ
CCL2
Producing cells (%)
ns ***
WT Nos2-/- WT Nos2-/-
Unact LPS+IFN-γ
CCL2
Producing cells (gMFI)
**
WT Nos2-/-
LPS+IFN-γ
B
pro-IL-1β
Producing cells (%)
***
Unt L-NIL
LPS+IFN-γ
pro-IL-1β
Producing cells (gMFI)
***
Unt L-NIL
LPS+IFN-γ
CCL2
Producing cells (%)
**
Unt L-NIL
LPS+IFN-γ
CCL2
Producing cells (gMFI)
*
Unt L-NIL
LPS+IFN-γ
C
IL-1α
IL-1α (pg/mL)
***
WT Nos2-/- WT Nos2-/-
Unact LPS+IFN-γ
IL-1β
IL-1β (pg/mL)
ns *
WT Nos2-/- WT Nos2-/-
Unact LPS+IFN-γ
IL-6
IL-6 (pg/mL)
*
WT Nos2-/- WT Nos2-/-
Unact LPS+IFN-γ
IP-10 (CXCL10)
IP-10 (pg/mL)
*
WT Nos2-/- WT Nos2-/-
Unact LPS+IFN-γ
MCP-1 (CCL2)
MCP-1 (pg/mL)
ns ***
WT Nos2-/- WT Nos2-/-
Unact LPS+IFN-γ
MIP-1α (CCL3)
MIP-1α (pg/mL)
***
WT Nos2-/- WT Nos2-/-
Unact LPS+IFN-γ

Postat et al.
Figure 5

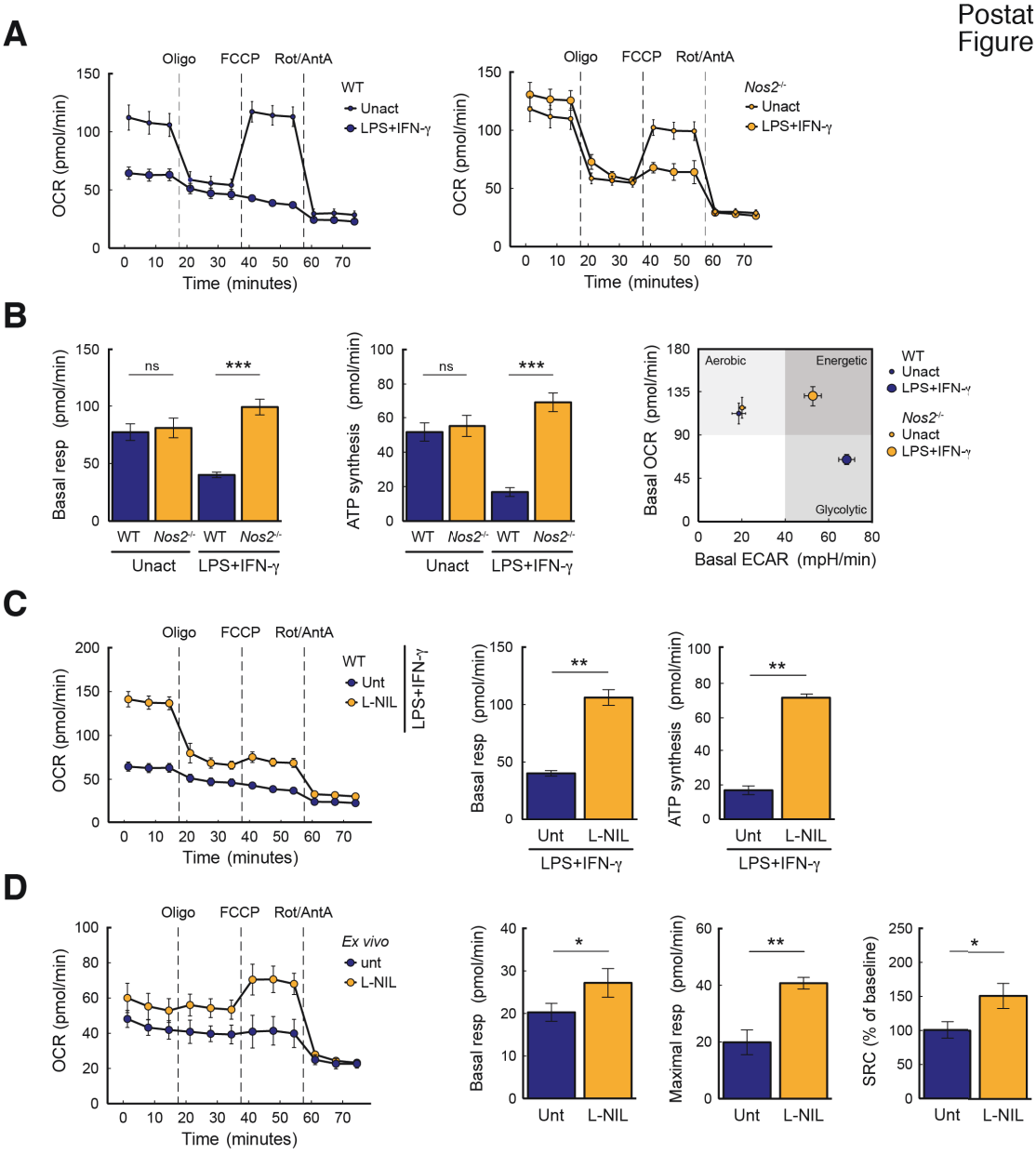

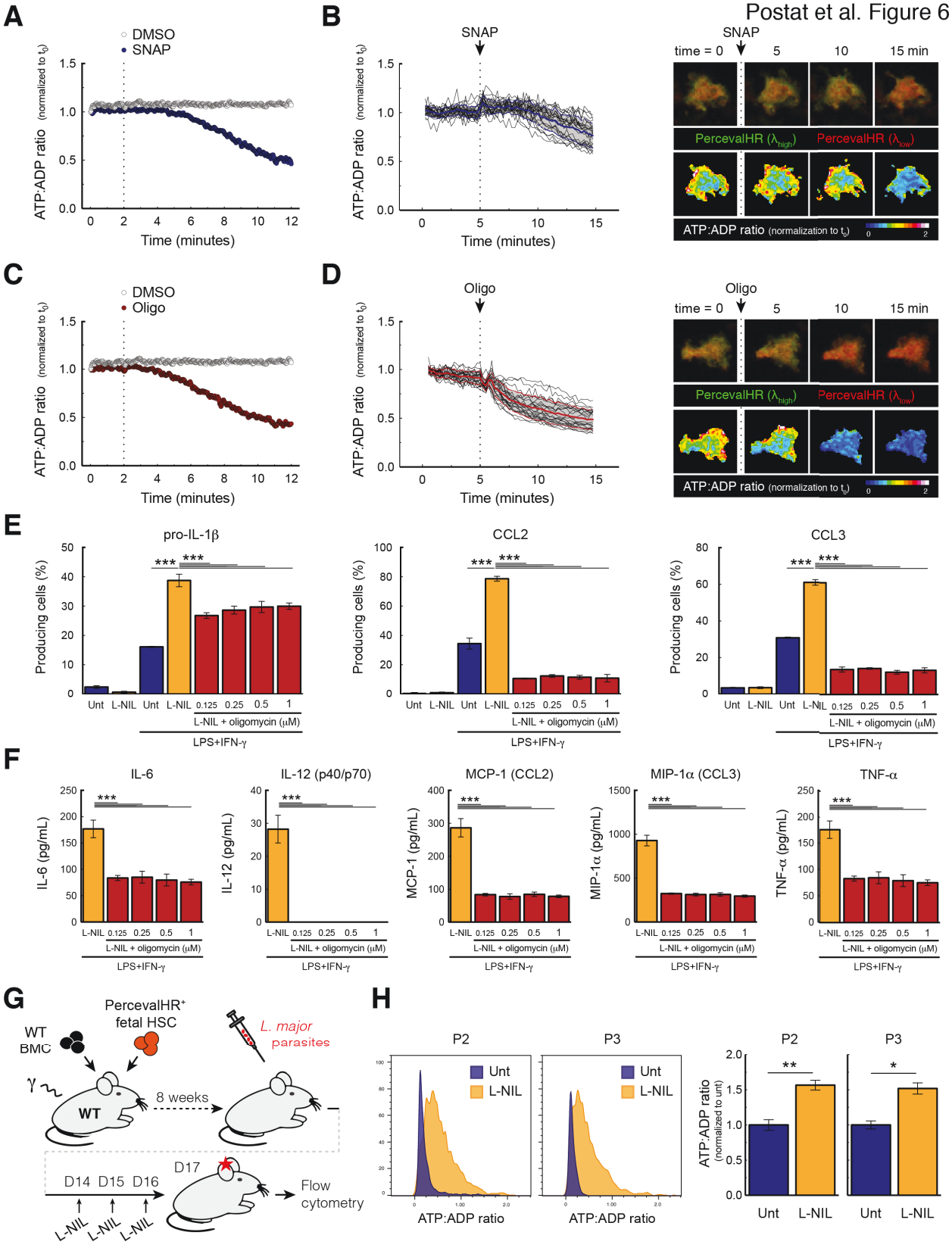
A
DMSO
SNAP
ATP:ADP ratio (normalized to t0)
Time (minutes)
B
SNAP
time = 0
5
10
15 min
PercevalHR (λhigh)
PercevalHR (λlow)
ATP:ADP ratio (normalization to t0)
C
DMSO
Oligo
D
Oligo
E
pro-IL-1β
CCL2
CCL3
Producing cells (%)
Unt
L-NIL
L-NIL + oligomycin (μM)
LPS+IFN-γ
F
IL-6
IL-12 (p40/p70)
MCP-1 (CCL2)
MIP-1α (CCL3)
TNF-α
IL-6 (pg/mL)
IL-12 (pg/mL)
MCP-1 (pg/mL)
MIP-1α (pg/mL)
TNF-α (pg/mL)
G
WT BMC
PercevalHR+ fetal HSC
L. major parasites
WT
8 weeks
D14 D15 D16
D17
L-NIL
Flow cytometry
H
P2
P3
Unt
L-NIL
ATP:ADP ratio
ATP:ADP ratio (normalized to unt)

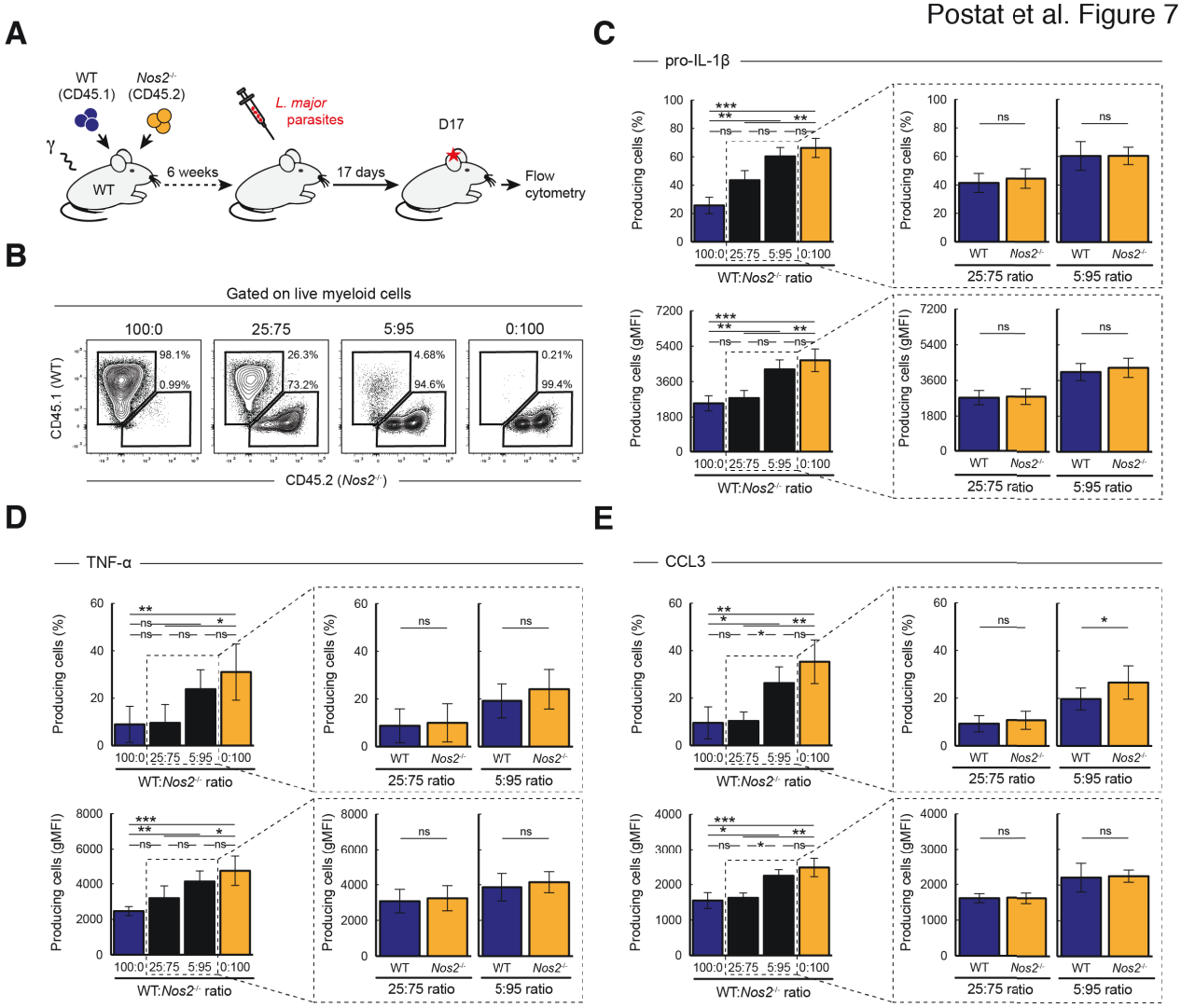
A
WT (CD45.1)
Nos2-/- (CD45.2)
γ
WT
6 weeks
L. major parasites
17 days
D17
Flow cytometry
B
Gated on live myeloid cells
100:0
25:75
5:95
0:100
98.1%
0.99%
26.3%
73.2%
4.68%
94.6%
0.21%
99.4%
CD45.1 (WT)
CD45.2 (Nos2-/-)
C
pro-IL-1β
Producing cells (%)
Producing cells (gMFI)
WT:Nos2-/- ratio
25:75 ratio
5:95 ratio
D
TNF-α
E
CCL3
ns
WT
Nos2-/-

Figure legends

Figure 1. NO dampens the inflammatory reaction at the site of *L. major* infection.
(A) Experimental set-up. WT mice were infected with DsRed-expressing *L. major* and treated 14 days later with the specific iNOS inhibitor L-NIL. Inflammatory reaction in infected ears was characterized 3 days later. **(B)** *Top*. Flow cytometry contour plots showing the gating strategy used to analyze mononuclear phagocytes (P1, P2 and P3) from extracted ear cells. *Bottom*. Absolute cell numbers of myeloid cells, neutrophils and mononuclear phagocytes in infected ears from untreated (blue circles) or L-NIL-treated (orange circles) WT mice as assessed by flow cytometry. A third of the ear cell preparation was used flow cytometric analysis and 200000 cells were acquired. Representative of 6 independent experiments. **(C)** *Left*. Representative images of two-photon intravital imaging performed on infected ears from untreated or L-NIL-treated *Lyz2*$^{+/EGFP}$ mice, showing DsRed-expressing *L. major* and myeloid cells (GFP^{+}). Scale bar: 50 μm. *Right*. Quantification of GFP fluorescence in infected ears from untreated or L-NIL-treated mice. Results are representative of 2 independent experiments. **(D)** Cytokines (IL-1α, IL-1β, TNF-α, IL-6, IL-12 (p40 and p70), IL-4, IL-5 and IL-10) and chemokines (CXCL10, CXCL1, CCL2 and CCL3) quantification in ear lysates from untreated (blue bars) or L-NIL-treated (orange bars) mice as assessed by multiplex assay. Ears from age and sex-matched uninfected mice were analyzed to assess cytokine basal concentrations. Results are representative of 3 independent experiments. Data are represented as mean ± SD.

Figure 2. NO impacts immune cell recruitment at the site of *L. major* infection
(A) Experimental set up. WT mice were infected with DsRed-expressing *L. major* and treated 14 days later with the specific iNOS inhibitor L-NIL. Cell recruitment was assessed 3 days later by transferring i.v. fluorescently-labeled bone marrow cells. **(B)** *Left*. Representative images of two-photon intravital imaging performed on infected ears from untreated or L-NIL-treated mice, showing DsRed-expressing *L. major* (red), Evans blue-labeled vessels (magenta) and GFP^{+} extravasated cells (green). Scale bar: 100 μm. *Right*. The absolute numbers of extravasated cells in the imaging field were measured for untreated (blue bar) or L-NIL-treated (orange bar) mice. Representative of 2 independent experiments. **(C)** Percentages and absolute cell numbers of total GFP^{+} cells and GFP^{+} neutrophils in infected ears from untreated (blue circles) and L-NIL-treated (orange circles) mice as assessed by flow cytometry. **(D)** *Top*. Contour plot and quantification of infection among recruited GFP^{+} cells in untreated mice. *Bottom*. Pie chart showing the cellular composition of infected cells among the recruited GFP^{+} cells. Results are representative of 6 independent experiments. Data are represented as mean ± SD.

Figure 3. NO restricts monocyte-derived cells function *in vivo* at the single cell level.
(A) Experimental set-up. WT mice were infected with DsRed-expressing *L. major* and treated 14 days later with the specific iNOS inhibitor L-NIL. Monocyte-derived cell activity (P2 and P3 gates) was assessed 3 days later by intracellular cytokine staining on isolated ear cells. **(B)** Contours plots showing TNF-α staining in monocyte-derived cells from untreated or L-NIL-treated mice. Percentages and gMFI (in brackets) of producing cells are shown in respective plots. **(C)** Percentages (bars) and gMFI (scatter dot plots) of TNF-α-, pro-IL-1β- or CCL3-producing monocytes-derived cells (P2 and P3 gates) from untreated (blue) and L-NIL-treated (orange) mice as assessed by flow cytometry. Results are representative of 2 independent experiments with 6 ears analyzed per group and per experiment. Data are represented as mean ± SD. *See also Figure S1 and S2.*

Figure 4. NO broadly restricts bone-marrow derived macrophage functions *in vitro*.
WT or *Nos2*$^{-/-}$ BMDMs were activated 24 h with LPS+IFN-γ or left unactivated. **(A)** Percentages and gMFI of pro-IL-1β (left) and CCL2 (right) producing WT (blue bars) or *Nos2*$^{-/-}$ (orange bars) cells as

assessed using intracellular cytokine staining. Representative of 4 independent experiments. **(B)** Percentages and gMFI of pro-IL-1β- (left) and CCL2- (right) producing BMDMs cultured in the absence (blue bars) or presence (orange bars) of L-NIL. **(C)** Cytokines (IL-1α, IL-1β, IL-6) and chemokines (CXCL10, CCL2 and CCL3) quantification in WT or *Nos2*$^{-/-}$ BMDM supernatants as assessed by multiplex assay. Results are representative of 2 independent experiments with 6 replicates per conditions and per experiment. Data are represented as mean ± SD. *See also Figure S3 and S5.*

Figure 5. NO dampens mitochondrial respiration *in vitro* and *in vivo*.
(A,B) WT or *Nos2*$^{-/-}$ BMDMs were activated 24 h with LPS+IFN-γ or left unactivated before extracellular flux analysis. **(A)** Oxygen consumption rate (OCR) measured during sequential treatments with oligomycin, FCCP and rot/antA on WT and *Nos2*$^{-/-}$ BMDMs. **(B)** Quantification of ATP synthesis and basal respiration based on OCR variations for WT (blue bars) and *Nos2*$^{-/-}$ (orange bars) BMDMs. Basal OCR and ECAR are graphed for the indicated populations to represent their metabolic phenotypes. Representative of 3 independent experiments. **(C)** *Left*. OCR was measured on untreated or L-NIL-treated WT activated BMDMs. *Right*. Quantification of ATP synthesis and basal respiration based on OCR variations for untreated (blue bars) or L-NIL-treated WT (orange bars) activated BMDMs. **(D)** *Left*. OCR was measured on monocyte-derived cells isolated from infected ears. Cells were left untreated or treated with L-NIL for 2 h *ex vivo*. *Right*. Quantification of basal respiration, maximal respiration and spare respiratory capacity (SRC) based on OCR variations for untreated (blue bars) or L-NIL-treated (orange bars) cells. Results were evaluated using a two-tailed unpaired Student's t-test with Welch's correction. Results are representative of six mice analyzed in 2 independent experiments. Data are represented as mean ± SD. *See also Figure S4 and S5*

Figure 6. NO alters ATP:ADP ratio *in vitro* and *in vivo*, restricting macrophage activity.
(**A-D**) Single-cell measurement of ATP:ADP ratio in BMDMs. PercevalHR-expressing BMDMs were activated 24 h with LPS+IFN-γ in the presence of L-NIL. (**A**) ATP:ADP ratio was measured in BMDMs immediately following incubation with the NO donor SNAP (100 μM) (or DMSO as a control) by time-resolved flow cytometry. Normalized cellular ATP:ADP ratio was calculated using PercevalHR fluorescence measured at λ_{low} = 405 nm and λ_{high} = 488 nm excitation wavelengths (see Experimental procedure). The graph shows the geometric mean for the normalized ATP:ADP ratio as a function of the acquisition time. (**B**) Live-imaging of ATP:ADP ratio in BMDMs exposed to SNAP (100 μM) using two-photon excitation (λ_{low} = 830 nm and λ_{high} = 1040 nm). Quantification for multiple cells (left) and representative time-lapse images (right) are shown. (C) ATP:ADP ratio was measured in BMDMs immediately following incubation with the ATP synthase inhibitor oligomycin (1 μM) (or DMSO as a control) by time-resolved flow cytometry. (D) Live-imaging of ATP:ADP ratio in BMDMs exposed to oligomycin (1 μM). Results are representative of three independent experiments. (**E-F**) BMDMs were activated 24 h with LPS+IFN-γ in the presence or in the absence of L-NIL or left untreated. When indicated BMDMs were incubated with various concentration of oligomycin for the last 4 h of the culture. (**E**) Percentages of cytokine-producing cells were assessed by intracellular cytokine staining for pro-IL-1β, CCL2 and CCL3. Representative of 3 independent experiments. (**F**) Cytokines and chemokines in BMDM supernatants cultured in the presence or absence of oligomycin were measured by multiplex assay. Medium was changed in all samples at the time of oligomycin addition. (**G-H**) NO decreases ATP:ADP ratio in monocyte-derived cells *in vivo*. (G) Experimental set-up. Chimeric mice reconstituted with PercevalHR HSCs were infected with *L. major*. Two weeks later, some mice were treated with L-NIL for 3 consecutive days. Monocyte-derived cells recovered at the site of infection were analyzed for ATP:ADP ratio (based on PercevalHR fluorescences) by flow cytometry. (**H**) Representative histograms (left) and bar plot (right) of the ATP:ADP ratio in P2 and P3 populations recovered from infected mice with or

without iNOS inhibition. Results were evaluated using a two-tailed unpaired Student's t-test with Welch's correction. Data are represented as mean ± SD. *See also Figure S6.*

Figure 7. Collective NO production provides a quorum-sensing mechanism to dampen inflammation.

(A) Experimental set-up. CD45.1 WT recipient mice were lethally irradiated and reconstituted with CD45.1 WT and CD45.2 *Nos2*$^{-/-}$ bone marrow cells, mixed at different ratios. Chimeras were infected 6 weeks later with DsRed-expressing *L. major*. Monocyte-derived cells activity was assessed 17 days later by intracellular cytokine staining on extracted ear cells. **(B)** Cellular composition in the ear of infected mixed-bone marrow chimeras. (**C-E**) Percentages (top) and gMFI (bottom) of pro-IL-1β- **(C)**, TNF-α- **(D)** and CCL3- **(E)** producing Ly6C^{+} MHC-II^{+} monocyte-derived cells (P2 gate) among the overall population (100:0 (blue bars), 0:100 (orange bars), mixed chimeras (black bars)) as assessed by intracellular cytokine staining. The inset shows the analysis of WT (CD45.1) and *Nos2*$^{-/-}$ (CD45.2) cells in the same chimeric mice prepared at the indicated WT:*Nos2*$^{-/-}$ ratio. Representative of 7 mice per group in 2 independent experiments. Data are represented as mean ± SD. *See also Figure S7.*

STAR Methods Text

Contact for reagent and resource sharing

Further information and requests for resources and reagents should be directed to and will be fulfilled by the Lead Contact, Philippe Bousso (philippe.bousso@pasteur.fr)

Experimental model and subject details

Mice

C57BL/6J mice were obtained from Charles River France. C57BL/6J-Ptprc[a] (CD45.1), C57BL/6J-Tg(UBC-GFP)30Scha/J (Ubi-GFP), C57BL/6J-*Lyz2*$^{tm1.1Graf[EGFP]}$ (*Lyz2*$^{+/EGFP}$), C57BL/6-Tg(Csf1r-EGFP-NGFR/FKBP1A/TNFRSF6)2Bck/J (MaFIA) and B6.129P2-Nos2tm1Lau/J (*Nos2*$^{-/-}$) transgenic mice were bred in our animal facility. All mice were housed under SPF conditions, sex-matched and aged between 6 and 10 weeks for each experiment. All procedures were performed in agreement with the Institut Pasteur institutional guidelines for animal care. Experimental protocols were approved by the Animal Ethics Committee #1 of the Comité Régional d'Éthique pour l'Expérimentation Animale (CREEA), Ile-de-France (MESR N° 01264).

Parasites

DsRed-expressing *Leishmania major* parasites were grown at 26°C for a maximum of 5 passages in M119 medium supplemented with 10% heat-inactivated fetal bovine serum, 0.1 mM adenine, 1 µg/mL biotin, 5 µg/mL hemin and 2 µg/mL biopterin.

Bone marrow-derived macrophages (BMDMs)

Femurs and tibias were isolated from adult WT or *Nos2*$^{-/-}$ mice, sterilized in 70% ethanol and flushed with PBS. Single cell suspensions were prepared by filtering the marrow through a 30 µm cell strainer. 20×10^6 BMC were cultured in 150 mm non-treated Petri dishes for 7 days, 37°C, 5% CO_2, in 30 mL RPMI medium 1640 - GlutaMAX™ supplemented with 10% heat-inactivated fetal bovine serum, 100 U/mL penicillin, 100 ng/mL streptomycin, 1 mM sodium pyruvate, 1 mM HEPES and 5 mM 2-mercaptoethanol (complete RPMI) and 20% L929-cell conditioned supernatant. 30 mL of fresh medium was added 3 days after plating.

Method details

Infection, inflammation model and L-NIL treatment

For infection, stationary-phase promastigotes were resuspended at 10^8 parasites/mL in PBS and 5 µL were injected intradermally into the ear dermis. To induce a non-infectious inflammatory reaction, incomplete Freund's adjuvant was emulsified with an equal volume of saline and 10 µL were injected intradermally into the ear dermis. To inhibit iNOS activity, L-NIL was freshly prepared at 2 mg/mL in PBS and mice were injected with 100 µL i.p. once a day for 3 days, starting 14 days post infection or 4 days post challenge. Age and sex-matched controls were infected or challenged at the same time and did not received L-NIL injection.

Extraction of ear cells

Ears harvested from euthanized mice were separated into dorsal and ventral sheets using tissue forceps before being digested for 45 min, 37°C, 700 rpm, in RPMI medium 1640 supplemented with 100 U/mL penicillin, 100 ng/mL streptomycin, 0.5 mg/mL liberase TL and 50 ng/mL DNase. Single cell suspensions in PBS were prepared by crushing digested ears into a 70 µm cell strainer. After a

washing step in PBS and filtration, cells were analyzed by flow cytometry or subjected to extracellular flux analysis.

Adoptive transfer
Bone marrow cells were harvested from Ubi-GFP mice and filtered through a 30 µm cell strainer to generate a single cell suspension. 6×10^7 cells were injected i.v. per mice after anaesthesia.

Flow cytometry
In vitro generated BMDMs were washed with cold PBS and incubated for 10 min, 4°C, in 3 mL of Cell Dissociation Buffer to detach the cells. BMDMs were recovered by adding 10 mL of cold PBS and washed before seeding at 10^6 cells/well (6-well non-treated plates) in 2 mL complete RPMI supplemented with 20% L929-cell conditioned supernatant. To vary the density of iNOS competent cells in the culture, we mixed WT and *Nos2*$^{-/-}$ BMDMs at various ratios, keeping the total cell number constant to avoid confounding effects of varying cytokine and/or nutrients concentrations. The day after seeding, medium was removed and replaced with 2 mL of fresh complete RPMI supplemented with 1 µg/mL LPS + 50 ng/mL IFN-γ for activation. When needed, treatment with 20 µg/mL L-NIL was performed at the time of activation. Treatment with oligomycin or azide was performed 20 h post activation at the indicated doses. To monitor glucose uptake, 20 µM 2-deoxy-2-[(7-nitro-2,1,3-benzoxadiazol-4-yl)amino]-D-glucose (2-NBDG) was incubated with cells during 1 h. 24 h post activation, BMDMs were washed with cold PBS and incubated for 10 min, 4°C, in 300 µL Cell Dissociation Buffer to detach the cells. BMDMs were harvested by adding 1 mL of cold PBS to each well. Cells were stained with Zombie Violet fixable dye diluted at 1:200 in PBS supplemented with 2% FBS and 5 mM EDTA (FACS buffer) for 15 min, 4°C, to assess cell viability. BMDMs were stained for 15 min, 4°C, in FACS buffer supplemented with 10 µg/mL anti-mouse CD16/32 (Fc-block) using a combination of fluorescently-labeled monoclonal antibodies among: PerCP-Cy5.5 anti-CD11b, APC-eFluor® 780 anti-MHC II (I-A/I-E). For intracellular staining, prior harvesting the cells, BD GolgiPlug diluted at 1:1000 was added to every well without volume variation, 20 h post activation. Cells were harvested and stained as described above. BMDMs were fixed for 30 min, 4°C, using formaldehyde solution diluted at 2% in PBS. Cells were permeabilized using PermWash buffer following manufacturer's instructions and stained for 45 min, 4°C, using a combination of fluorescently-labeled monoclonal antibodies among: PE anti-mouse CCL2, PE anti-mouse CCL3, APC anti-mouse IL-1β Pro-form.

For *ex vivo* analyses, extracted ear cells were stained with Zombie Violet fixable dye diluted at 1:200 or LIVE/DEAD blue fixable dye diluted at 1:500 in FACS buffer for 15 min, 4°C, to assess cell viability. Cells were then fixed for 30 min, 4°C, using formaldehyde solution diluted to 2% in PBS. Surface staining of cells was performed for 15 min, 4°C, in FACS buffer supplemented with 10 µg/mL anti-mouse CD16/32 (Fc-block) using a combination of fluorescently-labeled monoclonal antibodies among: BUV395 anti-CD45, BV421 anti-MHC II (I-A/I-E), BV510 anti-Gr-1, BV510 anti-Ly-6G, BV605 anti-Ly-6C, PerCP-Cy5.5 anti-CD11b, PE-Cy7 anti-CD45.1, APC anti-CD11c, APC-eFluor® 780 anti-CD45.2, APC-eFluor® 780 anti-MHC II (I-A/I-E). For intracellular staining, extracted cells were plated in 48-well plates in 1 mL complete RPMI supplemented with BD GolgiPlug (diluted at 1:1000) for 4 h, 37°C. iNOS inhibition was maintained adding 20 µg/mL L-NIL to dedicated wells. Cells were harvested by flushing all wells and submitted to staining as described above. After surface staining, cells were permeabilized using PermWash buffer following manufacturer's instructions and stained 45 min, 4°C, using a combination of fluorescently-labeled monoclonal antibodies among: Alexa Fluor® 488 anti-mouse TNF-α, eFluor® 660 anti-CCL3, APC anti-mouse IL-1β Pro-form. Samples were analyzed using a BD CantoII or a BD Fortessa flow cytometer equipped with FACSDiva software (BD Bioscience) or a CytoFLEX LX flow cytometer equipped with CytExpert software (Beckman Coulter).

For analysis of PercevalHR-expressing cells, two fluorescence signals were acquired. F_{low} was collected by exciting PercevalHR with a violet laser (λ_{low} = 405 nm) and filtering the signal through a 525/40 filter. F_{high} was collected by exciting PercevalHR with a blue laser (λ_{high} = 488 nm) and filtering the signal through a 510/20+OD1 filter. Cellular ATP:ADP ratio was determined by calculating F_{high}:F_{low} ratio for each acquired cell. For time-resolved (kinetic) flow cytometry, ATP:ADP ratio was normalized to the first value acquired (t_0). Data analysis was performed using FlowJo 10.2 software.

MitoTracker staining

After activation, cells were loaded with MitoTracker® dyes using 40 nM MitoTracker® GreenFM and 50 nM MitoTracker® Red CMXRos during 30 min, 37°C, 5% CO_2. Cells were washed with cold PBS before flow cytometry analysis.

Hypoxic culture

Hypoxic cultures were conducted using PetakaG3 FLAT hypoxic devices (balancing the partial pressure of dissolved oxygen in the media at 25 mmHg). 15×10^6 BMDMs were loaded into each chamber in 20 mL complete RPMI supplemented with 20% L929-cell conditioned medium and cultivated horizontally overnight to allow cell seeding. The day after, medium was replaced for activation. Cell treatments and flow cytometry were performed as described earlier.

Extracellular flux analysis

BMDMs were analyzed using an XF^{e}96 Extracellular Flux Analyzer (Seahorse Bioscience). BMDMs were plated in XF^{e}96 cell culture microplates (10^5 cells/well in 200 µL final) and either left untreated or activated with 1 µg/mL LPS + 50 ng/mL IFN-γ, 37°C, 5% CO_2. 24 h post activation, cells were washed with XF Base medium supplemented with 10 mM glucose, 2 mM glutamine and 1 mM sodium pyruvate (MitoStress XF running buffer, pH adjusted to 7.4) or supplemented with 2 mM glutamine (GlycoStress XF running buffer, pH adjusted to 7.4), and 175 µL of appropriate XF running buffer was added as final volume. BMDMs were stored 1 h at 37°C in a non-CO_2 incubator before starting the analysis. Following manufacturer's instruction, OCR and ECAR were measured in response to 1 µM oligomycin, 1.5 µM Carbonyl cyanide-*4*-(trifluoromethoxy)phenylhydrazone (FCCP) and 0.5 µM rotenone and antimycin A (MitoStress Test Kit) or in response to 10 mM glucose, 1 µM oligomycin and 50 mM 2-deoxy-glucose (2-DG) (GlycoStress Test Kit).

For *ex vivo* isolation of mononuclear phagocytes from infected ears, we relied on the expression of the CD11c marker on both P2 and P3 populations (Olekhnovitch et al., 2014). $CD11c^+$ cells were isolated from infected ears using positive selection on MACS columns. The isolated population contained at least 90% of $CD11b^+MHC\text{-}II^+$ monocyte-derived cells. Cells were washed and plated at 10^5 cells/well in 175 µL of MitoStress XF running buffer and treated with 20 µg/mL L-NIL or left untreated during 2 h, 37°C, non-CO_2 incubator. Following manufacturer's instruction, OCR and ECAR were measured in response to 1 µM oligomycin, 1.5 µM FCCP and 0.5 µM rotenone and antimycin A (MitoStress Test Kit).

Data analysis was performed using Wave software.

Multiplex assay for cytokine and chemokine quantification

Ears harvested from euthanized mice were separated into dorsal and ventral sheets and snap frozen before storage at -80°C until analysis. For tissue lysates preparation, ears were thawed out and chopped in 1 mL RIPA buffer on ice. After 20 min incubation, samples were grounded during 2 min with a Potter-Elvehjem PTFE pestle into an appropriate glass tube. Lysates were subsequently clarified by centrifugation for 15 min at 4°C, 15.000 rcf. Multiplex assay was performed following manufacturer's instructions. Lysates were diluted at 1:2 in assay diluent. Standards were reconstituted with RIPA buffer diluted at 1:2 in assay diluent. For analyte capture, the plate was incubated

overnight at 4°C under agitation on an orbital shaker. Plate reading was performed using a Bio-Plex 200 system equipped with Bio-Plex Manager software (Bio-Rad).
For *in vitro* analyses, BMDMs were cultivated and activated as indicated during 24 h. Supernatants were harvested and cleared by centrifugation before being snap frozen and stored at -80°C until analysis. The day of analysis, supernatants were diluted 1:4 in assay diluent and multiplex assay was performed as described previously.

PercevalHR probe and virus generation
The original PercevalHR construct was cloned into a murine stem cell viral (MSCV) vector. HEK 293 cells were co-transfected with 6 µg pMSCV-PercevalHR and 4 µg pCL-Eco plasmids using JetPRIME reagent following manufacturer instructions. Medium was changed 4 h after with complete RPMI. 48 h after transfection, retrovirus containing supernatant was harvested from HEK 293 cells, 0.45 µm-filtered and supplemented with 10 µg/mL polybrene to generate retroviral-conditioned medium.

Retroviral transduction of BMDMs
BMDMs were retrovirally transduced during their differentiation. On day 3, differentiation medium was exchanged with 25 mL retroviral-conditioned medium supplemented with 20% L929-cell conditioned medium for an overnight incubation. On day 4, retroviral medium was replaced with complete RPMI supplemented with 20% L929-cell conditioned supernatant for an additional 3 days. Transduction efficiencies of >60% were routinely achieved.

Generation of mixed-bone marrow chimeras
WT CD45.1 recipient mice were γ-irradiated with a single lethal dose of 9 *Gy*. Femurs and tibias were isolated from adult WT CD45.1 or *Nos2*$^{-/-}$ CD45.2 mice, sterilized in 70% ethanol and flushed with PBS. Single cell suspensions were prepared by filtering the marrow through a 30 µm cell strainer. Mice were anaesthetized 2 hours post irradiation and reconstituted with a total of 5×10^7 bone marrow cells (WT, *Nos2*$^{-/-}$ or a mixture of both) by retro-orbital i.v. injection. Chimeras were infected 6 to 8 weeks after reconstitution. The same protocol was used to generate mixed-bone marrow chimeras using WT and MAFIA cells.

Generation of PercevalHR-expressing fetal liver chimeras
WT recipient mice were γ-irradiated with a single lethal dose of 9 *Gy*. Mice were anaesthetized 2 hours post irradiation and reconstituted with a total of 1×10^6 PercevalHR-expressing fetal HSCs plus 5×10^5 WT bone marrow cells by retro-orbital i.v. injection. For PercevalHR-expressing HSC generation, fetal liver of E14.5 embryos were harvested and multipotent HSCs were isolated by negative selection on MACS columns using biotin anti-mouse TER-119 antibody. Isolated HSCs were cultivated overnight in complete RPMI supplemented with 200 ng/mL rmSCF, 200 ng/mL rmFlt3-L and 200 ng/mL rmIL-3 at a density of 1×10^6 cells/mL. The day after, 1×10^6 HSCs in 2 mL retroviral-conditioned medium were retrovirally transduced by spin infection (800 *g*, 2 h, 32°C). After the spin infection, medium was replaced with complete RPMI supplemented with the same cytokine cocktail for an overnight incubation before injection into irradiated recipients. Chimeras were infected 8 weeks after reconstitution.

Intravital imaging
Mice were anaesthetized and prepared for intravital two-photon imaging. Each mouse was placed on a custom-designed heated stage, one ear was placed onto a metal piece and immobilized with double sided tape. The ear was kept moisturized using ophthalmic gel covered by a coverslip. Two-photon imaging was performed using a 25X/1.05 NA objective (Olympus) immerged in deionized water and installed into a DM6000 upright microscope equipped with a SP5 confocal head (Leica Microsystem)

and a Chameleon Ultra Ti::Sapphire Laser (Coherent) tuned at 920 nm. Emitted fluorescence was split with dichroic mirrors (Semrock) and filtered with appropriate filters (Semrock) for each channel before collection with nondescanned detectors. Typically, images from 15 to 20 z planes spaced by 5 µm were collected every 2 minutes for up to 3 hours. For *in vitro* analysis of PercevalHR-expressing BMDMs, two-photon imaging was performed using a 25X/1.05 NA objective (Olympus) installed into a FVMPE-RS upright microscope (Olympus) equipped with an Insight deep see dual laser (Spectra physics) and a resonant scanner. PercevalHR excitation was achieved using λ_{low} = 830 nm and λ_{high} = 1040 nm. Emitted fluorescence, collected sequentially for each λ, was split with dichroic mirrors (Semrock) and filtered with a 520/35 filter (PercevalHR signal) and a 483/32 filter (background) before collection with GaAsP detectors. Images in a single plan were collected every 15 s for 5 to 10 min. Data collected were analyzed and processed using Fiji (ImageJ) and Imaris software.

Quantification and statistical analysis

Data are reported as the mean ± SD, and numbers of experiments are reported in figure legends. For *in vitro* analyses, statistical differences between two groups were evaluated using a two-tailed unpaired Student's t-test with Welch's correction or using an ordinary one-way ANOVA with post hoc Holm-Sidak test for multiple comparison. For *in vivo* analyses, unless indicated otherwise, statistical differences between two groups were evaluated using a Mann-Whitney U test. Correlation between the density of iNOS competent cell and cellular respiration and cytokine production was further analyzed *in vitro* and *in vivo* by exponential one-phase decay regression. Significance was defined by a p-value<0.05. All statistical tests were performed using GraphPad Prism 6.0a software. p-values were reported as stars: * $p<0.05$; ** $p<0.01$; *** $p<0.005$

Key Resources Table

REAGENT or RESOURCE	SOURCE	IDENTIFIER
Antibodies		
Purified anti-mouse CD16/32 (Fc-block) (clone: 93)	BioLegend	Cat#101302; RRID: AB_312801
Biotin anti-mouse TER-119/Erythroid cells (clone: TER-119)	BioLegend	Cat#116203; RRID: AB_313705
BUV395 anti-mouse CD45 (clone: 30-F11)	BD Biosciences	Cat#564279; RRID: AB_2651134
BV421 anti-mouse MHC II (I-A/I-E) (clone: M5/114.15.2)	BioLegend	Cat#107632; RRID: AB_2650896
BV510 anti-mouse Ly-6G/Ly-6C (Gr-1) (clone: RB6-8C5)	BioLegend	Cat#108438; RRID: AB_2562215
BV510 anti-mouse Ly-6G (clone: 1A8)	BioLegend	Cat#127633; RRID: AB_2562937
BV605 anti-mouse Ly-6C (clone: HK1.4)	BioLegend	Cat#128036; RRID: AB_2562353
Alexa Fluor 488 anti-mouse TNF-a (clone: MP6-XT12)	BioLegend	Cat#506313; RRID: AB_493328
Alexa Fluor 488 anti-mouse Ly-6G (clone: 1A8)	BioLegend	Cat#127626; RRID: AB_2561340
PE anti-mouse/rat/human MCP-1 (clone: 2H5)	BioLegend	Cat#505904; RRID: AB_315410
PerCP/Cy5.5 anti-mouse/human CD11b (clone: M1/70)	BioLegend	Cat#101228; RRID: AB_893232
PE anti-mouse CCL3 (MIP-1alpha) (clone: DNT3CC)	Invitrogen	Cat#12-7532-80; RRID: AB_2572661
PE/Cy7 anti-mouse CD45.1 (clone: A20)	BioLegend	Cat#110730; RRID: AB_1134168
eFluor 660 anti-mouse CCL3 (MIP-1 alpha) (clone: DNT3CC)	eBioscience	Cat#50-7532-82; RRID: AB_2574295
APC anti-mouse CD11c (clone: N418)	BioLegend	Cat#117310; RRID: AB_313779
APC anti-mouse IL-1b Pro-form (clone: NJTEN3)	eBioscience	Cat#17-7114-80; RRID: AB_10670739
APC-eFluor 780 anti-mouse CD45.2 (clone: 104)	eBioscience	Cat#47-0454-82; RRID: AB_1272175
APC-eFluor 780 anti-mouse MHC II (I-A/I-E) (clone: M5/114.15.2)	eBioscience	Cat#47-5321-82; RRID: AB_1548783
Alexa Fluor 488 Rat IgG1, kappa isotype ctrl (clone: RTK2071)	BioLegend	Cat#400417; RRID: AB_389319
PE Armenian Hamster IgG isotype ctrl (clone: HTK888)	Biolegend	Cat#400908; RRID: AB_326593
PE Rat IgG2a, kappa isotype ctrl (clone: RTK2758)	Biolegend	Cat#400508; RRID: AB_326529
APC Rat IgG1 isotype ctrl (clone: eBRG1)	eBioscience	Cat#17-4310-82; RRID: AB_470178
Biological Samples		
Leishmania major, strain: LRC-L137 V121, DsRed-expressing parasites	Misslitz *et al.* (2000); Sörensen *et al.* (2003)	N/A
Chemicals, peptides, or recombinant proteins		
Lipopolysaccharide from *Escherichia coli* O26:B6	Sigma-Aldrich	Cat#L2654; CAS ID: 93572-42-0
Mouse IFN gamma Recombinant Protein Carrier-Free	eBisocience	Cat#34-8311-85; CAS ID: 98059-61-1
L-NIL (hydrochloride)	Cayman Chemical	Cat#80310; CAS ID: 159190-45-1
Oligomycin A	Cayman Chemical	Cat#11342; CAS ID: 579-13-5
SNAP	Cayman Chemical	Cat#82250; CAS ID: 67776-06-1
Oligomycin A	Cayman Chemical	Cat#11342; CAS ID: 579-13-5
MitoTracker Green FM	Molecular Probes	Cat#M7514; CAS ID: 201860-17-5
Sodium azide 10% solution	Interchim Uptima	Cat#NJK63A; CAS ID: 26628-22-8
MitoTracker Red CMXRos	Molecular Probes	Cat#M7512
Liberase TL Research Grade 10 mg	Sigma-Aldrich (Roche)	Cat#05401020001
BD GolgiPlug (Protein Transport Inhibitor)	BD Biosciences	Cat#555029
2-NBDG	Sigma-Aldrich	Cat#72987; CAS ID: 186689-07-6
Cell Dissociation Buffer, enzyme-free, PBS	Gibco	Cat#13151014
Perm/Wash Buffer	BD Biosciences	Cat#554723
RIPA buffer	Sigma-Aldrich	Cat#R0278
cOmplete™ Protease Inhibitor Cocktail	Sigma-Aldrich	Cat#11697498001
XF Base Medium Minimal DMEM	Seahorse Bioscience	Cat#102353-100
Recombinant Murine SCF	Peprotech	Cat#250-03

Recombinant Murine Flt3-ligand	Peprotech	Cat#250-31L
Recombinant Murine IL-3	Peprotech	Cat#213-13
Polybrene Transfection Reagent	Merck Millipore	Cat#TR-1003-G
Freund's Adjuvant, Incomplete	Sigma-Aldrich	Cat#F5506
Critical Commercial Assays		
AccuCheck Counting Beads	Invitrogen	Cat#PCB100
Cytokine 20-plex Mouse Panel	Invitrogen	Cat#LMC0006M
LIVE/DEAD Fixable Blue Dead Cell Stain Kit	Invitrogen	Cat#L23105
jetPRIME	Polyplus-transfection	Cat#114-07
Zombie Violet^{FM} Fixable Viability Kit	BioLegend	Cat#423114
CD11c MicroBeads UltraPure, mouse	Miltenyi Biotec	Cat#130-108-338
Seahorse XF96e FluxPak mini	Seahorse Bioscience	Cat#102601-100
Seahorse XF Cell Mito Stress Test Kit	Seahorse Bioscience	Cat#103015-100
Seahorse XF Glycolysis Stress Test Kit	Seahorse Bioscience	Cat#103020-100
Experimental Models: Cell Lines		
HEK 293 cells	N/A	N/A
Experimental Models: Cell strains		
Mouse: C57BL/6J	Charles River France	JAX:000664
Mouse: C57BL/6J-Ptprc[a]	Komuro *et al.* (1975)	N/A; MGI ID: 4819849
Mouse: C57BL/6J-Tg(UBC-GFP)30Scha/J	Schaefer *et al.* (2001)	N/A; MGI ID: 3057178
Mouse: C57BL/6J-Lyz2$^{tm1.1Graf[EGFP]}$	Faust *et al.* (2000)	N/A; MGI ID: 2654931
Mouse: C57BL/6-Tg(Csf1r-EGFP-NGFR/FKBP1A/TNFRSF6)2Bck/J	Burnett *et al.* (2004)	N/A; MGI ID: 3051865
Mouse: B6.129P2-Nos2^{tm1Lau}/J	Laubach *et al.* (1995)	N/A; MGI ID: 1857228
Recombinant DNA		
GW1-PercevalHR plasmid (from Gary Yellen)	Tantama *et al.* (2013)	Addgene plasmid #49082
pCL-Eco	N/A	N/A
pMSCV	N/A	N/A
Software and Algorithms		
FlowJo 10.2	Tree Star	https://www.flowjo.com/
Fiji (Image J)	Schindelin *et al.* (2012)	https://fiji.sc/
Imaris	Bitplane	https://www.bitplane.com/
GraphPad Prism 6.0a	GraphPad Software	https://www.graphpad.com/
Wave Desktop	Agilent Technologies	https://www.agilent.com/
Zotero	Zotero	https://www.zotero.org/
Other		
PetakaG3 FLAT	Celartia	Cat#FLPTK25 (Tebu-bio)

Supplemental information

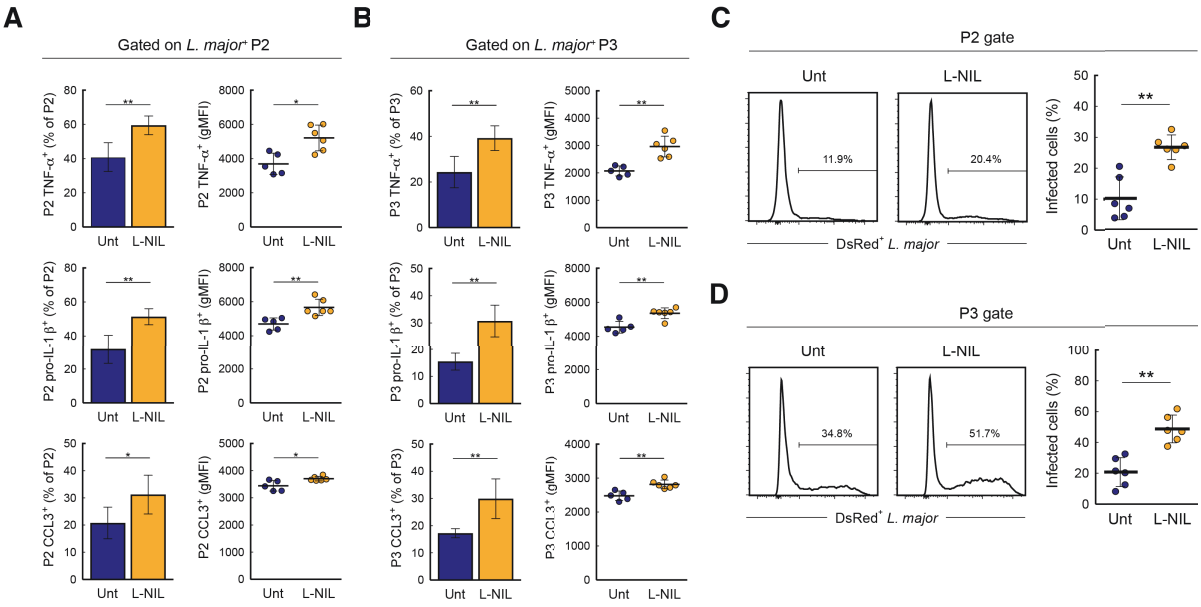

Figure S1. The suppression of cytokine production by NO is also observed in infected monocyte-derived cells. *Related to Figure 3*

WT mice were infected with DsRed-expressing *L. major* and treated 14 days later with the specific iNOS inhibitor L-NIL. The activity of infected (DsRed$^+$) monocyte-derived cells was assessed 3 days later by intracellular cytokine staining on isolated ear cells**.** Percentages (bars) and gMFI (scatter dot plots) of TNF-α-, pro-IL-1β- or CCL3-producing monocytes-derived cells in P2 **(A)** or P3 **(B)** gates. **(C-D)** Effect of iNOS inhibition on monocyte-derived cells infection. WT mice were infected with DsRed-expressing *L. major* and treated 14 days later with the specific iNOS inhibitor L-NIL. Three days later, the percentage of infected monocyte-derived cells in the P2 **(C)** and P3 **(D)** populations was measured by flow cytometry. Numbers indicate the percentage of DsRed$^+$ cells. Plots shows the percentage of infected cells in individual ears. Data are represented as mean ± SD.

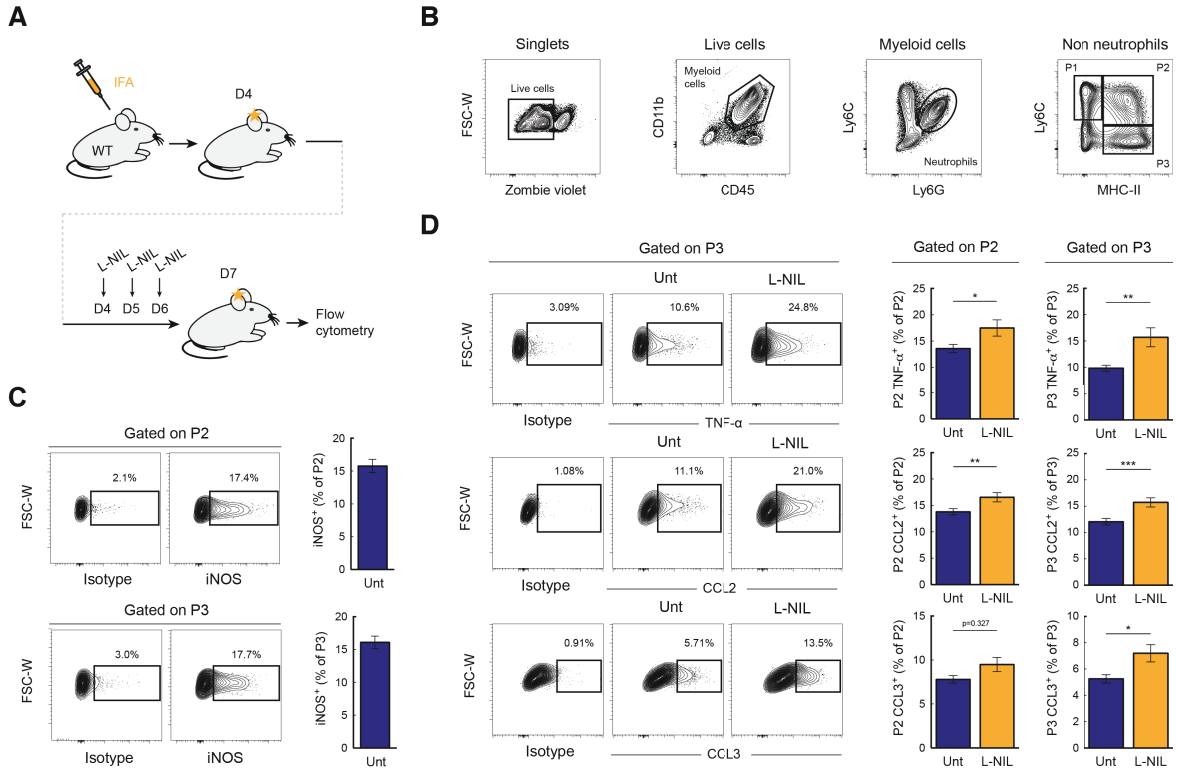

Figure S2. NO restricts inflammation and monocyte-derived cells function *in vivo* in a non-infectious model of inflammation. *Related to Figure 3*

(A) Experimental set-up. WT mice were intradermally injected with emulsified incomplete Freund's adjuvant and treated 4 days later with the specific iNOS inhibitor L-NIL. Monocyte-derived cells activity in inflamed ears were characterized 3 days later. **(B)** Flow cytometry contour plots showing the accumulation of mononuclear phagocytes (P1, P2 and P3) in the inflamed ear. A third of the ear cell preparation was used flow cytometric analysis and >200000 cells were acquired. **(C)** *Left.* Contour plots showing iNOS staining in monocyte-derived cells isolated from a WT mouse. *Right*. Percentages of iNOS expressing monocyte-derived cells in inflamed ear from untreated mice. **(D)** Representative contour plots showing cytokine stainings in monocyte-derived cells. **(E)** Percentages of TNF-α-, CCL2- or CCL3-producing monocytes-derived cells (P2 and P3 gates) from untreated and L-NIL-treated mice as assessed by flow cytometry. Data are represented as mean ± SEM with 16 ears analyzed for each condition.

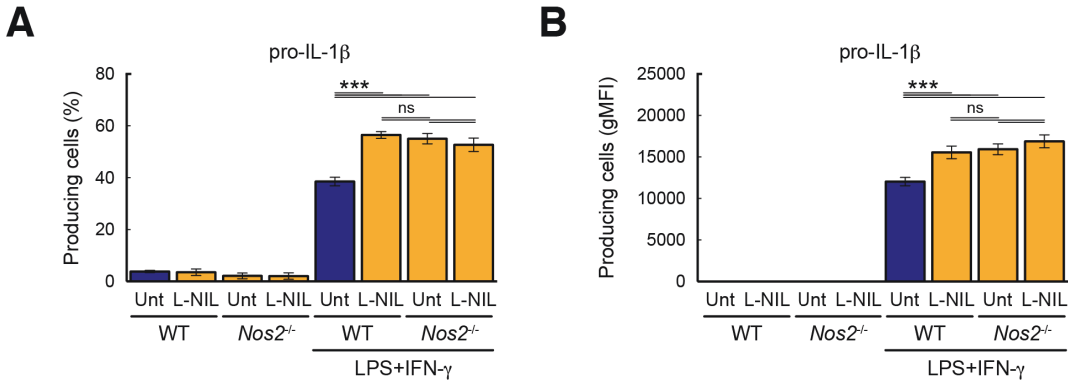

Figure S3. L-NIL treatment does not affect unactivated BMDMs or activated *Nos2*$^{-/-}$ BMDMs. *Related to Figure 4*

WT or *Nos2*$^{-/-}$ BMDMs were activated 24h with LPS+IFN-γ or left unactivated in the presence or absence of L-NIL. Percentages **(A)** and gMFI **(B)** of pro-IL-1β producing WT or *Nos2*$^{-/-}$ cells treated with L-NIL or left untreated as assessed by intracellular cytokine staining. Data are represented as mean ± SD.

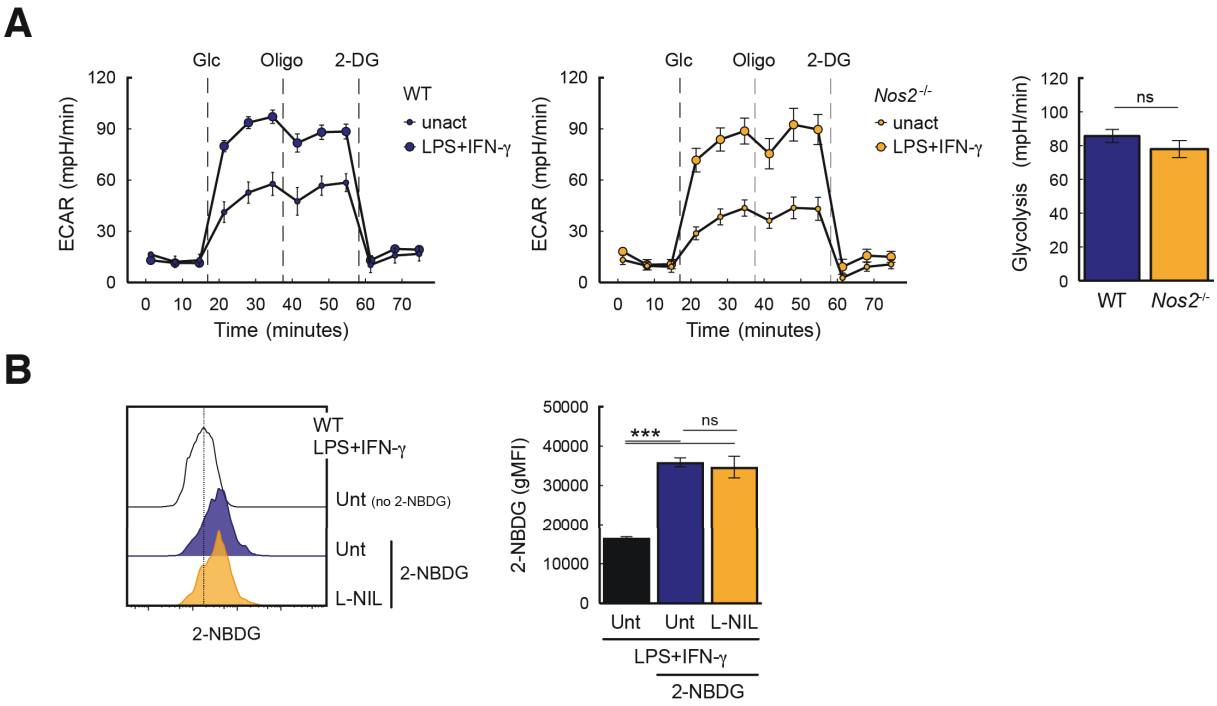

Figure S4. iNOS activity in activated BMDMs has no detectable effect on glycolysis and glucose uptake. *Related to Figure 5*

WT or *Nos2*$^{-/-}$ BMDMs were activated 24 h with LPS+IFN-γ or left unactivated before extracellular flux analysis. **(A)** Extracellular acidification rate (ECAR) measured during sequential treatments with glucose, oligomycin and 2-DG on WT and *Nos2*$^{-/-}$ BMDMs (left and middle panels). Quantification of glycolysis based on ECAR variations is shown for on WT and *Nos2*$^{-/-}$ BMDMs (right panel). **(B)** WT BMDMs were activated 24 h with LPS+IFN-γ in the presence or absence of L-NIL and incubated with 2-NBDG for an additional hour. Uptake was measured by flow cytometry. Representative histograms (left) and bar plots (right) are shown for the indicated conditions. Data are represented as mean ± SD.

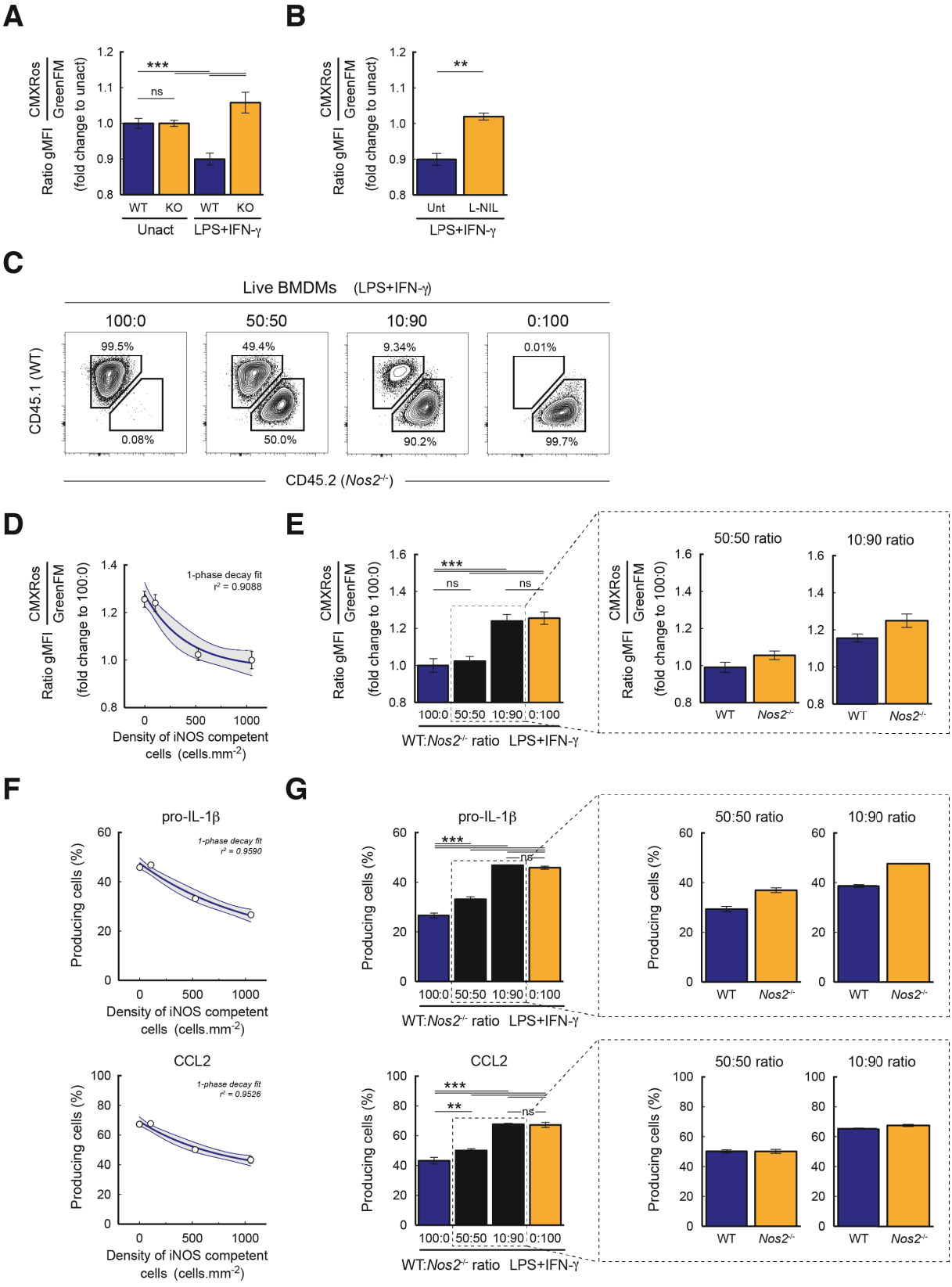

Figure S5. Collective NO production dampens BMDMs respiration and activity *in trans*. *Related to Figure 4 and 5*

(A-B) WT or *Nos2*$^{-/-}$ BMDMs were activated 24 h with LPS+IFN-γ or left unactivated and loaded with MitoTracker GreenFM (total mitochondria) and MitoTracker CMXRos (respiring mitochondria) to assess

mitochondrial activity by flow cytometry. The ratio between MitoTracker CMXRos gMFI and MitoTracker GreenFM gMFI was calculated for each condition. Results are shown as fold change for the activated compared to the unactivated condition for **(A)** WT and *Nos2*$^{-/-}$ cells or **(B)** untreated or L-NIL-treated WT cells. **(C)** WT or *Nos2*$^{-/-}$ BMDMs were activated 24 h with LPS+IFN-γ either alone (ratios 100:0 and 0:100) or mixed at different ratios (50:50 and 10:90). (**D-E**) WT (CD45.1) or *Nos2*$^{-/-}$ (CD45.2) BMDMs were activated 24 h with LPS+IFN-γ either alone (ratios 100:0 and 0:100) or mixed at different ratios (50:50 and 10:90) and loaded with MitoTracker GreenFM and MitoTracker CMXRos. (**D**) Mitochondrial activity was normalized to the value of activated WT (100:0 ratio) for each group and graphed as a function of the density of iNOS competent cells in the culture. (**E**) Bar plots showing the normalized mitochondrial activity for the different mixed culture conditions. The inset shows the analysis of WT (CD45.1) and *Nos2*$^{-/-}$ (CD45.2) cells in mixed cultures at the indicated ratio. **(F-G)** Percentages of cytokine-producing cells were assessed by intracellular cytokine staining for pro-IL-1β and CCL2. **(F)** Percentages of cytokine producing cells were graphed as a function of the density of iNOS competent cells in the culture. **(G)** Bar plots showing the percentages of producing cells for pro-IL-1β (top panel) and CCL2 (bottom panel) for the different mixed culture conditions. The inset shows the analysis of WT (CD45.1) and *Nos2*$^{-/-}$ (CD45.2) cells in mixed cultures at the indicated ratio. Data are represented as mean ± SD.

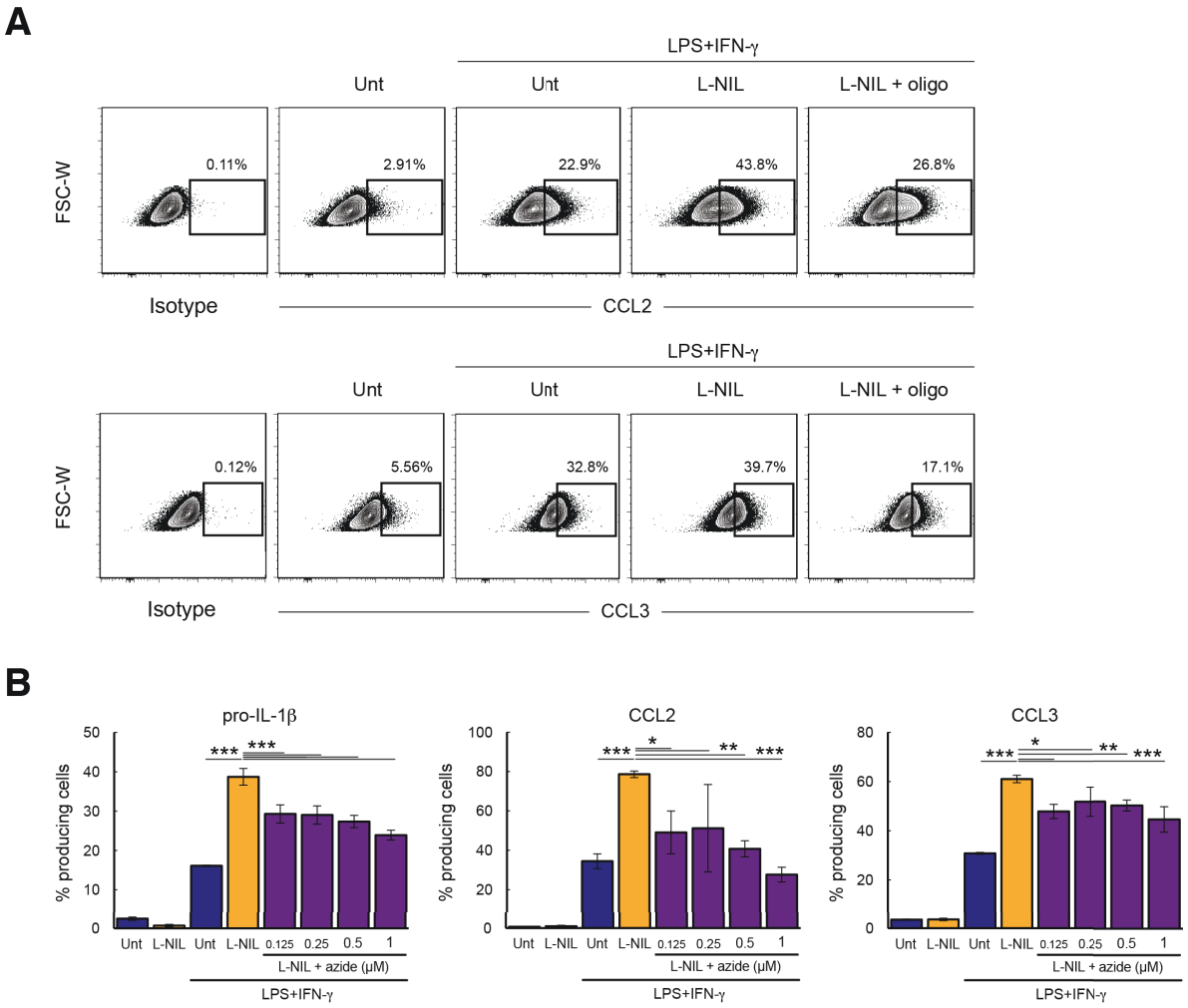

Figure S6. NO also reduces cytokine production under hypoxic conditions and azide also reduces cytokine production in BMDMs. *Related to Figure 6*

(A) WT BMDMs cultivated under hypoxia (pO_2=25mmHg) were activated 24 h with LPS+ IFN-γ in the presence or absence of L-NIL or left unactivated. When indicated, BMDMs were incubated with oligomycin (1 μM) for the last 4 h of culture. Production of CCL2 (top panel) and CCL3 (bottom panel) was assessed by intracellular cytokine staining. Numbers indicate the percentage of producing cells for each condition. **(B)** BMDMs were activated 24 h with LPS+IFN-γ in the presence or in the absence of L-NIL or left untreated. When indicated BMDMs were incubated with various concentration of azide for the last 4 h of the culture. Percentages of cytokine-producing cells were assessed by intracellular cytokine staining for pro-IL-1β, CCL2 and CCL3. Data are represented as mean ± SD.

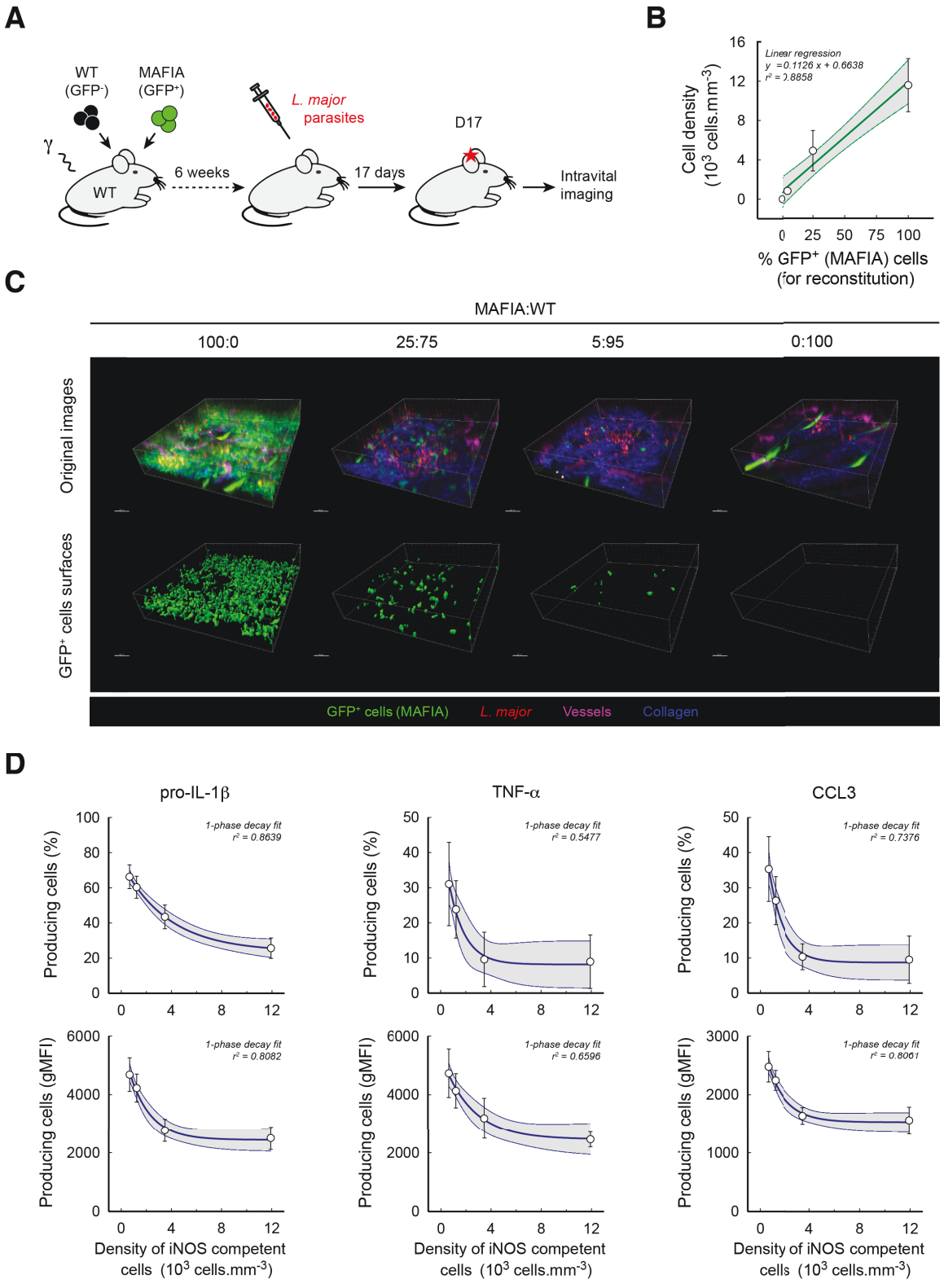

Figure S7. Tissue density of iNOS competent cells at the site of infection regulates cytokine production in monocyte-derived cells in mixed bone-marrow chimeras. *Related to Figure 7*

(A) Experimental set-up. WT recipient mice were lethally irradiated and reconstituted with WT (GFP^-) and MAFIA (GFP^+) bone marrow cells, mixed at different ratios. Chimeras were infected 6 weeks later with DsRed-expressing *L. major*. 17 days later, intravital imaging was performed to visualize GFP^+ cells in the infected skin. **(B)** GFP^+ cell density (number of GFP^+ cells per mm^3) was correlated with the percentage of

GFP^+ cells used to reconstitute chimera recipients. **(C)** 3D volume reconstruction was used to determine GFP^+ cell numbers and the corresponding cell densities at the site of infection. **(D)** CD45.1 WT recipient mice were lethally irradiated and reconstituted with CD45.1 WT and CD45.2 *Nos2*$^{-/-}$ bone marrow cells, mixed at different ratios to modulate the tissue density of iNOS competent cells. Chimeras were infected 6 weeks later with DsRed-expressing *L. major*. Monocyte-derived cells activity was assessed 17 days later by intracellular cytokine staining on extracted ear cells. Percentages (top) and gMFI (bottom) of pro-IL-1β-, TNF-α- and CCL3-producing $Ly6C^+$ $MHC\text{-}II^+$ monocyte-derived cells (P2 gate) were graphed as a function of the estimated density of iNOS competent cells. Data are represented as mean ± SD.